

AD-A126 767

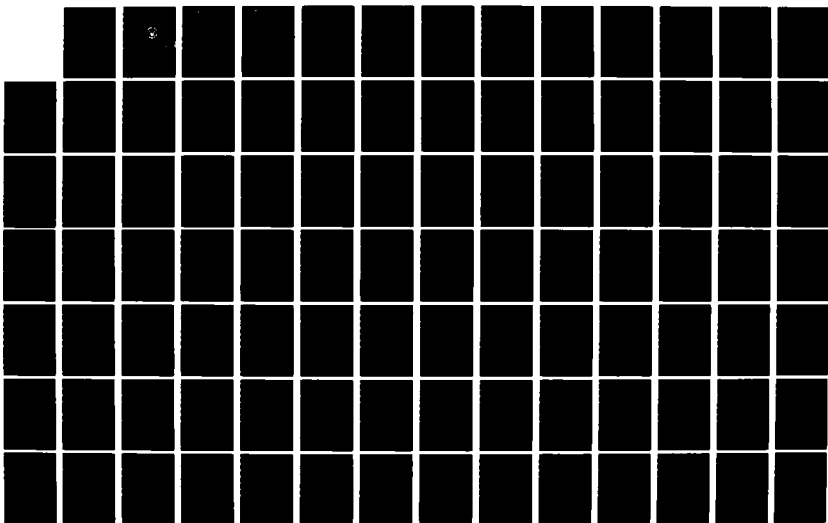
A NUMERICAL ANALYSIS OF PIPE FLOW STABILITY(U) NAVAL
POSTGRADUATE SCHOOL MONTEREY CA D B WALLACE DEC 82

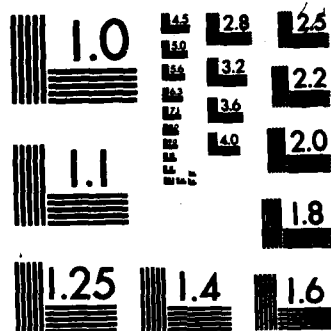
1/3

UNCLASSIFIED

F/G 20/4

NL





MICROCOPY RESOLUTION TEST CHART
NATIONAL BUREAU OF STANDARDS-1963-A

NAVAL POSTGRADUATE SCHOOL
Monterey, California



THESIS

A NUMERICAL ANALYSIS OF PIPE FLOW STABILITY

by

David Bruce Wallace

December 1982

Thesis Advisor:

T. H. Gawain

Approved for public release; distribution unlimited

DTIC
ELECTE
APR 14 1983

A

ADA 126767

DTIC FILE COPY

83 04 14 054

UNCLASSIFIED

SECURITY CLASSIFICATION OF THIS PAGE (When Data Entered)

REPORT DOCUMENTATION PAGE		READ INSTRUCTIONS BEFORE COMPLETING FORM
1. REPORT NUMBER	2. GOVT ACCESSION NO.	3. RECIPIENT'S CATALOG NUMBER
	A126767	
4. TITLE (and Subtitle)		5. TYPE OF REPORT & PERIOD COVERED
A Numerical Analysis of Pipe Flow Stability		Master's Thesis December 1982
7. AUTHOR(s)		6. PERFORMING ORG. REPORT NUMBER
David Bruce Wallace		
8. PERFORMING ORGANIZATION NAME AND ADDRESS		9. CONTRACT OR GRANT NUMBER(s)
Naval Postgraduate School Monterey, California 93940		
10. CONTROLLING OFFICE NAME AND ADDRESS		11. REPORT DATE
Naval Postgraduate School Monterey, California 93940		December 1982
12. MONITORING AGENCY NAME & ADDRESS (if different from Controlling Office)		13. NUMBER OF PAGES
		236
		14. SECURITY CLASS. (of this report)
		Unclassified
		15. DECLASSIFICATION/DOWNGRADING SCHEDULE
16. DISTRIBUTION STATEMENT (of this Report)		
Approved for public release; distribution unlimited		
17. DISTRIBUTION STATEMENT (of the abstract entered in Block 20, if different from Report)		
18. SUPPLEMENTARY NOTES		
19. KEY WORDS (Continue on reverse side if necessary and identify by block number)		
pipe flow stability critical Reynolds number vorticity transport equations hydrodynamic stability		
20. ABSTRACT (Continue on reverse side if necessary and identify by block number)		
<p>Standard theoretical methods of analysis which work well for seemingly more complex problems fail to predict the experimentally observed instability of fully developed, incompressible pipe flow at any Reynolds number. Past research by Harrison and Arnold on the stability of pipe flow yielded erroneous results due to errors in the setup of the problem and formulation of the boundary conditions at the axis.</p>		

DD FORM 1 JAN 73 1473

EDITION OF 1 NOV 68 IS OBSOLETE
S/N 0102-014-6001

UNCLASSIFIED

SECURITY CLASSIFICATION OF THIS PAGE (When Data Entered)

DECLASSIFICATION OF THIS DOCUMENT HAS BEGUN

finite differencing techniques
velocity vector potential
least stable eigenvalue
eigenfunctions
eigensystem
axial perturbation velocity

A revised theory with particular attention to the rather complex boundary conditions at the axis has recently been developed. Improved finite differencing techniques with consistent fourth order truncation error were also used to approximate the governing differential equations.

Numerical results for angular wave numbers zero and six show that the flow is stable at all Reynolds numbers. Results for angular wave number one contain instabilities at all Reynolds numbers for small values of the axial wave number. These results are tabulated, plotted, and discussed in detail in this paper.

[illegible]

SECURITY CLASSIFICATION OF THIS PAGE(When Data Entered)

Approved for public release; distribution unlimited

A Numerical Analysis of Pipe Flow Stability

by

David Bruce Wallace
Lieutenant, United States Navy
B.S., University of Kansas, 1975

Submitted in partial fulfillment of the requirements
for the degree of

MASTER OF SCIENCE IN AERONAUTICAL ENGINEERING

from the

NAVAL POSTGRADUATE SCHOOL
December 1982

Author:

David Bruce Wallace

Approved by:

T.H. Gausman Thesis Advisor

Donald B. Leuten
Chairman, Department of Aeronautics

William M. Folger
Dean of Science and Engineering



ABSTRACT

Standard theoretical methods of analysis which work well for seemingly more complex problems fail to predict the experimentally observed instability of fully developed, incompressible pipe flow at any Reynolds number. Past research by Harrison and Arnold on the stability of pipe flow yielded erroneous results due to errors in the setup of the problem and formulation of the boundary conditions at the axis.

A revised theory with particular attention to the rather complex boundary conditions at the axis has recently been developed. Improved finite differencing techniques with consistent fourth order truncation error were also used to approximate the governing differential equations.

Numerical results for angular wave numbers zero and six show that the flow is stable at all Reynolds numbers. Results for angular wave number one contain instabilities at all Reynolds numbers for small values of the axial wave number. These results are tabulated, plotted, and discussed in detail in this paper.




TABLE OF CONTENTS

I.	INTRODUCTION -----	14
II.	THE VORTICITY TRANSPORT EQUATION -----	19
	A. BASIC THEORY -----	19
	B. THE VORTICITY TRANSPORT EQUATION -----	23
	C. THE VORTICITY TRANSPORT MATRIX EQUATION -----	30
	D. EQUATION FOR $n = 0$ -----	32
	E. EQUATIONS FOR $n = 1$ -----	33
	F. EQUATIONS FOR $n = 6$ -----	35
III.	BOUNDARY CONDITIONS -----	36
IV.	PERTURBATION VELOCITY -----	49
V.	NUMERICAL METHODS -----	52
	A. GENERAL METHODS USED -----	52
	B. FINITE DIFFERENCE EQUATIONS -----	57
	C. SPECIFIC METHODS FOR $n = 0, 1, \text{ AND } 6$ -----	67
	D. COMPUTER PROGRAM USEAGE -----	83
VI.	RESULTS -----	86
	A. RESULTS FOR $n = 0$ -----	86
	B. RESULTS FOR $n = 1$ -----	99
	C. RESULTS FOR $n = 6$ -----	118
	D. NUMERICAL ACCURACY -----	134
VII.	RECOMMENDATIONS AND CONCLUSIONS -----	139

APPENDIX A:	COEFFICIENTS OF THE VORTICITY TRANSPORT EQUATIONS -----	142
APPENDIX B:	COEFFICIENTS OF THE TRANSFORMED VORTICITY TRANSPORT EQUATIONS FOR $n = 0, 1,$ AND 6 -----	144
APPENDIX C:	COEFFICIENTS OF THE BOUNDARY EQUATIONS AT THE AXIS -----	151
APPENDIX D:	SPECIAL CONDITIONS AT THE AXIS -----	154
COMPUTER PROGRAMS	-----	156
A.	MAIN INVESTIGATIVE PROGRAM FOR $n = 0$ -----	156
B.	MAIN INVESTIGATIVE PROGRAM FOR $n = 1$ -----	172
C.	MAIN INVESTIGATIVE PROGRAM FOR $n = 6$ -----	199
D.	PROGRAM TO COMPUTE THE NONCENTRAL FINITE DIFFERENCE COEFFICIENTS -----	220
LIST OF REFERENCES	-----	234
INITIAL DISTRIBUTION LIST	-----	236

LIST OF FIGURES

2-1	Velocity Profile of Fluid Flow in a Pipe -----	22
5-1	Radial Mesh, Standard Method -----	53
5-2	Radial Mesh, Half Station Method -----	54
5-3	[A] Matrix for $n = 0$ -----	69
5-4	[B] Matrix for $n = 0$ -----	70
5-5	[A] Matrix for $n \geq 6$ -----	74
5-6	[B] Matrix for $n \geq 6$ -----	75
5-7	[A] Matrix for $n = 1$ -----	80
5-8	[B] Matrix for $n = 1$ -----	81
6-1	Normalized Perturbation Velocity vs. Radius -----	90
6-2	Normalized Perturbation Velocity vs. Radius -----	91
6-3	Normalized Perturbation Velocity vs. Radius -----	92
6-4	Normalized Perturbation Velocity vs. Radius -----	93
6-5	Normalized Perturbation Velocity vs. Radius -----	94
6-6	Normalized Perturbation Velocity vs. Radius -----	95
6-7	Normalized Perturbation Velocity vs. Radius -----	96
6-8	Normalized Perturbation Velocity vs. Radius -----	97
6-9	Normalized Perturbation Velocity vs. Radius -----	98
6-10	GAMMA^* vs. ALPHA, Reynolds Number Contours, $n = 1$ -----	104
6-11	GAMMA^* vs. ALPHA, Reynolds Number Contours, $n = 1$ -----	105
6-12	GAMMA^* vs. Reynolds Number, Alpha Contours, $n = 1$ -----	106
6-13	Normalized Perturbation Velocity vs. Radius -----	107
6-14	Normalized Perturbation Velocity vs. Radius -----	108

6-15	Normalized Perturbation Velocity vs. Radius -----	109
6-16	Normalized Perturbation Velocity vs. Radius -----	110
6-17	Normalized Perturbation Velocity vs. Radius -----	111
6-18	Normalized Perturbation Velocity vs. Radius -----	112
6-19	Normalized Perturbation Velocity vs. Radius -----	113
6-20	Normalized Perturbation Velocity vs. Radius -----	114
6-21	Normalized Perturbation Velocity vs. Radius -----	115
6-22	Normalized Perturbation Velocity vs. Radius -----	116
6-23	Normalized Perturbation Velocity vs. Radius -----	117
6-24	GAMMA* vs. ALPHA, Reynolds Number Contours, $n = 6$ -----	121
6-25	GAMMA* vs. ALPHA, Reynolds Number Contours, $n = 6$ -----	122
6-26	GAMMA* vs. Reynolds Number, Alpha Contours, $n = 6$ -----	123
6-27	Normalized Perturbation Velocity vs. Radius -----	124
6-28	Normalized Perturbation Velocity vs. Radius -----	125
6-29	Normalized Perturbation Velocity vs. Radius -----	126
6-30	Normalized Perturbation Velocity vs. Radius -----	127
6-31	Normalized Perturbation Velocity vs. Radius -----	128
6-32	Normalized Perturbation Velocity vs. Radius -----	129
6-33	Normalized Perturbation Velocity vs. Radius -----	130
6-34	Normalized Perturbation Velocity vs. Radius -----	131
6-35	Normalized Perturbation Velocity vs. Radius -----	132
6-36	Normalized Perturbation Velocity vs. Radius -----	133
6-37	Normalized Perturbation Velocity vs. Radius -----	136
6-38	Normalized Perturbation Velocity vs. Radius -----	137
6-39	Normalized Perturbation Velocity vs. Radius -----	138

LIST OF TABLES

2-1	Properties of the Vorticity Transport Equations -----	29
5-1	Properties of the [A] and [B] Matrices for $n \geq 6$ -----	73
6-1	Stability Data for Angular Wave Number $n = 0$ -----	88
6-2	Stability Data for Angular Wave Number $n = 1$ -----	100
6-3	Stability Data for Angular Wave Number $n = 1$ -----	101
6-4	Stability Data for Angular Wave Number $n = 6$ -----	119
6-5	Stability Data for Angular Wave Number $n = 6$ -----	120

TABLE OF SYMBOLS

D	Differential operator $\partial/\partial r$
D^2, D^3, D^4	Higher order partial derivatives with respect to r.
e	Base of natural logarithms.
$\vec{e}_x, \vec{e}_r, \vec{e}_\theta$	Unit vectors along the x, r, and θ axes in cylindrical coordinates.
F, G, H	Components of the velocity vector potential function defined in equation (2-28).
h	The increment of the radius in the finite difference equations, $h = 1/N$.
i	$+\sqrt{-1}$, the imaginary unit.
i	Used as an index to distinguish the transformed coefficient matrices $[M_i]$ of equation (2-43) and in the discrete finite difference equations.
j	Used as an index to distinguish the transformed coefficient matrices $[N_j]$ of equation (2-43).
N	The number of interior points along the pipe radius used in the finite difference mesh.
n	Angular wave number of the perturbation in the θ direction, where $n = 0, 1, 2, 3, \dots$
O	Symbol denoting the phrase "of order".
P	Pressure appearing in equations (2-4, 5, 11, and 12).

P	Component of the velocity vector potential derived from the component G after a change of variable.
Q	Component of the velocity vector potential derived from the component H after a change of variable.
R	Normalized pipe radius, $R = 1$.
\bar{R}	The dimensional pipe radius used to define Re in equation (2-6).
Re	Reynolds number based on pipe radius and mean volumetric velocity, as defined in equation (2-6).
t	Time.
U	The axial component of the mean dimensionless velocity of the flow as defined in equation (2-13).
\bar{U}	The mean dimensional volumetric velocity of the flow used to define Re in equation (2-6).
u, v, w	Components of the complex perturbation velocity.
\vec{V}	Velocity vector of the mean flow.
\vec{V}'	Velocity vector of the total or resultant flow.
\vec{v}	Complex perturbation velocity vector.
\vec{W}	The velocity vector potential function defined in equation (2-28).
x, r, θ	Cylindrical coordinates.
X	Symbol for $iax + in\theta + yt$, defined in equation (2-29).

$\{X^*\}$	Eigenvector corresponding to the least stable eigenvalue.
α	The real axial wave number of the perturbation in the x direction, where $\alpha \geq 0$.
γ	The complex frequency of the perturbation defined in equation (2-30).
γ^*	The maximum algebraic value of the real part of the complex frequency which is also the least stable eigenvalue, also referred to as GAMMA*.
$\vec{\Gamma}$	Shorthand notation of the vorticity transport equations as defined in equation (2-32).
$\Gamma_x, \Gamma_r, \Gamma_\theta$	Components of $\vec{\Gamma}$ in cylindrical coordinates.
ϵ	The residual error of the least stable eigenvalue solution of the governing equations.
ν	Kinematic viscosity.
μ	Viscosity.
ρ	Density.
$\vec{\Omega}$	Mean vorticity vector.
$\vec{\Omega}'$	Total or resultant vorticity vector.
$\vec{\omega}$	Perturbation vorticity vector.
∇	Linear vector operator (nabla).
\times	Vector cross-product operator.
$\nabla \times$	Vector curl operator.

- $\nabla \cdot$ Vector dot product operator.
- $[]$ Brackets enclosing a matrix.
- $\{\}$ Brackets enclosing a column vector.

I. INTRODUCTION

Osborne Reynolds [Ref. 1] conducted his classical experiments on the transition from laminar to turbulent flow of fluids in circular pipes nearly 100 years ago. Based on his experiments the critical Reynolds number for pipe flow was found to be 2300. An analytical solution for the problem of predicting instabilities of fully developed, three dimensional, incompressible flow of constant viscosity fluids in pipes has been pursued actively since then. Several approaches have been taken in solving the inherently nonlinear Navier-Stokes equations, which along with the continuity equation, govern the behavior of fluid flow in pipes of circular cross-section.

Salwen and Grosch [Ref. 2] studied pipe flow with purely sinusoidal streamwise (axial) perturbations. Infinitesimal velocity and pressure perturbations, which were explicit functions of time and not complex or exponential in form, were introduced into the flow field. Numerical calculations were carried out at various angular wave numbers and it was concluded that the flow was stable for all axial wave numbers and Reynolds numbers. Perturbations with exponential growth in space but a purely sinusoidal variation in time were explored by Garg and Rouleau [Ref. 3] and found to be stable. Gill [Ref. 4] studied combinations of exponential growth in space and in time using power series analysis and concluded that these flows were all stable.

Because of the general agreement that pipe flow is stable to infinitesimal disturbances, two other approaches to the problem of predicting instabilities at the experimentally observed critical Reynolds number have been pursued. First, investigations by Davy and Drazin [Ref. 5] confirmed that pipe Poiseuille flow was stable at all Reynolds numbers for infinitesimal disturbances that were both temporally and axially complex and exponential in nature. However, despite the fact that the governing equations must necessarily remain nonlinear with the introduction of disturbances of finite amplitude, they concluded that the flow is unstable with respect to finite disturbances. Similar theoretical examinations of plane Poiseuille flow between two parallel plates led McIntire and Lin [Ref. 6] to this same conclusion. Second, it was postulated by Huang and Chen [Ref. 7] and Leite [Ref. 8] that the origin of flow instabilities occur in the entrance region of the pipe, where the flow has not yet become fully developed. Both theoretical and experimental studies have been done to support these hypotheses. Garg [Ref. 9] also found that flow instabilities existed near the entry region for developing pipe flow. He concluded that results using the Hornbeck velocity profile more nearly approximated experimentally determined values of the critical Reynolds number. While these investigations have shown instabilities to exist in pipe flow, a completely generalized solution to the linearized problem of fully developed pipe flow has never been accomplished.

Recently, a more general theory consisting of perturbations which have a fully complex exponential form with respect to time and the axial

coordinate, a purely imaginary exponential form in the angular coordinate and are three dimensional in nature have been explored. Development of this theory by Harrison [Ref. 10] and further numerical investigations by Arnold [Ref. 11] failed to produce conclusive results that instabilities exist in fully developed pipe flow. Errors in the setup of the problem and inadequate formulation of the boundary conditions at the pipe axis contributed to these erroneous results. Arnold, however, was on the right track in his research by incorporating newly formulated boundary conditions at the axis developed by Gawain [Ref. 12].

Arnold's work, for the most part, remains valid except that he overlooked a small but significant detail that resulted in unclear definitions of stability and instability. He used a complex axial wave number α , of the form $\alpha = \alpha_R + i\alpha_I$, whereas the correct version should simply be a purely imaginary quantity of the form $i\alpha$. Thus, Arnold introduced an extra degree of freedom, namely the fictitious and incorrect quantity α_R . This accounts for the erroneous instabilities which he obtained in his numerical investigation of pipe flow.

Further work by Gawain [Ref. 13] refined the boundary conditions at the axis and incorporated the previously defined imaginary axial wave number, in exponential form, which represents only sinusoidal oscillations with respect to the axial coordinate. Using these advancements in the linearized theory, Gawain showed an asymptotic trend toward neutral stability of the flow with increasing Reynolds numbers for angular wave number, $n = 0$. This paper duplicates and confirms the results for $n = 0$, that the flow is stable at all Reynolds numbers and axial wave numbers. It is further shown that fully developed pipe flow for $n = 6$

is also stable and shows the same trends as for $n = 0$. Instabilities are shown to exist in the numerical analysis of the vorticity transport equations for $n = 1$. The paradox that now appears is that for angular wave numbers $n = 0$ and 6 the flow is apparently stable at all Reynolds numbers while for $n = 1$ the flow is apparently unstable at all Reynolds numbers. Neither of these theoretical results is consistent with the known experimental fact that there exists a critical Reynolds number below which pipe flow is stable and above which it is unstable. However, the new result for $n = 1$, while it can hardly be called correct, is at least encouraging in that it shows for the first time that instabilities can in fact exist in the solution of the linearized vorticity transport equations for fully developed pipe flow.

In addition to implementing the improved axis boundary conditions and the advancement in the linearized theory, improved finite differencing techniques were used to approximate the vorticity transport equations along a uniform radial mesh. Highly accurate numerical solutions for the previously mentioned angular wave numbers, $n = 0, 1$, and 6 , were obtained using double precision, complex numbers. Additionally, finite difference equations with consistent fourth order truncation error were used throughout. Details of the development of the vorticity transport equations and the central and non-central finite difference equations are discussed in later chapters. Systematic and extensive calculations remain to be accomplished for angular wave numbers, $n = 2, 3, 4, 5$, and $n > 6$. The results of these numerical analyses should prove to be fruitful in establishing a theory which

adequately explains the experimentally observed fact of the onset of flow instabilities at the critical Reynolds number.

II. THE VORTICITY TRANSPORT EQUATION

A. BASIC THEORY

The governing equations for laminar flow of fluids in a circular pipe are derived from Newton's second law of motion,

$$\vec{F} = m \vec{a} \quad (2-1)$$

and the conservation of mass principle through an infinitesimal control volume. Equation (2-1) results in the familiar Navier-Stokes equation, which is a vector equation in three cylindrical coordinates and in time. The equation for conservation of mass results in the continuity equation for incompressible flow and is given by,

$$\nabla \cdot \vec{V} = 0 \quad (2-2)$$

For the case at hand, the following assumptions are made,

1. The fluid is incompressible, $\rho = \text{constant}$
2. The fluid has constant viscosity, $\mu = \text{constant}$
3. The flow is fully developed, $U = f(r)$ only
4. The flow is three dimensional in nature
5. The mean flow is steady, $\partial \vec{V} / \partial t = 0$
6. The perturbation flow is unsteady, $\partial \vec{V} / \partial t \neq 0$
7. The effects of body forces are negligible

The resulting Navier-Stokes equation can be stated as the sum of the forces per unit mass is equal to the acceleration or,

$$\Sigma \frac{\text{Force}}{\text{mass}} = \text{acceleration} \quad (2-3)$$

The forces acting on the fluid are pressure forces and viscous forces. Body forces and hydrostatic forces balance out and are not a factor here.

Equation (2-3) in its dimensional form can be expressed as,

$$-\nabla^* \frac{p^*}{\rho^*} + \left(\frac{\mu^*}{\rho^*}\right) \nabla^{2*} \vec{v}^* = \frac{d\vec{v}^*}{dt^*} \quad (2-4)$$

where the starred quantities are fully dimensional.

It should be noted here that the equations presented through equation (2-18) represent the mean flow. Equation (2-4) can also be expressed in a nondimensional form as,

$$-\nabla p + \frac{1}{Re} \nabla^2 \vec{v} = \frac{d\vec{v}}{dt} \quad (2-5)$$

where Re is the Reynolds number and is defined as,

$$Re = \frac{\bar{R} \bar{U}}{\nu} \quad (2-6)$$

This definition of Reynolds number is based on the pipe radius \bar{R} as the characteristic length, the mean volumetric velocity \bar{U} as the characteristic velocity, and the kinematic viscosity ν which is constant. The three quantities on the right side of equation (2-6) are dimensional, but Re is a dimensionless quantity. On this basis, the critical Reynolds number for transition from laminar to turbulent flow becomes 1150 (vice the value of 2300 which is obtained if the Reynolds number is

defined in terms of pipe diameter). All subsequent equations presented in this paper are in nondimensional form.

Returning to the derivation of the mean flow, the acceleration term or substantial derivative, $d\vec{V}/dt$ can be expanded to the form,

$$\frac{d\vec{V}}{dt} = (\vec{V} \cdot \nabla) \vec{V} + \frac{\partial \vec{V}}{\partial t} \quad (2-7)$$

but $(\vec{V} \cdot \nabla)\vec{V}$ can be further expanded by a well known vector identity to,

$$(\vec{V} \cdot \nabla)\vec{V} = \nabla \left(\frac{U^2}{2} \right) - \vec{V} \times (\nabla \times \vec{V}) \quad (2-8)$$

Additionally, $\nabla^2 \vec{V}$ from equation (2-5) can be expanded to,

$$\nabla^2 \vec{V} = \nabla (\nabla \cdot \vec{V}) - \nabla \times (\nabla \times \vec{V}) \quad (2-9)$$

but $\nabla \cdot \vec{V} = 0$, since continuity must be satisfied and equation (2-9) becomes,

$$\nabla^2 \vec{V} = - \nabla \times (\nabla \times \vec{V}) \quad (2-10)$$

With appropriate substitutions, the final form of the Navier-Stokes equation becomes,

$$- \nabla P - \frac{1}{Re} \nabla \times (\nabla \times \vec{V}) = \nabla \left(\frac{U^2}{2} \right) - \vec{V} \times (\nabla \times \vec{V}) + \frac{\partial \vec{V}}{\partial t} \quad (2-11)$$

A more convenient form of equation (2-11) is,

$$- \nabla \left(P + \left(\frac{U^2}{2} \right) \right) = \frac{1}{Re} \nabla \times (\nabla \times \vec{V}) - \vec{V} \times (\nabla \times \vec{V}) + \frac{\partial \vec{V}}{\partial t} \quad (2-12)$$

As previously discussed, all the quantities in the equations have been nondimensionalized. Dimensionless cylindrical coordinates x , r , and θ are used with \vec{e}_x , \vec{e}_r and \vec{e}_θ denoting the unit vectors in the three coordinate directions, respectively. It is well known that the velocity profile for fully developed, three dimensional, incompressible flow in circular pipes can be expressed analytically by,

$$U = 2 (1 - r^2) \quad (2-13)$$

This function has the shape of a paraboloid of revolution as shown in Figure 2-1.

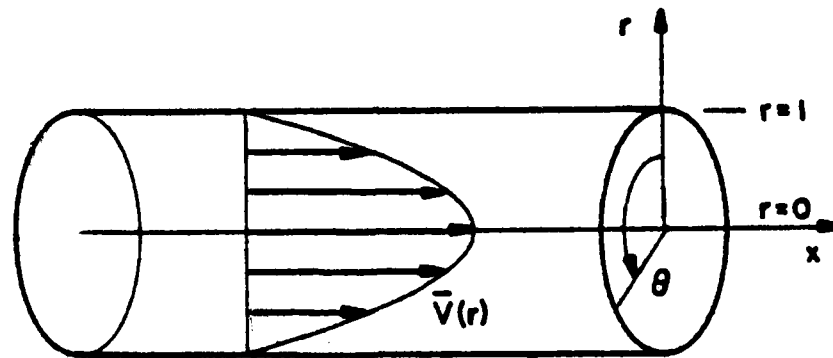


Figure 2-1. Velocity Profile of Fluid Flow in a Pipe

The nondimensional mean velocity vector $\vec{V}(r)$ of the flow is given by,

$$\vec{V}(r) = U \vec{e}_x = 2 (1 - r^2) \vec{e}_x \quad (2-14)$$

A second vector quantity $\vec{\Omega}$, the mean vorticity, is defined as the curl of the mean velocity vector and is given by,

$$\vec{\Omega} = \nabla \times \vec{V} = 4 r \vec{e}_\theta \quad (2-15)$$

which will be used later.

B. THE VORTICITY TRANSPORT EQUATION

The vorticity transport equation is now obtained by taking the curl of the Navier-Stokes equation (2-12), resulting in,

$$-\nabla \times \nabla \left(P + \left(\frac{U^2}{2} \right) \right) = \frac{1}{Re} \nabla \times (\nabla \times (\nabla \times \vec{V})) - \nabla \times (\vec{V} \times (\nabla \times \vec{V})) + \frac{\partial (\nabla \times \vec{V})}{\partial t} \quad (2-16)$$

The primary reason for taking the curl of the Navier-Stokes equation is to eliminate the unknown scalar on the left side of equation (2-16). Since the curl of the gradient of a scalar is equal to zero, equation (2-6) reduces to,

$$\frac{1}{Re} \nabla \times (\nabla \times (\nabla \times \vec{V})) - \nabla \times (\vec{V} \times (\nabla \times \vec{V})) + \frac{\partial (\nabla \times \vec{V})}{\partial t} = 0 \quad (2-17)$$

Equation (2-17) can be simplified by substituting the mean vorticity vector relation equation (2-15) into equation (2-17) resulting in,

$$\frac{1}{Re} \nabla \times (\nabla \times \vec{\Omega}) - \nabla \times (\vec{V} \times \vec{\Omega}) + \frac{\partial \vec{\Omega}}{\partial t} = 0 \quad (2-18)$$

In order to analyze this flow field and in particular to determine the transition from laminar to turbulent flow, a disturbance of small amplitude is introduced into the flow. It is assumed that the resulting flow is made up of the steady state, laminar flow and a small perturbation flow superimposed on the laminar flow. The total velocity and vorticity respectively become,

$$\vec{V}' = \vec{V} + \vec{v} \quad (2-19)$$

and

$$\vec{\Omega}' = \vec{\Omega} + \vec{\omega} \quad (2-20)$$

where \vec{v} and $\vec{\omega}$ are the velocity perturbations and vorticity perturbations, respectively. It is of course a necessary requirement that the continuity equation for the total flow be satisfied here as well,

$$\nabla \cdot \vec{V}' = \nabla \cdot \vec{V} + \nabla \cdot \vec{v} = 0 \quad (2-21)$$

In view of this relation and of equation (2-2), the perturbation flow independently satisfies the continuity condition and

$$\nabla \cdot \vec{v} = 0 \quad (2-22)$$

The introduction of the perturbation quantities into the vorticity transport equation is accomplished by substituting \vec{V}' for \vec{V} and $\vec{\Omega}'$ for $\vec{\Omega}$ into equation (2-18). This results in,

$$\frac{1}{Re} \nabla \times (\nabla \times (\vec{\Omega} + \vec{\omega})) - \nabla \times [(\vec{V} + \vec{v}) \times (\vec{\Omega} + \vec{\omega})] + \frac{\partial(\vec{\Omega} + \vec{\omega})}{\partial t} = 0 \quad (2-23)$$

which is the equation for the total or resultant flow field. Upon expanding equation (2-23), applying the mean steady flow assumption, $\partial \vec{V}/\partial t = 0$, and subtracting equation (2-18) from it, equation (2-23) becomes,

$$\frac{1}{Re} \nabla \times (\nabla \times \vec{\omega}) - \nabla \times [(\vec{V} \times \vec{\omega}) - (\vec{\Omega} \times \vec{v}) + (\vec{v} \times \vec{\omega})] + \frac{\partial \vec{\omega}}{\partial t} = 0 \quad (2-24)$$

Now equation (2-23) is linear in the perturbation quantities except for the second order term, $(\vec{v} \times \vec{\omega})$. Since the perturbations are assumed to be small, this term can be neglected.

The perturbation vorticity is defined as,

$$\vec{\omega} = \nabla \times \vec{v} \quad (2-25)$$

which is analogous to equation (2-15) for the mean flow. Making this substitution in equation (2-24) yields the linearized vorticity transport equation,

$$\frac{1}{Re} \nabla \times (\nabla \times (\nabla \times \vec{v})) - \nabla \times (\vec{V} \times (\nabla \times \vec{v})) + \nabla \times (\nabla \times (\vec{V} \times \vec{v})) + \nabla \times \frac{\partial \vec{v}}{\partial t} = 0 \quad (2-26)$$

As previously mentioned, the continuity equation (2-22) for the perturbation velocity must be satisfied. A convenient way to insure this is to express \vec{v} in terms of a velocity vector potential function \vec{W} as follows,

$$\vec{v} = \nabla \times \vec{W} \quad (2-27)$$

It can be verified that if \vec{v} is defined in this way, equation (2-22) is satisfied identically for any arbitrary vector function \vec{W} .

Instead of proceeding directly with the real vector functions \vec{v} and \vec{W} , it is advantageous to work with the Fourier transforms of \vec{v} and \vec{W} , which are in general complex functions. This is the form which is used here. It can be shown, because of the linearity of the basic equation, that if a solution can be found for the Fourier transforms, then the corresponding real vector functions will satisfy the basic equation as well. A detailed explanation of these functions was presented more elegantly by Gawain [Ref. 13]. The vector potential function \vec{W} , now representing the Fourier transform, can be expressed as,

$$\vec{W} = [F(r) \vec{e}_x + G(r) \vec{e}_r + H(r) \vec{e}_\theta] e^X \quad (2-28)$$

where X is a convenient abbreviation for the complex quantity,

$$X = i\alpha x + in\theta + \gamma t \quad (2-29)$$

The axial wave number α is a real quantity greater than or equal to zero which in the exponential form represents purely sinusoidal axial variations of \vec{v} . The angular wave number n is a positive integer and represents sinusoidal angular variations of \vec{v} which are periodic with respect to coordinate θ . The complex frequency γ contained in the exponent is of the form,

$$e^{\gamma t} = e^{(\gamma_R + i\gamma_I)t} = e^{\gamma_R t} (\cos \gamma_I t + i \sin \gamma_I t) \quad (2-30)$$

The quantity γ_R clearly represents the exponential time rate of growth or decay of the perturbation amplitude. The basic criteria for hydrodynamic stability can be defined in terms of γ_R . Positive values of γ_R represent growth and signify flow instability while negative values of γ_R represent decay and signify flow stability.

The vorticity transport equation can now be expressed in terms of the velocity vector, \vec{V} and the complex vector potential, \vec{W} . By making the substitution for \vec{v} , equation (2-26) now becomes,

$$\begin{aligned} \frac{1}{Re} \nabla \times (\nabla \times (\nabla \times (\nabla \times \vec{W}))) - \nabla \times (\vec{V} \times (\nabla \times (\nabla \times \vec{W}))) \\ + \nabla \times (\nabla \times (\vec{V} \times (\nabla \times \vec{W}))) + \nabla \times (\nabla \times \frac{\partial \vec{W}}{\partial t}) = 0 \end{aligned} \quad (2-31)$$

In convenient shorthand notation, equation (2-31) becomes,

$$\text{Equation (2-31)} = \vec{f}(r)e^x = [\Gamma_x(r) \vec{e}_r + \Gamma_r(r) \vec{e}_\theta + \Gamma_\theta(r) \vec{e}] e^x = 0 \quad (2-32)$$

and can be expressed in matrix notation as,

$$\vec{f} = \begin{Bmatrix} \Gamma_x \\ \Gamma_r \\ \Gamma_\theta \end{Bmatrix} = \begin{Bmatrix} 0 \\ 0 \\ 0 \end{Bmatrix} \quad (2-33)$$

Therefore, the three components of the vorticity transport equation are equivalent to three simultaneous scalar equations, namely,

$$\begin{aligned}\Gamma_x &= 0 \\ \Gamma_r &= 0 \\ \Gamma_\theta &= 0\end{aligned}\tag{2-34}$$

Of these three equations, only two are actually independent since, as can be seen from equation (2-31), $\vec{\Gamma} \cdot \vec{e}^x$ is itself the curl of another vector. Therefore $\vec{\Gamma} \cdot \vec{e}^x$ must necessarily be nondivergent. It can be shown that the components of $\vec{\Gamma}$ satisfy the identity, $\nabla \cdot (\vec{\Gamma} \cdot \vec{e}^x) \equiv 0$, or,

$$i\alpha\Gamma_x + \frac{1}{r} D (r\Gamma_r) + \left(\frac{i\alpha}{r}\right) \Gamma_\theta \equiv 0\tag{2-35}$$

where D is the symbol for the differential operator d/dr . Two linearly independent equations can now be formulated from equations (2-34) given the constraint of equation (2-35). This can be reduced to some appropriate linear combination of two of the equations which is set equal to zero and to the third equation which is also set equal to zero. This results in a system of two coupled, fourth order differential equations in three unknowns. Recall that the vector potential function \vec{W} is expressed in terms of $F(r)$, $G(r)$, and $H(r)$. It can be shown that one of these variables is redundant and may be eliminated without any loss of generality in the solution of the equations. For the present case, the solution assumes its most convenient form if,

$$F(r) = 0\tag{2-36}$$

This convention has therefore been adopted and now $G(r)$ and $H(r)$ become the two coupled eigenfunctions of the governing fourth order differential equations. Returning to the problem of selecting the proper linear combination of equations comprising \vec{f} , it is important to choose this combination in an optimum fashion by analyzing the algebraic structure of these equations. Table 2-1 is taken from reference [13], corrected, and duplicated here for that purpose. Notice that equations (1) and (3) in the table are third order in G . If the particular linear combination of these equations is chosen as appears in equation (4), the result reduces to an equation of second order in G . This does not affect the order of the result since the function H remains fourth order.

Table 2-1. Properties of the Vorticity Transport Equations

EQUATION	TERM OF HIGHEST ORDER IN G	TERM OF HIGHEST ORDER IN H	HIGHEST NEGATIVE POWER OF r
(1) $\Gamma_x(r) = 0$	$\frac{i\alpha}{Re} D^3G$	$-\frac{n\alpha}{rRe} D^2H$	r^{-3}
(2) $\Gamma_r(r) = 0$	$\frac{1}{Re} (\alpha^2 + \frac{n^2}{r^2}) D^2G$	$\frac{in}{rRe} D^3H$	r^{-4}
(3) $\Gamma_\theta(r) = 0$	$\frac{in}{rRe} D^3G$	$-\frac{1}{Re} D^4H$	r^{-4}
(4) $-\frac{n}{\alpha r} \Gamma_x(r) + \Gamma_\theta(r) = 0$	$-\frac{4in}{r^2Re} D^2G$	$-\frac{1}{Re} D^4H$	r^{-4}

The formulation of the problem is simplified greatly by choosing two independent vorticity transport equations in the form,

$$\Gamma_r = 0 \quad (2-37)$$

and

$$-\frac{n}{ar} \Gamma_x + \Gamma_\theta = 0 \quad (2-38)$$

C. THE VORTICITY TRANSPORT MATRIX EQUATION

While the fourth order linear vector operations and the associated algebra becomes very lengthy and rather tedious, the investigator attempting to expand the final form of the linearized vorticity transport equation (2-31) should pay sufficient attention to these details. Recall that the curl operation on a vector in cylindrical coordinates takes the form,

$$\nabla \times \vec{W} = \begin{vmatrix} \frac{1}{r} \vec{e}_x & \frac{1}{r} \vec{e}_r & \vec{e}_\theta \\ \frac{\partial}{\partial x} & \frac{\partial}{\partial r} & \frac{\partial}{\partial \theta} \\ 0 & Ge^x & rHe^x \end{vmatrix} \quad (2-39)$$

After all the nabla (∇) operations are complete, the final equation will be in the form of a vector equation as defined in equation (2-32). The first vorticity transport equation consists of the coefficient represented by Γ_r and is set equal to zero. The second equation consists of

the previously defined linear combination of the coefficients represented by Γ_x and Γ_θ and is also set equal to zero. The two resulting simultaneous ordinary differential equations are then expanded and the coefficients of the derivatives regrouped so that equations (2-37) and (2-38) can be conveniently expressed in matrix format as follows,

$$\begin{aligned}
 & [M_4] \begin{Bmatrix} D^4 G \\ D^4 H \end{Bmatrix} + [M_3] \begin{Bmatrix} D^3 G \\ D^3 H \end{Bmatrix} + [M_2] \begin{Bmatrix} D^2 G \\ D^2 H \end{Bmatrix} + [M_1] \begin{Bmatrix} D G \\ D H \end{Bmatrix} \\
 & + [M_0] \begin{Bmatrix} G \\ H \end{Bmatrix} = \gamma \left([N_2] \begin{Bmatrix} D^2 G \\ D^2 H \end{Bmatrix} + [N_1] \begin{Bmatrix} D G \\ D H \end{Bmatrix} + [N_0] \begin{Bmatrix} G \\ H \end{Bmatrix} \right) \quad (2-40)
 \end{aligned}$$

As it turns out, the equations are a pair of coupled homogeneous differential equations that can be solved as an eigenvalue problem. This technique is discussed in the chapter on Numerical Methods.

The matrices which appear in equation (2-40) are 2 X 2 matrices and are summarized in detail in Appendix A. Equation (2-40) and the respective matrix elements contained in Appendix A are the generalized vorticity transport equations for all angular wave numbers n , at all axial wave numbers α , and all Reynolds numbers. As will be explained in detail in the chapter on Boundary Conditions, the generalized equations are transformed by appropriate changes of variable depending on the angular wave number. The changes of variables from the eigenfunctions $G(r)$ and $H(r)$ to the new eigenfunctions $P(r)$ and $Q(r)$, respectively, are determined by the original boundary conditions that must be satisfied, particularly at the pipe axis.

D. EQUATIONS FOR $n = 0$

For the case $n = 0$, equation (2-40) is greatly simplified in that the two equations uncouple and allow an independent investigation of either eigenfunction, $G(r)$ or $H(r)$. Miscellaneous trial calculations made earlier suggest that the solutions for $G(r)$ are probably stable for all values of α and Re . Therefore, only the solutions for $H(r)$ were investigated. It should also be noted that the examination of the axial perturbation velocity is of particular interest in this analysis and, in the case for $n = 0$, is not a function of $G(r)$. The change of variable required to satisfy the boundary conditions is,

$$H(r) = r Q(r) \quad (2-41)$$

Taking the derivatives of $H(r)$ yields,

$$\begin{aligned} DH &= r DQ + Q \\ D^2H &= r D^2Q + 2 DQ \\ D^3H &= r D^3Q + 3 D^2Q \\ D^4H &= r D^4Q + 4 D^3Q \end{aligned} \quad (2-42)$$

With the substitution of equations (2-41) and (2-42) into equation (2-40), the following expression is obtained,

$$M_4' D^4Q + M_3' D^3Q + M_2' D^2Q + M_1' DQ + M_0' Q = \gamma (N_2' D^2Q + N_1' DQ + N_0' Q) \quad (2-43)$$

The primed coefficients are actually the elements from row 2 and column 2 of the newly transformed coefficient matrices and are not enclosed in matrix brackets. However, in general, the new coefficient matrices $[M_i']$ and $[N_j']$, (where the indices $i = 0, 1, 2, 3, 4$ and $j = 0, 1, 2$), are formed after the change of variable is made and the terms are collected. The primed coefficients used to solve the transformed vorticity transport equation in terms of $Q(r)$ for $n = 0$ are defined in Appendix B, Part A.

E. EQUATIONS for $n = 1$

For the case $n = 1$, eigenfunctions $G(r)$ and $H(r)$ do not become uncoupled and must be solved for in a system of simultaneous equations in a form similar to equation (2-40). An additional parameter $H(0)$ is introduced into the equations by the change of variables. This particular change of variables is required because of the complicated nature of the boundary conditions at the axis and is thoroughly explained in the chapter on Boundary Conditions. For $n = 1$, the change of variables required to satisfy the boundary conditions are,

$$\begin{aligned} G(r) &= -i H(0) + r^2 P(r) \\ H(r) &= H(0) + r^2 Q(r) \end{aligned} \tag{2-44}$$

Taking the derivatives of $G(r)$ yields,

$$\begin{aligned} DG &= r^2 DP + 2r P \\ D^2G &= r^2 D^2P + 4r DP + 2 P \end{aligned} \tag{2-45}$$

and taking the derivatives of $H(r)$ yields,

$$\begin{aligned}
 DH &= r^2 DQ + 2r Q \\
 D^2H &= r^2 D^2Q + 4r DQ + 2 Q \\
 D^3H &= r^2 D^3Q + 6r D^2Q + 6 DQ \\
 D^4H &= r^2 D^4Q + 8r D^3Q + 12 D^2Q
 \end{aligned}
 \tag{2-46}$$

Remember that in general $D(H(0)) \neq DH(0)$, where $DH(0)$ is the value of the first derivative of $H(r)$ evaluated at the point $r = 0$. Since $D(H(0)) = 0$ here, it vanishes from the expressions for the derivatives of $G(r)$ and $H(r)$. In order to accommodate $H(0)$ in the system of equations where it appears explicitly, two additional 2×1 column matrices are required, namely $[M'_5]$ and $[N'_3]$. After the changes of variable have been made, equation (2-40) now becomes,

$$\begin{aligned}
 &[M'_4] \begin{Bmatrix} D^4P \\ D^4Q \end{Bmatrix} + [M'_3] \begin{Bmatrix} D^3P \\ D^3Q \end{Bmatrix} + [M'_2] \begin{Bmatrix} D^2P \\ D^2Q \end{Bmatrix} + [M'_1] \begin{Bmatrix} DP \\ DQ \end{Bmatrix} + [M'_0] \begin{Bmatrix} P \\ Q \end{Bmatrix} \\
 &+ [M'_5] \{H(0)\} = \gamma \left([N'_2] \begin{Bmatrix} D^2P \\ D^2Q \end{Bmatrix} + [N'_1] \begin{Bmatrix} DP \\ DQ \end{Bmatrix} + [N'_0] \begin{Bmatrix} P \\ Q \end{Bmatrix} + [N'_3] \{H(0)\} \right)
 \end{aligned}
 \tag{2-47}$$

The coefficient matrices of equation (2-47) used to solve the transformed vorticity transport equations in terms of $P(r)$ and $Q(r)$ for $n = 1$ are defined in Appendix B, Part B.

F. EQUATIONS FOR $n = 6$

For the case $n = 6$, eigenfunctions $G(r)$ and $H(r)$ remain coupled. The change of variables does not introduce any additional parameters and the system of simultaneous equations is solved in the form of equation (2-40) once again. The change of variables required to satisfy the boundary conditions for $n = 6$ and additionally for all angular wave numbers $n > 6$ are,

$$\begin{aligned} G(r) &= r^4 P(r) \\ H(r) &= r^3 Q(r) \end{aligned} \quad (2-48)$$

Taking the derivatives of $G(r)$ yields,

$$\begin{aligned} DG &= r^4 DP + 4r^3 P \\ D^2G &= r^4 D^2P + 8r^3 DP + 12r^2 P \end{aligned} \quad (2-29)$$

and taking the derivatives of $H(r)$ yields,

$$\begin{aligned} DH &= r^3 DQ + 3r^2 Q \\ D^2H &= r^3 D^2Q + 6r^2 DQ + 6r Q \\ D^3H &= r^3 D^3Q + 9r^2 D^2Q + 18r DQ + 6 Q \\ D^4H &= r^3 D^4Q + 12r^2 D^3Q + 36r D^2Q + 24 DQ \end{aligned} \quad (2-50)$$

Substituting equations (2-48), (2-49), and (2-50) into equation (2-40) results in the transformed coefficient matrices for the system of equations. The coefficient matrices of the functions $P(r)$ and $Q(r)$ and their respective derivatives for $n = 6$ are defined in Appendix B, Part C.

III. BOUNDARY CONDITIONS

The incorrect formulation of the boundary conditions for the linearized vorticity transport equations at the pipe axis has probably been the primary reason that previous investigators have failed to predict the onset of flow instabilities in circular pipes at any Reynolds number. Gawain [Ref. 13] suggested that if these boundary conditions are formulated in a rigorous and systematic fashion and applied to the vorticity transport equations, a correct numerical solution may be computed which agrees with experimental results. It can be seen from equations (2-40) and from the coefficient matrices of Appendix A that the two vorticity transport equations are coupled, except for the case $n = 0$. The resulting pair of differential equations are second order in $G(r)$ and fourth order in $H(r)$. In order to obtain a determinate solution of the equations, a total of six boundary conditions are required. More specifically, at least two of the boundary conditions must involve $G(r)$ or its derivatives and at least four of the boundary conditions must involve $H(r)$ or its derivatives. It might be expected that when the equations are coupled, the boundary conditions may also be coupled. That is to say that the boundary conditions may consist of various linear combinations of the functions and their derivatives, which turns out to be the case and is shown later.

The boundary conditions at the pipe wall are determined in a fairly straight forward manner. They are derived from the fact that the components of the perturbation velocity must vanish at the wall. From the definition of the perturbation velocity, defined previously as,

$$\vec{v} = \nabla \times \vec{W} \quad (2-27)$$

it can be shown that the following three boundary conditions result.

$$\begin{aligned} G(1) &= 0 \\ H(1) &= 0 \\ DH(1) &= 0 \end{aligned} \quad (3-1)$$

Since six boundary conditions are required and three have been determined at the pipe wall, there remain three boundary conditions to be determined at the pipe axis. Of these three conditions, at least one must involve $G(r)$ or its derivatives and at least two must involve $H(r)$ or its derivatives.

The proper derivation of the three boundary conditions at the axis turns out to be a non-trivial problem. As can be seen in Table 2-1, the highest negative power of r that appears in the equations is r^{-4} . Closer inspection of the vorticity transport equations of equation (2-40) and the coefficient matrices in Appendix A reveals that the equations contain terms in r^{-4} , r^{-3} , r^{-2} , r^{-1} , and r^0 . At first glance, it may appear that these equations are not satisfied in the limit as r approaches zero. It should be noted that it would be incorrect to multiply the equations through by any positive power of r since that would alter the degree of the singularity of the equations at the axis.

This problem can be resolved and subsequently the boundary conditions at the axis can be deduced rigorously by expanding the functions $G(r)$ and $H(r)$ as power series in r . The highest negative power of r is r^{-4} and appears in the coefficient matrix $[M_0]$ for the pair of functions $G(r)$ and $H(r)$. The series expansion for $G(r)$, and similarly for $H(r)$, is carried to the fourth derivative as follows,

$$G(r) = G(0) + DG(0)r + D^2G(0) \frac{r^2}{2!} + D^3G(0) \frac{r^3}{3!} + D^4G(0) \frac{r^4}{4!} + \dots \quad (3-2)$$

It can be seen that when the series expansion expressions for $G(r)$ and $H(r)$ are substituted into equation (2-40), the higher order terms of equation (3-2) that contain powers of r greater than four will vanish in the limit as r approaches zero. For the first derivatives of $G(r)$ and $H(r)$, the highest negative power of r that appears in the coefficient matrix $[M_1]$ is r^{-3} . Therefore, the series expansion for the first derivative of $G(r)$, and similarly for $H(r)$, up to the fourth derivative term is,

$$DG(r) = 0 + DG(0) + D^2G(0)r + D^3G(0) \frac{r^2}{2!} + D^4G(0) \frac{r^3}{3!} + \dots \quad (3-3)$$

The remaining derivatives of the functions are expanded in a similar manner through the fourth derivative term. The resulting power series approximations for $G(r)$ and $H(r)$ and their derivatives are then substituted into equation (2-40). The coefficients are then regrouped in ascending powers of r .

As mentioned previously, the equations must be satisfied in the limit as r approaches zero. Therefore, the coefficients of the functions that contain r^{-4} , r^{-3} , r^{-2} , r^{-1} , and r^0 must all be zero. The remaining coefficients will contain positive powers of r and will vanish in the limit as r approaches zero. By considering only the terms containing negative powers of r and setting those coefficients equal to zero, five pair of equations in ten unknowns remain so that the boundary conditions can be determined. The unknowns are the functions of $G(r)$ and $H(r)$ and their first four derivatives evaluated at the pipe axis, $r = 0$. It is convenient to summarize these equations in matrix format below,

$$\frac{(n^2-1)}{\text{Re}} [C_1] \begin{Bmatrix} G(0) \\ H(0) \end{Bmatrix} = \begin{Bmatrix} 0 \\ 0 \end{Bmatrix} \quad (3-4)$$

$$\frac{n^2}{\text{Re}} [C_2] \begin{Bmatrix} DG(0) \\ DH(0) \end{Bmatrix} = \begin{Bmatrix} 0 \\ 0 \end{Bmatrix} \quad (3-5)$$

$$\frac{(n^2-1)}{\text{Re}} [C_3] \begin{Bmatrix} D^2G(0) \\ D^2H(0) \end{Bmatrix} = \begin{Bmatrix} 0 \\ 0 \end{Bmatrix} + (i\alpha[C_4] - \gamma [D_4]) \begin{Bmatrix} G(0) \\ H(0) \end{Bmatrix} = \begin{Bmatrix} 0 \\ 0 \end{Bmatrix} \quad (3-6)$$

$$\frac{n(n^2-4)}{\text{Re}} [C_5] \begin{Bmatrix} D^3G(0) \\ D^3H(0) \end{Bmatrix} + n \left(2i\alpha \left(1 - \frac{i\alpha}{\text{Re}} \right) + \gamma \right) [C_6] \begin{Bmatrix} DG(0) \\ DH(0) \end{Bmatrix} = \begin{Bmatrix} 0 \\ 0 \end{Bmatrix} \quad (3-7)$$

$$\begin{aligned}
& \frac{(n^2-9)}{Re} [C_7] \begin{Bmatrix} D^4 G(0) \\ D^4 H(0) \end{Bmatrix} + (i\alpha [C_8] - \gamma [D_8]) \begin{Bmatrix} D^2 G(0) \\ D^2 H(0) \end{Bmatrix} \\
& + (i\alpha [C_9] - \gamma\alpha^2 [D_9]) \begin{Bmatrix} G(0) \\ H(0) \end{Bmatrix} = \begin{Bmatrix} 0 \\ 0 \end{Bmatrix} \quad (3-8)
\end{aligned}$$

The 2 X 2 matrices which appear in equations (3-4) through (3-8) are defined in detail in Appendix C. Special conditions at the axis arise when the determinants of these matrices are evaluated at specific angular wave numbers. They are summarized in Appendix D.

For each specific value of angular wave number n , it is possible to derive a set of boundary conditions at the axis. Special conditions at the axis occur for angular wave numbers that cause the coefficients in equations (3-4) through (3-8) to equal zero or the determinants in Appendix D to be zero. That is to say, if a coefficient vanishes or the pair of equations are linearly dependent, the functions may be arbitrarily specified and are in general not equal to zero. But if the coefficient, appearing in equations (3-4) through (3-8) is non-zero and the determinant exists, the pair of functions must be identically zero. This situation occurs for all five pairs of variables when the angular wave number $n \geq 6$.

By taking these special conditions into account for the case $n = 0$, it can be deduced from equations (3-6) and (3-8) that,

$$\begin{Bmatrix} G(0) \\ H(0) \end{Bmatrix} = \begin{Bmatrix} D^2 G(0) \\ D^2 H(0) \end{Bmatrix} = \begin{Bmatrix} 0 \\ 0 \end{Bmatrix} \quad (3-9)$$

Carrying out this procedure for $n = 1, 2, 3, 4, 5$, and 6 yields a simplified set of boundary conditions at the axis. The following sets of equations (3-10) through (3-16) are essentially the same as those of Gawain [Ref. 13] but were independently checked and appear here with a few minor corrections.

$n = 0$

$$\begin{array}{lll} G(0) = 0 & H(0) = 0 & (a) \\ \hline & & (3-10) \end{array}$$

$$\begin{array}{lll} D^2G(0) = 0 & D^2H(0) = 0 & (b) \\ \hline \end{array}$$

$n = 1$

$$\begin{array}{lll} G(0) + i H(0) = 0 & & (a) \\ \hline \end{array}$$

$$\begin{array}{lll} DG(0) = 0 & DH(0) = 0 & \\ \hline \end{array}$$

$$\begin{array}{lll} D^3G(0) = 0 & D^3H(0) = 0 & (3-11) \\ \hline \end{array}$$

$$- \frac{8}{Re} [C_7] \begin{Bmatrix} D^4G(0) \\ D^4H(0) \end{Bmatrix} + (i\alpha [C_8] - \gamma [D_8]) \begin{Bmatrix} D^2G(0) \\ D^2H(0) \end{Bmatrix} \quad (b)$$

$$+ (i\alpha [C_9] - \gamma \alpha^2 [D_9]) \begin{Bmatrix} G(0) \\ H(0) \end{Bmatrix} = \begin{Bmatrix} 0 \\ 0 \end{Bmatrix}$$

$n = 2$

$$\begin{array}{lll} G(0) = 0 & H(0) = 0 & (a) \\ \hline \end{array}$$

$$\begin{array}{lll} DG(0) + i DH(0) = 0 & & (3-12) \\ \hline \end{array}$$

$$\begin{array}{lll} D^2G(0) = 0 & D^2H(0) = 0 & (b) \\ \hline \end{array}$$

$$\begin{array}{lll} D^4G(0) = 0 & D^4H(0) = 0 & \\ \hline \end{array}$$

$n = 3$

$$G(0) = 0$$

$$H(0) = 0$$

$$DG(0) = 0$$

$$DH(0) = 0$$

(a)

$$D^2G(0) + i D^2H(0) = 0$$

$$D^3G(0) = 0$$

$$D^3H(0) = 0$$

(b)

(3-13)

$n = 4$

$$G(0) = 0$$

$$H(0) = 0$$

$$DG(0) = 0$$

$$DH(0) = 0$$

(a)

$$D^2G(0) = 0$$

$$D^2H(0) = 0$$

$$D^3G(0) + i D^3H(0) = 0$$

$$D^4G(0) = 0$$

$$D^4H(0) = 0$$

(b)

(3-14)

$n = 5$

$$G(0) = 0$$

$$H(0) = 0$$

$$DG(0) = 0$$

$$DH(0) = 0$$

(a)

$$D^2G(0) = 0$$

$$D^2H(0) = 0$$

$$D^4G(0) + i D^4H(0) = 0$$

$$D^3G(0) = 0$$

$$D^3H(0) = 0$$

(b)

(3-15)

$n \geq 6$

$$G(0) = 0$$

$$DG(0) = 0$$

$$D^2G(0) = 0$$

$$D^3G(0) = 0$$

$$D^4G(0) = 0$$

$$H(0) = 0$$

$$DH(0) = 0$$

$$D^2H(0) = 0$$

$$D^3H(0) = 0$$

$$D^4H(0) = 0$$

(a)

(b)

(3-16)

Recall that exactly three boundary conditions are required at the axis to finalize the solution of the vorticity transport equations. Equations (3-10) through (3-16) contain from four to ten boundary constraints including linear combinations of several boundary conditions, as suggested earlier. By introducing appropriate changes of variables, the pair of functions in $G(r)$ and $H(r)$ and their respective derivatives can be transformed to a new pair of functions in terms of $P(r)$ and $Q(r)$ and their derivatives. The transformed system of equations take the form of equation (2-40) for all values of n , except for $n = 1$ where equation (2-47) is applicable. The change of variables is dependent on each specific value of n up through six and is chosen in such a way that the boundary conditions in subset (a) of equation (3-10) through (3-16) are satisfied identically. The boundary conditions in subset (b) must be satisfied explicitly in the finite difference equations near the axis. Development of the finite difference equations is discussed in the chapter on Numerical Methods.

The following sets of equations are taken from Gawain [Ref. 13] and are included here so that a complete treatment of the subject on boundary conditions is contained in this paper.

n = 0

Change of Variables

$$\begin{aligned} G(r) &= rP(r) \\ H(r) &= rQ(r) \end{aligned} \quad (a)$$

Boundary Conditions at Axis (3-17)

$$\begin{aligned} DP(0) &= 0 & DQ(0) &= 0 \\ & & D^3Q(0) &= 0 \end{aligned} \quad (b)$$

Boundary Conditions at Wall

$$\begin{aligned} P(1) &= 0 & Q(1) &= 0 \\ & & DQ(1) &= 0 \end{aligned} \quad (c)$$

The solutions for $P(r)$ and $Q(r)$ become uncoupled for $n = 0$

n = 1

Change of Variables

$$\begin{aligned} G(r) &= -i H(0) + r^2 P(r) \\ H(r) &= H(0) + r^2 Q(r) \end{aligned} \quad (a)$$

Boundary Conditions at Axis (3-18)

$$DP(0) = 0 \quad DQ(0) = 0$$

$$- \frac{96}{Re} [C_7] \begin{Bmatrix} D^2P(0) \\ D^2Q(0) \end{Bmatrix} + 2i\alpha[C_8] \begin{Bmatrix} P(0) \\ Q(0) \end{Bmatrix} + i\alpha[C_9] \begin{Bmatrix} -i \\ 1 \end{Bmatrix} H(0)$$

$$= + \gamma \left(2[D_8] \begin{Bmatrix} P(0) \\ Q(0) \end{Bmatrix} + \alpha^2 [D_9] \begin{Bmatrix} -i \\ 1 \end{Bmatrix} H(0) \right) \quad (b)$$

Boundary Conditions at Wall

$$\begin{aligned} -i H(0) + P(1) &= 0 & H(0) + Q(1) &= 0 \\ & & -2H(0) + DQ(1) &= 0 \end{aligned} \quad (c)$$

$n = 2$

Change of Variables

$$G(r) = -i r DH(0) + r^2 P(r) \quad (a)$$

$$H(r) = r DH(0) + r^2 Q(r)$$

Boundary Conditions at Axis (3-19)

$$P(0) = 0 \quad Q(0) = 0 \quad (b)$$

$$D^2P(0) = 0 \quad D^2Q(0) = 0$$

Boundary Conditions at Wall

$$\begin{aligned} -i DH(0) + P(1) &= 0 & DH(0) + Q(1) &= 0 \\ & & -DH(0) + DQ(1) &= 0 \end{aligned} \quad (c)$$

$n = 3$

Change of Variables

$$G(r) = r^2 P(r) \quad (a)$$

$$H(r) = r^2 Q(r)$$

Boundary Conditions at Axis (3-20)

$$P(0) + i Q(0) = 0 \quad (b)$$

$$DP(0) = 0 \quad DQ(0) = 0$$

Boundary Conditions at Wall

$$\begin{aligned} P(1) &= 0 & Q(1) &= 0 \\ & & DQ(1) &= 0 \end{aligned} \quad (c)$$

$$n = 4$$

Change of Variables

$$G(r) = r^3 P(r) \quad (a)$$

$$H(r) = r^3 Q(r)$$

Boundary Conditions at Axis (3-21)

$$P(0) + i Q(0) = 0 \quad (b)$$

$$DP(0) = 0 \quad DQ(0) = 0$$

Boundary Conditions at Wall

$$\begin{aligned} P(1) = 0 \quad Q(1) = 0 \\ DQ(1) = 0 \end{aligned} \quad (c)$$

$$n = 5$$

Change of Variables

$$G(r) = r^3 P(r) \quad (a)$$

$$H(r) = r^3 Q(r)$$

Boundary Conditions at Axis (3-22)

$$P(0) = 0 \quad Q(0) = 0 \quad (b)$$

$$DP(0) + i DQ(0) = 0$$

Boundary Conditions at Wall

$$\begin{aligned} P(1) = 0 \quad Q(1) = 0 \\ DQ(1) = 0 \end{aligned} \quad (c)$$

$$n \geq 6$$

Change of Variables

$$G(r) = r^4 P(r) \tag{a}$$

$$H(r) = r^3 Q(r)$$

Boundary Conditions at Axis (3-23)

$$P(0) = 0 \qquad Q(0) = 0 \tag{b}$$

$$DQ(0) = 0$$

Boundary Conditions at Wall

$$P(1) = 0 \qquad Q(1) = 0 \tag{c}$$

$$DQ(1) = 0$$

It should be noted that the change of variable relations in subset (a) of equations (3-17) through (3-23) does not change the order of the derivatives appearing in the transformed vorticity transport equations. Upon close examination of subsets (b) and (c) of these equations, it is apparent that the correct number of boundary conditions required for the solution of the transformed equations has resulted from the change of variables. The vorticity transport equations are now expressed in terms of $P(r)$ and $Q(r)$ and their derivatives and have exactly three boundary conditions at the pipe wall for all values of n and three boundary conditions at the axis for all values of n , except for $n = 1$ and 2 . The fact that there are four boundary conditions at the axis for angular wave numbers $n = 1$ and 2 warrants further comment here.

Notice in equations (3-18a) and (3-19a) for the cases $n = 1$ and 2 that an additional parameter is introduced by the change of variable equations. The additional parameter for $n = 1$ is $H(0)$ and for $n = 2$ is $DH(0)$. The introduction of the parameter for each case requires the specification of four boundary conditions at the axis instead of the usual three. This conclusion was reached by Gawain [Ref. 13] and is analyzed in detail in his paper. There is one other peculiarity about the boundary conditions at the axis for $n = 1$ that should be mentioned. The axis boundary conditions in equation (3-18b) contain a pair of equations that involve the complex perturbation frequency γ , which represents an eigenvalue of the solution for the equations. The presence of γ in the axis boundary condition for $n = 1$ is an important factor in formulating a solution for the vorticity transport equations and is included in the eigensystem of the finite difference equations. The details of the implementation are discussed later.

The solution of the problem for predicting the onset of flow instabilities in circular pipes is now at hand. The original vorticity transport equations (2-40) are transformed to the functions $P(r)$ and $Q(r)$ and their respective derivatives by the appropriate change of variables depending on the specific angular wave number being investigated. After imposing the rigorously deduced boundary conditions, a solution can be determined in the perturbation quantities.

IV. PERTURBATION VELOCITY

The solution of the transformed vorticity transport equations developed in the previous chapter can now be expressed in terms of the perturbation quantities $P(r)$ and $Q(r)$. The original functions $G(r)$ and $H(r)$ are actually components of the vector potential function \vec{W} defined in equation (2-28),

$$\vec{W} = [F(r) \vec{e}_x + G(r) \vec{e}_r + H(r) \vec{e}_\theta] e^x \quad (2-28)$$

The axial component $F(r)$ was previously set to zero since one function could be arbitrarily specified. From equation (2-27) the perturbation velocity vector was expressed as,

$$\vec{v} = \nabla \times \vec{W} \quad (2-27)$$

Therefore the functions $G(r)$ and $H(r)$ represent the behavior of the perturbation velocity in the flow field. Referring back to the definition of the curl operation in equation (2-39), the relation for $\nabla \times \vec{W}$ has already been set up. The resulting expression for the perturbation velocity is given by,

$$\vec{v} = u \vec{e}_x + v \vec{e}_r + w \vec{e}_\theta \quad (4-1)$$

The components of the perturbation velocity are,

$$u = DH(r) + \frac{H(r)}{r} - \frac{in}{r} G(r) \quad (4-2)$$

$$v = -ia H(r) \quad (4-3)$$

$$w = ia G(r) \quad (4-4)$$

Digressing for a moment, it can be readily seen that since the perturbation velocity necessarily vanishes at the pipe wall, $r = 1$, the boundary conditions at the wall in equation (3-1) can be deduced.

Recall that the functions $P(r)$ and $Q(r)$ appear as the result of the change of variables for each specific angular wave number contained in subset (a) of equations (3-17) through (3-23). Analysis of the axial component of the perturbation velocity u becomes useful in interpreting the behavior of the functions $P(r)$ and $Q(r)$ along the radius of the pipe. Equations for the axial perturbation velocity in terms of $P(r)$ and $Q(r)$ are derived from equations (4-2) through (4-4) with the change of variable applied for each angular wave number being investigated and appear as follows,

$$n = 0 : u = 2 Q + r DQ \quad (4-5)$$

$$n = 1 : u = 3 r Q + r^2 DQ - i r P \quad (4-6)$$

$$n = 6 : u = 4 r^2 Q + r^3 DQ - i 6 r^3 P \quad (4-7)$$

The axial perturbation velocity is computed in part VII of the main investigative program for each angular wave number. To prepare the perturbation velocity u for plotting versus pipe radius, it is first

normalized. Since this velocity is in general a complex quantity, the perturbation velocity with the largest magnitude is determined by,

$$|u_c|_{\text{MAX}} = (u_R^2 + u_I^2)^{\frac{1}{2}} \quad (4-8)$$

The normalizing velocity constant will then become u_c and the maximum normalized velocity will become,

$$\frac{u}{u_c} = 1 + i(0) \quad (4-9)$$

The remaining normalized velocities are found by dividing through by u_c . The normalized perturbation velocity is then plotted versus the normalized pipe radius for various axial wave numbers and Reynolds numbers at the three angular wave numbers investigated. The plots and results are discussed in detail in the chapter on Results.

V. NUMERICAL METHODS

A. GENERAL METHODS USED

In general, the vorticity transport equations are a pair of coupled homogeneous differential equations which are second order in the perturbation quantity $G(r)$ and fourth order in the perturbation quantity $H(r)$. A change of variables is introduced so that the number of boundary conditions at the axis is reduced to three for each angular wave number investigated, except for $n = 1$. Recall for this case that there are four boundary conditions imposed at the axis because of the introduction of the additional parameter $H(0)$. By applying the change of variables to the original pair of equations, the vorticity transport equations are transformed into an equivalent pair of coupled homogeneous differential equations that are second order in $P(r)$ and fourth order in $Q(r)$. The solution of the vorticity transport equations will now be in terms of the perturbation quantities $P(r)$ and $Q(r)$ which are also referred to as eigenfunctions, and γ which is an eigenvalue. The axial perturbation velocity is expressed in terms of $P(r)$ and $Q(r)$ as derived previously and is examined to determine the behavior of the perturbation quantities. The resulting eigenvalue γ is of primary interest since the magnitude and sign of the real part of γ determines the relative stability or instability of the pipe flow problem.

A numerical solution of the transformed vorticity transport equations is now sought. The convenient matrix format of the equations is given below.

$$\begin{aligned}
& [M_4] \begin{Bmatrix} D^4 P \\ D^4 Q \end{Bmatrix} + [M_3] \begin{Bmatrix} D^3 P \\ D^3 Q \end{Bmatrix} + [M_2] \begin{Bmatrix} D^2 P \\ D^2 Q \end{Bmatrix} + [M_1] \begin{Bmatrix} DP \\ DQ \end{Bmatrix} + [M_0] \begin{Bmatrix} P \\ Q \end{Bmatrix} = \\
& \gamma [N_2] \begin{Bmatrix} D^2 P \\ D^2 Q \end{Bmatrix} + [N_1] \begin{Bmatrix} DP \\ DQ \end{Bmatrix} + [N_0] \begin{Bmatrix} P \\ Q \end{Bmatrix}
\end{aligned} \tag{5-1}$$

The details of the transformed coefficient matrices for $n = 0, 1$, and 6 are given in Appendix B. It is convenient to approximate the derivatives of $P(r)$ and $Q(r)$ by a finite number of discrete unknowns along a radial mesh consisting of N interior points. It is not possible to compute the continuous values of the functions and their derivatives along the pipe radius using a digital computer. Therefore, discrete finite difference techniques are used. For the problem at hand, the normalized nondimensional radius of the pipe, which becomes the independent variable, is divided into a computational mesh. The standard method of representing this mesh is with uniformly spaced stations over the interval $0 < r < 1$, Figure 5-1.

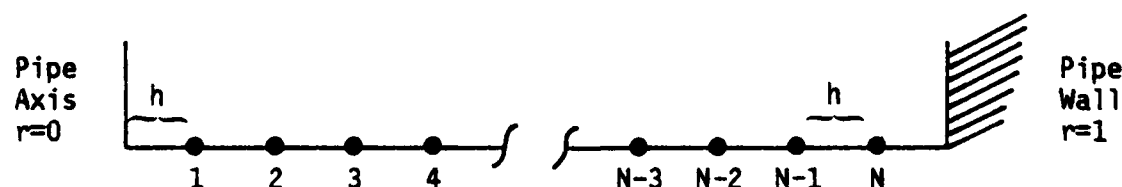


Figure 5-1. Radial Mesh, Standard Method

The vorticity transport equation coefficients are then evaluated at each station of the radial mesh resulting in N uniformly spaced discrete values with $N + 1$ equal intervals and $N + 2$ total points, including $r = 0$ and $r = 1$. The spacing between the stations is denoted by $h = 1/(N + 1)$.

A refinement of the method for generating a computational mesh is referred to as the half station method and is used in this numerical analysis. All the radial stations of Figure 5-1 are moved to mid-interval or one half station ($h/2$) toward the axis with an additional station appearing at one half station from the pipe wall, as shown in Figure 5-2.

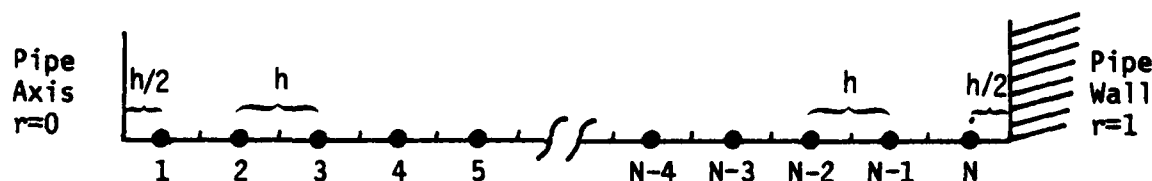


Figure 5-2. Radial Mesh, Half Station Method

Therefore for N interior stations, the method results in N intervals and $N + 2$ total points including the boundaries. The first station, r_1 , is a distance $h/2$ from the axis and the N th station, r_N , is a distance $h/2$ from the wall. The general expression for the i th station, corresponding to the i th increment of the radius, is given by,

$$r_i = h \left(i - \frac{1}{2} \right) ; i = 1, 2, 3, \dots, N \quad (5-2)$$

where $h = 1/N$.

An advantage of the half station method over the standard method is that there is better resolution at the stations near the boundaries where instabilities are thought to originate and where boundary layer effects are a factor. Therefore, the behavior of the perturbation quantities can be examined more closely. Additionally, better approximations for the derivatives of the functions $P(r)$ and $Q(r)$ can be realized with a smaller incremental distance to the points immediately adjacent to the boundaries. Even better resolution at the boundaries can be achieved by using a nonuniform computational mesh. Arnold [Ref. 11] introduced a change of independent variable by means of hyperbolic functions which included a mesh offset parameter so that he could control the concentration of mesh points at either the axis or wall. The method would certainly be useful in reducing computational time by reducing the total number of mesh points required for a satisfactory solution of the governing equations. However, the full implications of the nonuniform mesh with respect to α and γ dependence on the mesh offset parameter have not been fully explored. While this method is not used here, it may well prove to be useful in follow-on numerical investigations of the pipe flow problem.

The solution for the vorticity transport equations in terms of the perturbation quantities $P(r)$ and $Q(r)$ are now represented by a finite number of discrete unknowns. The governing differential equations are rewritten in finite difference form for N stations along the mesh resulting in a finite number of unknowns namely, $P_1, P_2, P_3, \dots, P_N$ and $Q_1, Q_2, Q_3, \dots, Q_N$. In general, this produces $2N$ simultaneous equations in $2N$

unknowns. The details of the derivation of the finite difference equations are explained shortly. Substituting the finite difference equations into the vorticity transport equation matrix format of equation (5-1) will result in N pairs of coupled simultaneous equations. These equations are regrouped and subsequently solved in the following eigenvalue problem format,

$$[A] \{X\} = \gamma [B] \{X\} \quad (5-3)$$

The column vector $\{X\}$ represents the rearranged unknowns as

$$\{X\} = \begin{Bmatrix} P_1 \\ P_2 \\ \vdots \\ P_i \\ \vdots \\ P_N \\ Q_1 \\ Q_2 \\ \vdots \\ Q_i \\ \vdots \\ Q_N \end{Bmatrix} \quad (5-4)$$

The symbol γ denotes the characteristic value or eigenvalue of the solution. Details of the composition of the $[A]$ and $[B]$ matrices are discussed for each specific angular wave number investigated.

B. FINITE DIFFERENCE EQUATIONS

The use of finite differencing techniques is the basis for solving the governing vorticity transport equations in the eigensystem equation (5-3). It is required that the governing equations must be satisfied at each of the interior stations $i = 1, 2, 3, \dots, N$, therefore producing $2N$ equations in $2N$ unknowns.

Except for stations adjacent to the boundaries, the derivatives of the perturbation quantities in the governing equations at the interior stations are usually approximated by standard central finite difference equations. These equations were taken from Table 7.27 of Ketter and Prawel [Ref. 14] and are summarized below,

$$DF_i = \frac{1}{12h} \left\{ F_{i-2} - 8F_{i-1} + 8F_{i+1} - F_{i+2} \right\} + \frac{1}{30} h^4 D^5 F_i \quad (5-5)$$

$$D^2 F_i = \frac{1}{12h^2} \left\{ -F_{i-2} + 16F_{i-1} - 30F_i + 16F_{i+1} - F_{i+2} \right\} + \frac{1}{90} h^4 D^6 F_i \quad (5-6)$$

$$D^3 F_i = \frac{1}{8h^3} \left\{ F_{i-3} - 8F_{i-2} + 13F_{i-1} - 13F_{i+1} + 8F_{i+2} - F_{i+3} \right\} + \frac{7}{120} h^4 D^7 F_i \quad (5-7)$$

$$D^4 F_i = \frac{1}{6h^4} \left\{ -F_{i-3} + 12F_{i-2} - 39F_{i-1} + 56F_i - 39F_{i+1} + 12F_{i+2} - F_{i+3} \right\} + \frac{7}{240} h^4 D^8 F_i \quad (5-8)$$

where F is an arbitrary function.

As can be seen from the equations above, the derivative of a function at a particular station can be approximated by a linear combination of the discrete unknown functions about a central point. The term outside the brackets in each equation represents the truncation error of the corresponding finite difference approximation. Notice that the truncation error of equations (5-5) through (5-8) are all of order h^4 ($O(h^4)$). It was hypothesized and shown by Gawain and Ball [Ref. 15] that finite difference approximations of consistent order truncation error reduced the overall error of the numerical solution in a typical problem by a factor of five for truncation error $O(h^2)$. For the present numerical analysis, a computational mesh of $N = 50$ was used for all cases. Now with the interval $h = 1/N = 0.02$, examination of the consistent fourth order truncation error term will yield an error of the order of 5×10^{-9} for all four derivatives approximated, since the magnitude of the normalized functions and derivatives are of order one. For an interval size of $h = 0.02$, a consistent truncation error $O(h^4)$ should significantly reduce the overall error of the solution.

Special problems arise in the derivation of the finite difference equations at stations near the boundaries. Several approaches can be taken to approximate the derivatives at these stations, which include backward, forward and central finite differencing techniques. Unfortunately, the central method previously discussed will involve imaginary stations outside the boundaries for stations close to the axis and wall, i.e., stations $i = -1, -2, -3$, and $N+1, N+2, N+3$ are involved in the fourth derivative approximation at station $i = 1$ and $i = N$, respectively. Unlike the boundary conditions for many problems well suited for this

type of numerical analysis, the vorticity transport equation boundary conditions for the pipe flow problem are very complicated by comparison. The boundary conditions for each angular wave number are different; some involve additional parameters while others contain the eigenvalue γ . In other words, the conditions at the imaginary stations for conventional problems can normally be expressed in terms of conditions at the real stations in the computational mesh. It is therefore impractical to use the central method for the pipe flow problem because of the complicated nature of the boundary conditions.

The method of forward differencing is used near the pipe axis and backward differencing is used near the wall. These two differencing methods will be referred to, collectively, as noncentral finite differencing techniques. It will be shown later that the two methods are essentially equivalent. A rigorous derivation of the noncentral finite difference equations is based on the Taylor series (power series) expansion of the function at a point. Since the governing equations contain the fourth order derivative of $Q(r)$, the derivation for this case is examined in detail here.

The Taylor series approximation of $Q_i(r)$ at station $i = 1$ appears as equation (5-9).

$$\begin{aligned}
 Q_1 = Q(0) + DQ(0) \frac{h}{2} + D^2Q(0) \frac{\left(\frac{h}{2}\right)^2}{2!} + D^3Q(0) \frac{\left(\frac{h}{2}\right)^3}{3!} + D^4Q(0) \frac{\left(\frac{h}{2}\right)^4}{4!} \\
 + D^5Q(0) \frac{\left(\frac{h}{2}\right)^5}{5!} + D^6Q(0) \frac{\left(\frac{h}{2}\right)^6}{6!} + D^7Q(0) \frac{\left(\frac{h}{2}\right)^7}{7!} + \dots \quad (5-9)
 \end{aligned}$$

The approximation for Q_i at stations $i = 1, 2, 3, 4, 5, 6$ are expressed in convenient matrix format below,

$$\begin{pmatrix} Q_1 \\ Q_2 \\ Q_3 \\ Q_4 \\ Q_5 \\ Q_6 \end{pmatrix} = \begin{bmatrix} 1 & \frac{1}{2} & \frac{(\frac{1}{2})^2}{2!} & \frac{(\frac{1}{2})^3}{3!} & \frac{(\frac{1}{2})^4}{4!} & \frac{(\frac{1}{2})^5}{5!} & \frac{(\frac{1}{2})^6}{6!} & \frac{(\frac{1}{2})^7}{7!} \\ 1 & \frac{3}{2} & \frac{(\frac{3}{2})^2}{2!} & \frac{(\frac{3}{2})^3}{3!} & \frac{(\frac{3}{2})^4}{4!} & \frac{(\frac{3}{2})^5}{5!} & \cdot & \cdot \\ 1 & \frac{5}{2} & \frac{(\frac{5}{2})^2}{2!} & \cdot & \cdot & \cdot & \cdot & \cdot \\ 1 & \frac{7}{2} & \frac{(\frac{7}{2})^2}{2!} & \cdot & \cdot & \cdot & \cdot & \cdot \\ 1 & \frac{9}{2} & \frac{(\frac{9}{2})^2}{2!} & \cdot & \cdot & \cdot & \cdot & \cdot \\ 1 & \frac{11}{2} & \frac{(\frac{11}{2})^2}{2!} & \cdot & \cdot & \cdot & \cdot & \cdot \end{bmatrix}$$

6×8

$$\begin{pmatrix} Q(0) \\ hDQ(0) \\ h^2D^2Q(0) \\ h^3D^3Q(0) \\ h^4D^4Q(0) \\ h^5D^5Q(0) \\ h^6D^6Q(0) \\ h^7D^7Q(0) \end{pmatrix} + \{E_1\} h^8D^8Q(0) \quad (5-10)$$

where the dots represent matrix elements that can be easily deduced.

Since the fourth order derivative of $Q(r)$ is present in the vorticity transport equations, there will be two boundary conditions specified at the axis and two at the wall. It can be shown that two columns of the matrix in equation (5-10) can be eliminated since two of the functions in the column vector are either zero or can be expressed in terms of additional parameters. The matrix, which will be denoted as $[AA]$, now becomes a square 6×6 matrix. Notice that the column vector $\{E_1\}$ represents the last nonvanishing term in the Taylor series. The approximation for the first derivative of $Q_i(r)$ at station $i = 1$ is given by,

$$\begin{aligned} DQ_1 = & DQ(0) + D^2Q(0) \frac{h}{2} + D^3Q(0) \frac{\left(\frac{h}{2}\right)^2}{2!} + D^4Q(0) \frac{\left(\frac{h}{2}\right)^3}{3!} + D^5Q(0) \frac{\left(\frac{h}{2}\right)^4}{4!} \\ & + D^6Q(0) \frac{\left(\frac{h}{2}\right)^5}{5!} + D^7Q(0) \frac{\left(\frac{h}{2}\right)^6}{6!} + \dots \end{aligned} \quad (5-11)$$

The Taylor series expansion for the second, third, and fourth derivative can be found by successive differentiation of equation (5-11). The first four derivatives of Q_i at station $i = 1$ can be expressed in matrix format as,

$$\begin{Bmatrix} hDQ_1 \\ h^2D^2Q_1 \\ h^3D^3Q_1 \\ h^4D^4Q_1 \end{Bmatrix} = \begin{bmatrix} 0 & 1 & (\frac{1}{2}) & \frac{(\frac{1}{2})^2}{2!} & \frac{(\frac{1}{2})^3}{3!} & \frac{(\frac{1}{2})^4}{4!} & \frac{(\frac{1}{2})^5}{5!} & \frac{(\frac{1}{2})^6}{6!} \\ 0 & 0 & 1 & (\frac{1}{2}) & \frac{(\frac{1}{2})^2}{2!} & \frac{(\frac{1}{2})^3}{3!} & \frac{(\frac{1}{2})^4}{4!} & \frac{(\frac{1}{2})^5}{5!} \\ 0 & 0 & 0 & 1 & (\frac{1}{2}) & \frac{(\frac{1}{2})^2}{2!} & \frac{(\frac{1}{2})^3}{3!} & \frac{(\frac{1}{2})^4}{4!} \\ 0 & 0 & 0 & 0 & 1 & (\frac{1}{2}) & \frac{(\frac{1}{2})^2}{2!} & \frac{(\frac{1}{2})^3}{3!} \end{bmatrix}$$

4×8

$$\begin{Bmatrix} Q(0) \\ hDQ(0) \\ h^2D^2Q(0) \\ h^3D^3Q(0) \\ h^4D^4Q(0) \\ h^5D^5Q(0) \\ h^6D^6Q(0) \\ h^7D^7Q(0) \end{Bmatrix} + \{E_2\} h^8D^8Q(0) \quad (5-12)$$

It can be shown here as well that two columns of the matrix in equation (5-12) can be eliminated so that the matrix denoted [CC] is now a 4 X 6 matrix. The column vector $\{E_2\}$ also represents the last non-vanishing term in the Taylor series. It can be seen that the approximations for the derivatives of Q_i at stations $i = 2$ and $i = 3$ can be determined by replacing $(1/2)$ in the [CC] matrix with $(3/2)$ and $(5/2)$, respectively.

To show how the noncentral finite difference approximations near the axis are formulated, the case for angular wave number $n \geq 6$ is examined. The boundary conditions at the axis for the function Q are,

$$Q(0) = 0 \quad \text{and} \quad DQ(0) = 0 \quad (5-13)$$

Applying these conditions to equations (5-10) and (5-12) will eliminate the first two columns of the $[AA]$ and $[CC]$ matrices since the first two terms of the column vectors vanish. The truncation error terms $\{E_1\}$ and $\{E_2\}$ are very small quantities and are neglected at this point. In shorthand notation, equation (5-10) now becomes,

$$\begin{Bmatrix} Q_1 \\ Q_2 \\ Q_3 \\ Q_4 \\ Q_5 \\ Q_6 \end{Bmatrix} = [AA]_{6 \times 6} \begin{Bmatrix} h^2 D^2 Q(0) \\ h^3 D^3 Q(0) \\ h^4 D^4 Q(0) \\ h^5 D^5 Q(0) \\ h^6 D^6 Q(0) \\ h^7 D^7 Q(0) \end{Bmatrix} \quad (5-14)$$

and equation (5-12) becomes,

$$\begin{Bmatrix} h D Q_1 \\ h^2 D^2 Q_1 \\ h^3 D^3 Q_1 \\ h^4 D^4 Q_1 \end{Bmatrix} = [CC]_{4 \times 6} \begin{Bmatrix} h^2 D^2 Q(0) \\ h^3 D^3 Q(0) \\ h^4 D^4 Q(0) \\ h^5 D^5 Q(0) \\ h^6 D^6 Q(0) \\ h^7 D^7 Q(0) \end{Bmatrix} \quad (5-15)$$

Equation (5-14) is multiplied through $[AA]^{-1}$ and becomes,

$$\begin{Bmatrix} h^2 D^2 Q(0) \\ h^3 D^3 Q(0) \\ h^4 D^4 Q(0) \\ h^5 D^5 Q(0) \\ h^6 D^6 Q(0) \\ h^7 D^7 Q(0) \end{Bmatrix} = [AA]_{6 \times 6}^{-1} \begin{Bmatrix} Q_1 \\ Q_2 \\ Q_3 \\ Q_4 \\ Q_5 \\ Q_6 \end{Bmatrix} \quad (5-16)$$

and is then substituted into equation (5-15) giving,

$$\begin{Bmatrix} h D Q_1 \\ h^2 D^2 Q_1 \\ h^3 D^3 Q_1 \\ h^4 D^4 Q_1 \end{Bmatrix} = [CC]_{4 \times 6} [AA]_{6 \times 6}^{-1} \begin{Bmatrix} Q_1 \\ Q_2 \\ Q_3 \\ Q_4 \\ Q_5 \\ Q_6 \end{Bmatrix} \quad (5-17)$$

Now, the fourth derivative of Q_1 at station $i = 1$ is approximated in terms of the discrete functions of Q at the interior mesh points with truncation error Oh^4 . The values on the bottom row of the resulting 4×6 matrix after multiplication in equation (5-17) are the coefficients of the column vector Q_1 through Q_6 for $D^4 Q_1$. In order to have consistent truncation error Oh^4 , the last row and last column of the $[AA]$ and $[CC]$ matrices are deleted for the third derivative of Q . Matrix $[AA]$ becomes a 5×5 and is now inverted and matrix $[CC]$ becomes a 3×5 . The values on the bottom row of the resulting 3×5 matrix are

the coefficients of Q_1 through Q_5 which approximates D^3Q_1 . The rows and columns of matrices [AA] and [CC] are successively reduced to determine the coefficients for D^3Q_1 in terms of Q_1 through Q_4 , and DQ_1 in terms of Q_1 through Q_3 so that consistent truncation error Oh^4 is preserved throughout. The noncentral finite difference equation for D^4Q_1 will now appear as,

$$D^4Q_1 = \frac{1}{h^4} (A_1Q_1 + A_2Q_2 + A_3Q_3 + A_4Q_4 + A_5Q_5 + A_6Q_6) + Oh^4 \quad (5-18)$$

where A_1 through A_6 are the coefficients taken from the bottom row of the resulting matrix in equation (5-17)

In a similar manner, by imposing the required boundary conditions, this process can be carried out to determine the noncentral finite difference equations for the first two derivatives of $P(r)$ at several points near the boundaries as required.

It is important to note here that the noncentral finite difference approximations near the wall can be formulated by using the same techniques as those used near the axis. Once again taking the case for angular wave number $n \geq 6$, the boundary conditions at the pipe wall for the function Q are,

$$Q(1) = 0 \quad \text{and} \quad DQ(1) = 0 \quad (5-19)$$

Rather than set up complete new [AA] and [CC] matrices at different values of r in the Taylor series expansion near the wall, assume that the boundary conditions in equation (5-19) are imposed at the axis,

$r = 0$. Notice that the boundary conditions in equation (5-19) are now identical to the boundary conditions in equation (5-13). The method for computing the coefficients of the noncentral finite difference approximations at the wall can be carried out as discussed previously and, in this case, have already been computed. It can be shown that the A_i coefficients of equation (5-18) are applicable to D^4Q_N at the wall but will appear in reverse order. The noncentral finite difference equation for D^4Q_N is given by,

$$D^4Q_N = \frac{1}{h^4} (A_6Q_{N-5} + A_5Q_{N-4} + A_4Q_{N-3} + A_3Q_{N-2} + A_2Q_{N-1} + A_1Q_N) + Oh^4 \quad (5-20)$$

The method for determining the coefficients for the remaining derivatives of Q and P near the wall proceed as though the boundary conditions were imposed at the axis; the coefficients are computed, their order reversed and coefficients of the odd order derivatives undergo a sign change. Order reversal and sign changes are accomplished in part II of the main investigative program when the precomputed noncentral finite difference coefficients are read in as data.

As can be seen from the central finite difference approximations of equations (5-5) through (5-8), the third and fourth derivatives of a function require three points either side of the central point being approximated. The first and second derivatives require only two points either side of the central point. Therefore the central finite difference approximations are applicable only to interior stations $i = 4$ through $N-3$ for D^4Q_i and D^3Q_i , and stations $i = 3$ through $N-2$ for D^2Q_i ,

DQ_i , D^2P_i , and DP_i . This leaves either two or three points immediately adjacent to the boundaries to be approximated by the noncentral finite difference equations just developed.

Since the central finite difference approximations are applicable to the above mentioned interior mesh points and are valid for all the derivatives of $P(r)$ and $Q(r)$ as well, the coefficients are computed only once in part I of the main investigative program in double precision format. The coefficients of the noncentral finite difference approximations, which are dependent on the boundary conditions for each angular wave number, are computed in an independent computer program. The resulting noncentral coefficients for the derivatives of $P(r)$ and $Q(r)$ at mesh points near the boundaries are also computed in double precision format and are read into part II of the main investigative program as data.

C. SPECIFIC METHODS FOR $n = 0, 1$, AND 6

The vorticity transport equations have now been expanded into a set of discrete simultaneous equations with respect to a half station computational mesh of N points (stations). The derivatives of the governing equations were approximated by central and noncentral finite difference coefficients, with consistent fourth order truncation error, in terms of the discrete unknown functions of the system. The convenient matrix format of the eigensystem in equation (5-3) can now be solved on a digital computer using a specialized Fortran subroutine, which will be discussed later. It is important to understand the composition of the $[A]$ and $[B]$ matrices and the column vector of unknowns

{X}. The problem setup is examined in detail for each angular wave number investigated. In the following discussions, the vorticity transport equations are referred to in the transformed state after the change of variables to $P(r)$ and $Q(r)$ have been made. The boundary conditions in equations (3-17), (3-18), and (3-23), and the coefficients in Appendix B also apply.

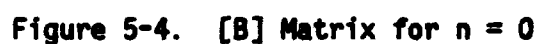
For the case $n = 0$, the pipe flow problem becomes greatly simplified in that the equations become uncoupled and only the solution for $Q(r)$ is investigated for reasons explained earlier. The governing equation in terms of $Q(r)$ is represented by equation (2-38). At the outset, it was determined that a mesh size of $N = 50$ was sufficient to produce a satisfactory numerical solution of the problem. It was necessary to determine when the solution was relatively independent of mesh size. Preliminary trial computations were performed for various mesh sizes, $N = 25$ to 100. From $N = 45$ to 100, the solution of the equation for $n = 0$ did not vary appreciably. Additionally, the solution was relatively independent of Reynolds numbers below 15,000 for mesh sizes of about 50. In order to reduce computation time and the eigensystem matrix size, a mesh of $N = 50$ was used in this analysis.

In general for angular wave number $n = 0$, the $[A]$ and $[B]$ matrices are 50×50 and appear as banded diagonal matrices. For a consistent order truncation error $O(h^4)$ used here, the derivative of highest order requires the greatest band width. From the governing equation in Q , it can be seen that the highest order derivative in $[A]$ is D^4Q and in $[B]$ is D^2Q . At stations near the boundaries, the noncentral finite difference coefficients require a band width of six in matrix $[A]$ and four in

matrix [B]. At interior stations, the central finite difference coefficients require a band width of seven for [A] and five for [B]. Therefore the [A] and [B] matrices of equation (5-3) contain nonzero elements as shown in Figures 5-3 and 5-4. The X elements contain non-central finite difference coefficients and the 0 elements contain central difference coefficients. The X and 0 symbols denote the station at which the approximation is made. The composition of the column vector {X} can also be seen in Figures 5-3 and 5-4.

$$\begin{bmatrix}
 \text{XXXXXX} \\
 \text{XXXXXX} \\
 \text{XXXXXX} \\
 000000 \\
 000000 \\
 \dots\dots \\
 000000 \\
 \dots\dots \\
 000000 \\
 000000 \\
 \text{XXXXXX} \\
 \text{XXXXXX} \\
 \text{XXXXXX}
 \end{bmatrix}
 \begin{Bmatrix}
 Q_1 \\
 Q_2 \\
 Q_3 \\
 \vdots \\
 Q_i \\
 \vdots \\
 Q_{N-2} \\
 Q_{N-1} \\
 Q_N
 \end{Bmatrix}$$

Figure 5-3. [A] Matrix for $n = 0$


$$M'_{4i} D^4 Q_i + M'_{3i} D^3 Q_i + M'_{2i} D^2 Q_i + M'_{1i} D Q_i + M'_{0i} Q_i = \gamma (N'_{2i} D^2 Q_i + N'_{1i} D Q_i + N'_{0i} Q_i) \quad (5-21)$$

where the primed quantities are element (2,2) of the corresponding transformed vorticity transport equation matrices given in Appendix B, Part A. At station $i = 1$, the top row of the [A] matrix will have six elements and the top row of [B] will have four elements.

For example, the matrix elements for the first row of [A] can be found as follows, where the a_i coefficients are analogous to the coefficients A_i of equation (5-18) and are equal to $a_i = A_i/h^4$. Similarly $b_i = B_i/h^3$, $c_i = C_i/h^2$, and $d_i = D_i/h$, where b_i , c_i , and d_i are the noncentral finite difference coefficients of the remaining three derivatives.

$$A_{1,1} \{Q_1\} = (M_{4,1}' a_1 + M_{3,1}' b_1 + M_{2,1}' c_1 + M_{1,1}' d_1 + M_{0,1}') \{Q_1\} \quad (5-22)$$

$$A_{1,2} \{Q_2\} = (M_{4,1}' a_2 + M_{3,1}' b_2 + M_{2,1}' c_2 + M_{1,1}' d_2) \{Q_2\} \quad (5-23)$$

$$A_{1,3} \{Q_3\} = (M_{4,1}' a_3 + M_{3,1}' b_3 + M_{2,1}' c_3 + M_{1,1}' d_3) \{Q_3\} \quad (5-24)$$

$$A_{1,4} \{Q_4\} = (M_{4,1}' a_4 + M_{3,1}' b_4 + M_{2,1}' c_4) \{Q_4\} \quad (5-25)$$

$$A_{1,5} \{Q_5\} = (M_{4,1}' a_5 + M_{3,1}' b_5) \{Q_5\} \quad (5-26)$$

$$A_{1,6} \{Q_6\} = (M_{4,1}' a_6) \{Q_6\} \quad (5-27)$$

where $A_{1,1}$ is the matrix element in the first row and the first column of [A], and so forth. This procedure is carried out for N equations along the computational mesh until all the nonzero matrix elements of [A] and [B] are computed.

Derivation of the noncentral finite difference coefficients for other angular wave numbers is fairly straightforward when accomplished by the methods outlined in the previous section. The boundary conditions for Q at the axis for $n = 0$ are,

$$DQ(0) = 0 \quad \text{and} \quad D^3Q(0) = 0 \quad (5-28)$$

After imposing these conditions, the second and fourth columns of the matrices in equations (5-10) and (5-12) can be eliminated since the corresponding terms in the column vectors vanish. The coefficients are then computed as described before in an independent computer program and then read into the main investigative program as data. Notice that the boundary conditions for the function Q at the wall are the same for $n = 0$ and $n \geq 6$. Therefore, the noncentral finite difference coefficients need to be computed only once.

The case for angular wave number $n \geq 6$ will be examined next since it more nearly represents the general case. Since the vorticity transport equations remain coupled for $n \geq 6$ and no additional parameters are introduced, a system of $2N$ equations in $2N$ unknowns will result. For a mesh size of 50, the $[A]$ and $[B]$ matrices become 100×100 and are solved in the form of equation (5-3). The first N equations of the system are represented by the discrete form of equation (2-37), which after transformation by the appropriate change of variables corresponds to the top equation of (5-1). The second N set of equations are represented by the discrete form of equation (2-38), which after transformation by the appropriate change of variables corresponds to the bottom equation of (5-1). As a matter of convenience for programming, the $[A]$ and $[B]$ matrices are partitioned into four 50×50 quadrants, which are individually banded diagonal matrices. The properties of the $[A]$ and $[B]$ matrices for $n \geq 6$ are summarized in Table 5-1.

Table 5-1. Properties of the [A] and [B] Matrices for $n \geq 6$

MATRIX	QUADRANT	HIGHEST ORDER DERIVATIVE PRESENT	NONCENTRAL COEFFICIENTS REQUIRED	*	CENTRAL COEFFICIENTS REQUIRED
A	I	D^2P	5	2	5
A	II	D^3Q	5	3	7
A	III	D^2P	5	2	5
A	IV	D^4Q	6	3	7
B	I	P	-	-	1
B	II	DQ	3	2	5
B	III	P	-	-	1
B	IV	D^2Q	4	2	5
* Number of stations near the boundaries where the noncentral finite difference approximations apply.					

It can be deduced from the data given in Table 5-1 that the [A] and [B] matrices will contain nonzero elements as shown in Figures 5-5 and 5-6. The column vector $\{X\}$ of unknowns is also given.

The method for determining the noncentral finite difference coefficients for $n \geq 6$ was discussed in a previous example.

The case for $n = 1$ is unique in that an additional parameter $H(0)$ is introduced by the change of variables and a pair of coupled boundary conditions at the axis in equation (3-18b) contain the eigenvalue γ . These peculiarities are significant factors in correctly setting up the problem. Recall that in the coupled governing equations (2-47) the additional parameter $H(0)$ appears explicitly and two additional column



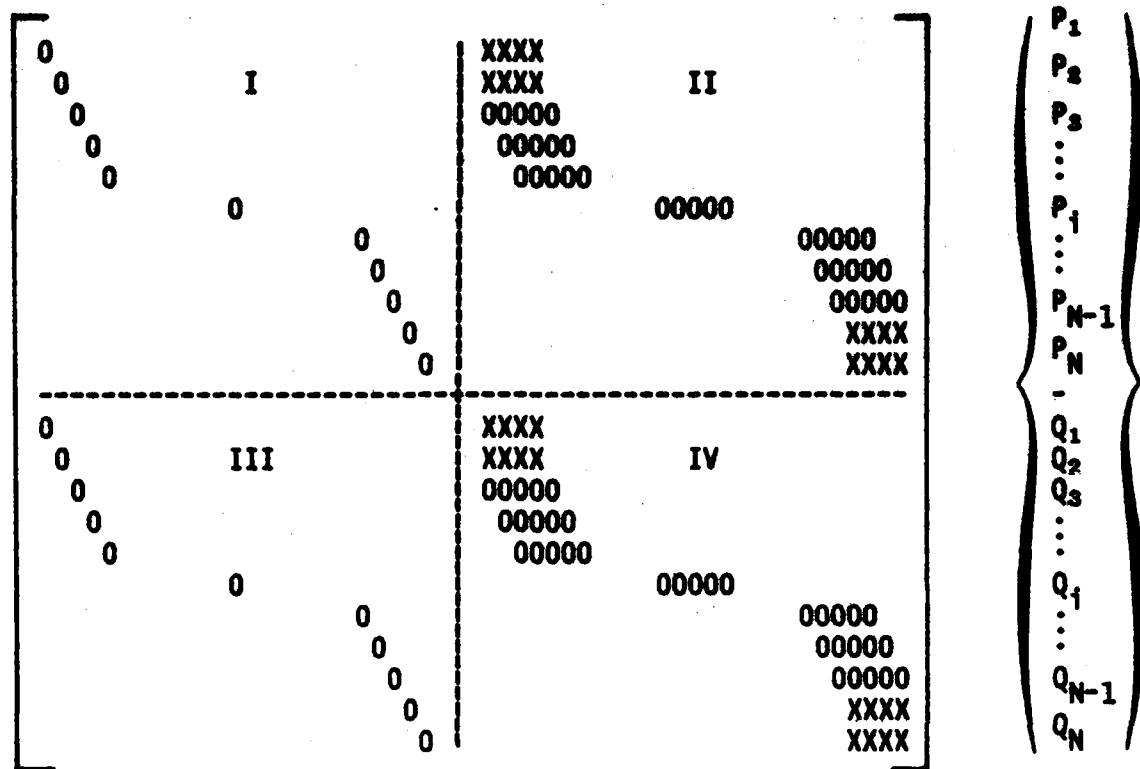


Figure 5-6. [B] Matrix for $n \geq 6$

matrices are required in the system of equations. This was due to the change of variables introduced by equations (2-44). The appearance of the eigenvalue γ in the pair of boundary equations at the axis comes about from the rigorous method in which the boundary conditions were derived in Chapter III. The coupled axis boundary conditions in equation (3-18b) are repeated here,

$$\begin{aligned}
 & -\frac{96}{Re} [C_7] \begin{Bmatrix} D^2P(0) \\ D^2Q(0) \end{Bmatrix} + 2i\alpha[C_8] \begin{Bmatrix} P(0) \\ Q(0) \end{Bmatrix} + i\alpha[C_9] \begin{Bmatrix} -1 \\ 1 \end{Bmatrix} H(0) \\
 & = \gamma \left(2 [D_8] \begin{Bmatrix} P(0) \\ Q(0) \end{Bmatrix} + \alpha^2 [D_9] \begin{Bmatrix} -1 \\ 1 \end{Bmatrix} H(0) \right)
 \end{aligned}
 \tag{5-29}$$

where the coefficient matrices are contained in Appendix C. Notice that the parameter $H(0)$ appears explicitly in these two equations as well. Additionally, the parameters $D^2P(0)$, $D^2Q(0)$, $P(0)$, and $Q(0)$ are also introduced. Obviously, this poses some problems since there are only two additional equations and five unknown parameters. $H(0)$ can be used since it appears in the 2N discrete equations of the system. $Q(0)$ is chosen as the second variable as a matter of convenience. The remaining three functions can be approximated in terms of discrete functions of P_i in the case for $D^2P(0)$ and $P(0)$, and Q_i and $Q(0)$ in the case of $D^2Q(0)$. By referring to the matrix form of the Taylor series expansion of a function at a point in equation (5-10), it can be seen how the approximations of these functions are made. For the present situation where

$DP(0) = 0$, eliminate the second column of the matrix and equation (5-10) will become,

$$\begin{Bmatrix} P_1 \\ P_2 \\ P_3 \\ P_4 \\ P_5 \end{Bmatrix} = [AA]_{5 \times 5} \begin{Bmatrix} P(0) \\ h^2 D^2 P(0) \\ h^3 D^3 P(0) \\ h^4 D^4 P(0) \\ h^5 D^5 P(0) \end{Bmatrix} + Oh^6 \quad (5-30)$$

Recall that the matrix in equation (5-30) is denoted $[AA]$ as before. After multiplying each side of the equation by $[AA]^{-1}$, the result becomes,

$$\begin{Bmatrix} P(0) \\ h^2 D^2 P(0) \\ h^3 D^3 P(0) \\ h^4 D^4 P(0) \\ h^5 D^5 P(0) \end{Bmatrix} = [AA]_{5 \times 5}^{-1} \begin{Bmatrix} P_1 \\ P_2 \\ P_3 \\ P_4 \\ P_5 \end{Bmatrix} - Oh^6 \quad (5-31)$$

Now $P(0)$ is approximated by the coefficients in the first row of $[AA]^{-1}$ and $D^2 P(0)$ is approximated by the coefficients in the second row of $[AA]^{-1}$ divided by h^2 , both expressed in terms of P_1 through P_5 . Notice that the approximation for $D^2 P(0)$ has truncation error Oh^4 and $P(0)$ has truncation error Oh^6 , which is acceptable in this analysis.

The approximation for $D^2 Q(0)$ is similar except that $Q(0)$ will appear explicitly in the approximations with $DQ(0) = 0$. Equation (5-10) now becomes,

$$\begin{Bmatrix} Q_1 \\ Q_2 \\ Q_3 \\ Q_4 \\ Q_5 \\ Q_6 \end{Bmatrix} = \begin{bmatrix} 1 \\ 1 \\ 1 \\ 1 \\ 1 \\ 1 \end{bmatrix} \{Q(0)\} + [AA]_{6 \times 6} \begin{Bmatrix} h^2 D^2 Q(0) \\ h^3 D^3 Q(0) \\ h^4 D^4 Q(0) \\ h^5 D^5 Q(0) \\ h^6 D^6 Q(0) \\ h^7 D^7 Q(0) \end{Bmatrix} + Oh^8 \quad (5-32)$$

After rearranging, equation (5-32) is multiplied through by $[AA]^{-1}$ and becomes,

$$\begin{Bmatrix} h^2 D^2 Q(0) \\ h^3 D^3 Q(0) \\ h^4 D^4 Q(0) \\ h^5 D^5 Q(0) \\ h^6 D^6 Q(0) \\ h^7 D^7 Q(0) \end{Bmatrix} = [AA]_{6 \times 6}^{-1} \begin{Bmatrix} Q_1 - Q(0) \\ Q_2 - Q(0) \\ Q_3 - Q(0) \\ Q_4 - Q(0) \\ Q_5 - Q(0) \\ Q_6 - Q(0) \end{Bmatrix} - Oh^8 \quad (5-33)$$

The coefficients for $D^2 Q(0)$ are taken from the first row of $[AA]^{-1}$ and divided by h^2 . $D^2 Q(0)$ is now expressed in terms of $Q(0)$ and Q_1 through Q_6 and will have a truncation error Oh^8 .

The two additional boundary condition equations involving y can now be solved in the eigensystem of equations with $H(0)$ and $Q(0)$ appearing explicitly as the two required unknowns. It is convenient to express the $[C_9]$ and $[D_9]$ matrices of equation (5-29) in slightly different form,

$$[C_9] \begin{Bmatrix} -1 \\ 1 \end{Bmatrix} H(0) \quad \text{as} \quad [C_9^*] \{H(0)\}$$

and

(5-34)

$$[D_9] \begin{Bmatrix} -1 \\ 1 \end{Bmatrix} H(0) \quad \text{as} \quad [D_9^*] \{H(0)\}$$

where $[C_9^*]$ and $[D_9^*]$ become 2 X 1 column matrices,

$$[C_9^*] = \begin{bmatrix} \left(\frac{\alpha^3}{Re} - 4i + 2i\alpha^2 \right) \\ \left(-2\alpha^2 + \frac{i\alpha^3}{Re} \right) \end{bmatrix} \quad \text{and} \quad [D_9^*] = \begin{bmatrix} -1 \\ 1 \end{bmatrix}$$
(5-35)

Substituting equations (5-35) into equation (5-29) yields,

$$- \frac{96}{Re} [C_7] \begin{Bmatrix} D^2P(0) \\ D^2Q(0) \end{Bmatrix} + 2i\alpha [C_8] \begin{Bmatrix} P(0) \\ Q(0) \end{Bmatrix} + i\alpha [C_9^*] \{H(0)\}$$
(5-36)

$$= \gamma \left(2 [D_8] \begin{Bmatrix} P(0) \\ Q(0) \end{Bmatrix} + \alpha^2 [D_9^*] \{H(0)\} \right)$$

The solution of the eigensystem of $2N + 2$ equations in $2N + 2$ unknowns is now accomplished in the form of equation (5-3). The appearance of the $[A]$ and $[B]$ matrices are identical to those for $n \geq 6$ in Figures 5-5 and 5-6 except for the addition of two columns to accommodate the parameters $H(0)$ and $Q(0)$, and two rows to accommodate the pair of boundary equations in (5-36). Nonzero elements are present in the $[A]$ and $[B]$ matrices for $n = 1$ as shown in Figures 5-7 and 5-8.

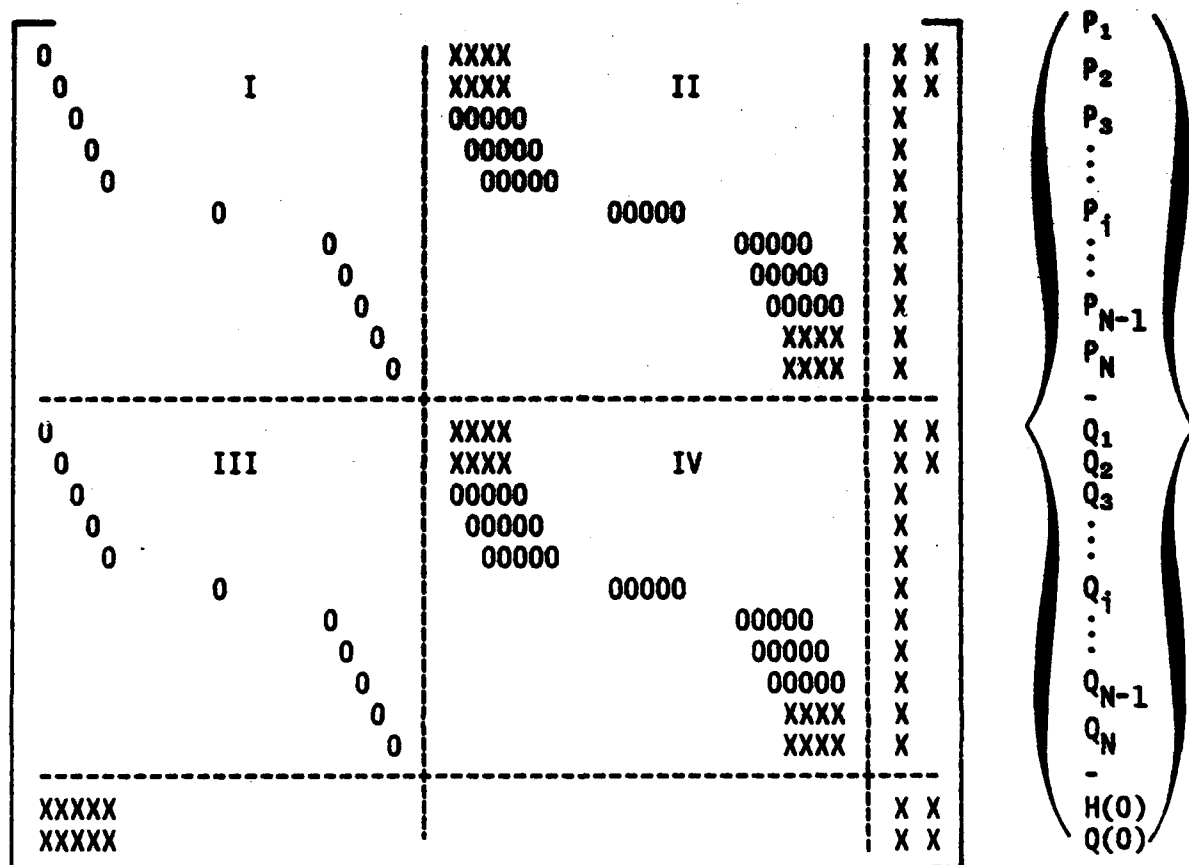


Figure 5-8. [B] Matrix for $n = 1$

Derivation of the noncentral finite difference coefficients for the derivatives of P and Q at the wall are straightforward as shown for the other angular wave numbers. The columns of the [AA] and [CC] matrices are eliminated based on the fact that parameters P(1), Q(1), and DQ(1) are all expressed in terms of H(0), as seen in equations (3-18c). By imposing the boundary conditions for Q at the wall,

$$Q(1) = -H(0) \quad \text{and} \quad DQ(1) = 2H(0) \quad (5-37)$$

equation (5-17) becomes,

$$\begin{Bmatrix} hDQ_1 \\ h^2D^2Q_1 \\ h^3D^3Q_1 \\ h^4D^4Q_1 \end{Bmatrix} = \begin{bmatrix} 2h \\ 0 \\ 0 \\ 0 \end{bmatrix} \{H(0)\} + \underset{4 \times 6}{[CC]} \underset{6 \times 6}{[AA]}^{-1} \begin{Bmatrix} Q_1 + (1-h)H(0) \\ Q_2 + (1-3h)H(0) \\ Q_3 + (1-5h)H(0) \\ Q_4 + (1-7h)H(0) \\ Q_5 + (1-9h)H(0) \\ Q_6 + (1-11h)H(0) \end{Bmatrix} \quad (5-38)$$

The coefficients in the resultant 4 X 6 matrix of equation (5-38) are in fact the same coefficients computed for $n \geq 6$ at the wall, and recall that they appear in reverse order when used at the wall. The details of the complete derivation of the noncentral finite difference coefficients near the boundaries is lengthy and not included here.

D. COMPUTER PROGRAM USEAGE

The solutions for the discrete transformed vorticity transport equations for the three angular wave numbers investigated are accomplished in the main investigative computer programs. Three separate programs were written rather than developing one program for the general case. The rationale for this is as follows: the changes of variables for each angular wave number $n \leq 6$ are different, the boundary conditions are different, the equations uncouple for $n = 0$, additional parameters are introduced for some, and $n = 1$ has a coupled boundary equation that contains γ that must be dealt with separately in the setup of the problem. It would be practical to write a general program for angular wave numbers $n \geq 6$, however.

For each specific angular wave number analyzed, the main computer program is divided into eight parts. Their functions are summarized below:

- Part I The central finite difference coefficient for the derivatives of P and Q are computed.
- Part II The noncentral finite difference coefficients for the derivatives of P and Q at the axis and wall are read in as data. Problem variables, Re and α , are read in as data.
- Part III Coefficients of the vorticity transport matrix equations are computed along the radial mesh.
- Part IV The [A] and [B] matrix elements are computed.
- Part V The eigenvalues and respective eigenvectors are computed in the subroutine EIGZC and the least stable eigenvalue is determined.
- Part VI Verification that the least stable eigenvalue and corresponding eigenvector satisfy the governing equations.

Part VII The normalized axial perturbation velocity is computed from the least stable eigenvalue and its eigenvector.

Part VIII The normalized axial perturbation velocity is plotted versus normalized pipe radius utilizing the Versatec plotter.

The numerical analysis of the pipe flow stability problem is centered around the subroutine EIGZC once the problem is properly set up. The eigensystem of equation (5-3) is solved by this subroutine which returns a set of N , $2N + 2$, or $2N$ eigenvalues for $n = 0$, 1 , or 6 , respectively, and a corresponding set of normalized eigenvectors. Each eigenvalue and its eigenvector represent a solution of the governing equations. The primary objective of the main program and of this investigation is to determine the least stable eigenvalue which indicates flow characteristics. Recall that if γ_R is positive, the flow is unstable. For each value of α and Re chosen, the maximum algebraic value of γ_R is found, denoted as γ^* , to determine if instabilities exist in the flow field. The corresponding eigenvector of γ^* , denoted as $\{X^*\}$, is used to compute the incremental axial perturbation velocity along the radius. Plots of the normalized perturbation velocity versus normalized pipe radius have no significance in determining stability or instability of the flow but are indicators of the general nature and behavior of the flow field perturbations. Another independent program was written to plot Reynolds number stability contours using data taken from program results for $n = 1$ and 6 . The subroutines used to make plots on Versatec plotter are PLOTG, standard Versatec plotting functions and TITLE1 to print titles and legends on the plots.

The numerical accuracy of the solution was determined by substituting y^* and its eigenvector into the governing equations. For this purpose, the residual error vector $\{e\}$ was computed by equation (5-39) and the magnitude of the error was examined.

$$\{e\} = [A] \{X^*\} - y^* [B] \{X^*\} \quad (5-39)$$

The Fortran subroutine EIGZC is contained in the International Mathematical and Statistical Library (IMSL) available in most large computer system libraries utilizing Fortran compilers. Specifically, the numerical analysis of the vorticity transport equations in the form of equation (5-3) was computed on the IBM 370/3033 (assigned processor) system with the Fortran H Extended compiler at the U.S. Naval Postgraduate School. All calculations were performed in full double precision format to improve the accuracy of the solution by minimizing truncation and round off errors inherently introduced by digital computations. The main investigative programs and other auxiliary programs were all written in Fortran programming language to be compatible with all versions of Fortran compilers. The computer program listings with applicable data sets are included after the appendices in this paper.

VI. RESULTS

A. RESULTS FOR $n = 0$

Results of the pipe flow stability problem are obtained from the solution of the linearized vorticity transport equations by the methods previously described. A generalized solution of the governing differential equations for fully developed, three-dimensional pipe flow has been accomplished for three angular wave numbers, $n = 0, 1$, and 6 . The characteristics of the flow field perturbations for each angular wave number investigated are established by the parameters Re and α . The purpose of this numerical investigation was to determine flow stability at various Reynolds numbers and axial wave numbers for each angular wave number. Recall that the perturbation velocity vector \vec{v} is defined in equation (2-27) as the curl of the velocity vector potential \vec{W} . This function is expressed in terms of $G(r)$ and $H(r)$ and a complex exponential form e^X in equations (2-28) and (2-29). After appropriate changes of variables were introduced, solutions were determined from the eigen-system of equations which consists of a set of eigenvalues and their corresponding normalized eigenvectors for fixed values of Re and α . The resulting perturbation quantities now appear in terms of the eigenfunctions $P(r)$ and $Q(r)$ and are represented in discrete form in the eigenvector $\{X\}$ as P_i and Q_i , where $i = 1, 2, 3, \dots, N$. As can be seen from equation (2-30), the real part of the complex eigenvalue γ_R will determine the growth or decay rate in time of the perturbation. Positive

values of γ_R indicate that the flow is unstable. The eigenvalue whose real part has the largest algebraic value, denoted as γ^* , is the least stable and is reported in these results to show stability trends.

Gawain [Ref. 13] reported the numerical results for angular wave number $n = 0$ for the solution of the governing equation in his paper. Those numerical results which incorporated a purely imaginary axial wave number and the advancements in the derivation of the boundary conditions at the pipe axis were duplicated in this investigation. They are essentially the same results except for variations in the fourth decimal place of the value of γ^* . This is due to the improved accuracy of the solution as a result of the numerical methods used here. The primary emphasis of this investigation is centered on determining the onset of flow instabilities at a theoretical critical Reynolds number near 1150. However, solutions were obtained at other Reynolds numbers to show stability trends and are presented in tabular and plotted form.

Stability data for angular wave number $n = 0$ for various combinations of Re and α are given in Table 6-1. The least stable eigenvalue solution of the governing equation is based on a computational mesh of $N = 50$. Table entries which contain dashes indicate that the solution of the governing equations was not sufficiently accurate to be included as valid data. Two facts become very clear in examining Table 6-1. First of all, the flow is stable at all Re and α for $n = 0$. Secondly, there is an asymptotic trend towards neutral stability for increasing Reynolds numbers. This second result agrees with experimental observations in that increasing Reynolds number has a destabilizing effect on the flow. It can also be seen that increasing the axial wave number has

Table 6-1. Stability Data for Angular Wave Number $n = 0$

Growth or Decay Trends of Least Stable Eigenvalue, γ^*

Re	$\alpha=0.0$	$\alpha=0.05$	$\alpha=1.0$	$\alpha=2.0$	$\alpha=4.0$	$\alpha=8.0$	$\alpha=16.0$	$\alpha=32.0$
300	-0.0879	-0.1544	-0.2360	-0.3399	-0.5152	-0.8665	-1.7770	-4.7194
575	-0.0459	-0.1196	-0.1685	-0.2429	-0.3614	-0.5831	-1.1122	-2.7236
1150	-0.0229	-0.0836	-0.1188	-0.1703	-0.2498	-0.3891	-0.6937	-1.5548
2300	-0.0115	-0.0591	-0.0838	-0.1197	-0.1737	-0.2633	-0.4429	-0.9099
4600	-0.0057	-0.0418	-0.0592	-0.0842	-0.1212	-0.1796	-0.2871	-
9200	-0.0029	-0.0295	-0.0418	-0.0593	-0.0846	-0.1225	-	-
18400	-0.0014	-0.0209	-0.0295	-0.0416	-0.0586	-	-	-

Note: Values are based on 50 mesh points.

a stabilizing effect on the flow. Normalized axial perturbation velocity plots versus pipe radius were made at various Re and α to examine the behavior of the perturbation quantities corresponding to the least stable eigenvalue solution. Figures 6-1 through 6-9, on the following pages, are representative of the behavior of the axial perturbation velocity. The activity is concentrated near the pipe axis for $n = 0$ and dies out quickly as r approaches 1.0. Additionally, the perturbation velocity plots were made in order to determine if mesh fineness was sufficient to obtain an accurate solution of the equations. Trial calculations were made for uniform mesh sizes up to 100 where the numerical results did not vary appreciably from those reported here.

NORMALIZED PERTURBATION VELOCITY VS RADIUS

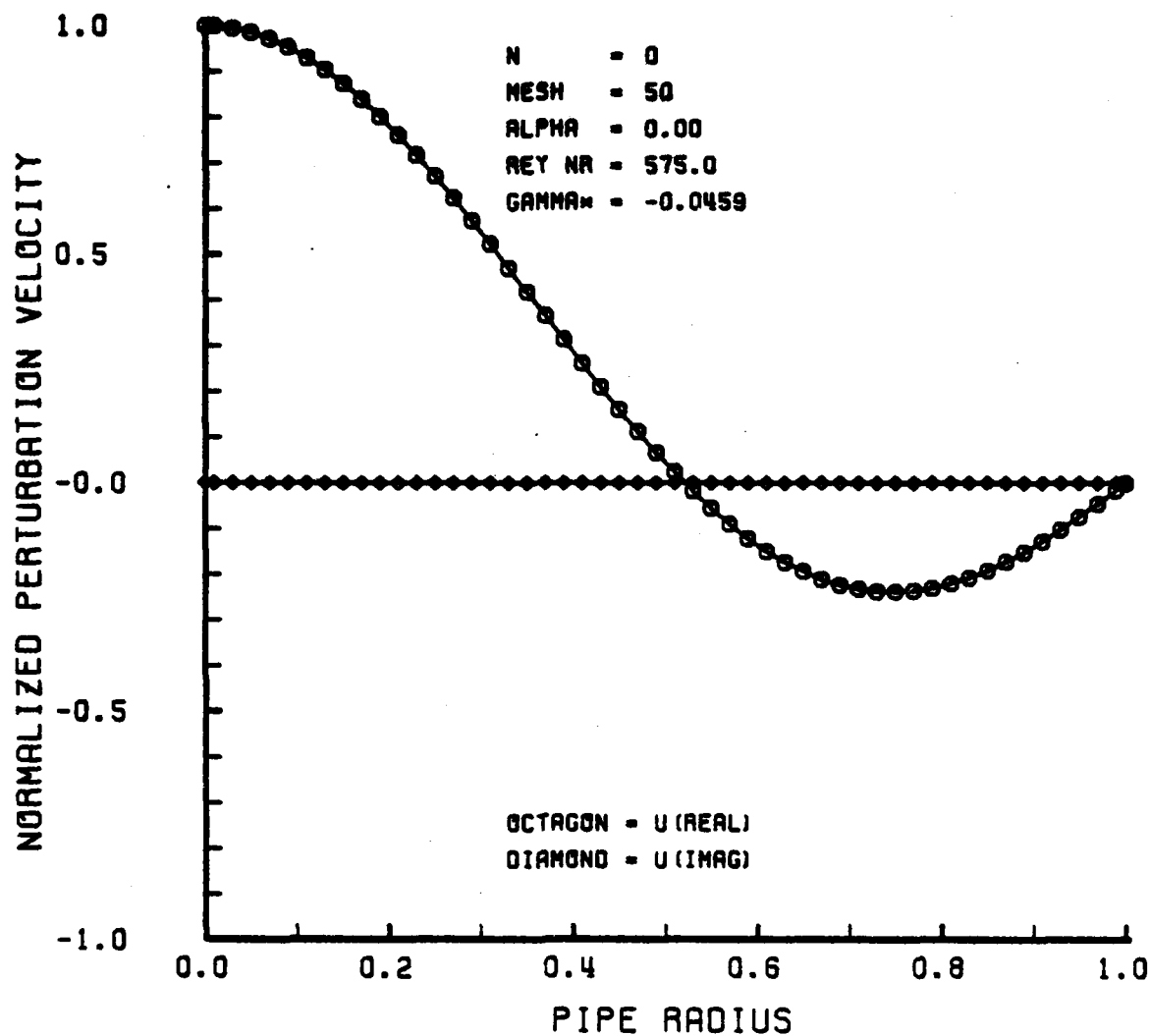


Figure 6-1

NORMALIZED PERTURBATION VELOCITY VS RADIUS

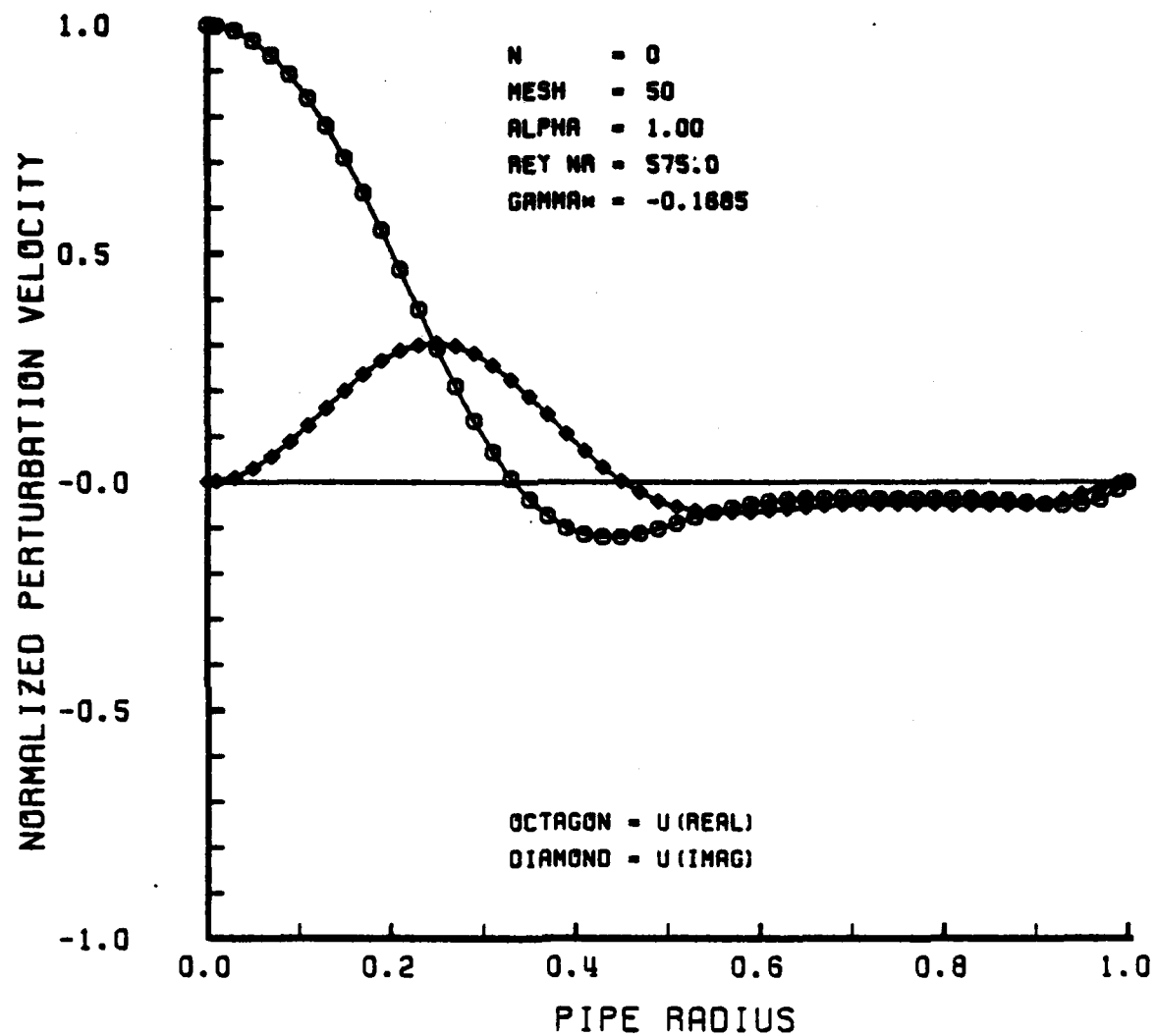


Figure 6-2

NORMALIZED PERTURBATION VELOCITY VS RADIUS

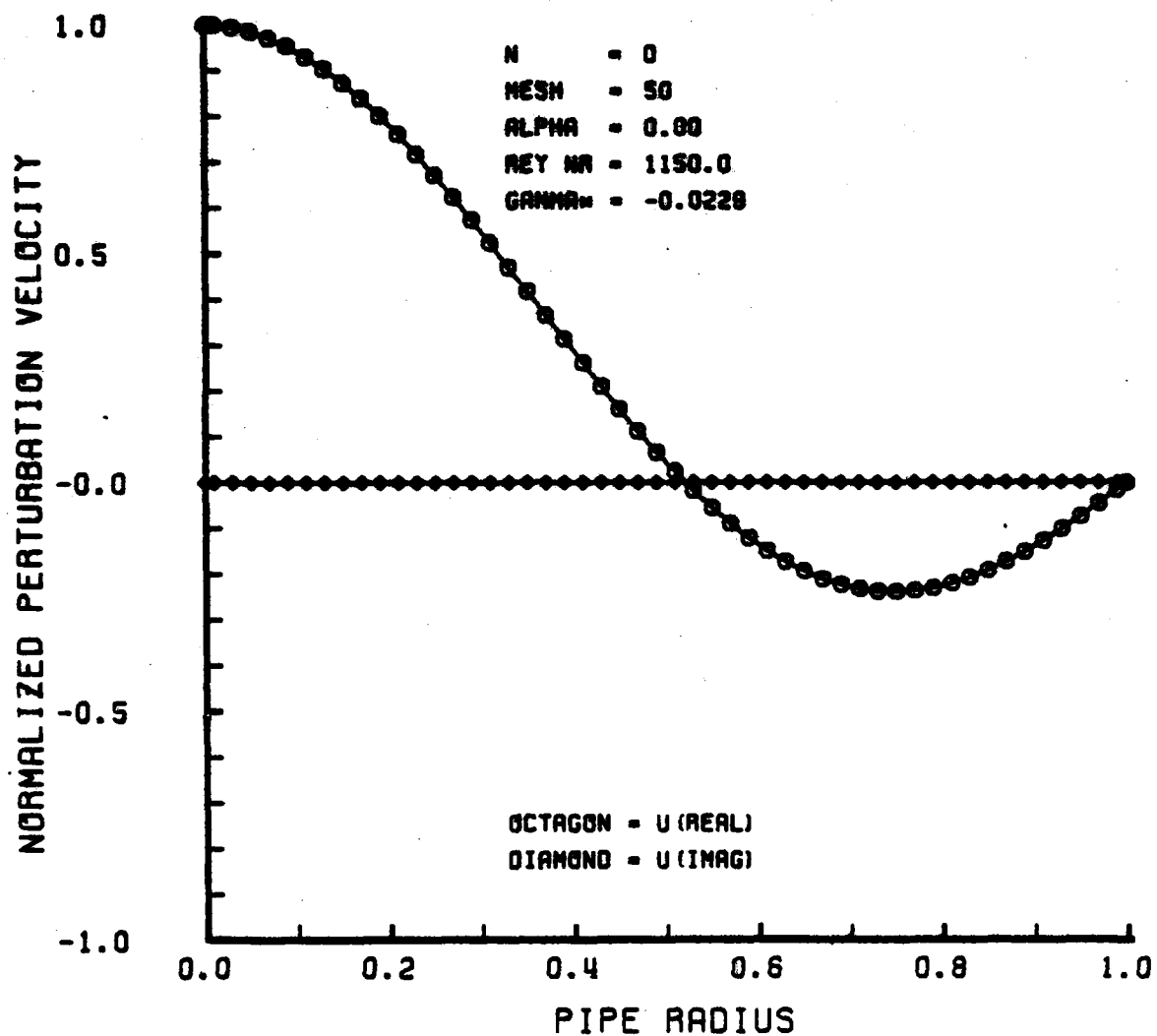


Figure 6-3

NORMALIZED PERTURBATION VELOCITY VS RADIUS

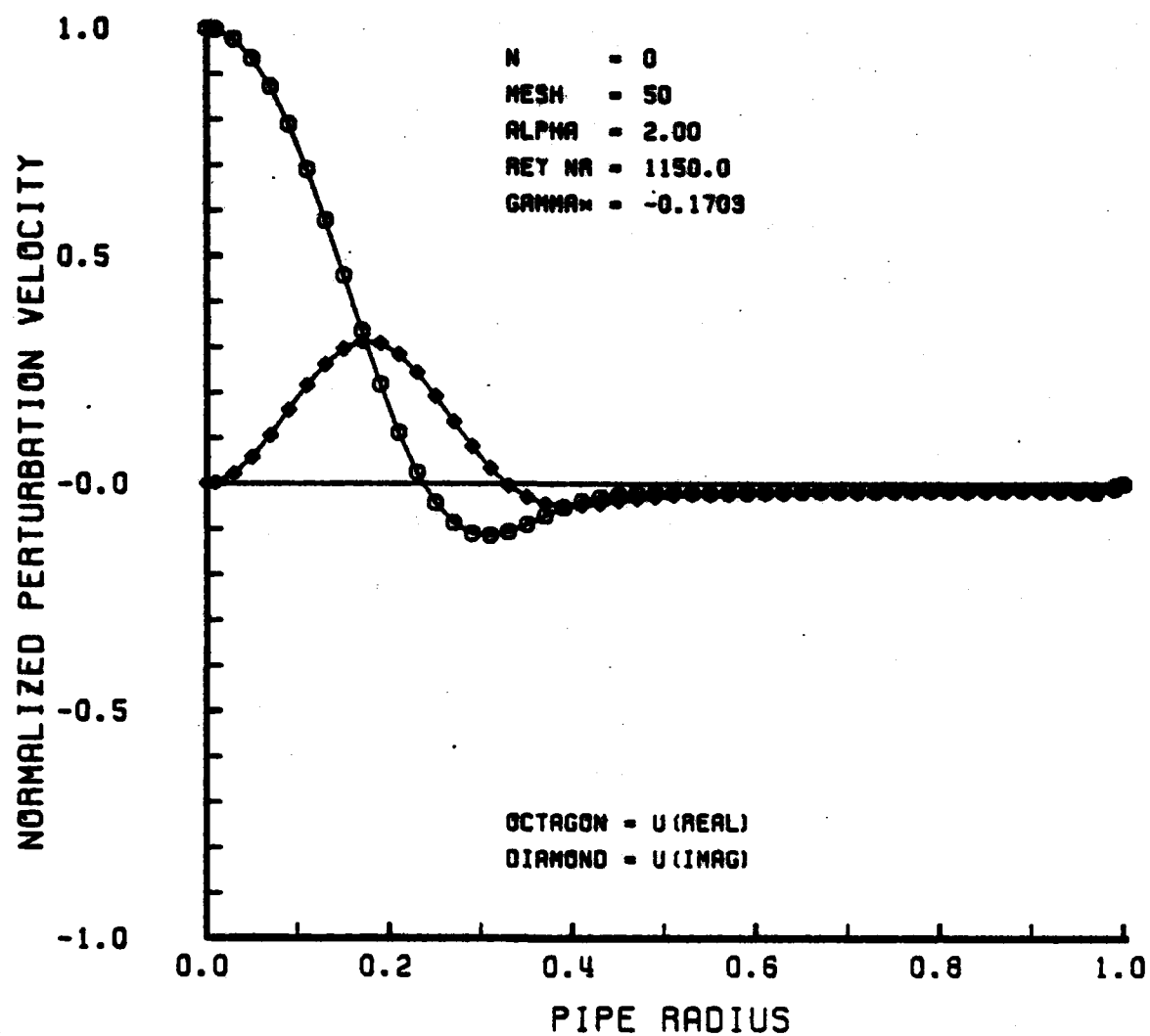


Figure 6-4

NORMALIZED PERTURBATION VELOCITY VS RADIUS

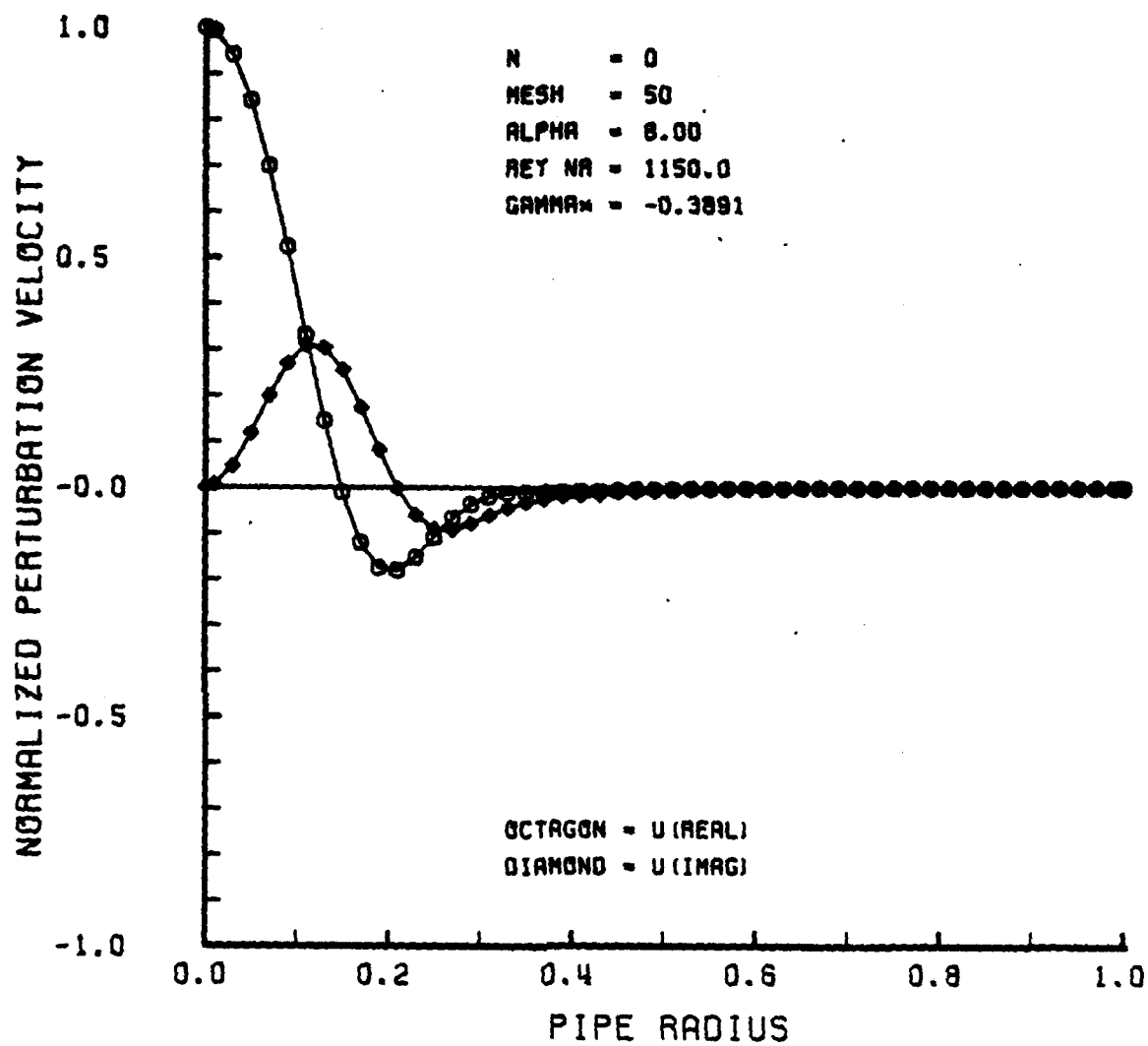


Figure 6-5

NORMALIZED PERTURBATION VELOCITY VS RADIUS

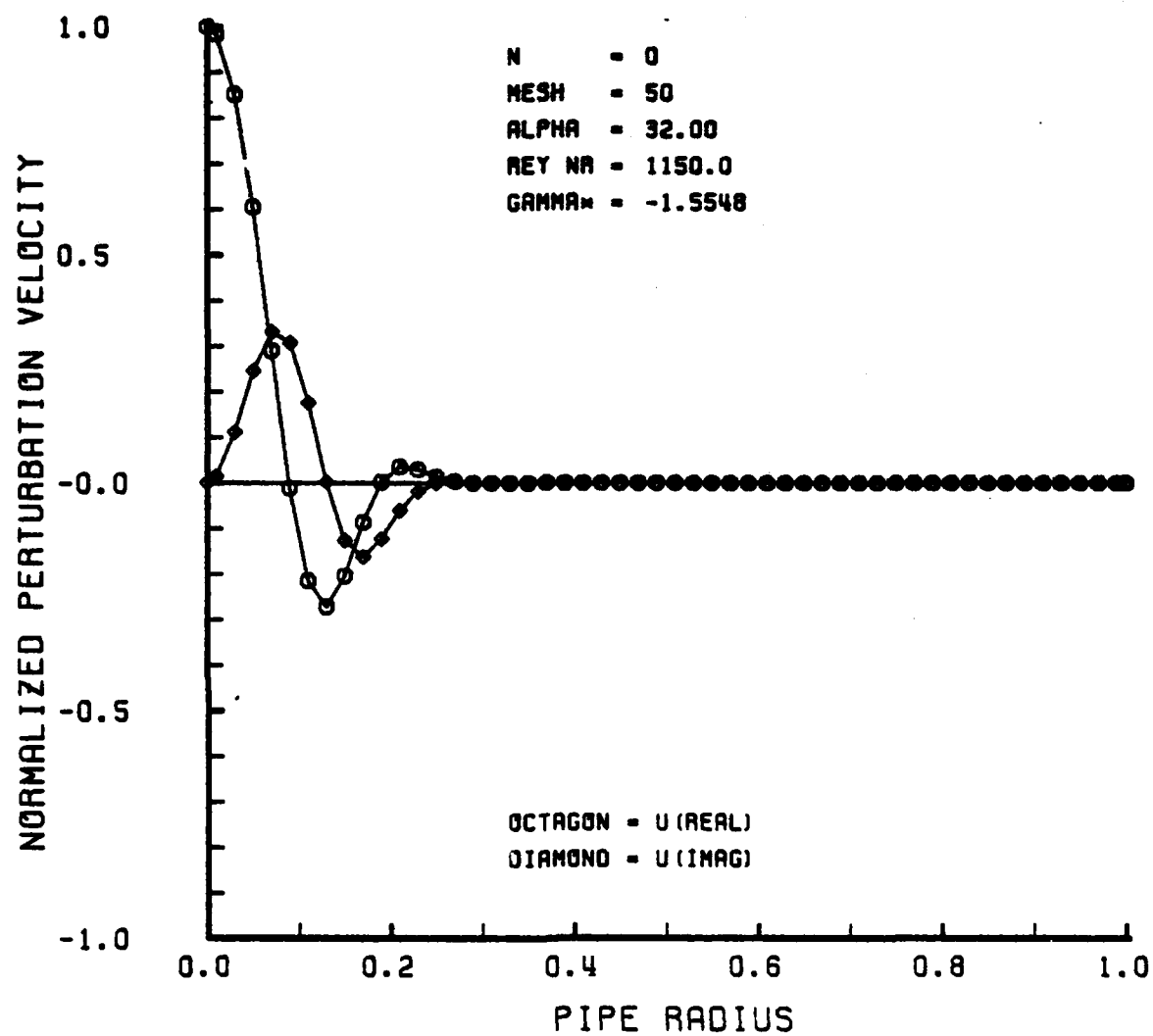


Figure 6-6

AD-A126 767

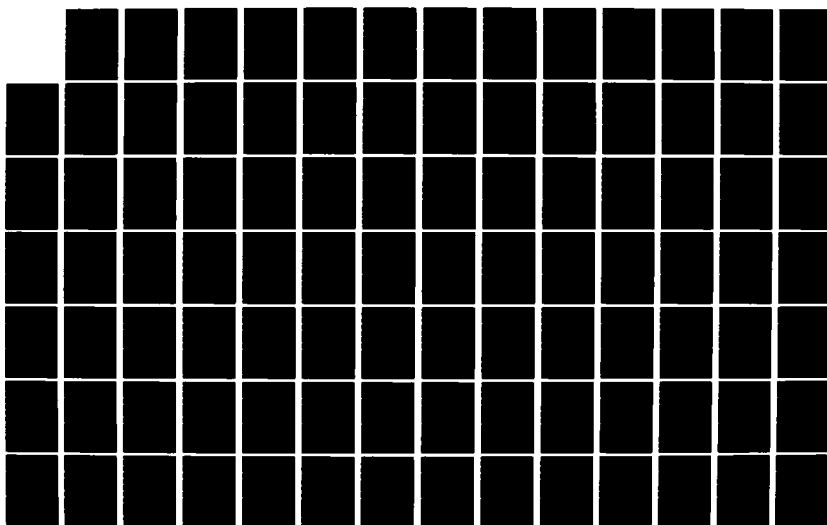
A NUMERICAL ANALYSIS OF PIPE FLOW STABILITY(U) NAVAL
POSTGRADUATE SCHOOL MONTEREY CA D B WALLACE DEC 82

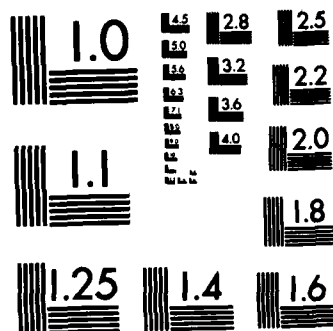
2/3

UNCLASSIFIED

.F/G 28/4

NL





MICROCOPY RESOLUTION TEST CHART
NATIONAL BUREAU OF STANDARDS-1963-A

NORMALIZED PERTURBATION VELOCITY VS RADIUS

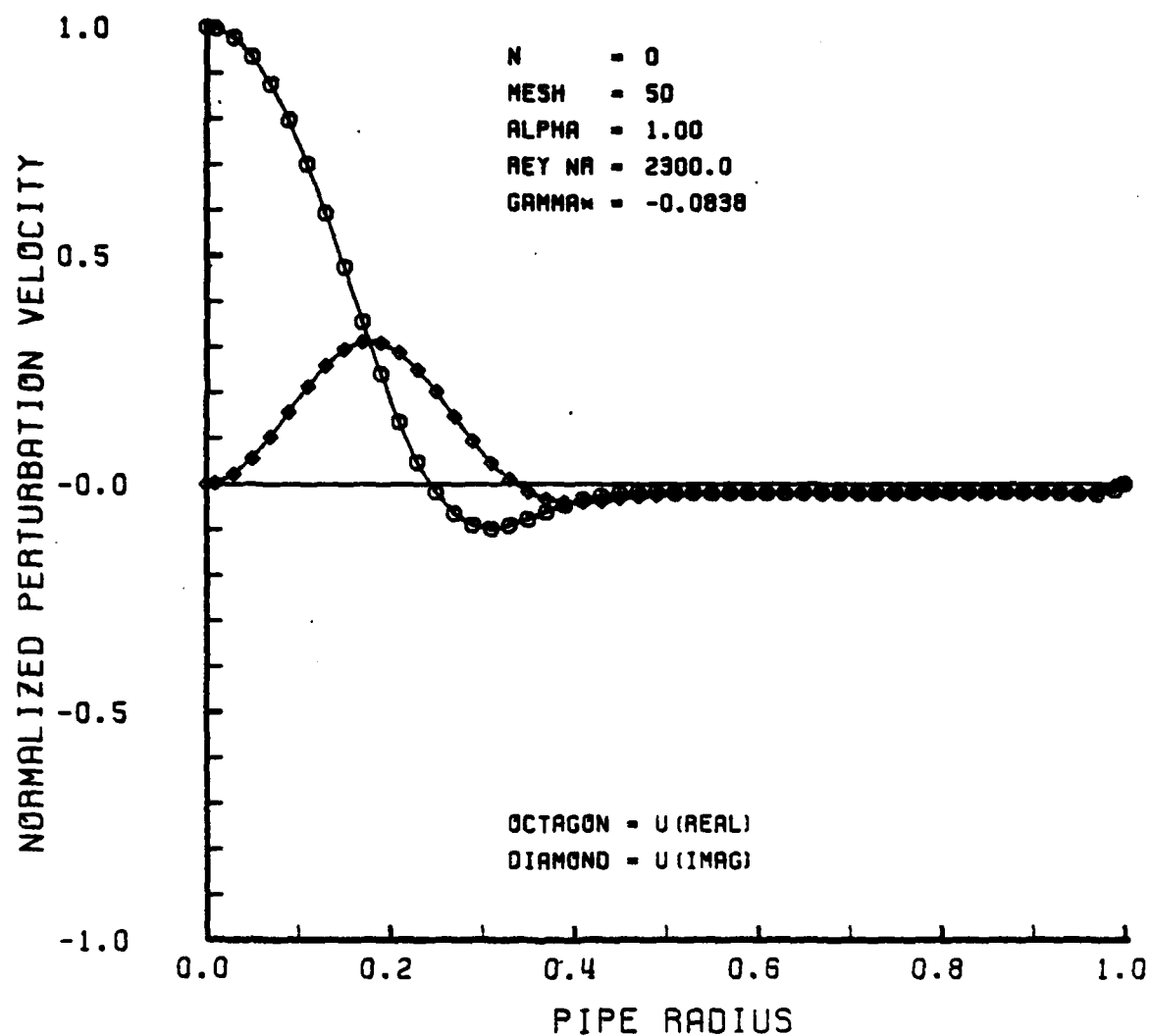


Figure 6-7

NORMALIZED PERTURBATION VELOCITY VS RADIUS

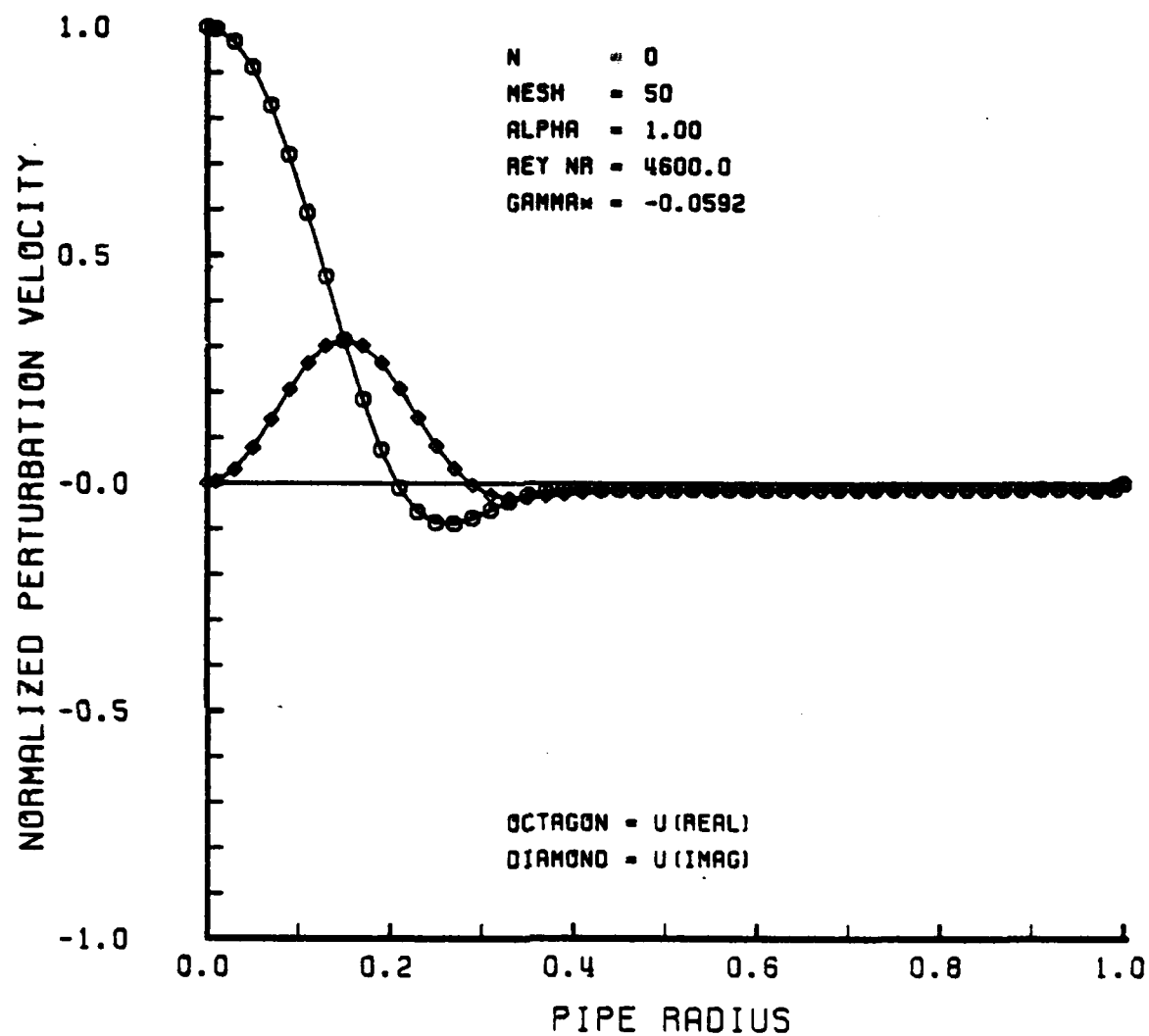


Figure 6-8

NORMALIZED PERTURBATION VELOCITY VS RADIUS

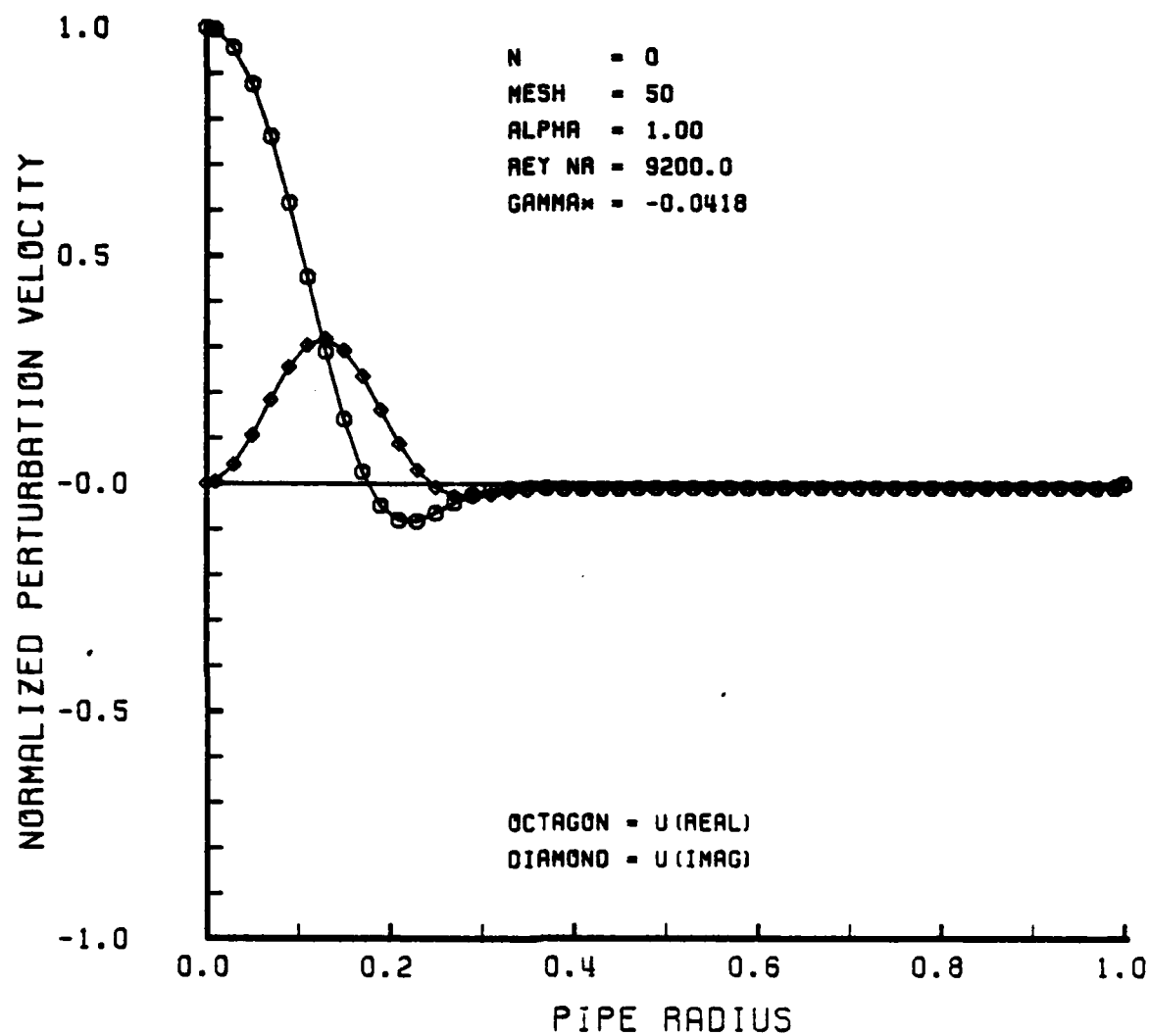


Figure 6-9

B. RESULTS FOR $n = 1$

The numerical results for angular wave number $n = 1$ indicate that flow instabilities indeed exist. There are four factors that may possibly account for the flow instabilities; (1) the complicated nature of the coupled governing equations for $n = 1$, (2) the rigorous way in which the boundary conditions at the axis were derived and enforced, (3) the introduction of additional parameters into the eigensystem, and (4) the appearance of the eigenvalue in a pair of the boundary condition equations. Table 6-2 summarizes the stability data for $n = 1$ over a wide range of Reynolds numbers and axial wave numbers. Once again the dashed table entries indicate inaccurate results. Notice that a mesh size of $n = 48$ was used for this case. This was necessary because of programming constraints that required the eigensystem to be less than or equal to 100×100 . It can be seen that flow instabilities exist at all Reynolds numbers. This occurs coincidentally with small values of α . More detailed stability data is presented in Table 6-3 for axial wave numbers $0 \leq \alpha \leq 1$. It is clear here that the flow becomes more unstable for very small values of $\alpha < 1$. The stability data presented in Tables 6-2 and 6-3 is more easily interpreted as Reynolds number contours in the plots of GAMMA^* vs. α . Figure 6-10 shows Reynolds number contours over a large range of α . It can be clearly seen that the flow is unstable at all Reynolds numbers for small values of axial wave numbers. Figure 6-11 shows a more detailed plot of the Reynolds number contours over a small range of α . Here it can be seen that the flow becomes more unstable for decreasing values of Reynolds numbers! It can

Table 6-2. Stability Data for Angular Wave Number $n = 1$

Growth or Decay Trends of Least Stable Eigenvalue, γ^*

Re	$\alpha=0.0$	$\alpha=0.05$	$\alpha=1.0$	$\alpha=2.0$	$\alpha=4.0$	$\alpha=8.0$	$\alpha=16.0$	$\alpha=32.0$
300	0.0606	0.0626	-0.0215	-0.2883	-0.3734	-0.7623	-1.3222	-
575	0.0316	0.0270	-0.0601	-0.1983	-0.2530	-0.4638	-1.1246	-0.7546
1150	0.0158	0.0026	-0.0876	-0.1362	-0.1723	-0.2805	-0.7067	-
2300	0.0079	-0.0131	-0.0675	-0.0947	-0.1205	-0.1745	-0.4004	-
4600	0.0039	-0.0237	-0.0476	-0.0664	-0.0860	-0.1117	-0.2327	-
9200	0.0020	-0.0239	-0.0336	-0.0467	-0.0617	-0.0736	-	-
18400	0.0010	-0.0169	-0.0238	-0.0328	-0.0436	-0.0497	-	-

Note: Values are based on 48 mesh points.

Table 6-3. Stability Data for Angular Wave Number $n = 1$

Growth or Decay Trends of Least Stable Eigenvalue, γ^*

Re	$\alpha=0.0$	$\alpha=0.05$	$\alpha=0.10$	$\alpha=0.15$	$\alpha=0.20$	$\alpha=0.50$	$\alpha=0.75$	$\alpha=1.0$
300	0.0606	0.0657	0.0718	0.0743	0.0743	0.0626	0.0322	-0.0215
575	0.0316	0.0374	0.0394	0.0395	0.0398	0.0270	-0.0057	-0.0601
1150	0.0158	0.0198	0.0204	0.0208	0.0202	0.0026	-0.0324	-0.0876
2300	0.0079	0.0103	0.0105	0.0096	0.0081	-0.0131	-0.0507	-0.0675
4600	0.0039	0.0053	0.0044	0.0028	0.0006	-0.0237	-0.0413	-0.0476
9200	0.0020	0.0022	0.0006	-0.0016	-0.0042	-0.0239	-0.0292	-0.0336
18400	0.0010	0.0003	-0.0018	-0.0044	-0.0074	-0.0169	-0.0206	-0.0238

Note: Values are based on 48 mesh points.

also be seen here that the flow becomes even more unstable for small values of α only slightly larger than zero. The reason for these results cannot be readily explained but it is obvious that they are in direct conflict with observed experimental results. When $\alpha > 1$, however, the contours show an asymptotic trend toward neutral stability for increasing Reynolds numbers; in other words, increasing Reynolds number has a destabilizing effect on the flow which agrees with experimental results. A slightly different method of presenting the data can be seen in Figure 6-12, as alpha contours in the plot of GAMMA* vs. Reynolds number. This plot further emphasizes the results discussed above; the flow is unstable at all Reynolds numbers for small alpha, increasing Reynolds number has a destabilizing effect on the flow and increasing axial wave number has a stabilizing effect.

Normalized perturbation velocity plots were also produced for this case and show some interesting trends. The behavior of the axial perturbation velocity for selected values of Re and α appear in Figures 6-13 through 6-23 on the following pages. Upon close examination of the perturbation velocity plots, it becomes apparent that the computational mesh is not sufficiently fine to adequately approximate the velocity function as α is increased. This problem will be discussed shortly.

It is interesting to note that the perturbation activity shifts from the pipe wall to the axis for increasing values of the axial wave number while Reynolds number remains constant. At small values of α , the activity originates at the wall. At larger values of α , the activity shifts to the axis, for the most part. At even larger values of α , the activity moves away from the axis to the region between the axis and

wall. However, some degree of activity remains at the wall for the last two cases. The change in the perturbation activity as described above can be seen in Figures 6-14 through 6-16 for $Re = 575$ and in Figures 6-19 through 6-21 for $Re = 2300$. The shift of perturbation activity to the axis with increasing axial wave number deserves comment here. Schlichting [Ref. 16] observed that the transition to turbulence is "characterized by the appearance of self-sustaining turbulent flashes which emanate from fluid layers near the wall along the tube." Therefore, it appears that unstable flows are associated with perturbation activity near the wall. As the activity shifts away from the wall with increasing axial wave number, the flow becomes stable. Additionally, after the activity moves to the axis, some degree of activity remains at the wall. While the solution appears to remain stable, it is recommended that this peculiarity be examined further. The use of a finer mesh to resolve this activity at the wall would be useful here.

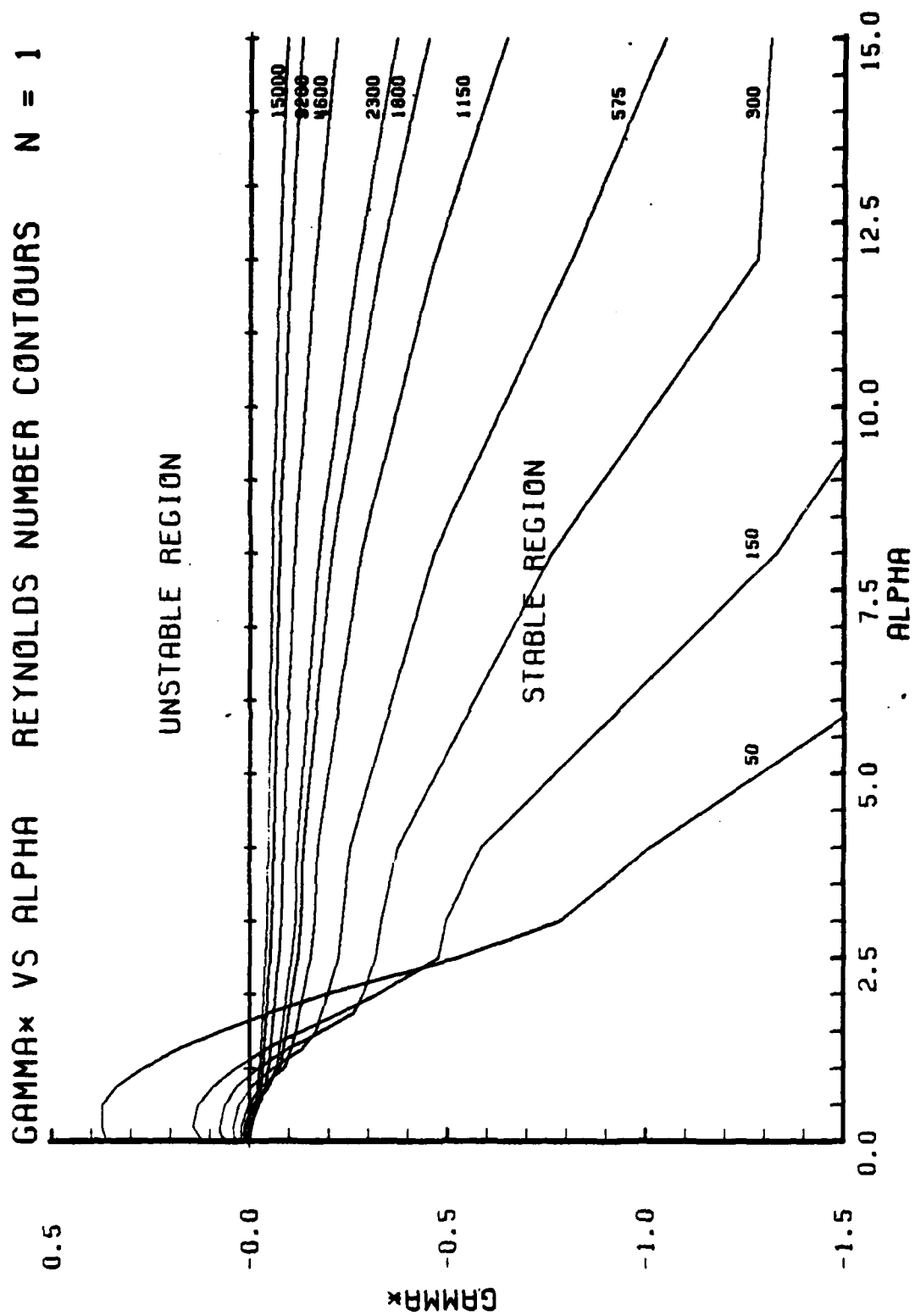


Figure 6-10

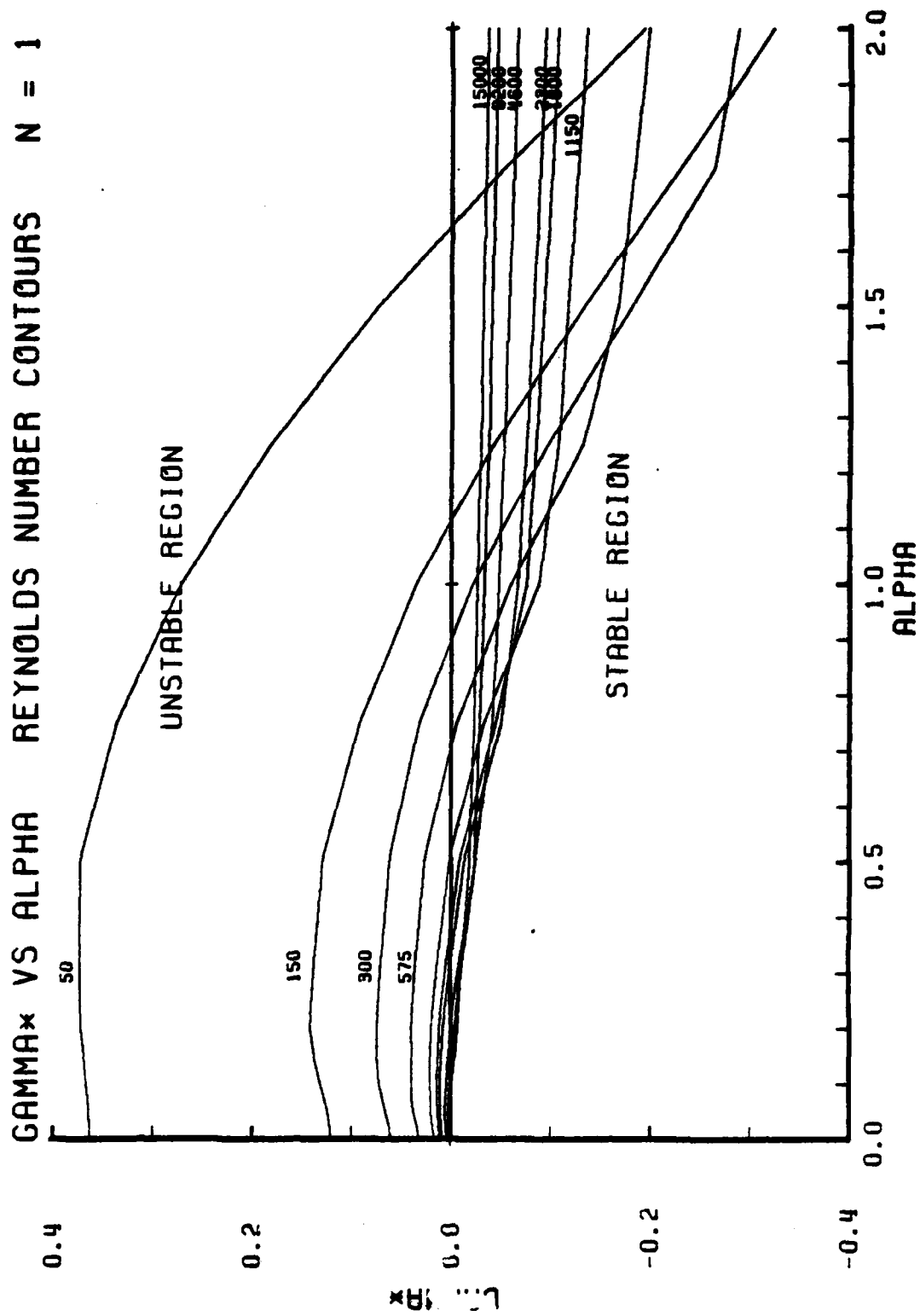


Figure 6-11

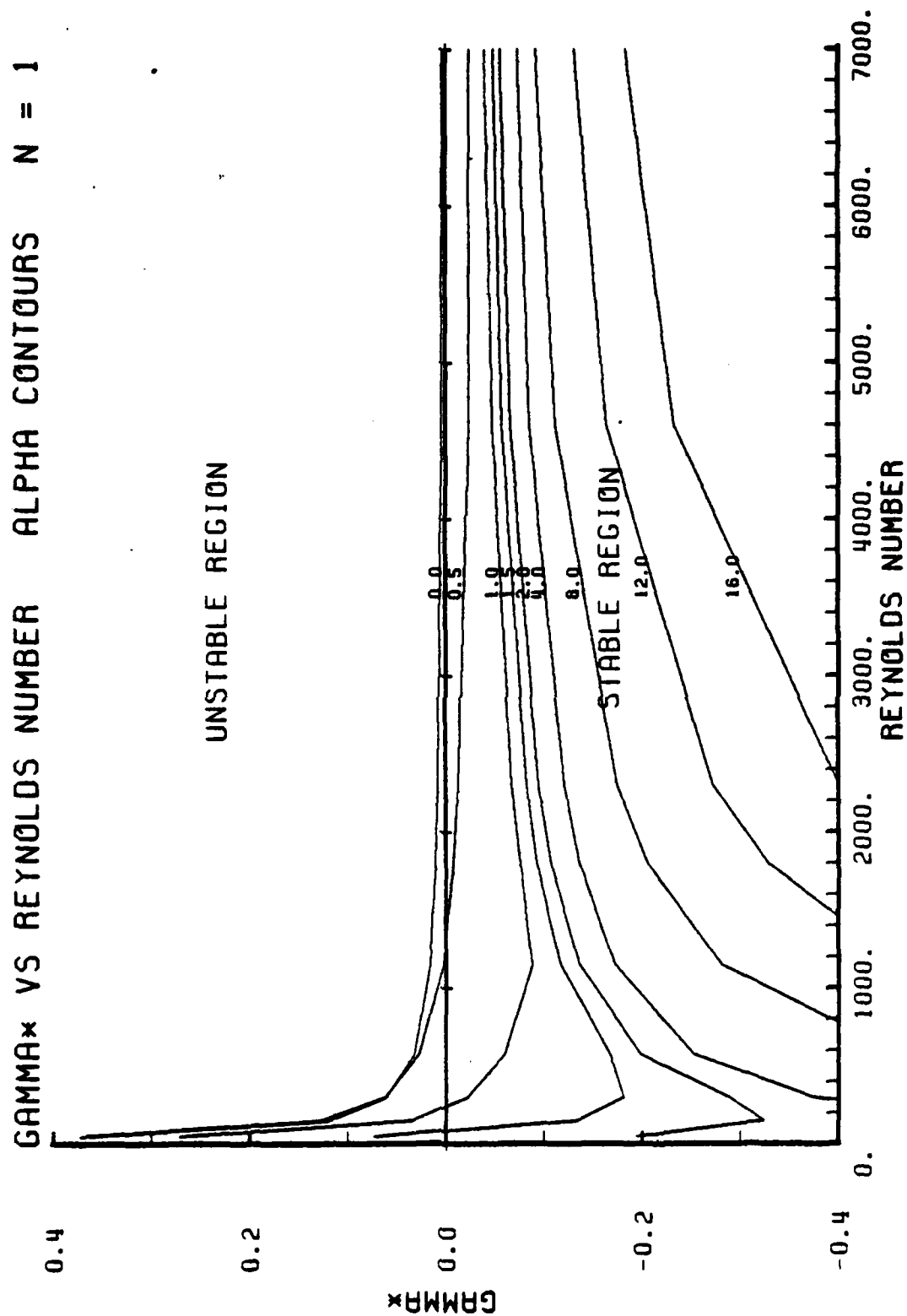


Figure 6-12

NORMALIZED PERTURBATION VELOCITY VS RADIUS

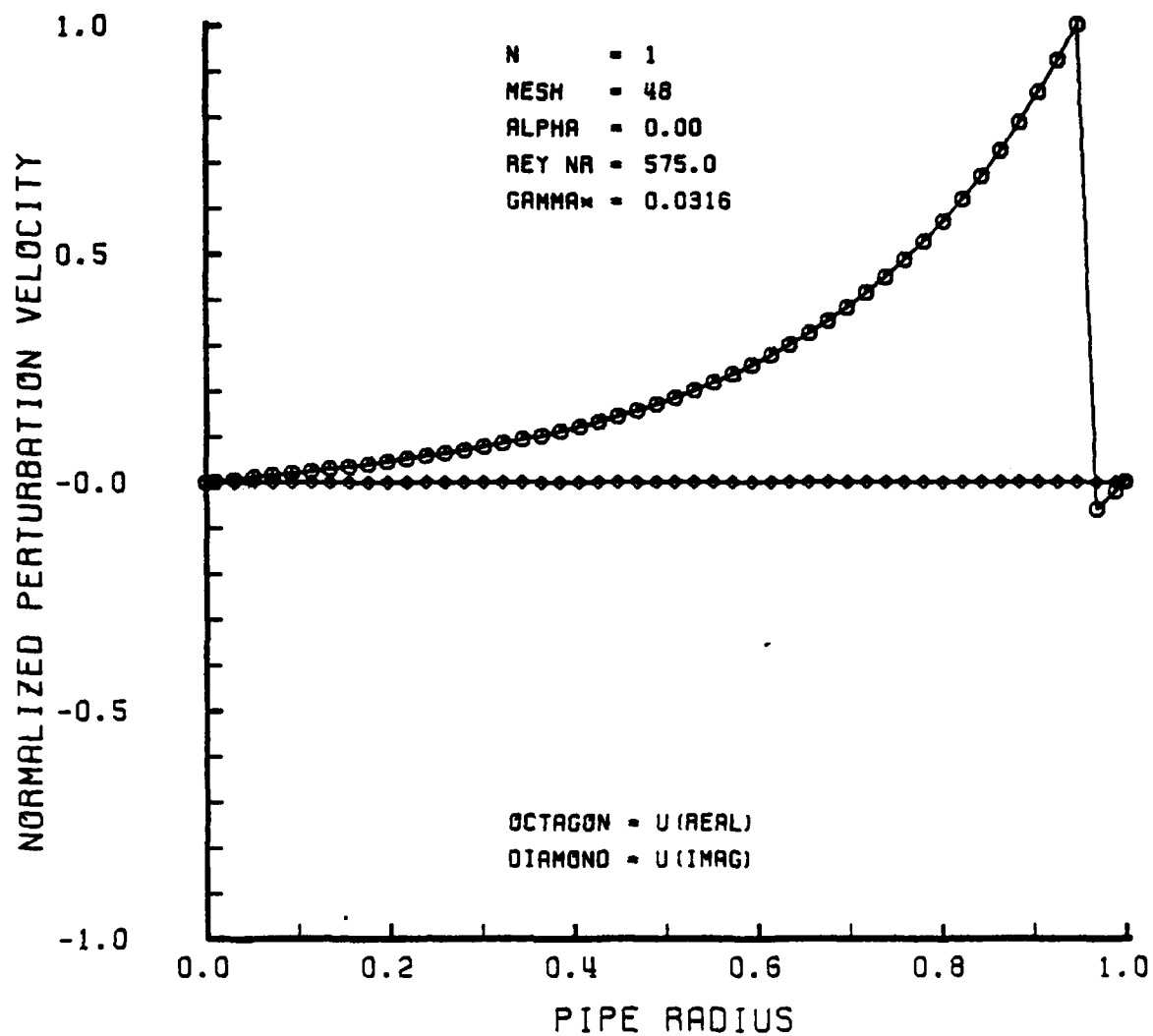


Figure 6-13

NORMALIZED PERTURBATION VELOCITY VS RADIUS

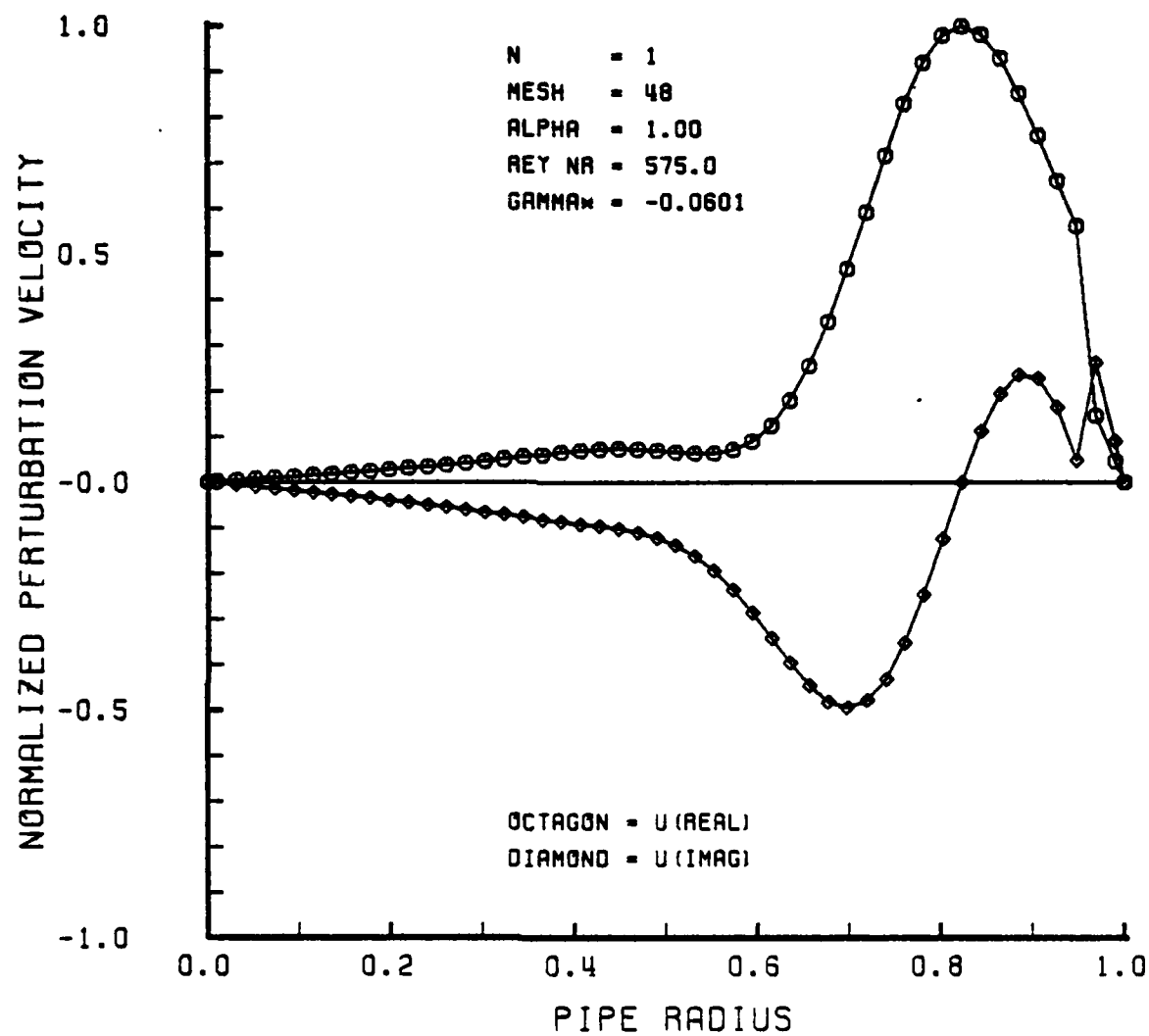


Figure 6-14

NORMALIZED PERTURBATION VELOCITY VS RADIUS

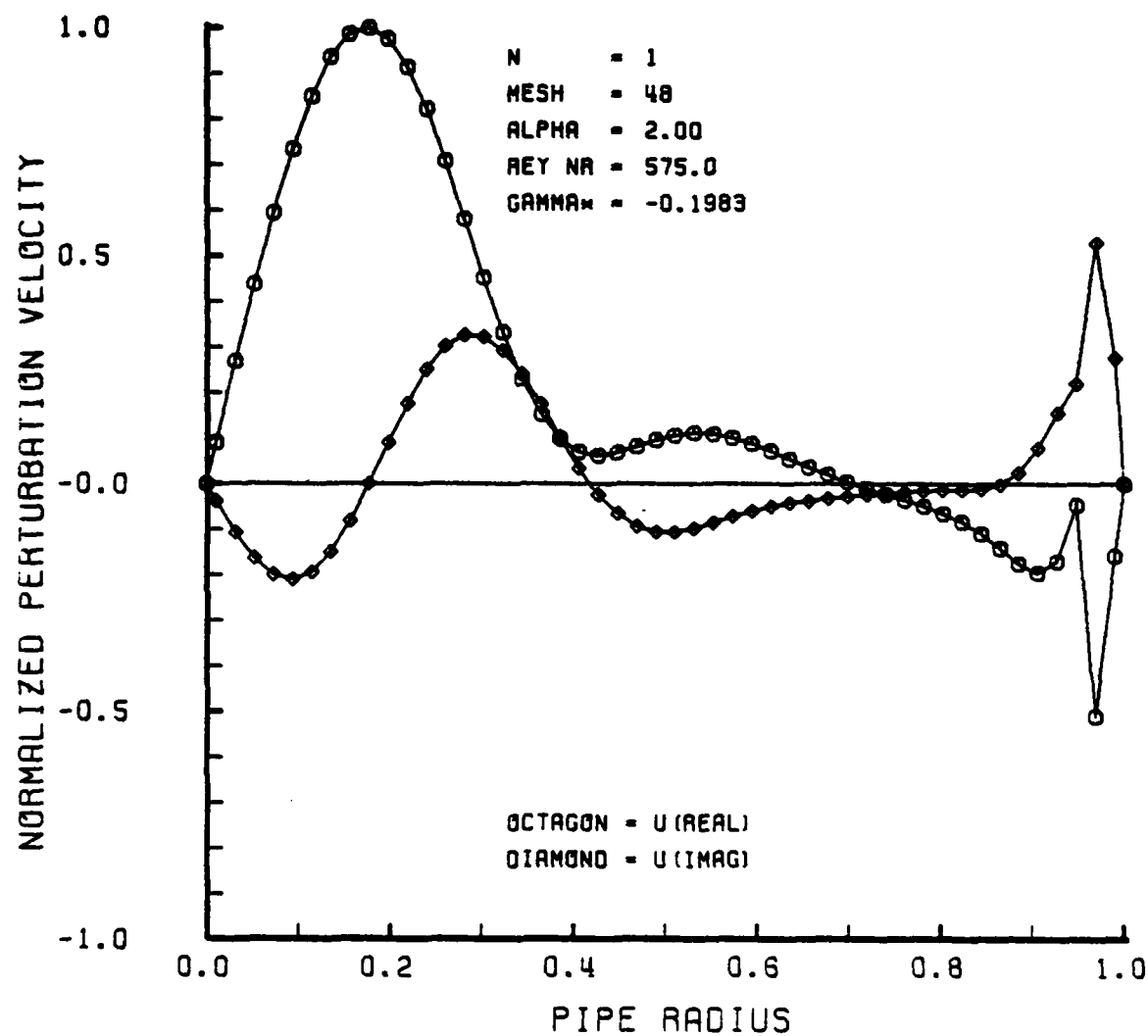


Figure 6-15

NORMALIZED PERTURBATION VELOCITY VS RADIUS

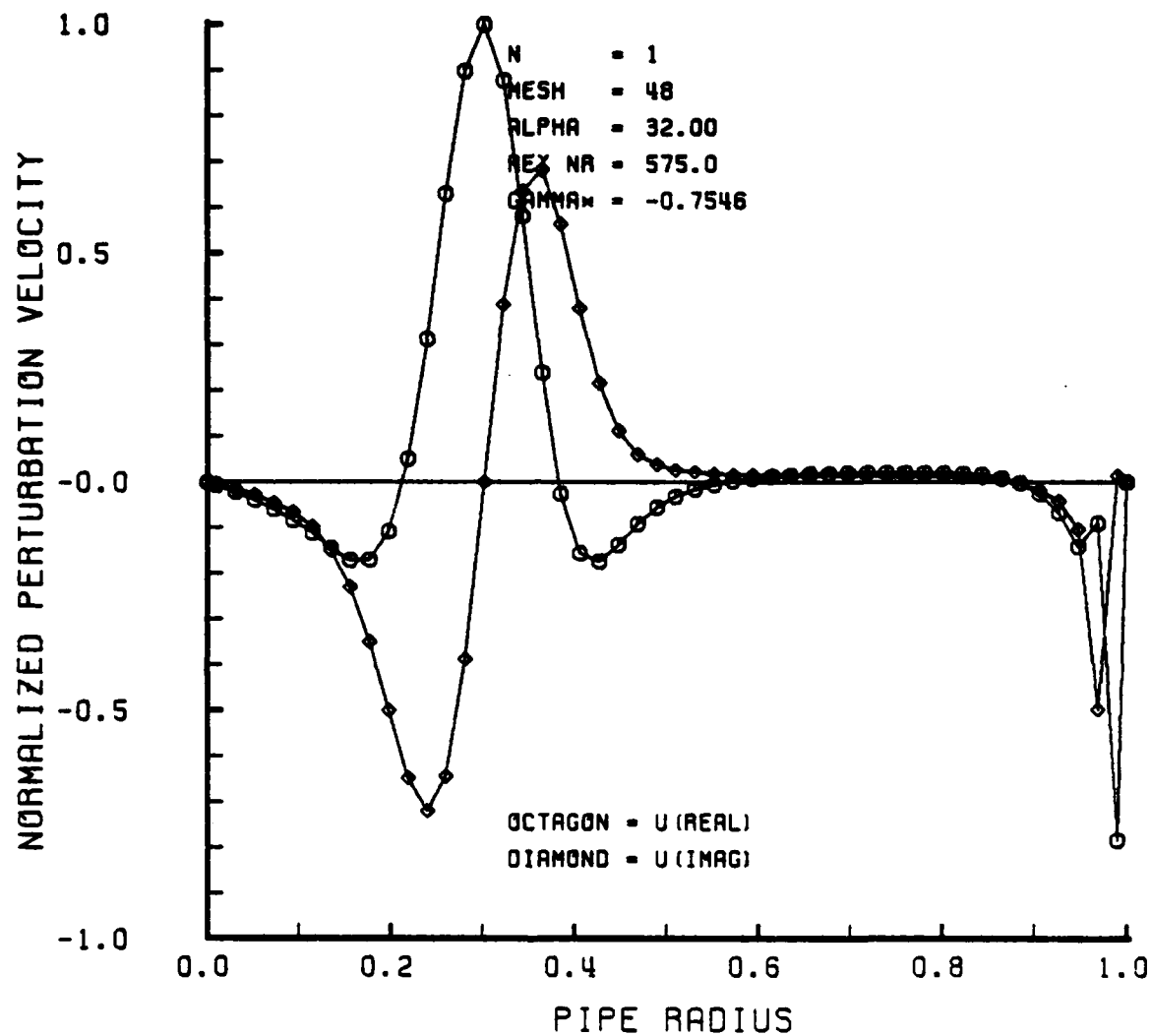


Figure 6-16

NORMALIZED PERTURBATION VELOCITY VS RADIUS

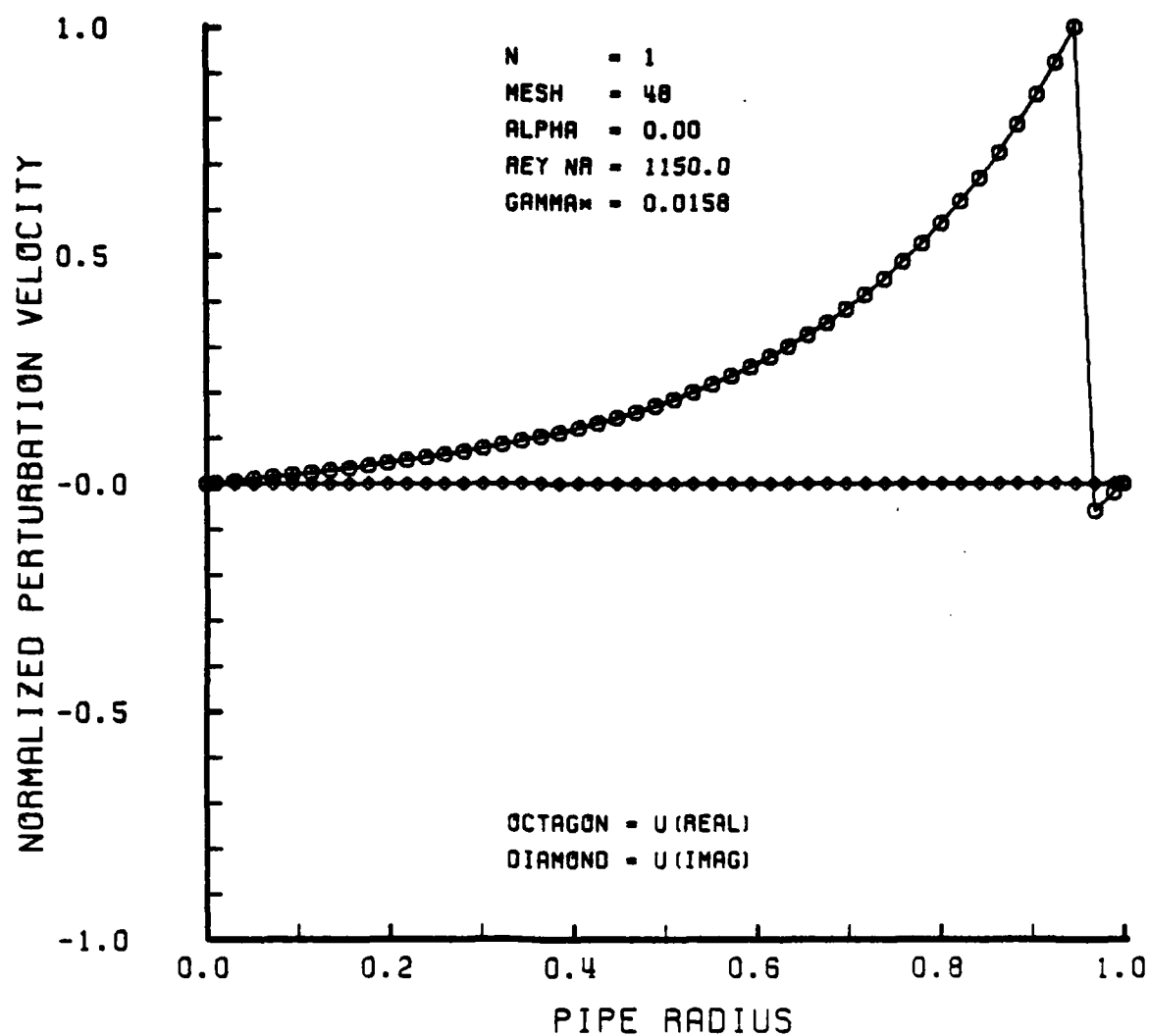


Figure 6-17

NORMALIZED PERTURBATION VELOCITY VS RADIUS

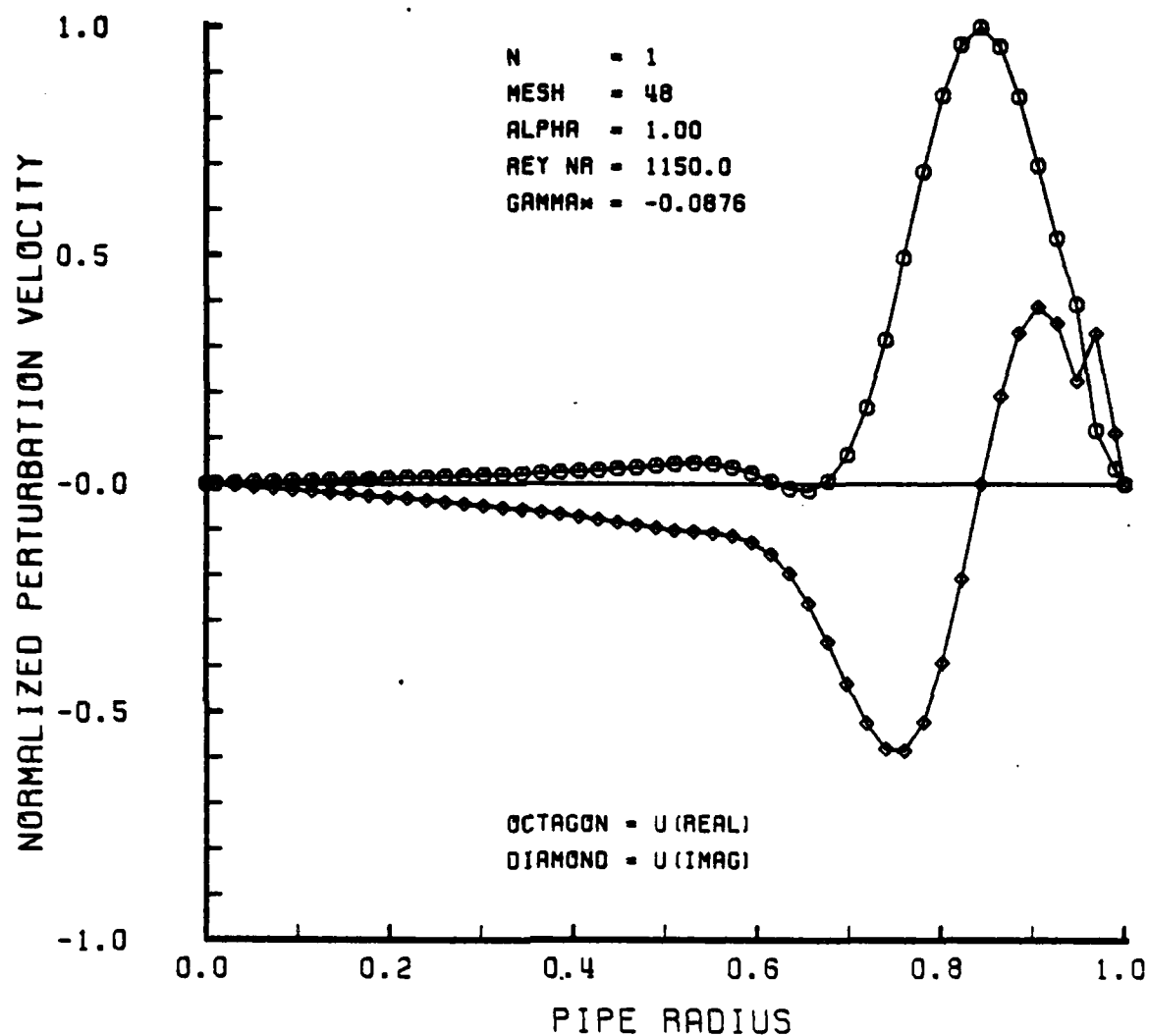


Figure 6-18

NORMALIZED PERTURBATION VELOCITY VS RADIUS

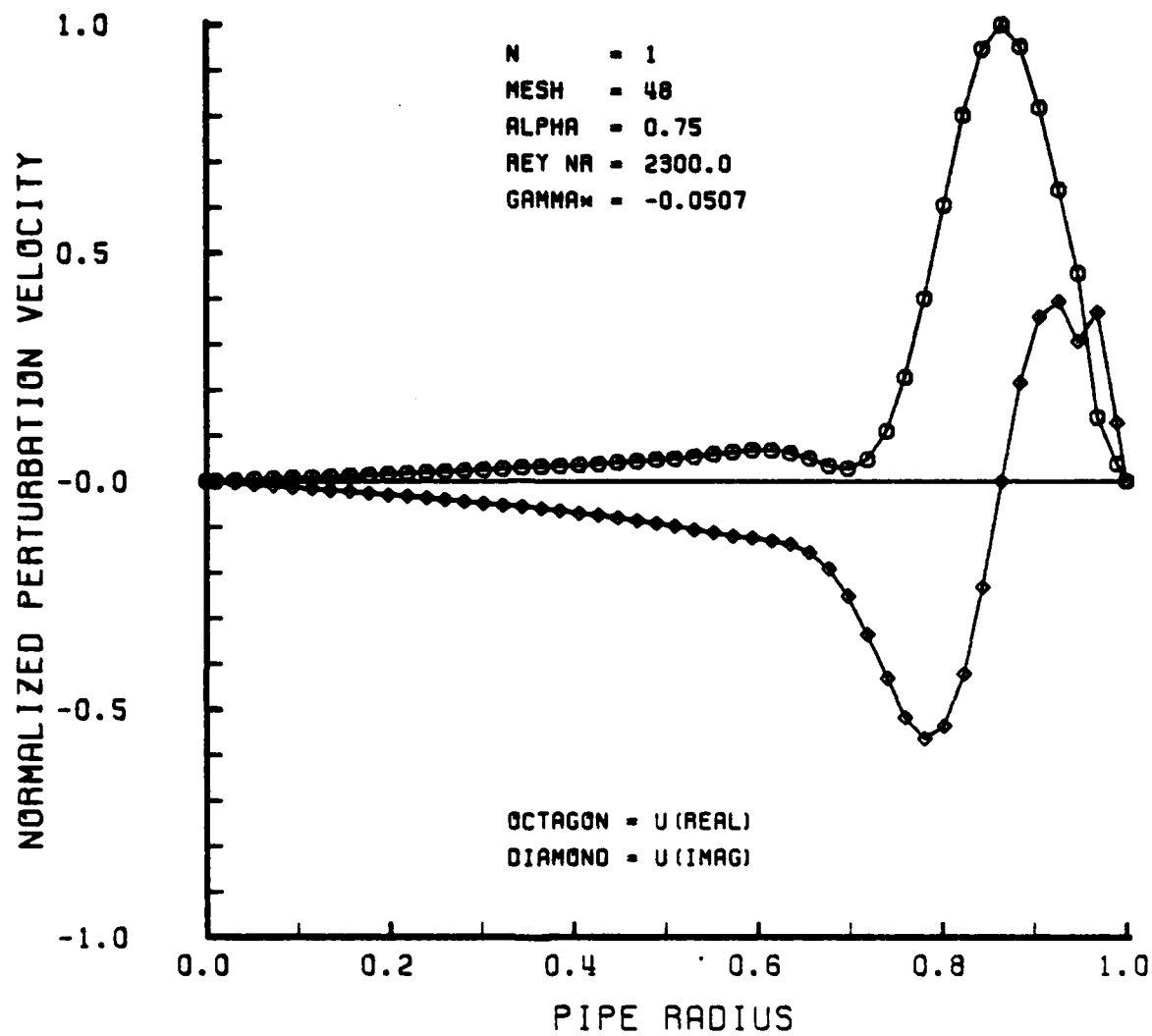


Figure 6-19

NORMALIZED PERTURBATION VELOCITY VS RADIUS

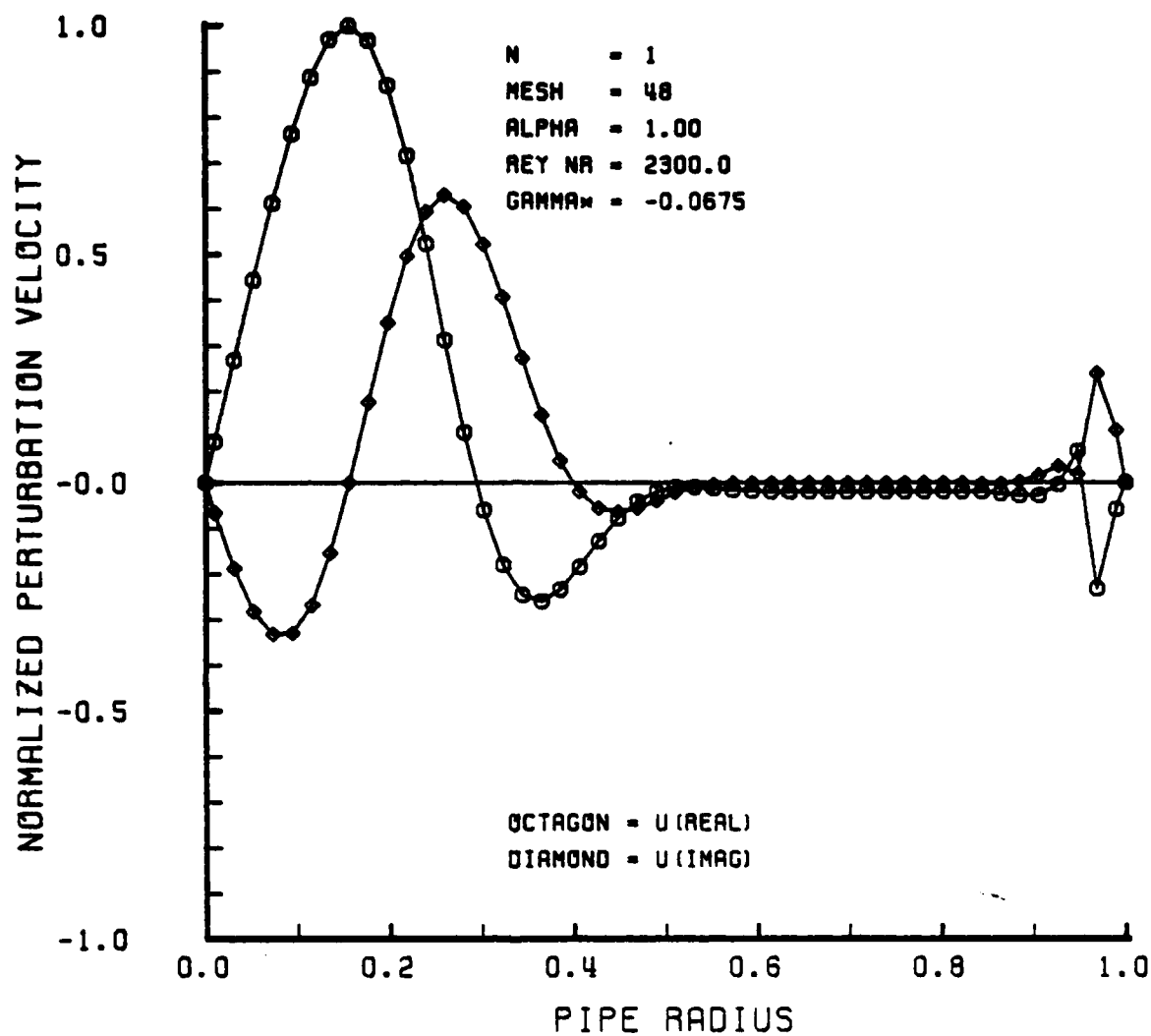


Figure 6-20

NORMALIZED PERTURBATION VELOCITY VS RADIUS

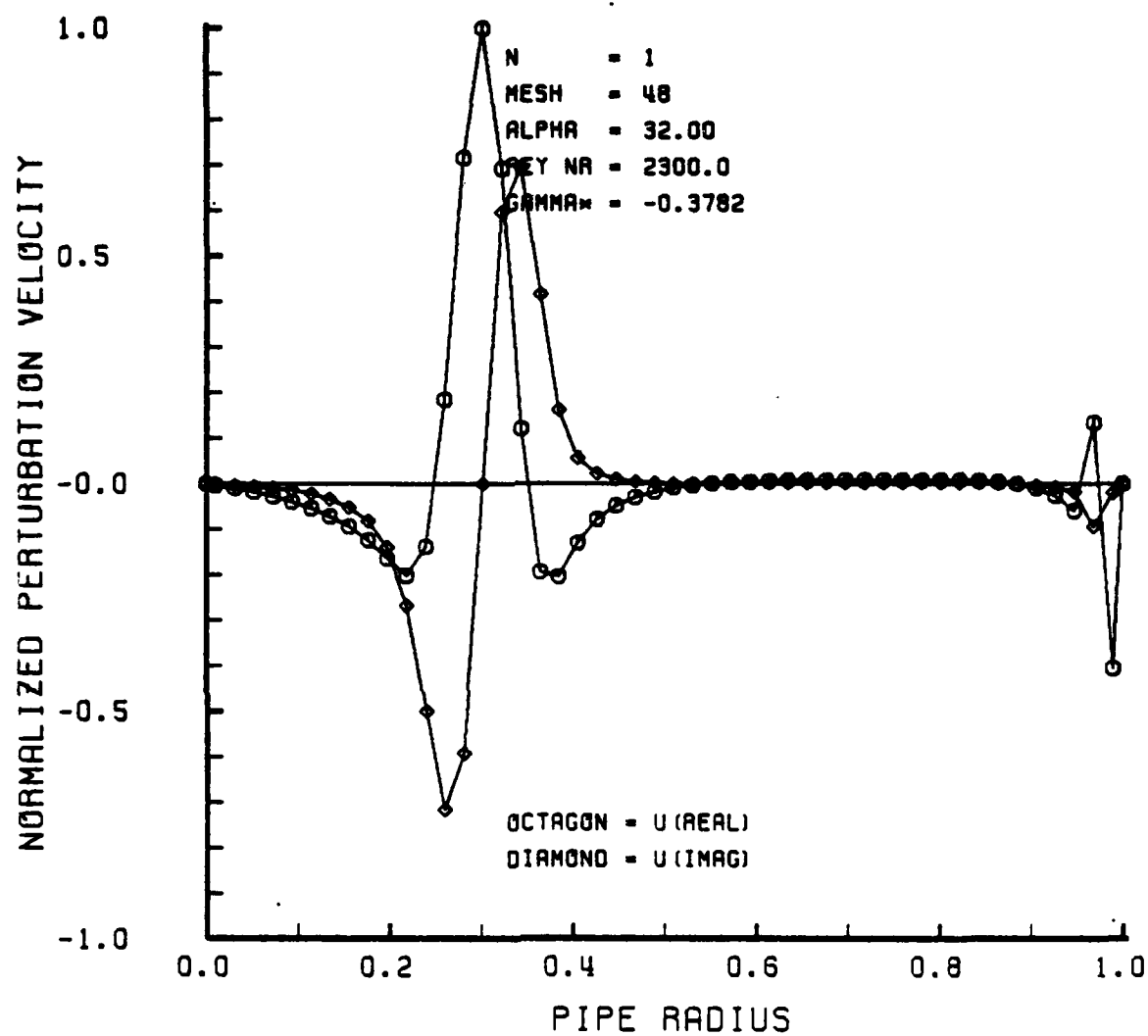


Figure 6-21

NORMALIZED PERTURBATION VELOCITY VS RADIUS

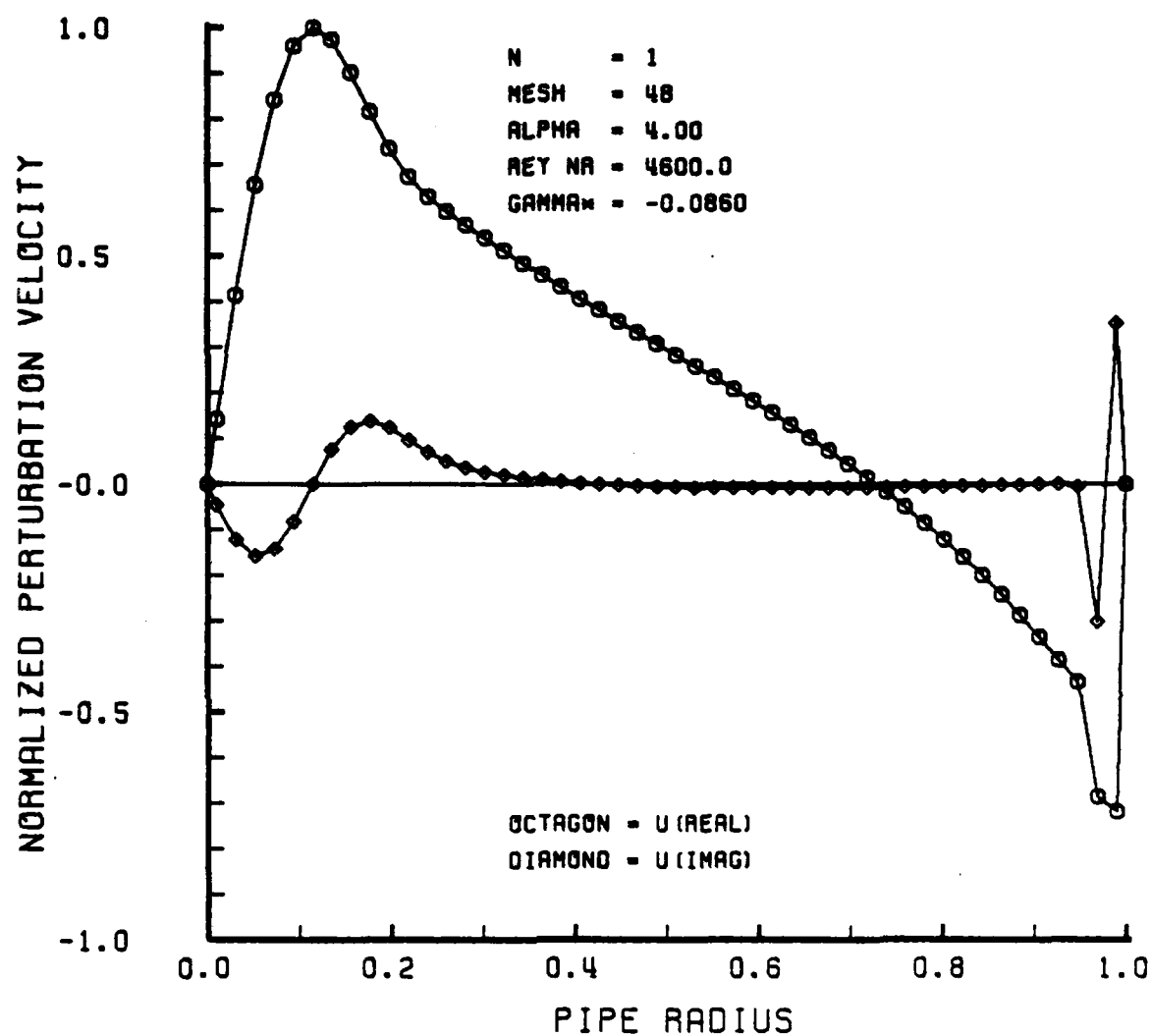


Figure 6-22

NORMALIZED PERTURBATION VELOCITY VS RADIUS

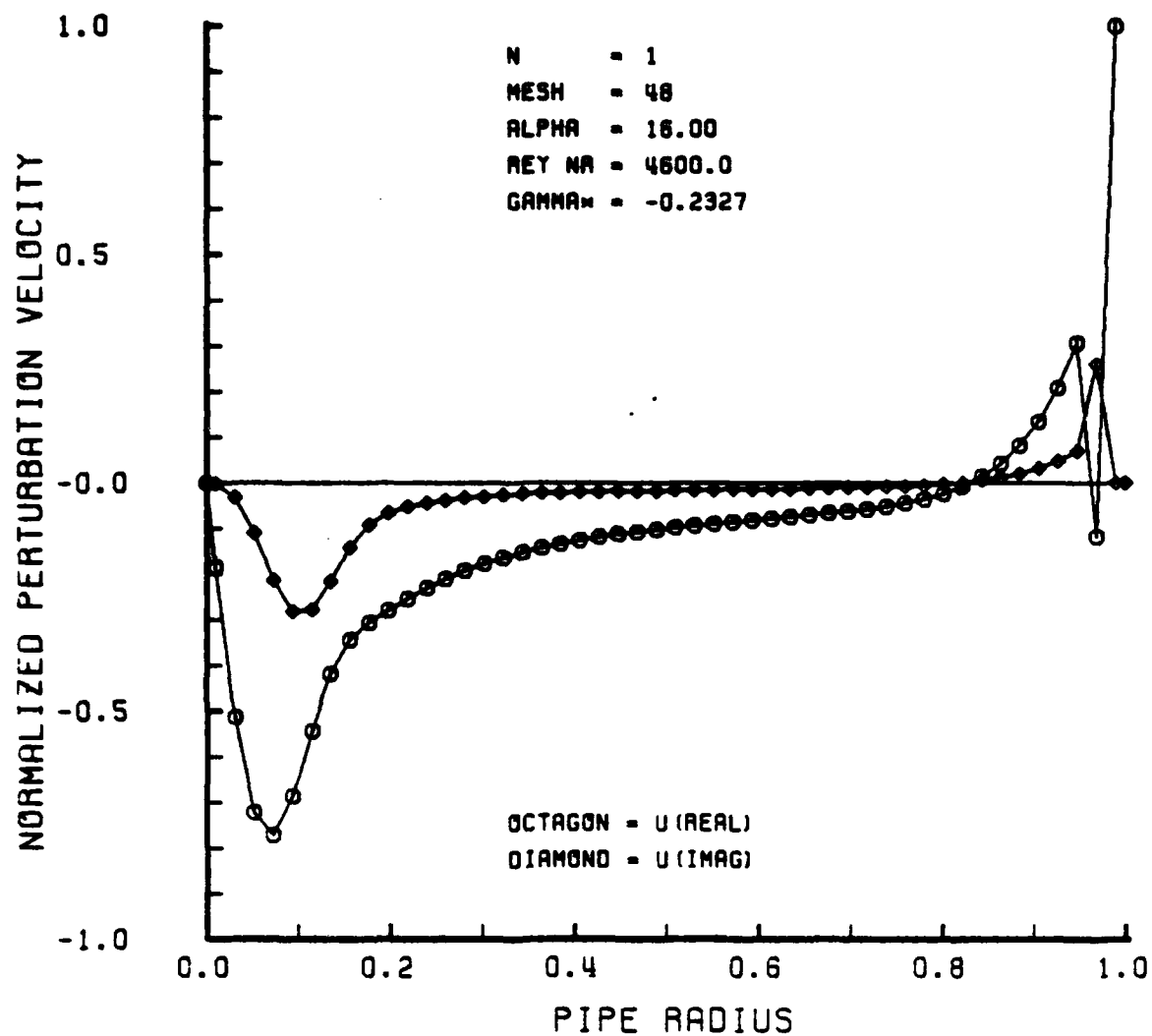


Figure 6-23

C. RESULTS FOR $n = 6$

Results for angular wave number $n = 6$ are similar to those for $n = 0$ in that the flow is stable at all Reynolds numbers. Stability data is presented in Tables 6-4 and 6-5 where it can be determined that this is the case. The data is once again presented as Reynolds number contours in the plots of GAMMA^* vs. α in Figures 6-24 and 6-25 and as α contours in the plot of GAMMA^* vs. Reynolds number in Figure 6-26. The trends are clear; the flow is stable at all Reynolds numbers, increasing Reynolds number has a destabilizing effect on the flow and increasing the axial wave number has a stabilizing effect.

Figures 6-27 through 6-36 are representative perturbation velocity plots for $n = 6$ at several Reynolds numbers and axial wave numbers. It can be seen in Figures 6-31 and 6-32 that the perturbation activity shifts from the wall to the axis for increasing α .

Table 6-4. Stability Data for Angular Wave Number $n = 6$

Growth or Decay Trends of Least Stable Eigenvalue, γ^*

Re	$\alpha=0.0$	$\alpha=0.05$	$\alpha=1.0$	$\alpha=2.0$	$\alpha=4.0$	$\alpha=8.0$	$\alpha=16.0$	$\alpha=32.0$
300	-0.3291	-0.3512	-0.4829	-0.7295	-1.1654	-1.9718	-2.8067	-4.6185
575	-0.1717	-0.2450	-0.3644	-0.5651	-0.9064	-1.4798	-2.0927	-
1150	-0.0858	-0.1814	-0.2789	-0.4386	-0.7049	-1.0532	-	-
2300	-0.0429	-0.1390	-0.2173	-0.3447	-0.5136	-	-	-
4600	-0.0215	-0.1084	-0.1712	-0.2549	-0.3631	-	-	-
9200	-0.0107	-0.0855	-0.1272	-0.1802	-0.2565	-	-	-
18400	-0.0054	-0.0636	-0.0899	-0.1273	-0.1811	-	-	-

Note: Values are based on 50 mesh points.

Table 6-5. Stability Data for Angular Wave Number $n = 6$

Growth or Decay Trends of Least Stable Eigenvalue, γ^*

Re	$\alpha=0.0$	$\alpha=0.05$	$\alpha=0.10$	$\alpha=0.15$	$\alpha=0.20$	$\alpha=0.50$	$\alpha=0.75$	$\alpha=1.0$
300	-0.3291	-0.3267	-0.3228	-0.3201	-0.3192	-0.3512	-0.4156	-0.4829
575	-0.1717	-0.1686	-0.1665	-0.1679	-0.1727	-0.2450	-0.3071	-0.3644
1150	-0.0858	-0.0833	-0.0864	-0.0960	-0.1092	-0.1814	-0.2325	-0.2789
2300	-0.0429	-0.0432	-0.0546	-0.0675	-0.0794	-0.1390	-0.1801	-0.2173
4600	-0.0215	-0.0273	-0.0397	-0.0505	-0.0603	-0.1084	-0.1414	-0.1712
9200	-0.0107	-0.0198	-0.0302	-0.0390	-0.0469	-0.0855	-0.1102	-0.1272
18400	-0.0054	-0.0151	-0.0234	-0.0305	-0.0368	-0.0636	-0.0779	-0.0899

Note: Values are based on 50 mesh points.

GAMMA* VS ALPHA REYNOLDS NUMBER CONTOURS N = 6

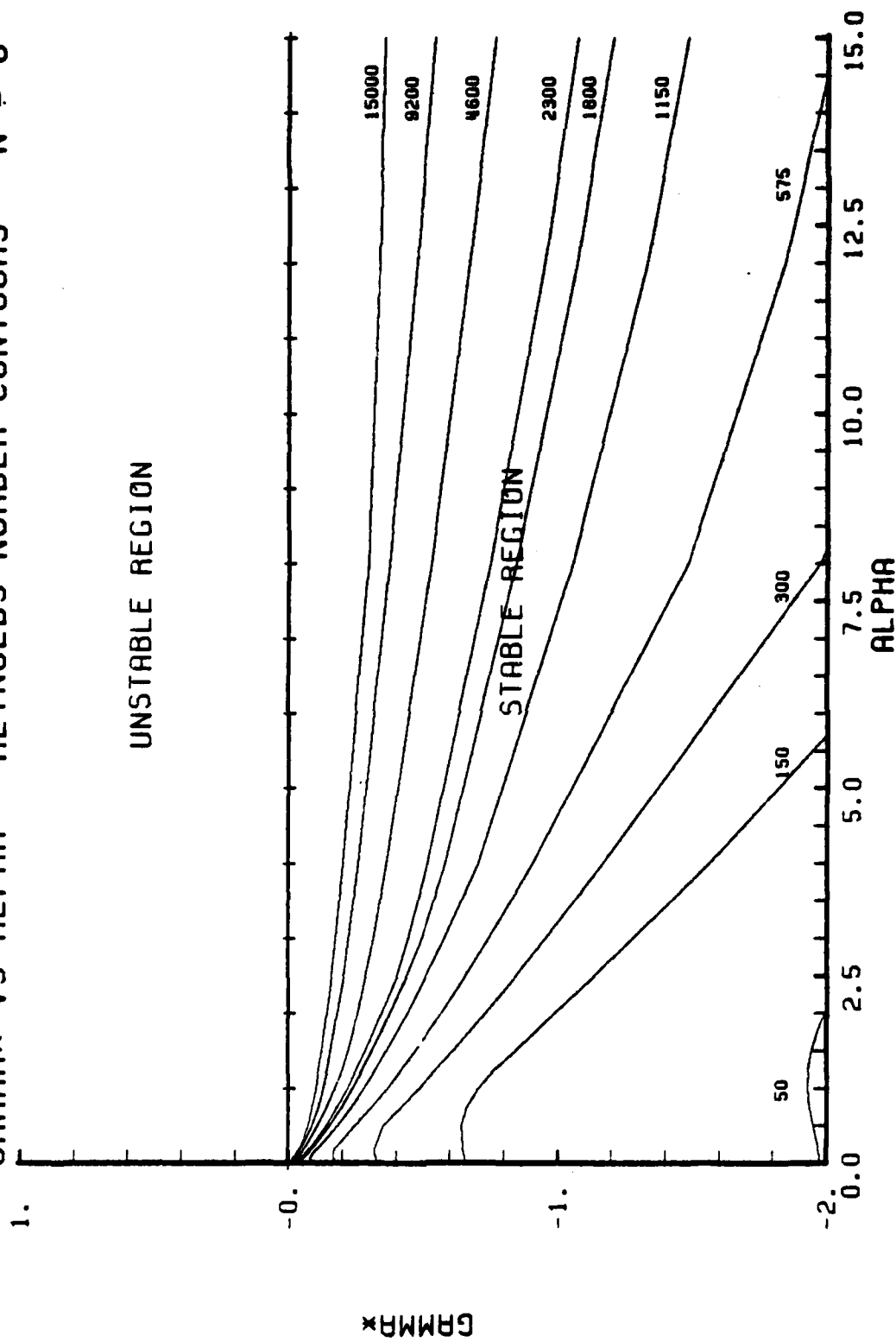


Figure 6-24

GAMMA* VS ALPHA REYNOLDS NUMBER CONTOURS N = 6

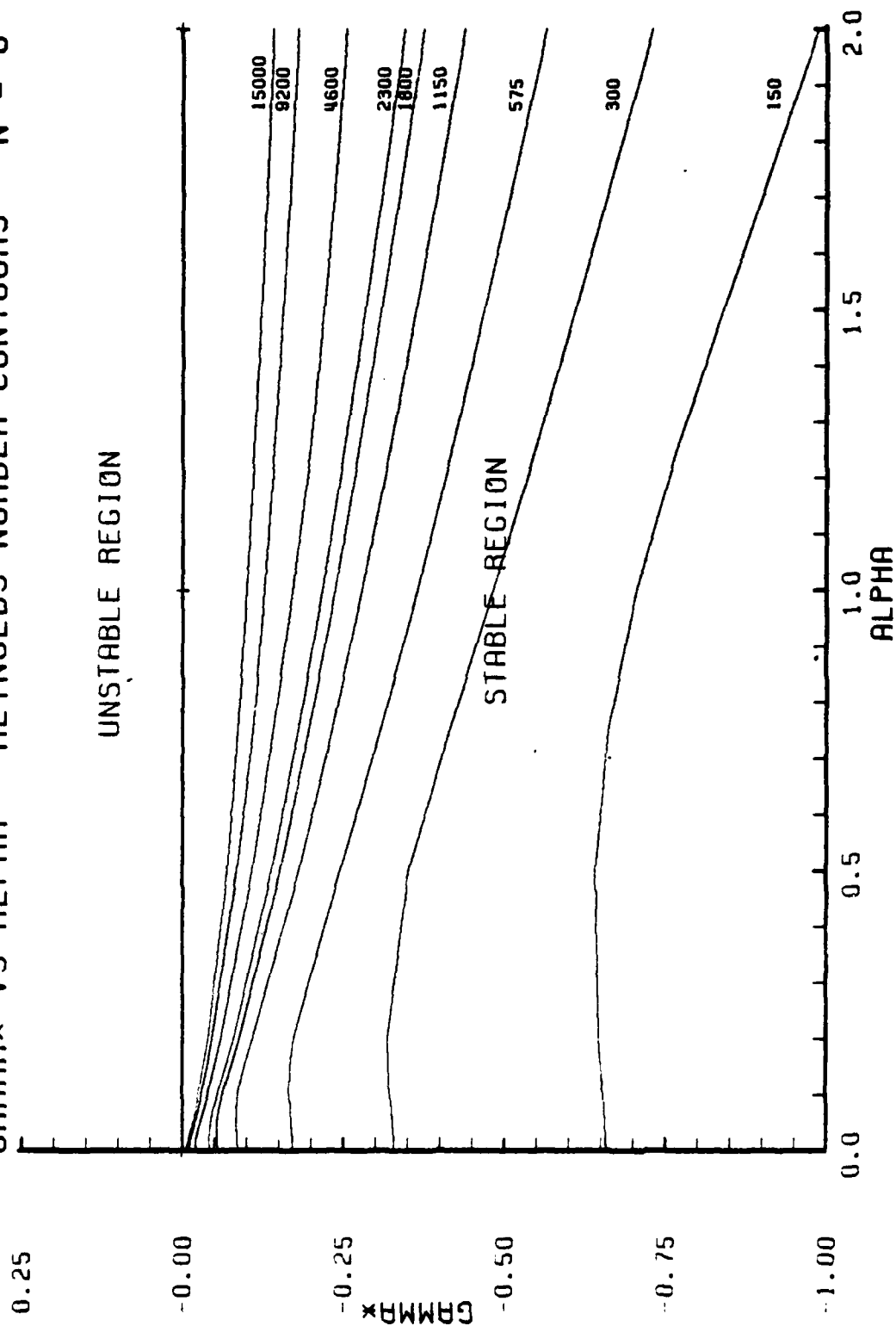


Figure 6-25

GAMMA* VS REYNOLDS NUMBER ALPHA CONTOURS N = 6

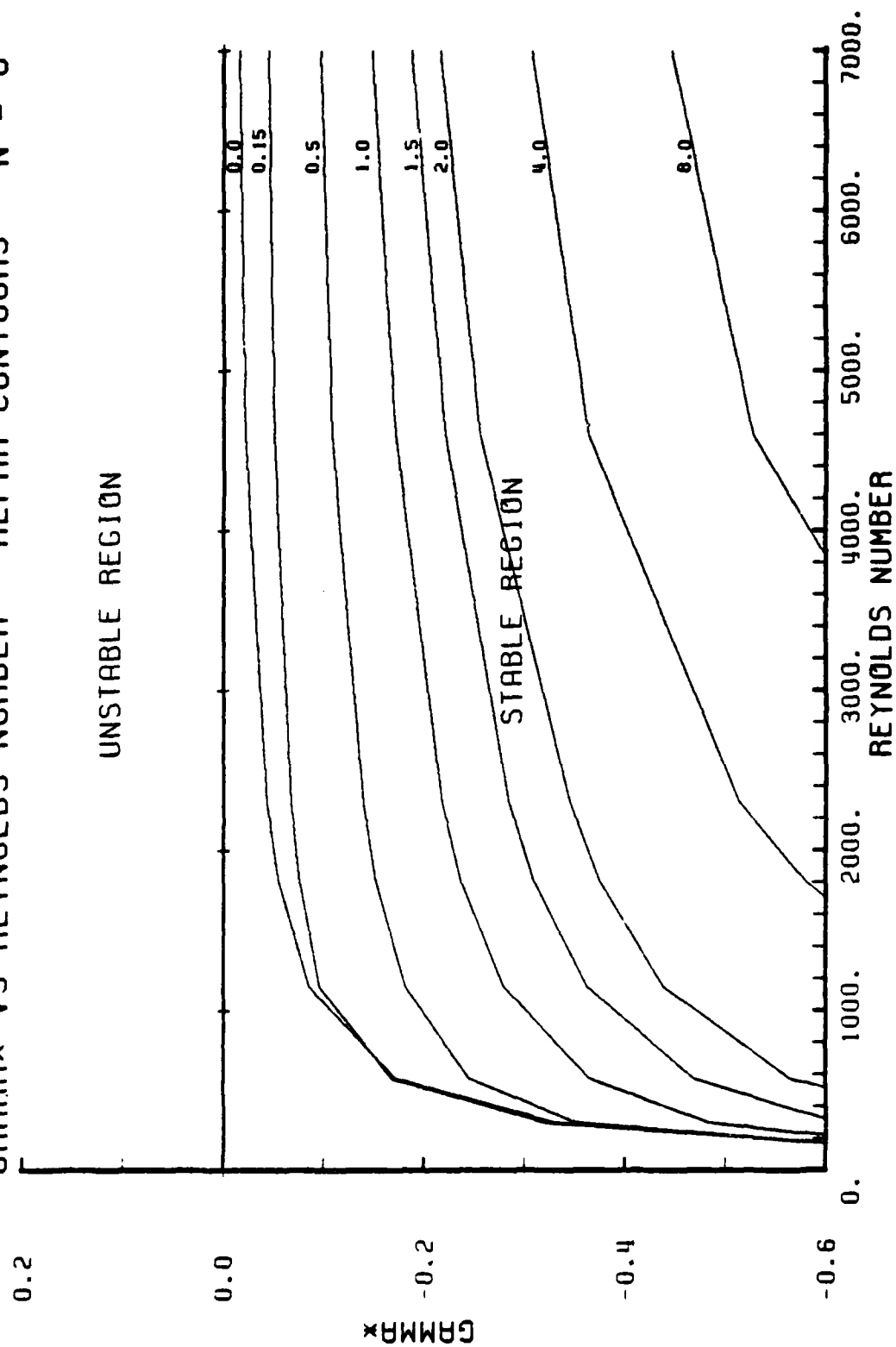


Figure 6-26

NORMALIZED PERTURBATION VELOCITY VS RADIUS

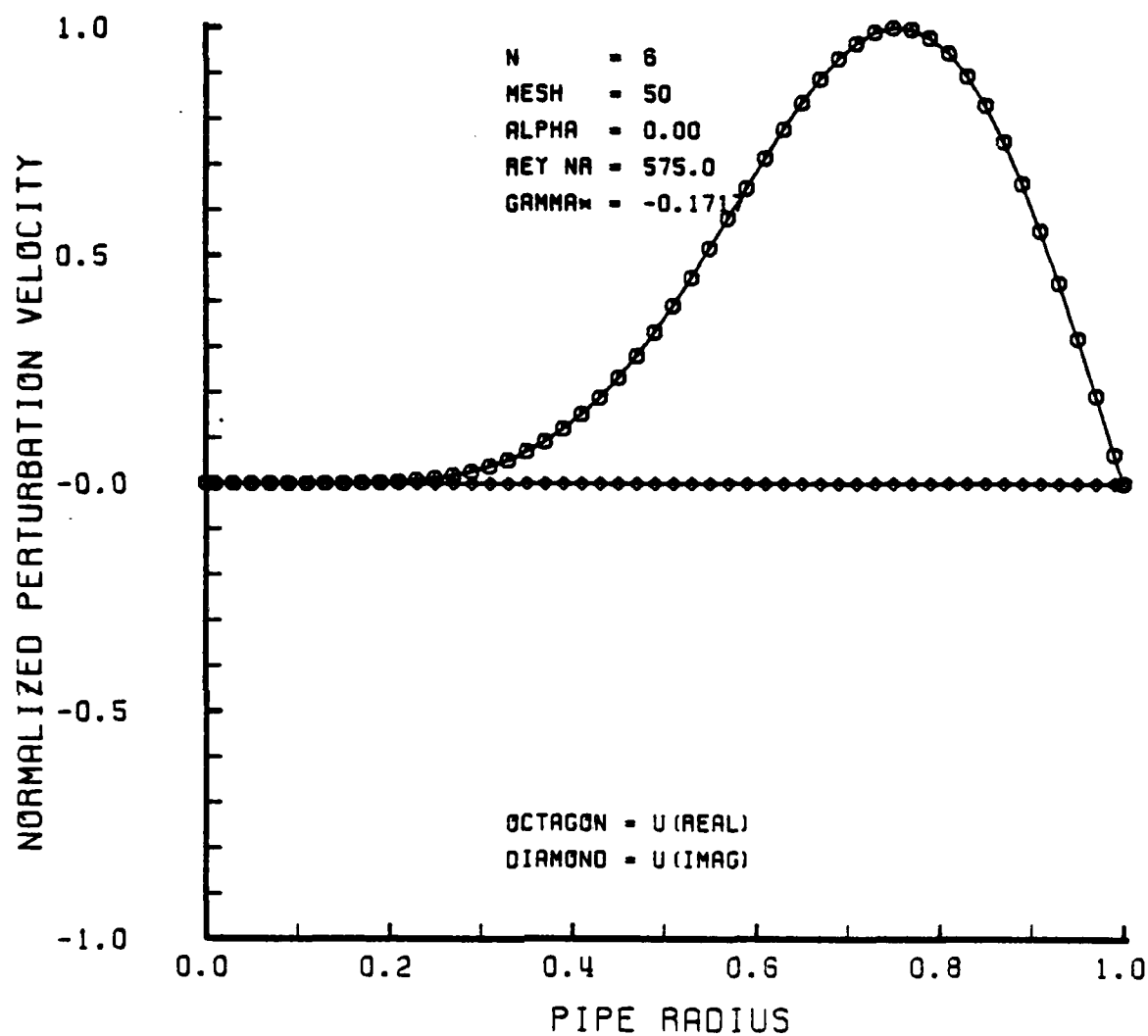


Figure 6-27

NORMALIZED PERTURBATION VELOCITY VS RADIUS.

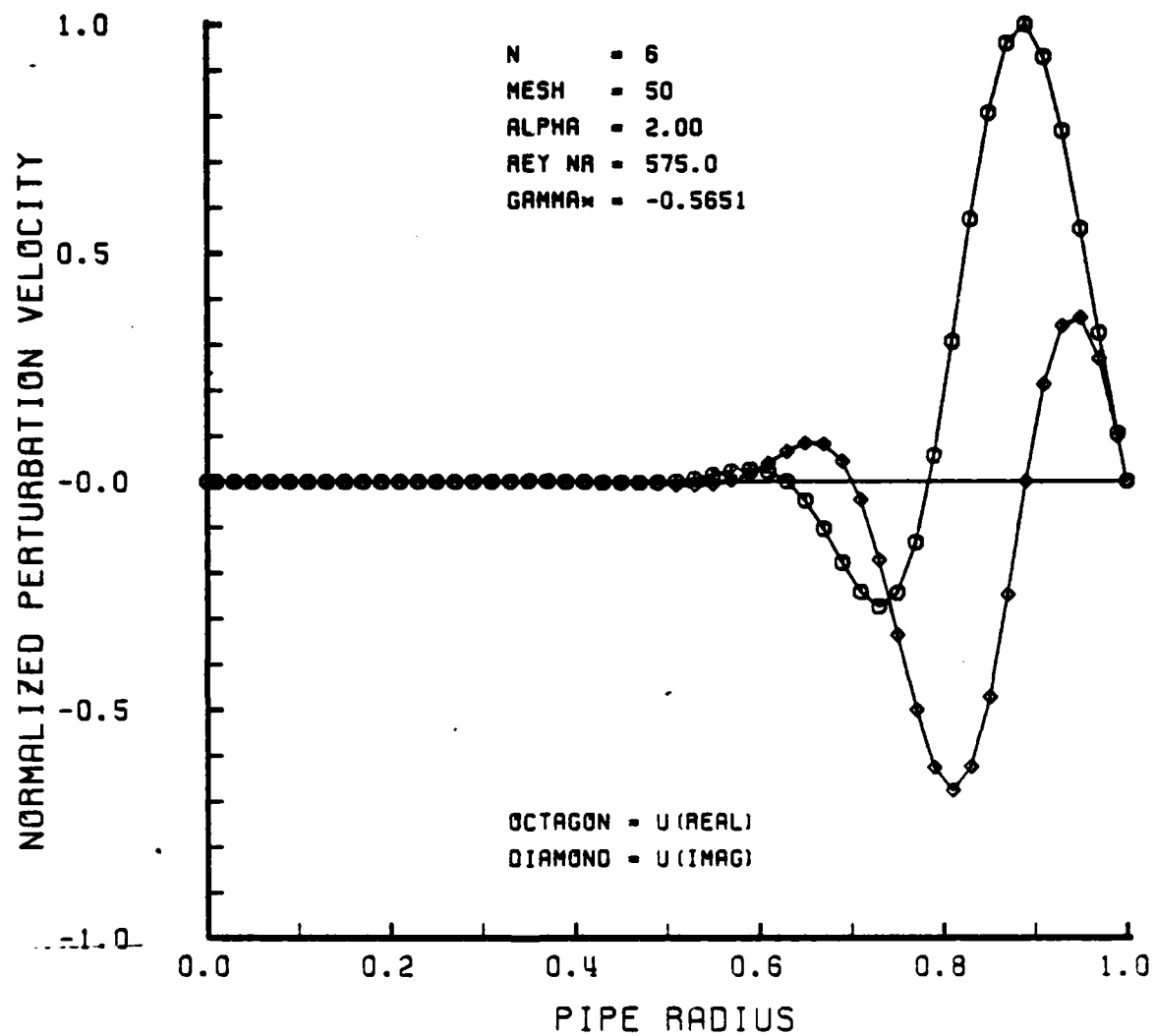


Figure 6-28

NORMALIZED PERTURBATION VELOCITY VS RADIUS

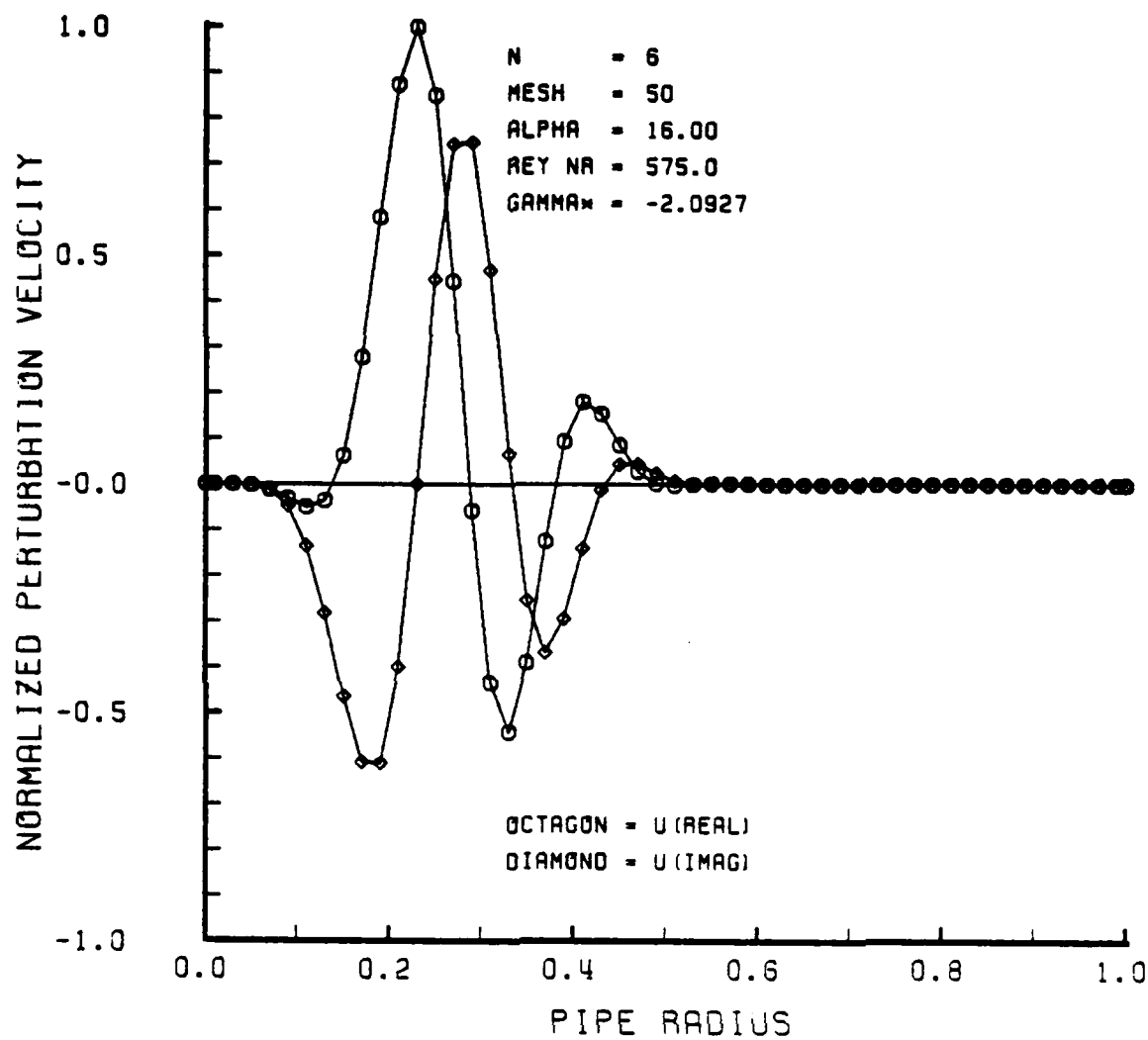


Figure 6-29

NORMALIZED PERTURBATION VELOCITY VS RADIUS

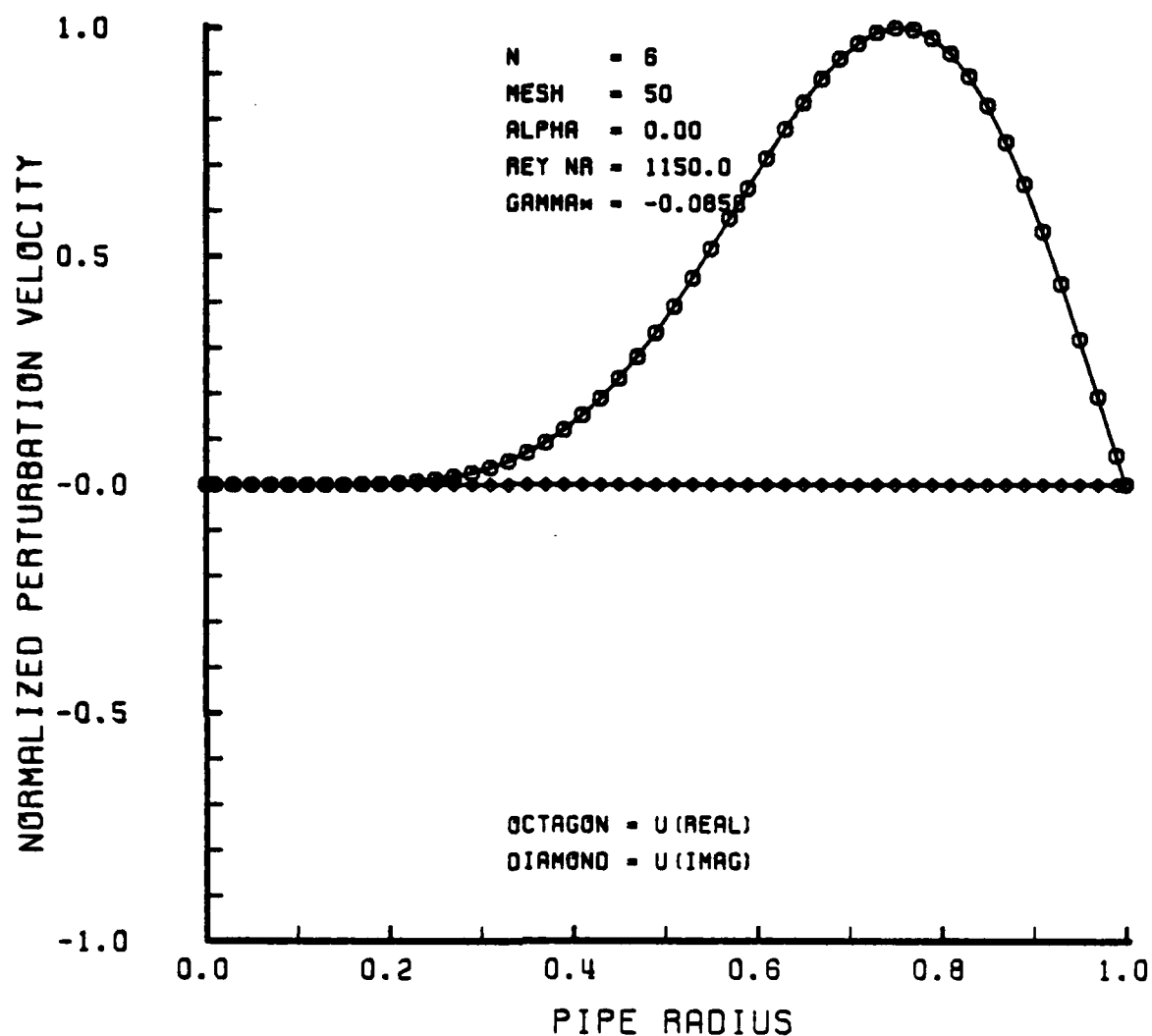


Figure 6-30

NORMALIZED PERTURBATION VELOCITY VS RADIUS

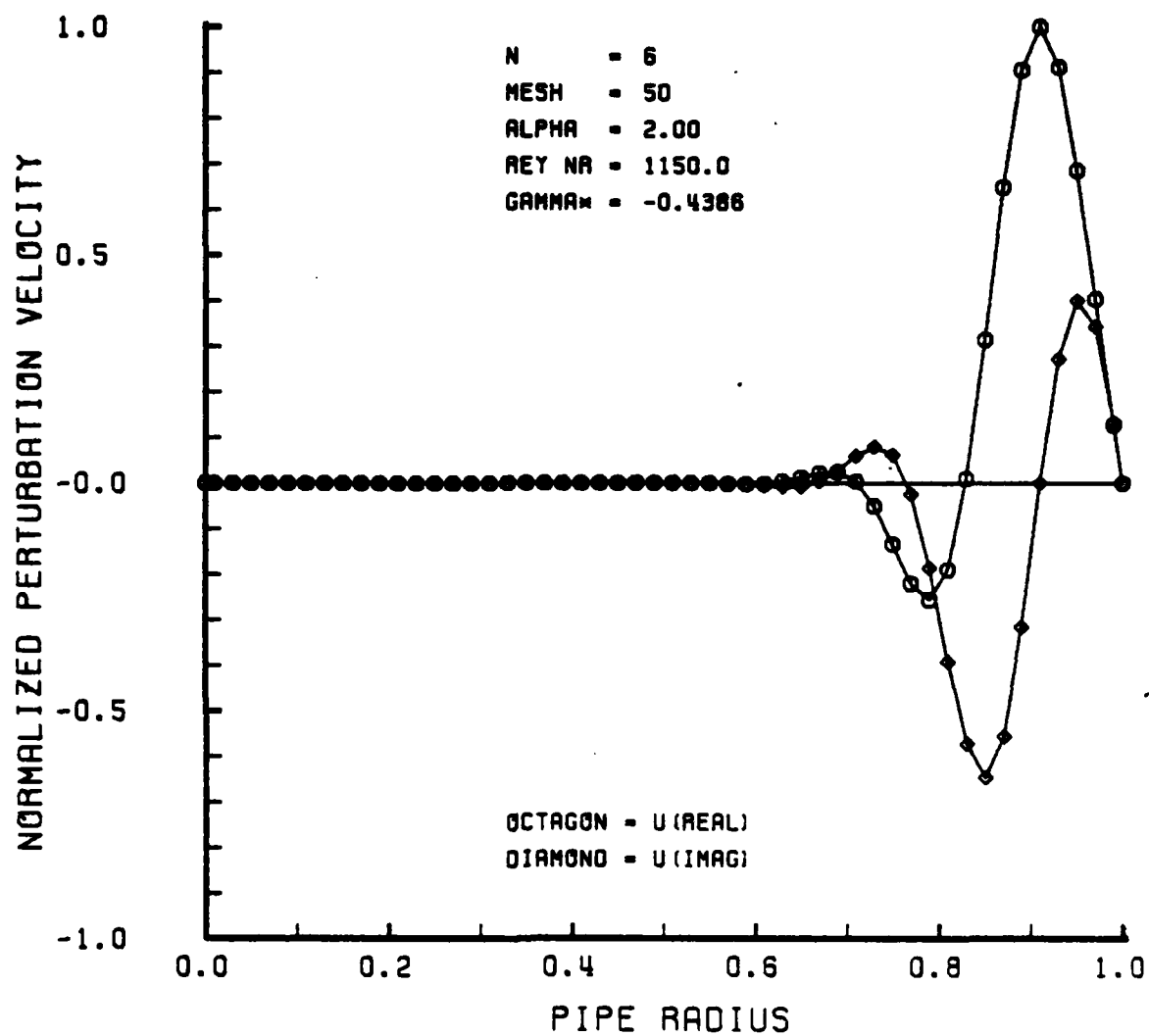


Figure 6-31

NORMALIZED PERTURBATION VELOCITY VS RADIUS

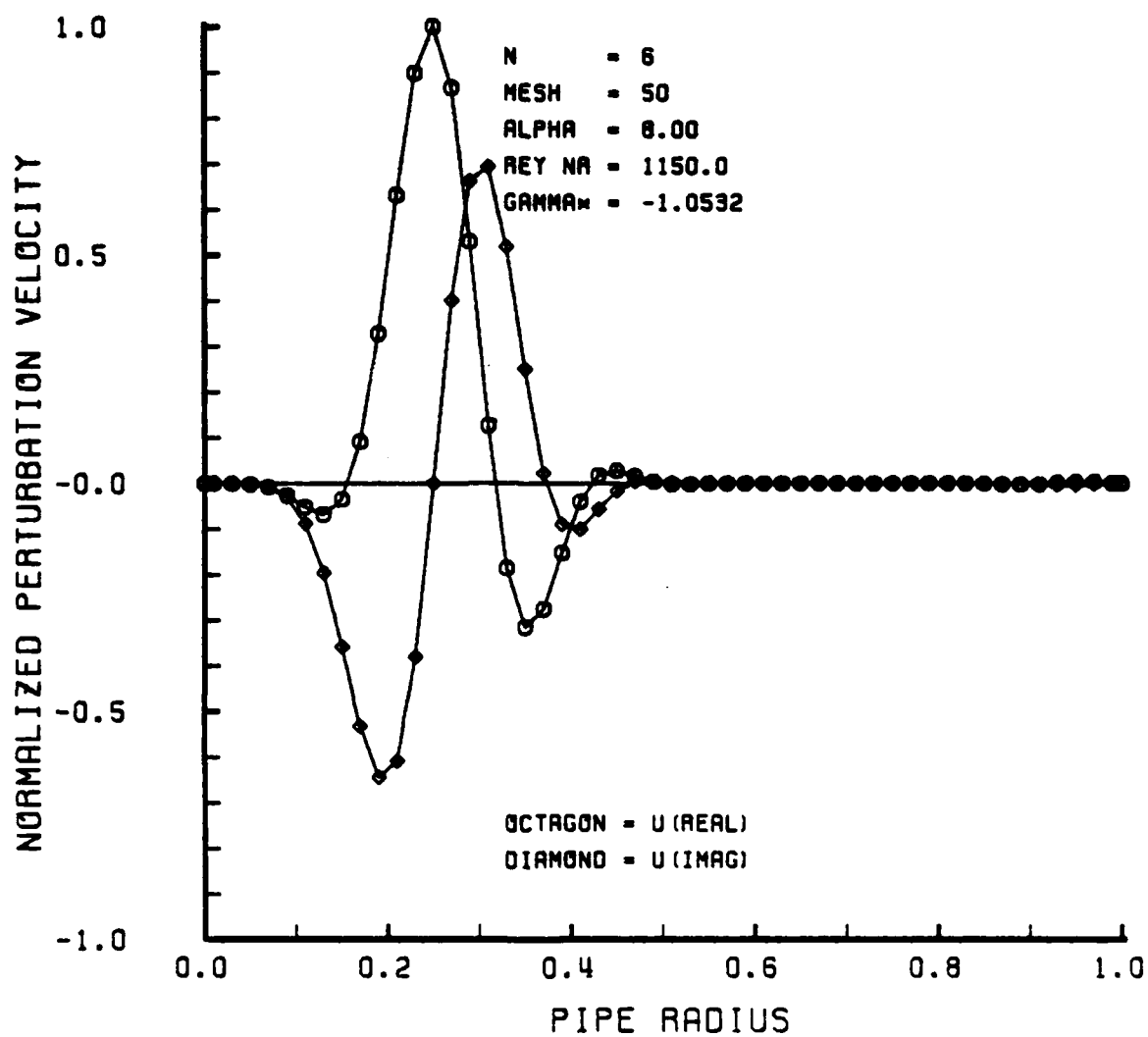


Figure 6-32

NORMALIZED PERTURBATION VELOCITY VS RADIUS

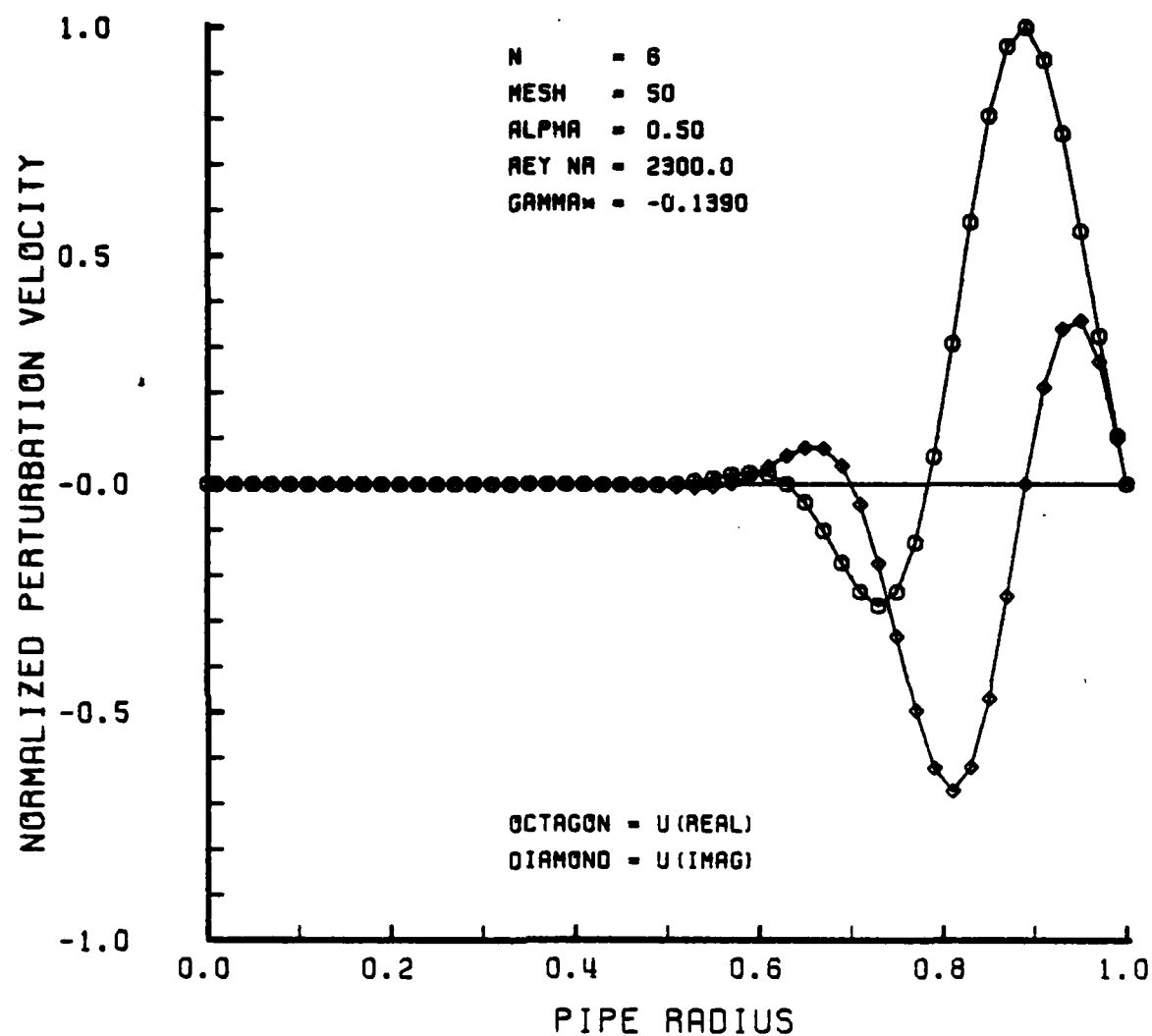


Figure 6-33

NORMALIZED PERTURBATION VELOCITY VS RADIUS

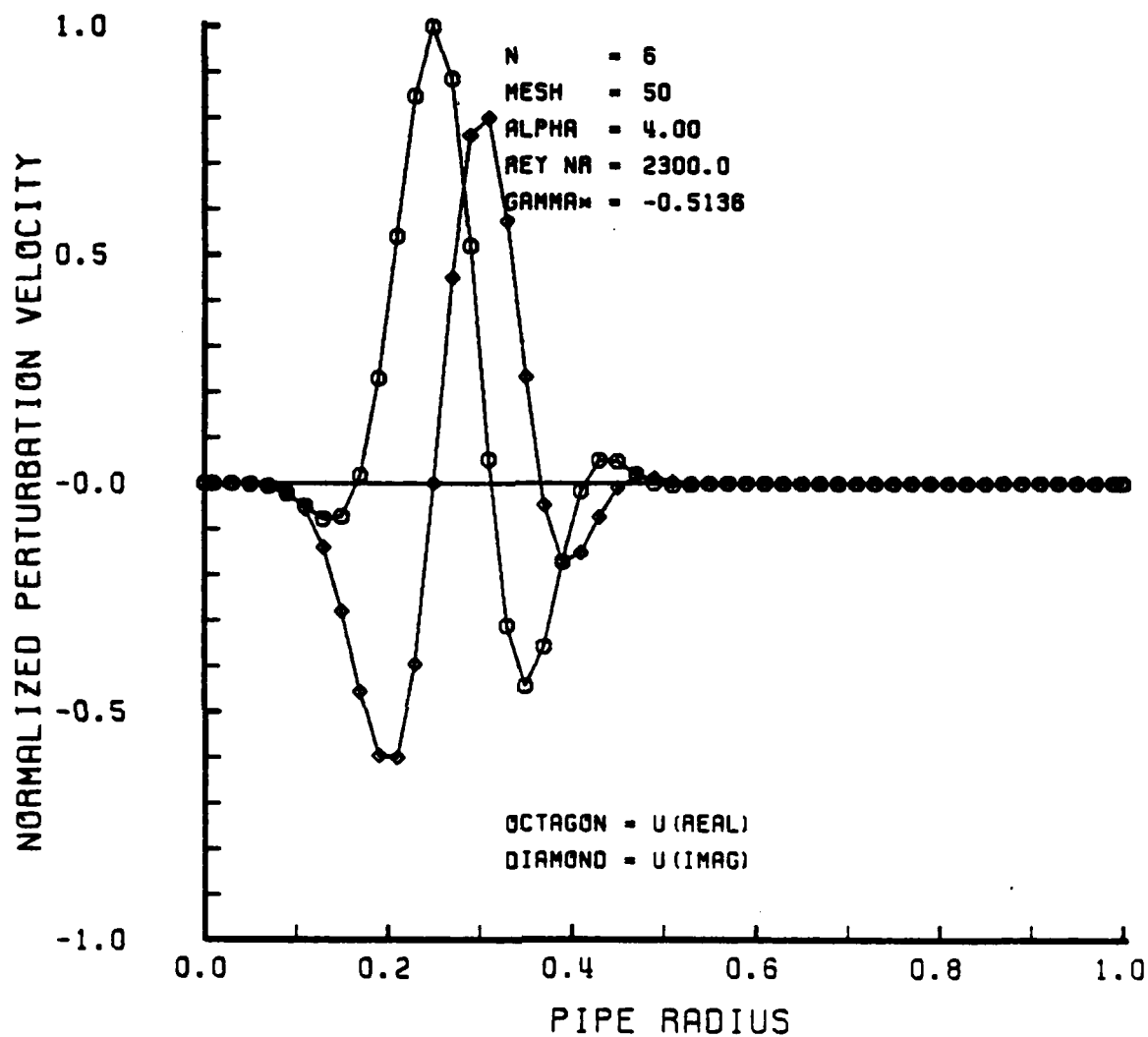


Figure 6-34

NORMALIZED PERTURBATION VELOCITY VS RADIUS

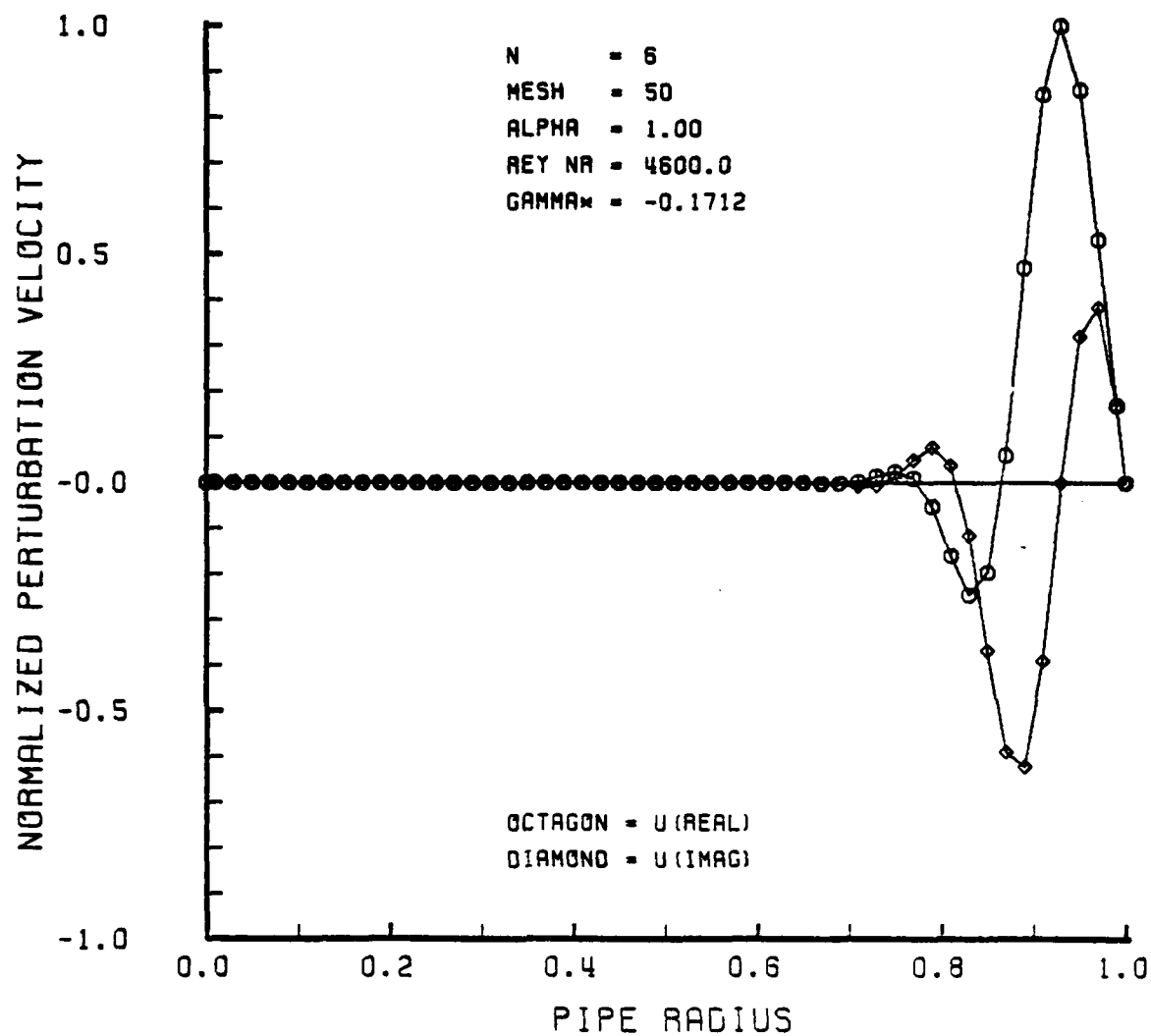


Figure 6-36

NORMALIZED PERTURBATION VELOCITY VS RADIUS

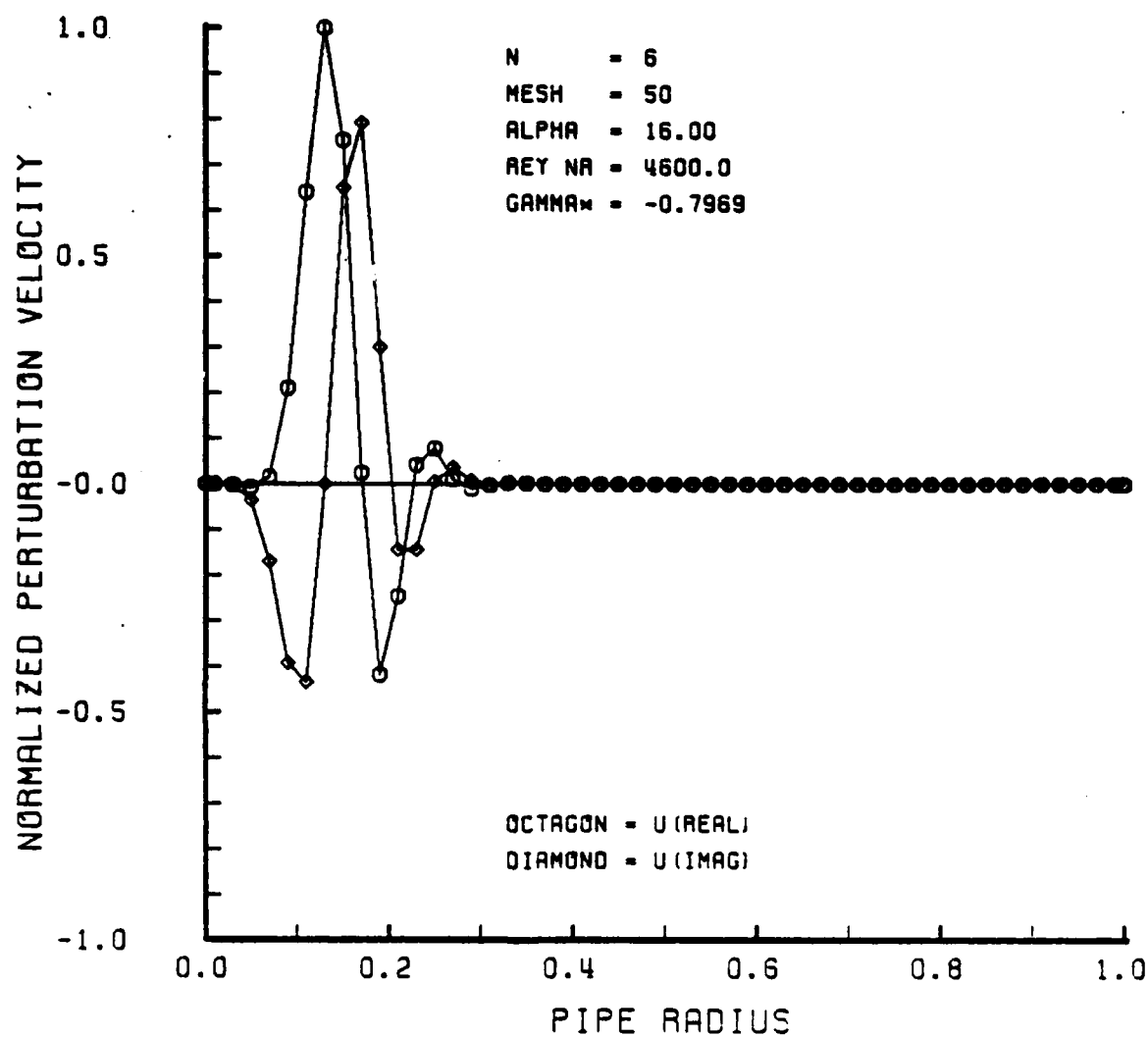


Figure 6-36

D. NUMERICAL ACCURACY

Numerical accuracy of the solutions of the governing vorticity transport equations was verified by substituting the least stable eigenvalue and its corresponding eigenvector into the eigensystem relation given in equation (5-39). The error vector was examined to determine the residual error of the solution. For the most part the error was of the order 10^{-12} to 10^{-9} , a most satisfactory result.

Upon closer examination of the error vector and the stability trends in the plots, it became evident that the accuracy of the numerical solution for the governing equations was not only dependent on the Reynolds number as previously mentioned but on the axial wave number as well. Plots of the perturbation velocity vs. radius for very large axial wave numbers are contained in Figures 6-37 through 6-39. The three figures, one for each angular wave number investigated, are examples of inaccurate solutions. Dependence of the solution on Reynolds number and axial wave number, became more evident as Re and α were increased. Rapid excursions of the perturbation velocity over a small portion of the pipe radius indicate that the computational mesh was not sufficiently fine to approximate the perturbation velocity function in the region of activity. This supposition can also be supported by examining the error vector where the residual error was found to be of the order 10^{-1} or worse, in the region of perturbation activity. Recall for $n = 1$ that some of the activity remained at the wall as α was increased. Refer to Figures 6-20 through 6-23. The residual error was

nominally of the order 10^{-5} in this region. Therefore, the true representation of the perturbation velocity is directly dependent upon an accurate numerical solution of the governing equations. These inaccuracies can be resolved by using a nonuniform mesh in the region of interest as suggested by Arnold. It is suspected, however, that after a thorough analysis of the effects of the problem parameters and mesh size on the solution have been investigated, only small values of the axial wave number below about 10.0 and Reynolds numbers in the vicinity of 1150 will be of primary interest. It is felt by this investigator that a mesh size of $N = 50$ and the wide range of problem parameters used here yielded solutions that satisfied the governing vorticity transport equations to a high degree and were sufficient to show stability trends.

NORMALIZED PERTURBATION VELOCITY VS RADIUS

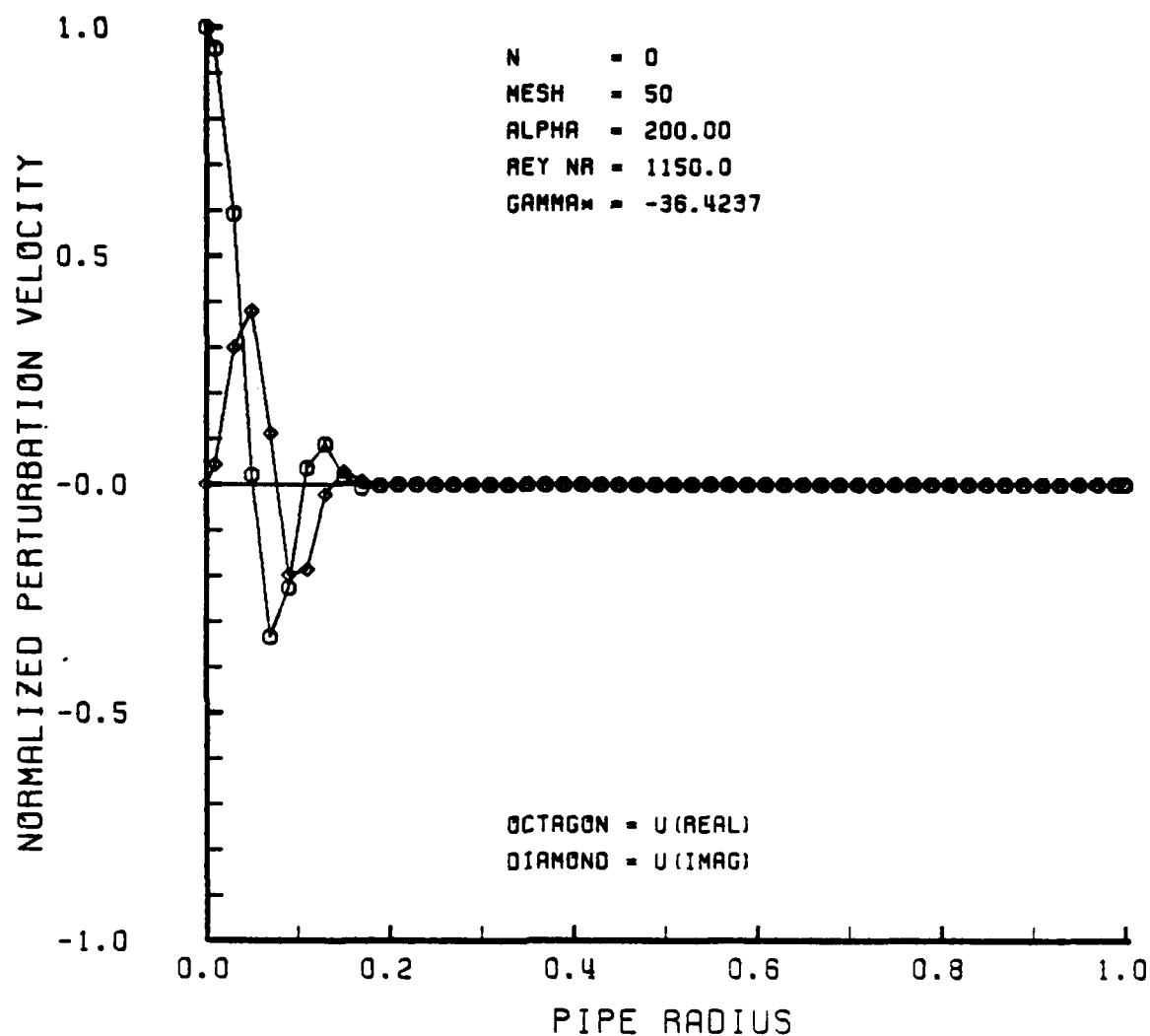


Figure 6-37

NORMALIZED PERTURBATION VELOCITY VS RADIUS

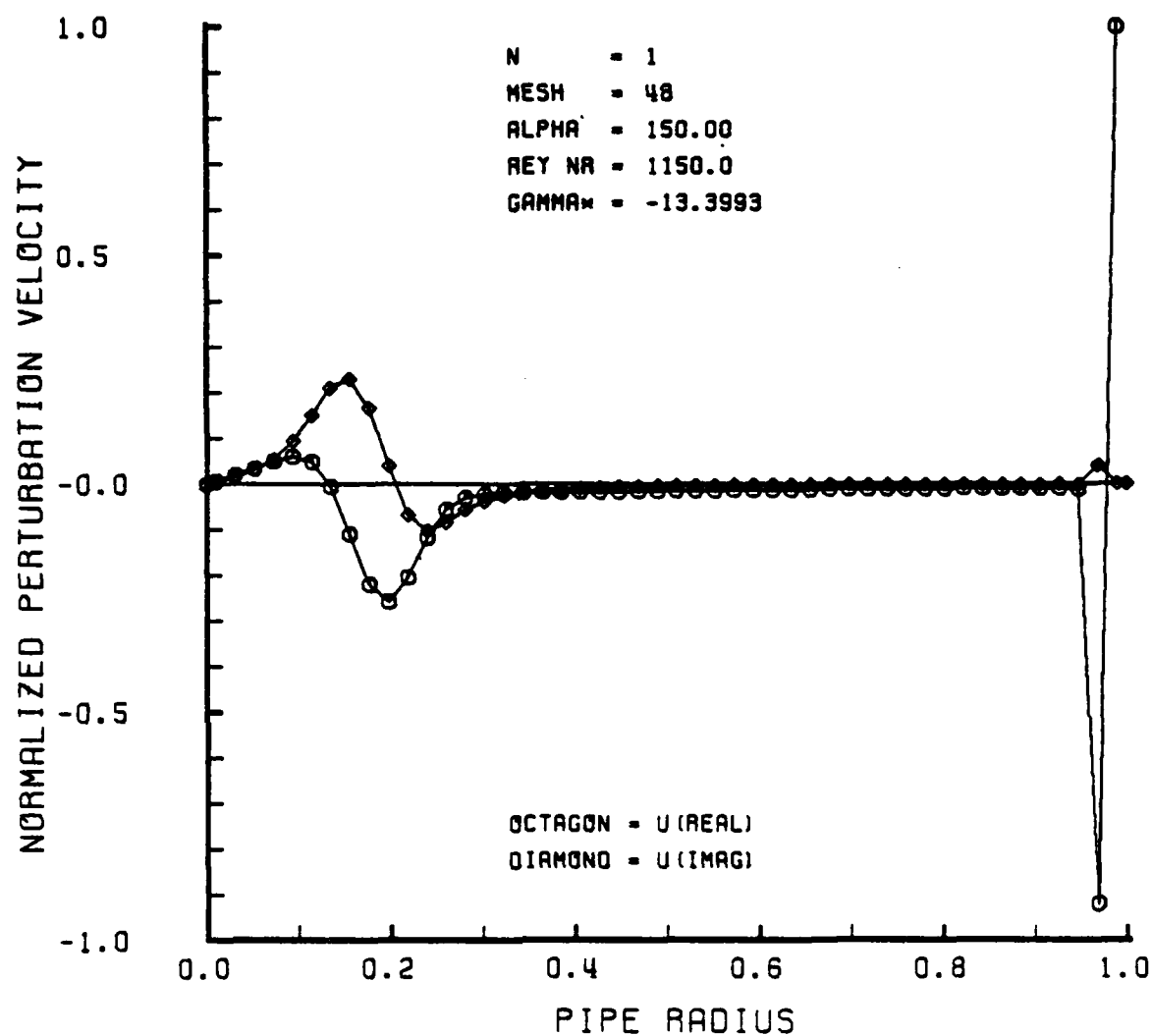


Figure 6-38

NORMALIZED PERTURBATION VELOCITY VS RADIUS

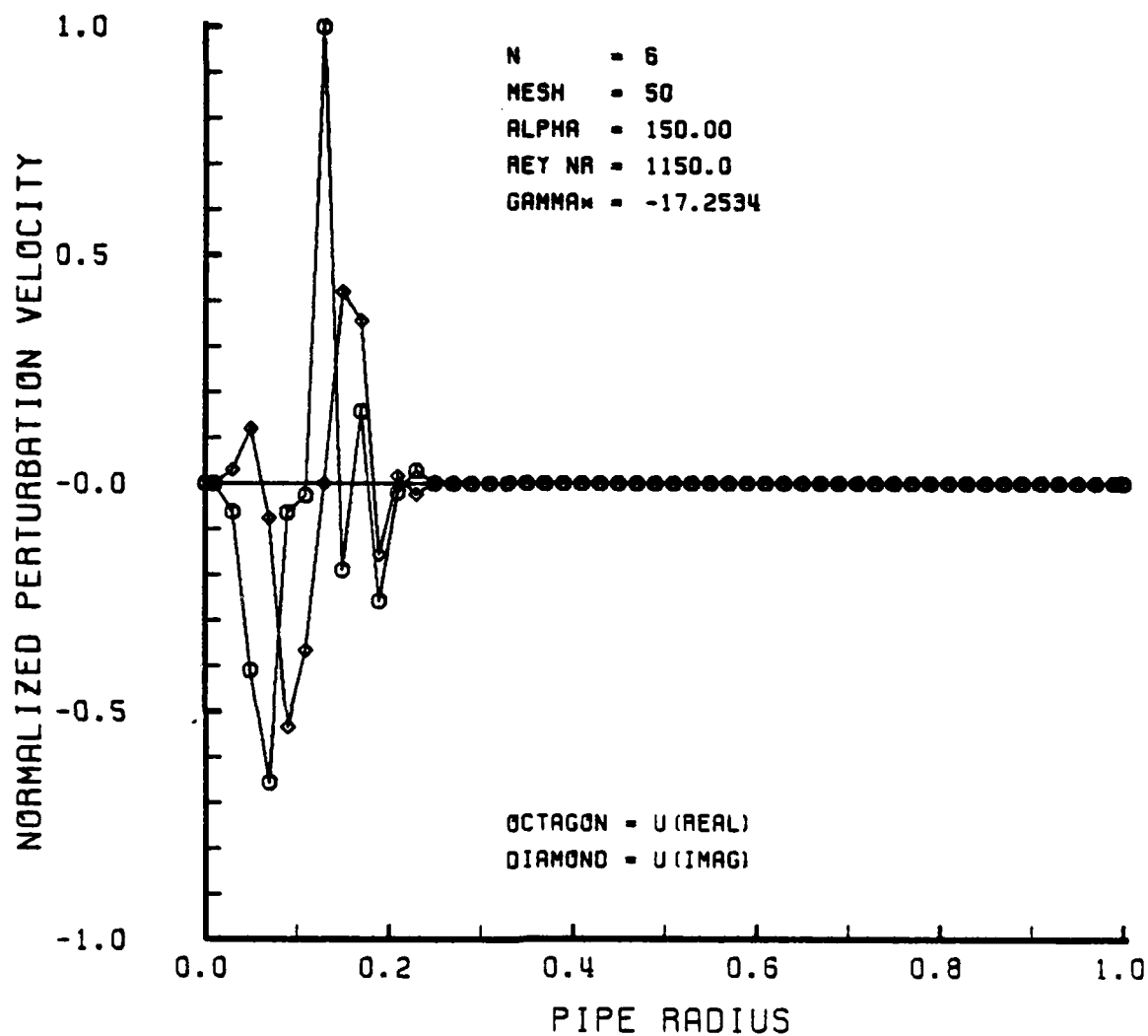


Figure 6-39

VII. RECOMMENDATIONS AND CONCLUSIONS

The problem of predicting the transition from laminar to turbulent flow of incompressible fluids in circular pipes has been pursued for nearly 100 years and has been presented here in a straightforward manner. The governing equations for the dynamics of this problem consist of the Navier-Stokes equation and the continuity equation. After taking the curl of the Navier-Stokes equation and applying the continuity principle, the linearized vorticity transport vector equation is obtained. The velocity vector potential function, which contains functions of r and a complex exponential factor, was then introduced. The resulting two linearly independent equations form the basis for the solution of the problem in the form of the vorticity transport matrix equation.

A valid solution of the governing equations was made possible because of two factors; (1) the advancements in the linearized theory by introducing a purely imaginary exponential form of the axial wave number, and (2) the rigorous method in which the boundary conditions at the pipe axis were derived and those constraints enforced. After an appropriate change of variables was performed, the governing equations were transformed into an equivalent pair of coupled, homogeneous differential equations that were solved in eigenvalue problem format. Accurate solutions of the governing equations were achieved by the refinement and combination of several standard methods of numerical analysis. These methods include; (1) the approximation of the governing equations along

a computational radial mesh developed by the half-station method, (2) the use of central and noncentral finite difference approximations having consistent fourth order truncation error, and (3) the use of complex, double precision number representations.

It was this author's intention from the outset to make this work as complete as possible. This was accomplished by including the development of the theory, the derivation of the boundary conditions, and a detailed explanation of the numerical methods used as well as obtaining solutions to the governing equations. This will enable future investigators to use this thesis as a starting point and as a single source reference for follow-on studies of this subject.

The conclusions of this numerical analysis follow directly from the results of the pipe flow stability problem which were discussed thoroughly in the previous chapter.

The most significant findings are:

- (1) for $n = 0$, the flow is stable at all Re and α .
- (2) for $n = 1$, the flow appears to be unstable at all Re for small values of α . This result is unfortunately in direct conflict with experimental observations.
- (3) for $n = 1$, unstable eigenvalues are associated with perturbation activity at the wall.
- (4) for $n = 6$, the flow is stable at all Re and α .

The following observations are also of interest:

- (5) for $n = 0, 1$, and 6 , increasing Reynolds number has a destabilizing effect on the flow.
- (6) for $n = 0, 1$, and 6 , increasing axial wave number has a stabilizing effect on the flow for fixed Re .
- (7) for $n = 1$ and 6 , increasing axial wave number causes a shift in the perturbation activity from the wall to the axis for fixed Re .

The results for angular wave numbers $n = 1$ and 6 are believed to be new. Conclusions (1), (5), (6), and (7) are in agreement with experimental results or previous theoretical investigations.

It is this author's opinion that the numerical analysis of the vorticity transport equations is now complete for angular wave numbers $n = 0$ and 6. It is felt, however, that the numerical results for angular wave number $n = 1$ warrant further study. The unresolved paradox is quite puzzling in that for $n = 1$ the flow appears to be unstable at all Reynolds numbers. Continued numerical investigations for $n = 1$ and follow-on studies of other angular wave numbers should prove fruitful in establishing a theory which predicts the transition from laminar to turbulent flow of fluids in pipes.

APPENDIX A

COEFFICIENTS OF THE VORTICITY TRANSPORT EQUATIONS

The generalized coefficient matrices which appear in the basic vorticity transport equations (2-40) are defined below.

$$[M_4] = \frac{1}{Re} \begin{bmatrix} 0 & 0 \\ 0 & -1 \end{bmatrix} \quad (A-1)$$

$$[M_3] = \frac{1}{Re} \begin{bmatrix} 0 & \frac{in}{r} \\ 0 & -\frac{2}{r} \end{bmatrix} \quad (A-2)$$

$$[M_2] = \frac{1}{Re} \begin{bmatrix} \left(\frac{n^2}{r^2} + \alpha^2 \right) & \frac{2 in}{r^2} \\ -\frac{4 in}{r^2} & \left(\frac{2n^2 + 3}{r^2} + 2\alpha^2 \right) \end{bmatrix} + \begin{bmatrix} 0 & 0 \\ 0 & 2i\alpha(1-r^2) \end{bmatrix} \quad (A-3)$$

$$[M_1] = \frac{1}{Re} \begin{bmatrix} -\left(\frac{n^2}{r^3} - \frac{\alpha^2}{r} \right) & -in \left(\frac{n^2 + 1}{r^3} + \frac{\alpha^2}{r} \right) \\ \frac{4 in}{r^3} & -\left(\frac{2n^2 + 3}{r^3} - \frac{2\alpha^2}{r} \right) \end{bmatrix} + \begin{bmatrix} 0 & 2n\alpha\left(\frac{1}{r} - r\right) \\ 0 & 2i\alpha\left(\frac{1}{r} - r\right) \end{bmatrix} \quad (A-4)$$

$$\begin{aligned}
[M_0] = \frac{1}{Re} & \begin{bmatrix} - \left(\frac{n^2(n^2 - 1)}{r^4} + \frac{(2n^2 + 1)\alpha^2}{r^2} + \alpha^4 \right) & -in \left(\frac{n^2 - 1}{r^4} + \frac{3\alpha^2}{r^2} \right) \\ 4 in \left(\frac{n^2 - 1}{r^4} + \frac{\alpha^2}{r^2} \right) & - \left(\frac{(n^2 + 3)(n^2 - 1)}{r^4} + \frac{2(n^2 + 1)\alpha^2}{r^2} + \alpha^4 \right) \end{bmatrix} \\
+ & \begin{bmatrix} -2i\alpha \left(\frac{n^2}{r^2} - (n^2 - \alpha^2) - \alpha^2 r^2 \right) & 2n\alpha \left(\frac{1}{r^2} + 1 \right) \\ -4n\alpha \left(\frac{1}{r^2} - 1 \right) & -2i\alpha \left(\frac{n^2 + 1}{r^2} - (n^2 + 1 - \alpha^2) - \alpha^2 r^2 \right) \end{bmatrix}
\end{aligned}
\tag{A-5}$$

$$[N_2] = \begin{bmatrix} 0 & 0 \\ 0 & -1 \end{bmatrix}
\tag{A-6}$$

$$[N_1] = \begin{bmatrix} 0 & \frac{in}{r} \\ 0 & -\frac{1}{r} \end{bmatrix}
\tag{A-7}$$

$$[N_0] = \begin{bmatrix} \left(\frac{n^2}{r^2} + \alpha^2 \right) & \frac{in}{r^2} \\ -\frac{2 in}{r^2} & \left(\frac{n^2 + 1}{r^2} + \alpha^2 \right) \end{bmatrix}
\tag{A-8}$$

APPENDIX B

COEFFICIENTS OF THE TRANSFORMED VORTICITY TRANSPORT

EQUATIONS FOR $n = 0, 1$, and 6

A. COEFFICIENTS FOR $n = 0$

Since the vorticity transport equations uncouple for $n = 0$, only the solution for the eigenfunction $Q(r)$ is sought. Therefore the details of the complete coefficient matrices are not required. The coefficients which appear here represent the matrix element (2,2) and correspond to the primed quantities of equation (2-43).

$$M_4' = - \frac{r}{Re} \quad (B-1)$$

$$M_3' = - \frac{6}{Re} \quad (B-2)$$

$$M_2' = \frac{1}{Re} \left(- \frac{3}{r} + 2\alpha^2 r \right) + 2i\alpha (r - r^3) \quad (B-3)$$

$$M_1' = \frac{1}{Re} \left(\frac{3}{r^2} + 6\alpha^2 \right) + 6i\alpha (1 - r^2) \quad (B-4)$$

$$M_0' = - \frac{\alpha^4 r}{Re} + 2i\alpha^3 (r^3 - r) \quad (B-5)$$

$$N_2' = - r \quad (B-6)$$

$$N_1' = - 3 \quad (B-7)$$

$$N_0' = \alpha^2 r \quad (B-8)$$

These coefficients also appear and are computed in part III of the main investigative computer program for $n = 0$.

B. COEFFICIENTS for $n = 1$

Since the vorticity transport equations do not uncouple for $n = 1$, the eigenfunctions $P(r)$ and $Q(r)$ must be solved for simultaneously. With the introduction of the additional parameter as a result of the change of variables, $H(0)$ appears explicitly as an unknown in the system of equations. This requires the addition of two coefficient matrices to equation (2-40). The 2×1 column matrix $[M'_5]$ appears on the left side of equation (2-47) and one 2×1 column matrix $[N'_3]$ appears on the right side of equation (2-47). The complete coefficient matrices for $n = 1$ are defined below.

$$[M'_4] = \begin{bmatrix} 0 & 0 \\ 0 & -\frac{r^2}{Re} \end{bmatrix} \quad (B-9)$$

$$[M'_3] = \begin{bmatrix} 0 & \frac{ir}{Re} \\ 0 & -\frac{10r}{Re} \end{bmatrix} \quad (B-10)$$

$$[M'_2] = \begin{bmatrix} \frac{1}{Re} (1 + \alpha^2 r^2) & \frac{8i}{Re} \\ -\frac{4i}{Re} & \frac{1}{Re} (2\alpha^2 r^2 - 19) + 2i\alpha (r^2 - r^4) \end{bmatrix} \quad (B-11)$$

$$\begin{aligned}
[M_1'] &= \begin{bmatrix} \frac{1}{Re} \left(\frac{3}{r} + 5\alpha^2 r \right) & 2\alpha(r - r^3) \\ 0 & \frac{1}{Re} \left(\frac{3}{r} + 10\alpha^2 r \right) \end{bmatrix} \\
&+ \begin{bmatrix} 0 & \frac{i}{Re} \left(\frac{12}{r} - \alpha^2 r \right) \\ -\frac{12i}{Re r} & 10i\alpha(r - r^3) \end{bmatrix} \quad (B-12)
\end{aligned}$$

$$\begin{aligned}
[M_0'] &= \begin{bmatrix} \frac{\alpha^2}{Re} (1 - \alpha^2 r^2) & 2\alpha(3 - r^2) \\ -4\alpha(1 - r^2) & \frac{1}{Re} (4\alpha^2 - \alpha^4 r^2) \end{bmatrix} \\
&+ \begin{bmatrix} -2i\alpha(1 - r^2 + \alpha^2 r^2 - \alpha^2 r^4) & \frac{-5i\alpha^2}{Re} \\ \frac{4i\alpha^2}{Re} & 2i\alpha\{2(1 - r^2) - \alpha^2(r^2 - r^4)\} \end{bmatrix} \quad (B-13)
\end{aligned}$$

$$[M_5'] = \begin{bmatrix} 2\alpha(2 - \alpha^2 + \alpha^2 r^2) + \frac{i\alpha^4}{Re} \\ -\frac{\alpha^4}{Re} - 2i\alpha^3(1 - \alpha r^2) \end{bmatrix} \quad (B-14)$$

$$[N_2'] = \begin{bmatrix} 0 & 0 \\ 0 & -r^2 \end{bmatrix} \quad (B-15)$$

$$[N_1'] = \begin{bmatrix} 0 & ir \\ 0 & -5r \end{bmatrix} \quad (B-16)$$

$$[N_0'] = \begin{bmatrix} 1 + \alpha^2 r^2 & 3i \\ -2i & -2 + \alpha^2 r^2 \end{bmatrix} \quad (B-17)$$

$$[N_3'] = \begin{bmatrix} -i\alpha^2 \\ \alpha^2 \end{bmatrix} \quad (B-18)$$

These coefficients also appear and are computed in Part III of the main investigative computer program for $n = 1$.

C. COEFFICIENTS for $n = 6$

The vorticity transport equations for $n = 6$ remain coupled. There are no additional parameters introduced with the change of variables to $P(r)$ and $Q(r)$. The system of equations take the form of equation (2-40) once again. The complete coefficient matrices for $n = 6$ are defined below.

$$[M_4'] = \begin{bmatrix} 0 & 0 \\ 0 & -\frac{r^3}{Re} \end{bmatrix} \quad (B-19)$$

$$[M_3'] = \begin{bmatrix} 0 & \frac{6ir^2}{Re} \\ 0 & -\frac{14r^2}{Re} \end{bmatrix} \quad (B-20)$$

$$[M_2'] = \begin{bmatrix} \frac{r^2}{Re} (36 + \alpha^2 r^2) & 0 \\ 0 & \frac{r}{Re} (21 + 2\alpha^2 r^2) \end{bmatrix} + \begin{bmatrix} 0 & \frac{66ir}{Re} \\ -\frac{24ir^2}{Re} & 2i\alpha(r^3 - r^5) \end{bmatrix} \quad (B-21)$$

$$\begin{aligned}
 [M_1] = & \begin{bmatrix} \frac{1}{Re} (252r + 9 \alpha^2 r^2) & 12\alpha(r^2 - r^4) \\ 0 & \frac{1}{Re} (315 + 14\alpha^2 r^2) \end{bmatrix} \\
 & + \begin{bmatrix} 0 & -\frac{i}{Re} (42 + 6\alpha^2 r^2) \\ -\frac{168ir}{Re} & 14i\alpha(r^2 - r^4) \end{bmatrix} \quad (B-22)
 \end{aligned}$$

$$\begin{aligned}
 [M_0] = & \begin{bmatrix} -\frac{1}{Re} (972 + 57\alpha^2 r^2 + \alpha^4 r^4) & 24\alpha(2r - r^3) \\ -24\alpha(r^2 - r^4) & -\frac{1}{Re} \left(\frac{1152}{r} + 56\alpha^2 r + \alpha^4 r^3 \right) \end{bmatrix} \\
 & + \begin{bmatrix} -2i\alpha r^2 \{36 - 36r^2 + \alpha^2 r^2 (1 - r^2)\} & -\frac{i}{Re} \left(\frac{768}{r} + 36\alpha^2 r \right) \\ \frac{i}{Re} (648 + 24\alpha^2 r^2) & -56i\alpha(r - r^3) - 2i\alpha^3(r^3 - r^5) \end{bmatrix} \quad (B-23)
 \end{aligned}$$

$$[N_2] = \begin{bmatrix} 0 & 0 \\ 0 & -r^3 \end{bmatrix} \quad (B-24)$$

$$[N_1'] = \begin{bmatrix} 0 & 6ir^2 \\ 0 & -7r^2 \end{bmatrix} \quad (B-25)$$

$$[N_0'] = \begin{bmatrix} 36r^2 + \alpha^2 r^4 & 24ir \\ -12ir^2 & 28r + \alpha^2 r^3 \end{bmatrix} \quad (B-26)$$

These coefficients also appear and are computed in part III of the main investigative computer program for $n = 6$.

APPENDIX C

COEFFICIENTS OF THE BOUNDARY EQUATIONS AT THE AXIS

The matrices which appear in the boundary equations at the axis, equations (3-4) through (3-8) are defined below.

$$[C_1] = \begin{bmatrix} -n^2 & -in \\ +4in & -(n^2 + 3) \end{bmatrix} \quad (C-1)$$

$$[C_2] = \begin{bmatrix} -n^2 & -2in \\ +4in & -(n^2 + 4) \end{bmatrix} \quad (C-2)$$

$$[C_3] = \begin{bmatrix} -\frac{n^2}{2} & -\frac{3}{2}in \\ +2in & -\frac{1}{2}(n^2 + 3) \end{bmatrix} \quad (C-3)$$

$$[C_4] = \begin{bmatrix} -\left\{ 2n^2 - (2n^2 + 1) \frac{i\alpha}{Re} \right\} & -in \left(2 - \frac{3i\alpha}{Re} \right) \\ +4in \left(1 - \frac{i\alpha}{Re} \right) & -2(n^2 + 1) \left(1 - \frac{i\alpha}{Re} \right) \end{bmatrix} \quad (C-4)$$

$$[D_4] = \begin{bmatrix} + n^2 & + in \\ - 2 in & + (n^2 + 1) \end{bmatrix} \quad (C-5)$$

$$[C_5] = \begin{bmatrix} - \frac{n}{6} & - \frac{2i}{3} \\ + \frac{2i}{3} & - \frac{n}{6} \end{bmatrix} \quad (C-6)$$

$$[C_6] = \begin{bmatrix} - n & - 2i \\ + 2i & - n \end{bmatrix} \quad (C-7)$$

$$[C_7] = \begin{bmatrix} - \frac{n^2}{24} & - \frac{5 in}{24} \\ + \frac{in}{6} & - \frac{(n^2 - 5)}{24} \end{bmatrix} \quad (C-8)$$

$$[C_8] = \begin{bmatrix} - \left\{ n^2 - \left(n^2 - \frac{3}{2} \right) \frac{i\alpha}{Re} \right\} & - in \left(3 - \frac{5i\alpha}{2Re} \right) \\ + 2 in \left(1 - \frac{i\alpha}{Re} \right) & - (n^2 - 3) \left(1 - \frac{i\alpha}{Re} \right) \end{bmatrix} \quad (C-9)$$

$$[D_8] = \begin{bmatrix} + \frac{n^2}{2} & + \frac{3 in}{2} \\ - in & + \frac{(n^2 - 3)}{2} \end{bmatrix} \quad (C-10)$$

$$[C_9] = \begin{bmatrix} \left(\frac{i\alpha^3}{Re} + 2n^2 - 2\alpha^2\right) & -2in \\ -4in & \left(\frac{i\alpha^3}{Re} + 2n^2 + 2 - 2\alpha^2\right) \end{bmatrix} \quad (C-11)$$

$$[D_9] = \begin{bmatrix} 1 & 0 \\ 0 & 1 \end{bmatrix} \quad (C-12)$$

Column matrices used in equation (5-36) for $n = 1$.

$$[C_9^*] = \begin{bmatrix} \left(\frac{\alpha^3}{Re} - 4i + 2i\alpha^2\right) \\ (-2\alpha^2 + \frac{i\alpha^3}{Re}) \end{bmatrix} \{H(0)\} \quad (C-13)$$

$$[D_9^*] = \begin{bmatrix} -i \\ 1 \end{bmatrix} \{H(0)\} \quad (C-14)$$

APPENDIX D

SPECIAL CONDITIONS AT THE AXIS

The determinates are formed from the corresponding matrices as defined in Appendix C. For angular wave numbers $n \geq 6$, all of the determinates become non-singular.

$$|C_1| = n^2 (n^2 - 1) \quad (D-1)$$

$$|C_2| = n^2 (n^2 - 4) \quad (D-2)$$

$$|C_3| = \frac{n^2}{4} (n^2 - 9) \quad (D-3)$$

$$\begin{aligned} |i\alpha[C_4] - \gamma[D_4]| = (n^2 - 1) \left\{ -2\alpha^2 \left(1 - \frac{i\alpha}{Re} \right) \left[2n^2 - (2n^2 - 1) \frac{i\alpha}{Re} \right] \right. \\ \left. + \gamma i\alpha \left[4n^2 - (4n^2 - 1) \frac{i\alpha}{Re} \right] + \gamma^2 n^2 \right\} \quad (D-4) \end{aligned}$$

$$|C_5| = \frac{1}{36} (n^2 - 16) \quad (D-5)$$

$$|C_6| = (n^2 - 4) \quad (D-6)$$

$$|C_7| = \frac{n^2}{576} (n^2 - 25) \quad (D-7)$$

$$\begin{aligned}
 |i\alpha[C_s] - \gamma[D_s]| &= (n^2 - 9) \left\{ -\alpha^2 \left(1 - \frac{i\alpha}{Re} \right) \left[- \left(n^2 - \frac{1}{2} \right) \frac{i\alpha}{Re} + n^2 \right] \right. \\
 &\quad \left. + \frac{\gamma i \alpha^3}{2} \left[- \left(n^2 - \frac{1}{2} \right) \frac{i\alpha}{Re} + 2n^2 \right] + \frac{\gamma^2 \alpha^4 n^2}{4} \right\} \quad (D-8)
 \end{aligned}$$

[illegible]

```

*****
THIS PROGRAM WAS DEVELOPED TO PERFORM A NUMERICAL ANALYSIS
OF THREE DIMENSIONAL PIPE FLOW STABILITY FOR AXIAL WAVE
NUMBER N = 0. THE PROGRAM IS DIVIDED INTO EIGHT PARTS.
THE FIRST PART COMPUTES THE CENTRAL FINITE DIFFERENCE
COEFFICIENTS FOR THE DERIVATIVES OF Q(R) ONLY, AT THE
INTERIOR MESH POINTS ALONG THE PIPE RADIUS. IN THE SECOND
PART, PRE-COMPUTED NON-CENTRAL FINITE DIFFERENCE
COEFFICIENTS FOR THE DERIVATIVES OF Q(R) AT POINTS
NEAR THE AXIS AND WALL ARE READ IN AS DATA. THE THIRD PART
COMPUTES THE VORTICITY TRANSPORT EQUATION COEFFICIENTS OF
Q(R) AND THEIR RESPECTIVE DERIVATIVES AT ALL RADIAL MESH
POINTS (STATIONS). THE FOURTH PART COMPUTES THE A AND B
MATRIX ELEMENTS, WHICH MAKE-UP THE EIGENSYSTEM TO BE SOLVED
IN THE FORMAT, A * X = GAMMA * B * X. IN THE FIFTH PART
THE A AND B MATRICES COMPRISING THE EIGENSYSTEM ARE SOLVED
IN THE SUBROUTINE EIGZC. THE RESULTING EIGENVALUES AND
CORRESPONDING EIGENVECTOR REPRESENT GAMMA AND THE COLUMN
VECTOR X, RESPECTIVELY, AND ARE SOLUTIONS OF THE GOVERNING
PARTIAL DIFFERENTIAL EQUATIONS. THE SIXTH PART VERIFIES
THE SOLUTION OF THE PDE AND THE MAGNITUDE OF THE RESIDUAL
IS DETERMINED. THE SEVENTH PART COMPUTES THE NORMALIZED
*****

```



```
DATA A1DER/7*{0.0D0,0.0D0}/,A2DER/7*{0.0D3,0.0D0}/,
DATA A3DER/7*{0.0D0,0.0D3}/,A4DER/7*{0.0D0,0.0D0}/,
DATA X1(1)/0.0/,Y1(1)/0.0/,X1(2)/1.0/,Y1(2)/0.0/,
DATA NESH/50/
```

[illegible]

PART I

COMPUTE CENTRAL DIFFERENCE COEFFICIENTS FOR THE

DERIVATIVES OF $Q(R)$ AT INTERIOR MESH POINTS.

COMPUTE CENTRAL DIFFERENCE COEFFICIENTS FOR FOURTH ORDER

DERIVATIVE OF $O(R)$ AT POINTS 4 - 47

```

DMESH = DFL0AT (MESH)
DH4TH = DMESH ** 4
A4TEMP (1) = (- 1.0 D0 / 6. 0 D3) * H4TH
A4TEMP (7) = DCMPLEX (A4TEMP, 0. 0 D3)
A4TEMP (2) = A4DER (1)
A4TEMP (6) = 2. 0 D0 * H4TH
A4TEMP (3) = DCMPLEX (A4TEMP, 0. 0 D3)
A4TEMP (5) = - 6. 5 D0 * H4TH
A4TEMP (4) = DCMPLEX (A4TEMP, 0. 0 D3)

```

COMPUTE CENTRAL DIFFERENCE COEFFICIENTS FOR THIRD ORDER

DERIVATIVE AT POINTS 4 - 47

```

H3RD = DMESH ** 3
ATEMP = 0.125D0 * H3RD
A3D(1) = DCHPLX{ATEMP,0.0D0}
A3D(2) = -A3D(1)
A3D(3) = DCHPLX{H3RD,0.0D0}
A3D(4) = -A3D(3)
A3D(5) = (13.0D0/8.0D0) * H3RD
A3D(6) = DCHPLX{ATEMP,0.0D0}
A3D(7) = -A3D(6)

```

COMPUTE CENTRAL DIFFERENCE COEFFICIENTS FOR SECOND ORDER

```

C C DERIVATIVE AT POINTS 2 - 43
H2ND = DMESH ** 2
ATEMP = (-1.0D0/12.0D0) * H2ND
A2DER(2) = DCMPLX(ATEMP,0.0D0)
A2DER(6) = A2DER(2)
ATEMP = (16.0D0/12.0D0) * H2ND
A2DER(3) = DCMPLX(ATEMP,0.0D0)
A2DER(5) = A2DER(3)
ATEMP = -2.5D0 * H2ND
A2DER(4) = DCMPLX(ATEMP,0.0D0)

      COMPUTE CENTRAL DIFFERENCE COEFFICIENTS FOR FIRST ORDER

      DERIVATIVE AT POINTS 2 - 43

H1ST = DMESH
ATEMP = (1.0D0/12.0D0) * H1ST
A1DER(2) = DCMPLX(ATEMP,0.0D0)
A1DER(6) = -A1DER(2)
ATEMP = (-8.0D0/12.0D0) * H1ST
A1DER(3) = DCMPLX(ATEMP,0.0D0)
A1DER(5) = -A1DER(3)

*****

      PART II

      READ IN PRE-COMPUTED NON-CENTRAL DIFFERENCE COEFFICIENTS FOR
      ALL DERIVATIVES OF Q(R) AT POINTS NEAR THE AXIS.

      BOUNDARY CONDITIONS AT THE AXIS ARE: D3Q(0)=0 AND DQ(0)=0.

      FOR SECOND EQUATION IN Q(R) ONLY, FOR N = 0.

51 READ(5,9) I,J,K
   IF(I.EQ.9) GO TO 54
   HTEMP = DMESH ** I
   DO 52 KKK = 1,K
     READ(5,* ) AATEMP, HTEMP
     AAXIS(I,J,KKK) = DCMPLX(AATEMP,0.0D0)
52 CONTINUE
   GO TO 51
54 CONTINUE

      READ IN PRE-COMPUTED NON-CENTRAL DIFFERENCE COEFFICIENTS FOR

```



```

CCCCCCCC
ALL DERIVATIVES OF Q(R) AT POINTS NEAR THE WALL.
BOUNDARY CONDITIONS AT THE WALL ARE: DQ(1)=0 AND Q(1)=0.
FOR SECOND EQUATION IN Q(R) ONLY, FOR N = 0.

55 READ(5,59) I,J,K
   IF(I.EQ.9) GO TO 57
   HTEMP = DRESH ** I
   JJ = 4 - J
   SIGN = 1.0 DO
   IF(I.EQ.1) SIGN = -SIGN
   IF(I.EQ.3) SIGN = -SIGN
   DO 56 KKK = 1, K
   KKK = 7 - KKK
   READ(5,* ) WATEMP
   WATEMP = WATEMP * HTEMP * SIGN
   AWALL(I,JJ,KKK) = DCMPLY(WATEMP,0.0D0)
56 CONTINUE
57 GO TO 55
59 FORMAT(I1,1X,I1,1X,I1)

REARRANGING SOME OF THE DATA IN THE AXIS AND WALL
COEFFICIENT MATRICES

DO 58 I = 1,6
  AAXIS(2,3,I) = A2DER(I + 1)
  AAXIS(1,3,I) = A1DER(I + 1)
  AWALL(2,1,I) = A2DER(I)
  AWALL(1,1,I) = A1DER(I)
58 CONTINUE

READ IN COEFFICIENTS TO DETERMINE Q(0)

DO 10 I = 1,6
  READ(5,*) A6INV(I)
  CONTINUE
10 CONTINUE

*****
READ IN ALPHA AND KEYNOLDS NR

IPIOT = 0
19 CONTINUE
  READ(5,*) ALPHA,RE

```

PIP01930
 PIP01940
 PIP01950
 PIP01960
 PIP01970
 PIP01980
 PIP01990
 PIP02000
 PIP02010
 PIP02020
 PIP02030
 PIP02040
 PIP02050
 PIP02060
 PIP02070
 PIP02080
 PIP02090
 PIP02100
 PIP02110
 PIP02120
 PIP02130
 PIP02140
 PIP02150
 PIP02160
 PIP02170
 PIP02180
 PIP02190
 PIP02200
 PIP02210
 PIP02220
 PIP02230
 PIP02240
 PIP02250
 PIP02260
 PIP02270
 PIP02280
 PIP02290
 PIP02300
 PIP02310
 PIP02320
 PIP02330
 PIP02340
 PIP02350
 PIP02360
 PIP02370
 PIP02380
 PIP02390
 PIP02400

IF (ALPHA.LT.0.0D0) GO TO 180

PART III

COMPUTATION OF THE VORTICITY TRANSPORT EQUATION COEFFICIENTS
FOR Q(R) ONLY AND THE RESPECTIVE DERIVATIVES.

PRE-COMPUTE CONSTANTS INVOLVING ALPHA IN THE COEFFICIENTS

```

DTEMPR = (-6.0D0/RE)
D3TEMP = DCMLPX(DTEMPR,0.0D0)
E1TEMP = DCMLPX(-3.0D0,0.0D0)
ALSO = ALPHA * ALPHA
AL2 = ALPHA + ALPHA
AL22 = ALSO + ALSO
AL6 = 6.0D0 * ALSO
AL3RD = ALSO * ALPHA
AL4TH = AL3RD * ALPHA
AL23 = AL3RD + AL3RD

```

```

DO 60 I = 1,MESH
R = (DFLOAT(I) - 0.5D0) / DMESH
R2 = R * R
R3 = R2 * R
RAD(I) = DCMLPX(R,0.0D0)
DTEMPR = (-R/RE)
D4(I) = DCMLPX(DTEMPR,0.0D0)
D3(I) = D3TEMP
DTEMPR = ((-3.0D0/R) + (AL22 * R))/RE
DTEMPI = AL2 * (R - R3)
D2(I) = DCMLPX(DTEMPR,DTEMPI)
DTEMPR = ((3.0D0/(R2)) + AL62)/RE
DTEMPI = AL6 * (1.0D) - R2
D1(I) = DCMLPX(DTEMPR,DTEMPI)
DTEMPR = -(AL4TH * R)/RE
DTEMPI = AL23 * (R3 - R)
D0(I) = DCMLPX(DTEMPR,DTEMPI)
ETEMP = -R
E2(I) = DCMLPX(ETEMP,0.0D0)
E1(I) = E1TEMP
ETEMP = ALSO * R
E0(I) = DCMLPX(ETEMP,0.0D0)
60 CONTINUE

```

PIP02410
 PIP02420
 PIP02430
 PIP02440
 PIP02450
 PIP02460
 PIP02470
 PIP02480
 PIP02490
 PIP02500
 PIP02510
 PIP02520
 PIP02530
 PIP02540
 PIP02550
 PIP02560
 PIP02570
 PIP02580
 PIP02590
 PIP02600
 PIP02610
 PIP02620
 PIP02630
 PIP02640
 PIP02650
 PIP02660
 PIP02670
 PIP02680
 PIP02690
 PIP02700
 PIP02710
 PIP02720
 PIP02730
 PIP02740
 PIP02750
 PIP02760
 PIP02770
 PIP02780
 PIP02790
 PIP02800
 PIP02810
 PIP02820
 PIP02830
 PIP02840
 PIP02850
 PIP02860
 PIP02870
 PIP02880

162


```

399 FORMAT(5X, D30.18, 3X, D30.18)
400 CONTINUE
C
C      COMPUTATION OF DQ(R)
DO 410 J = 1, 3
DO (J) = ZERO
DO 410 K = 1, 6
DO (J) = DQ(J) + Q(K) * AAXIS(1, J, K)
410 CONTINUE
C
M = MESH - 3
DO 420 J = 4, M
DO (J) = ZERO
DO 420 K = 1, 7
L = J - 4 + K
DQ(J) = DQ(J) + Q(L) * A1DER(K)
420 CONTINUE
C
MM = M - 3
DO 430 J = 1, 3
L = J + M
DQ(L) = ZERO
DO 430 K = 1, 6
N = MM + K
DQ(L) = DQ(L) + Q(N) * AVAL(1, J, K)
430 CONTINUE
C
DO 440 I = 1, MESH
U(I) = Q(I) * TWO + RAD(I) * DQ(I)
440 CONTINUE
C
C      COMPUTE Q(0)
Q06 = ZERO
DO 441 I = 1, 6
A6CPX = DCMPLEX(A6INV(I), 0.0D0)
Q06 = Q06 + (A6CPX * Q(I))
441 CONTINUE
C
C      REARRANGE DATA FOR PLOT ROUTINE
M2 = MESH + 2
DO 450 I = 1, MESH
II = M2 - I
III = II - 1
U(II) = U(III)
RAD(II) = RAD(III)

```

```

PIP04330
PIP04340
PIP04350
PIP04360
PIP04370
PIP04380
PIP04390
PIP04400
PIP04410
PIP04420
PIP04430
PIP04440
PIP04450
PIP04460
PIP04470
PIP04480
PIP04490
PIP04500
PIP04510
PIP04520
PIP04530
PIP04540
PIP04550
PIP04560
PIP04570
PIP04580
PIP04590
PIP04600
PIP04610
PIP04620
PIP04630
PIP04640
PIP04650
PIP04660
PIP04670
PIP04680
PIP04690
PIP04700
PIP04710
PIP04720
PIP04730
PIP04740
PIP04750
PIP04760
PIP04770
PIP04780
PIP04790
PIP04800

```



```

PIP05770
PIP05780
PIP05790
PIP05800
PIP05810
PIP05820
PIP05830
PIP05840
PIP05850
PIP05860
PIP05870
PIP05880
PIP05890
PIP05900
PIP05910
PIP05920
PIP05930
PIP05940
PIP05950
PIP05960
PIP05970
PIP05980
PIP05990
PIP06000
PIP06010
PIP06020
PIP06030
PIP06040
PIP06050
PIP06060
PIP06070
PIP06080
PIP06090
PIP06100
PIP06110
PIP06120
PIP06130
PIP06140
PIP06150
PIP06160
PIP06170
PIP06180
PIP06190
PIP06200
PIP06210
PIP06220
PIP06230
PIP06240

```

```

CALL SYMBOL(XO,YO,YHT,'GAMMA*','0.0,9)
CALL NUMBER(XN,YO,YHT,GAMPLT,0.0,4)
YO = YO - 3.4
CALL SYMBOL(XO,YO,YHT,'OCTAGON' = U(REAL)',0.0,17)
YO = YO - DELY
CALL SYMBOL(XO,YO,YHT,'DIAMOND' = U(IMAG)',0.0,17)
YO = YO - DELY
CALL SYMBOL(XO,YO,YHT,'TRIANGLE' = U AMPL ',0.0,17)

WRITE THE AXIS LABELS

XO = XO - 2.55
YO = YO + 0.3
YHT = 0.12
CALL SYMBOL(XO,YO,YHT,'NORMALIZED PERTURBATION VELOCITY',90.,32)
XO = XO + 2.8
YO = YO - 1.0
CALL SYMBOL(XO,YO,YHT,'PIPE RADIUS',0.0,11)
RETURN
END

```

```

/*GO,SYN DD *
4 1 6
0.149055277542135411D+01
-0.146728551300678589D+01
-0.952808034464035483D+00
0.131474814501754689D+01
-0.443066268162952040D+00
0.578588951948733141D-01
4 2 6
-0.529970874070089781D+01
0.109232811728783830D+02
-0.803543362016894491D+01
-0.276664742824026710D+01
-0.380985744383800062D+00
0.261995041349871033D-01
4 3 6
0.182995357263197173D+01
-0.649259024806782037D+01
0.932687952743622972D+01
-0.649679291508053325D+01
-0.199910835799184739D+01
-0.166558294911753445D+00
3 1 5
0.307102076124568124D+01
-0.551704152249136515D+01
-0.319074394463668409D+01
-0.848010380622840620D+00

```


0.000	575.000	0
0.500	575.000	0
1.000	575.000	0
2.000	575.000	0
4.000	575.000	0
8.000	575.000	0
16.000	575.000	0
32.000	575.000	0
0.500	1150.000	0
1.000	1150.000	0
2.000	1150.000	0
4.000	1150.000	0
8.000	1150.000	0
16.000	1150.000	0
32.000	1150.000	0
*/	1.000	
//		

B. MAIN INVESTIGATIVE PROGRAM FOR $n = 1$

```

//WALLACE JOB (2027,0084), 'THESIS N = 1', CLASS=C
//*MAIN LINES={10
//EXEC PRYICLSP, IMSL=DP, REGION.G0=2048K
//PORT.SYSIN DD *
C*****
THIS PROGRAM WAS DEVELOPED TO PERFORM A NUMERICAL ANALYSIS
OF THREE DIMENSIONAL PIPE FLOW STABILITY FOR AXIAL WAVE
NUMBER N = 1. THE PROGRAM IS DIVIDED INTO EIGHT PARTS.
THE FIRST PART COMPUTES THE CENTRAL FINITE DIFFERENCE
COEFFICIENTS FOR THE DERIVATIVES OF P(R) AND Q(R) AT THE
INTERIOR MESH POINTS ALONG THE PIPE RADIUS. IN THE SECOND
PART, PRE-COMPUTED NON-CENTRAL FINITE DIFFERENCE
COEFFICIENTS FOR THE DERIVATIVES OF P(R) AND Q(R) AT POINTS
NEAR THE AXIS AND WALL ARE READ IN AS DATA. THE THIRD PART
COMPUTES THE VORTICITY TRANSPORT EQUATION COEFFICIENTS OF
P(R) AND Q(R) AND THEIR RESPECTIVE DERIVATIVES AT ALL RADIAL
MESH POINTS (STATIONS). THE FOURTH PART COMPUTES THE A AND B
MATRIX ELEMENTS, WHICH MAKE-UP THE EIGENSYSTEM TO BE SOLVED
IN THE FORMAT, A * X = GAMMA * B * X. IN THE FIFTH PART
THE A AND B MATRICES COMPRISING THE EIGENSYSTEM ARE SOLVED
IN THE SUBROUTINE EIGZC. THE RESULTING EIGENVALUES AND
CORRESPONDING EIGENVECTOR REPRESENT GAMMA AND THE COLUMN
VECTOR X, RESPECTIVELY, AND ARE SOLUTIONS OF THE GOVERNING
PARTIAL DIFFERENTIAL EQUATIONS. THE SIXTH PART VERIFIES
THE SOLUTION OF THE PDE AND THE MAGNITUDE OF THE RESIDUAL
IS DETERMINED. THE SEVENTH PART COMPUTES THE NORMALIZED
PIP000010
PIP000020
PIP000030
PIP000040
PIP000050
PIP000060
PIP000070
PIP000080
PIP000090
PIP000100
PIP000110
PIP000120
PIP000130
PIP000140
PIP000150
PIP000160
PIP000170
PIP000180
PIP000190
PIP000200
PIP000210
PIP000220
PIP000230
PIP000240
PIP000250
PIP000260
PIP000270
PIP000280
PIP000290
PIP000300
PIP000310
PIP000320
PIP000330
PIP000340
PIP000350
PIP000360
PIP000370
PIP000380
PIP000390
PIP000400
PIP000410
PIP000420
PIP000430
PIP000440
PIP000450
PIP000460
PIP000470
PIP000480

```

173


```

A3DERQ(2) = -A3DERQ(5)
ATEMP = (13.0D0/8.0D0) * H3RD
A3DERQ(3) = DCMPLEX(ATEMP, 0.0D0)
A3DERQ(5) = -A3DERQ(3)

```

COMPUTE CENTRAL DIFFERENCE COEFFICIENTS FOR SECOND ORDER
DERIVATIVES OF P(R) AND Q(R) AT INTERIOR MESH POINTS.

```

H2ND = DMESH ** 2
ATEMP = (-1.0D0/12.0D0) * H2ND
A2DERQ(2) = DCMPLEX(ATEMP, 0.0D0)
A2DERQ(6) = A2DERQ(2)
ATEMP = (16.0D0/12.0D0) * H2ND
A2DERQ(3) = DCMPLEX(ATEMP, 0.0D0)
A2DERQ(5) = A2DERQ(3)
ATEMP = -2.5D0 * H2ND
A2DERQ(4) = DCMPLEX(ATEMP, 0.0D0)
A2DERP(1) = A2DERQ(2)
A2DERP(2) = A2DERQ(3)
A2DERP(3) = A2DERQ(4)
A2DERP(4) = A2DERQ(5)
A2DERP(5) = A2DERQ(5)

```

COMPUTE CENTRAL DIFFERENCE COEFFICIENTS FOR FIRST ORDER
DERIVATIVES OF P(R) AND Q(R) AT INTERIOR MESH POINTS.

```

H1ST = DMESH
ATEMP = (1.0D0/12.0D0) * H1ST
A1DERQ(2) = DCMPLEX(ATEMP, 0.0D0)
A1DERQ(6) = -A1DERQ(2)
ATEMP = (-8.0D0/12.0D0) * H1ST
A1DERQ(3) = DCMPLEX(ATEMP, 0.0D0)
A1DERQ(5) = -A1DERQ(3)
A1DERP(1) = A1DERQ(2)
A1DERP(2) = A1DERQ(3)
A1DERP(4) = A1DERQ(5)
A1DERP(5) = A1DERQ(5)

```

PART II

READ IN PRE-COMPUTED NON-CENTRAL DIFFERENCE COEFFICIENTS FOR
ALL DERIVATIVES OF P(R) AT POINTS NEAR THE AXIS.

```

PIP01450
PIP01460
PIP01470
PIP01480
PIP01490
PIP01500
PIP01510
PIP01520
PIP01530
PIP01540
PIP01550
PIP01560
PIP01570
PIP01580
PIP01590
PIP01600
PIP01610
PIP01620
PIP01630
PIP01640
PIP01650
PIP01660
PIP01670
PIP01680
PIP01690
PIP01700
PIP01710
PIP01720
PIP01730
PIP01740
PIP01750
PIP01760
PIP01770
PIP01780
PIP01790
PIP01800
PIP01810
PIP01820
PIP01830
PIP01840
PIP01850
PIP01860
PIP01870
PIP01880
PIP01890
PIP01900
PIP01910
PIP01920

```



```

47 CONTINUE
49 FORMAT(I1,1X,I1,1X,I1)
      READ IN PRE-COMPUTED NON-CENTRAL DIFFERENCE COEFFICIENTS FOR
      ALL DERIVATIVES OF Q(R) AT POINTS NEAR THE AXIS.
      BOUNDARY CONDITION AT THE AXIS IS: DQ(0) = 0.
51 READ(5,49) I,J,K
   IF(I.EQ.9) GO TO 54
   HTEMP = DMESH ** I
   DO 52 KKK = 1,K
     READ(5,*) AATEMP
     AATEMP = AATEMP * HTEMP
     AAXISQ(I,J,KKK) = DCMPLX(AATEMP,0.0D0)
52 CONTINUE
   GO TO 51
54 CONTINUE
      READ IN PRE-COMPUTED NON-CENTRAL DIFFERENCE COEFFICIENTS
      FOR D2Q(0).
55 READ(5,49) I,J,K
   IF(I.EQ.9) GO TO 57
   HTEMP = DMESH ** I
   JJ = 4 - J
   SIGN = 1.0D0
   IF(I.EQ.1) SIGN = -SIGN
   IF(I.EQ.3) SIGN = -SIGN
   DO 56 KKK = 1,K
     KK = 7 - KKK
     READ(5,*) WATEMP

```

```

PIP02410
PIP02420
PIP02430
PIP02440
PIP02450
PIP02460
PIP02470
PIP02480
PIP02490
PIP02500
PIP02510
PIP02520
PIP02530
PIP02540
PIP02550
PIP02560
PIP02570
PIP02580
PIP02590
PIP02600
PIP02610
PIP02620
PIP02630
PIP02640
PIP02650
PIP02660
PIP02670
PIP02680
PIP02690
PIP02700
PIP02710
PIP02720
PIP02730
PIP02740
PIP02750
PIP02760
PIP02770
PIP02780
PIP02790
PIP02800
PIP02810
PIP02820
PIP02830
PIP02840
PIP02850
PIP02860
PIP02870
PIP02880

```

[illegible]

PIP033370
 PIP033380
 PIP033390
 PIP033400
 PIP033410
 PIP033420
 PIP033430
 PIP033440
 PIP033450
 PIP033460
 PIP033470
 PIP033480
 PIP033490
 PIP033500
 PIP033510
 PIP033520
 PIP033530
 PIP033540
 PIP033550
 PIP033560
 PIP033570
 PIP033580
 PIP033590
 PIP033600
 PIP033610
 PIP033620
 PIP033630
 PIP033640
 PIP033650
 PIP033660
 PIP033670
 PIP033680
 PIP033690
 PIP033700
 PIP033710
 PIP033720
 PIP033730
 PIP033740
 PIP033750
 PIP033760
 PIP033770
 PIP033780
 PIP033790
 PIP033800
 PIP033810
 PIP033820
 PIP033830
 PIP033840

```

R = (DFLOAT(I) - 0.5D0) / DMESH
R2 = R * R
R3 = R2 * R
R4 = R3 * R
RAD(I) = DCMLPX(R, 0.3D0)

VORTICITY TRANSPORT EQN COEFFICIENTS FOR P(R), DP(R) & D2P(R)

FIRST EQUATION FIRST QUADRANT
TEMPR = (1.0D0 + ALSQ * R2) / RE
D2P1(I) = DCMLPX(TEMPR, 0.0D0)
TEMPR = ((3.0D0/R) + (R*ALSQ5)) / RE
D1P1(I) = DCMLPX(TEMPR, 0.0D0)
TEMPR = ALSQ * ((1.0D0 - ALSQ*R2) / RE
TEMP1(I) = -AL2 * ((1.0D0 - R2) + (ALSQ*R2)) - (ALSQ*R4)
DOF1(I) = DCMLPX(TEMPR, TEMP1)
TEMPR = 1.0D0 + (ALSQ * R2)
EOP1(I) = DCMLPX(TEMPR, 0.0D0)

V T E COEFFICIENTS FOR Q(R), DQ(R), D2Q(R) AND D3Q(R)

FIRST EQUATION SECOND QUADRANT
TEMP1 = R / RE
D3Q1(I) = DCMLPX(0.0D0, TEMP1)
TEMP1 = 8.0D0 / RE
D2Q1(I) = DCMLPX(0.0D0, TEMP1)
TEMPR = AL2 * (R - R3)
TEMP1 = ((12.0D0/R) - (ALSQ*R)) / RE
D1Q1(I) = DCMLPX(TEMPR, TEMP1)
TEMPR = AL2 * (3.0D0 - R2)
TEMP1 = -ALSQ5 / RE
DOQ1(I) = DCMLPX(TEMPR, TEMP1)
E1Q1(I) = DCMLPX(0.0D0, R)
EQQ1(I) = DCMLPX(0.0D0, 3.0D0)

VORTICITY TRANSPORT EQN COEFFICIENTS FOR H(O)

FIRST EQUATION
TEMPR = AL2 * (2.0D0 - ALSQ + (ALSQ*R2))
TEMP1 = AL4TH * RE
HOA1(I) = DCMLPX(TEMPR, TEMP1)
TEMP1 = -ALSQ
HOB1(I) = DCMLPX(0.0D0, TEMP1)

VORTICITY TRANSPORT EQN COEFFICIENTS FOR P(R), DP(R) & D2P(R)
  
```

CCCCC

CCCCC

CCCCC

CC

PIP03850
 PIP03860
 PIP03870
 PIP03880
 PIP03890
 PIP03900
 PIP03910
 PIP03920
 PIP03930
 PIP03940
 PIP03950
 PIP03960
 PIP03970
 PIP03980
 PIP03990
 PIP04000
 PIP04010
 PIP04020
 PIP04030
 PIP04040
 PIP04050
 PIP04060
 PIP04070
 PIP04080
 PIP04090
 PIP04100
 PIP04110
 PIP04120
 PIP04130
 PIP04140
 PIP04150
 PIP04160
 PIP04170
 PIP04180
 PIP04190
 PIP04200
 PIP04210
 PIP04220
 PIP04230
 PIP04240
 PIP04250
 PIP04260
 PIP04270
 PIP04280
 PIP04290
 PIP04300
 PIP04310
 PIP04320

```

C C C
SECOND EQUATION THIRD QUADRANT
TEMPI = -4.0D0 / RE
D2P2(I) = DCMPLX(0.0D0, TEMPI)
TEMPI = -12.0D0 / (RE * R)
D1P2(I) = DCMPLX(0.0D0, TEMPI)
TEMPI = -AL4 * (1.0D0 - R2)
TEMPI = ALSQ4 / RE
DOP2(I) = DCMPLX(TEMPI, TEMPI)
EOP2(I) = DCMPLX(0.0D0, -2.0D0)

V T E COEFFICIENTS FOR Q(R), DQ(R), D2Q(R), D3Q(R) AND D4Q(R)
C C C C C
SECOND EQUATION FOURTH QUADRANT
TEMPI = -R2 / RE
D4Q2(I) = DCMPLX(TEMPI, 0.0D0)
TEMPI = -(10.0D0 * R) / RE
D3Q2(I) = DCMPLX(TEMPI, 0.0D0)
TEMPI = (-19.0D0 + (ALSQ2 * R2)) / RE
TEMPI = AL2 * (R2 - R4)
D2Q2(I) = DCMPLX(TEMPI, TEMPI)
TEMPI = ((3.0D0 / R) + (ALSQ10 * R)) / RE
TEMPI = AL10 * (R - R3)
D1Q2(I) = DCMPLX(TEMPI, TEMPI)
TEMPI = (ALSQ4 - (AL4FH * R2)) / RE
TEMPI = AL2 * ((2.0D0 * (1.0D0 - R2)) - (ALSQ * (R2 - R4)))
D0Q2(I) = DCMPLX(TEMPI, TEMPI)
TEMPI = -R2
E2Q2(I) = DCMPLX(TEMPI, 0.0D0)
TEMPI = -5.0D0 * R
E1Q2(I) = DCMPLX(TEMPI, 0.0D0)
TEMPI = -2.0D0 + (ALSQ * R2)
E0Q2(I) = DCMPLX(TEMPI, 0.0D0)

VORTICITY TRANSPORT EQN COEFFICIENTS FOR H(O)
C C C C C
SECOND EQUATION
TEMPI = -AL4TH / RE
TEMPI = -AL3RD2 * (1.0D0 - (ALPHA * R2))
H0A2(I) = DCMPLX(TEMPI, TEMPI)
H0B2(I) = DCMPLX(ALS2, 6.0D0)
60 CONTINUE
C C C C C
*****

```



```

220 HOD1PA = HOD1PA + AVALLP(1,J,K)
    CONTINUE
221 HOD2PA = HOD2PA + D2P1(L)
    HOD1PA = HOD1PA + D1P1(L)
    HOD1(L) = HOD1(L) - (ONEING * (HOD2PA + HOD1PA))
    CONTINUE

C C C C C
      A AND B MATRIX ELEMENTS IN TERMS OF Q(R)
      FIRST EQUATION SECOND QUADRANT

DO 251 J = 1,3
  QOD1QA = ZERO
  QOD2QA = ZERO
  QOD3QA = ZERO
  QOD1QB = ZERO
  DO 250 K = 1,6
    KK = K + MESH
    AODER = ZERO
    IF(K.EQ.J) AODER = ONE
    A(J,KK) = AAXISO(3,J,K) * D3Q1(J) + AAXISO(2,J,K) * D2Q1(J) +
1      AAXISO(1,J,K) * D1Q1(J) + AODER * DQ1(J)
    B(J,KK) = AAXISO(2,J,K)
    AAXQ1 = AAXISO(1,J,K)
    AAXQ2 = AAXISO(2,J,K)
    IF(J.EQ.3) AAXQ1 = ZERO
    IF(J.EQ.3) AAXQ2 = ZERO
    QOD1QA = QOD1QA + AAXQ1
    QOD2QA = QOD2QA + AAXQ2
    QOD3QA = QOD3QA + AAXISO(3,J,K)
    QOD1QB = QOD1QB + AAXQ1
  CONTINUE
250 QOD1QA = D1Q1(J)
    QOD2QA = D2Q1(J)
    QOD3QA = D3Q1(J)
    QOD1QB = E1Q1(J)
    A(J,HQ) = -(QOD1QA + QOD2QA + QOD3QA)
    B(J,HQ) = -QOD1QB
  CONTINUE
251 M = MESH - 3
    DO 260 J = 4,M
      DO 260 K = 1,K
        LL = J - 4 + MESH
        AODER = ZERO
        IF(L.EQ.J) AODER = ONE
        A(J,LL) = AAXISO(3,K) * D3Q1(J) + AAXISO(2,K) * D2Q1(J) +
1      AAXISO(1,K) * D1Q1(J) + AODER * DQ1(J)

```

PIP05290
 PIP05300
 PIP05310
 PIP05320
 PIP05330
 PIP05340
 PIP05350
 PIP05360
 PIP05370
 PIP05380
 PIP05390
 PIP05400
 PIP05410
 PIP05420
 PIP05430
 PIP05440
 PIP05450
 PIP05460
 PIP05470
 PIP05480
 PIP05490
 PIP05500
 PIP05510
 PIP05520
 PIP05530
 PIP05540
 PIP05550
 PIP05560
 PIP05570
 PIP05580
 PIP05590
 PIP05600
 PIP05610
 PIP05620
 PIP05630
 PIP05640
 PIP05650
 PIP05660
 PIP05670
 PIP05680
 PIP05690
 PIP05700
 PIP05710
 PIP05720
 PIP05730
 PIP05740
 PIP05750
 PIP05760

```

260 B(J,LL) = AIDERQ(K)*E1Q1(J) + AODER*EQ1(J)
    CONTINUE
    MM = M - 3
    DO 266 J = 1,3
      L = J + M
      HOD3QA = ZERO
      HOD2QA = ZERO
      HOD1QA = ZERO
      HOD1QB = ZERO
      DO 265 K = 1,6
        KK = 7 - K
        NN = MM + K
        NN = NN + K
        AODER = ZERO
        IF(N.EQ.L) AODER = ONE
        A(L,NN) = AVALLO(3,J,K)*D3Q1(L) + AVALLO(2,J,K)*D2Q1(L) +
          AVALLO(1,J,K)*E1Q1(L) + AODER*EQ1(L)
        B(L,NN) = 1.0DO*(2:ODO*DFLAT(KK) - 1.0DO) / DMESH
        BTEMP = DCMPLX(HTMP,0.0DO)
        BETA = AVALLO(1,J,K)
        AWAQ1 = AVALLO(2,J,K)
        AWAQ2 = AVALLO(3,J,K)
        IF(J.EQ.1) AWAQ1 = ZERO
        IF(J.EQ.1) AWAQ2 = ZERO
        HOD1QA = HOD1QA + {AWAQ1*BETA}
        HOD2QA = HOD2QA + {AWAQ2*BETA}
        HOD3QA = HOD3QA + {AWALL2(3,J,K)}
        HOD1QB = HOD1QB + {AWAQ1*BETA}
      CONTINUE
      HOD1QA = HOD1QA + T2
      IF(J.EQ.1) HOD1QA = ZERO
      HOD1QB = HOD1QB + T2
      IF(J.EQ.1) HOD1QB = ZERO
      IF(J.EQ.1) HOD1QA = D121(L)
      HOD2QA = HOD2QA + D231(L)
      HOD3QA = HOD3QA + D331(L)
      HOD1QB = HOD1QB + E121(L)
      HOA1(L) = HOD1QA + HOD2QA + HOD3QA + HOA1(L)
      HOB1(L) = HOD1QB + HOD2QB + HOD3QB
    CONTINUE
266 CCCCCC

      A AND B MATRIX ELEMENTS IN TERMS OF H(0)
      FIRST EQUATION
      DO 267 I = 1,MESH
        A(I,MH0) = HOA1(I)
        B(I,MH0) = HOB1(I)
      CONTINUE
  
```



```

267 CONTINUE
C      A AND B MATRIX ELEMENTS IN TERMS OF P(R)
C      SECOND EQUATION THIRD QUADRANT
C
DO 270 J = 1, 2
JJ = J + MESH
DO 270 K = 1, 5
AODER = ZERO
IF (K.EQ.J) AODER = ONE
A(JJ,K) = AAXISP(2,J,K)*D2P2(J) + AAXISP(1,J,K)*D1P2(J) +
1 B(JJ,K) = AODER*EOP2(J)
270 CONTINUE
DO 275 J = 3, MP
JJ = J + MESH
DO 275 K = 1, 5
L = J - 3 + K
AODER = ZERO
IF (L.EQ.J) AODER = ONE
IF (JJ,L) = AODER*EOP2(J) + A1DERP(K)*D1P2(J) + AODER*DOP2(J)
B(JJ,L) = AODER*EOP2(J)
275 CONTINUE
DO 281 J = 1, 2
L = J + MP
LL = L + MESH
HOD1PA = ZERO
HOD2PA = ZERO
DO 280 K = 1, 5
N = MP + K
AODER = ZERO
IF (N.EQ.L) AODER = ONE
A(LL,N) = AODER*EOP2(L) + AODER*EOP2(L) + AODER*EOP2(L) + AODER*EOP2(L) +
1 B(LL,N) = AODER*EOP2(L) + AODER*EOP2(L) + AODER*EOP2(L) + AODER*EOP2(L) +
HOD1PA = HOD1PA + AODER*EOP2(L)
HOD2PA = HOD2PA + AODER*EOP2(L)
280 CONTINUE
HOD1PA = HOD1PA + D1P2(L)
HOD2PA = HOD2PA + D2P2(L)
HOD2PA = HOD2PA + HOD2PA
HOD2(L) = HOD2(L) - (ONEING * (HOD1PA + HOD2PA))
281 CONTINUE
C      A AND B MATRIX ELEMENTS IN TERMS OF Q(R)
C      SECOND EQUATION FOURTH QUADRANT
C

```

PIP06250
 PIP06260
 PIP06270
 PIP06280
 PIP06290
 PIP06300
 PIP06310
 PIP06320
 PIP06330
 PIP06340
 PIP06350
 PIP06360
 PIP06370
 PIP06380
 PIP06390
 PIP06400
 PIP06410
 PIP06420
 PIP06430
 PIP06440
 PIP06450
 PIP06460
 PIP06470
 PIP06480
 PIP06490
 PIP06500
 PIP06510
 PIP06520
 PIP06530
 PIP06540
 PIP06550
 PIP06560
 PIP06570
 PIP06580
 PIP06590
 PIP06600
 PIP06610
 PIP06620
 PIP06630
 PIP06640
 PIP06650
 PIP06660
 PIP06670
 PIP06680
 PIP06690
 PIP06700
 PIP06710
 PIP06720

```

DO 286 J = 1, 3
JJ = J + MESH
QDD1QA = ZERO
QDD2QA = ZERO
QDD3QA = ZERO
QDD4QA = ZERO
QDD1QB = ZERO
QDD2QB = ZERO
DO 285 K = 1, 6
KK = K + MESH
AODER = ZERO
IF (K.EQ.J) AODER = JNE
A(JJ, KK) = AAXISO(4, J, K) * D4Q2(J) + AAXISO(3, J, K) * D3Q2(J) +
1 AAXISO(2, J, K) * D2Q2(J) + AAXISO(1, J, K) * D1Q2(J) +
2 AODER * D0Q2(J)
1 B(JJ, KK) = AAXISO(2, J, K) * E2Q2(J) + AAXISO(1, J, K) * E1Q2(J) +
AAXQ1 = AAXISO(1, J, K)
AAXQ2 = AAXISO(2, J, K)
IF (J.EQ.3) AAXQ1 = ZERO
IF (J.EQ.3) AAXQ2 = ZERO
QDD1QA = QDD1QA + AAXQ1
QDD2QA = QDD2QA + AAXQ2
QDD3QA = QDD3QA + AAXISO(3, J, K)
QDD4QA = QDD4QA + AAXISO(4, J, K)
QDD1QB = QDD1QB + AAXQ1
QDD2QB = QDD2QB + AAXQ2
CONTINUE
285 QDD1QA = D1J22(J)
QDD2QA = D2J22(J)
QDD3QA = D3J22(J)
QDD4QA = D4J22(J)
QDD1QB = E1J22(J)
QDD2QB = E2J22(J)
= - (QDD1QA + QDD1QB + QDD2QA + QDD2QB)
B(JJ, HQO)
CONTINUE
286 DO 290 J = 4, M
JJ = J + MESH
DO 290 K = 1, 7
L = J - 4
LL = L + MESH
AODER = ZERO
IF (L.EQ.J) AODER = JNE
A(JJ, LL) = A4DERO(K) * D4Q2(J) + A3DERO(K) * D3Q2(J) +
1 A2DERO(K) * D2Q2(J) + A1DERO(K) * D1Q2(J) +
2 AODER * D0Q2(J)
B(JJ, LL) = A2DERO(K) * E2Q2(J) + A1DERO(K) * E1Q2(J) +
290 CONTINUE
  
```

PIP06730
PIP06740
PIP06750
PIP06760
PIP06770
PIP06780
PIP06790
PIP06800
PIP06810
PIP06820
PIP06830
PIP06840
PIP06850
PIP06860
PIP06870
PIP06880
PIP06890
PIP06900
PIP06910
PIP06920
PIP06930
PIP06940
PIP06950
PIP06960
PIP06970
PIP06980
PIP06990
PIP07000
PIP07010
PIP07020
PIP07030
PIP07040
PIP07050
PIP07060
PIP07070
PIP07080
PIP07090
PIP07100
PIP07110
PIP07120
PIP07130
PIP07140
PIP07150
PIP07160
PIP07170
PIP07180
PIP07190
PIP07200

```

DO 296 J = 1, 3
  L = J + M
  LL = L + MESH
  HOD1QA = ZERO
  HOD2QA = ZERO
  HOD3QA = ZERO
  HOD4QA = ZERO
  HOD1QB = ZERO
  HOD2QB = ZERO
  DO 295 K = 1, 6
    KK = MM + K
    NN = NN + K
    AORDER = ZERO
    IF (N.EQ.L) AORDER = ONE
    A(LL, NN) = AVALLO(4, J, K) * D4Q2(L) + AVALLO(3, J, K) * D3Q2(L) +
      AVALLO(2, J, K) * D2Q2(L) + AVALLO(1, J, K) * D1Q2(L)
    B(LL, NN) = AVALLO(2, J, K) * E2Q2(L) + AVALLO(1, J, K) * E1Q2(L)
    HTEMP = (1.0D0 - ((2.0D0 * DFLCAT(KK) - 1.0D0) / DMESH))
    BETA = DCMPLX(HTEMP, 0.0D0)
    AWAQ1 = AVALLO(1, J, K)
    AWAQ2 = AVALLO(2, J, K)
    IF (J.EQ.1) AWAQ1 = ZERO
    IF (J.EQ.1) AWAQ2 = ZERO
    HOD1QA = HOD1QA + (AWAQ1 * BETA)
    HOD2QA = HOD2QA + (AWAQ2 * BETA)
    HOD3QA = HOD3QA + (AVALLO(3, J, K) * BETA)
    HOD4QA = HOD4QA + (AVALLO(4, J, K) * BETA)
    HOD1QB = HOD1QB + (AWAQ1 * BETA)
    HOD2QB = HOD2QB + (AWAQ2 * BETA)
  CONTINUE
  HOD1QA = HOD1QA + THC
  HOD1QB = HOD1QB + THC
  IF (J.EQ.1) HOD1QA = ZERO
  IF (J.EQ.1) HOD1QB = ZERO
  HOD1QA = HOD1QA + D1Q2(L)
  HOD2QA = HOD2QA + D2Q2(L)
  HOD3QA = HOD3QA + D3Q2(L)
  HOD4QA = HOD4QA + D4Q2(L)
  HOD1QB = HOD1QB + E1Q2(L)
  HOD2QB = HOD2QB + E2Q2(L)
  HOD1QA = HOD1QA + HOD1QA + HOD3QA + HOD4QA
  HOD2QA = HOD2QA + HOD2QA + HOD3QA + HOD4QA
  HOD1QB = HOD1QB + HOD1QB + HOD3QB + HOD4QB
  HOD2QB = HOD2QB + HOD2QB + HOD3QB + HOD4QB
  HOD2(L) = HOD2(L) + HOD2(L)
  HOD2(L) = HOD2(L)
  CONTINUE
296 C
C      A AND B MATRIX ELEMENTS IN TERMS OF H(O)
C

```

```

PIP072210
PIP072220
PIP072230
PIP072240
PIP072250
PIP072260
PIP072270
PIP072280
PIP072290
PIP072300
PIP072310
PIP072320
PIP072330
PIP072340
PIP072350
PIP072360
PIP072370
PIP072380
PIP072390
PIP072400
PIP072410
PIP072420
PIP072430
PIP072440
PIP072450
PIP072460
PIP072470
PIP072480
PIP072490
PIP072500
PIP072510
PIP072520
PIP072530
PIP072540
PIP072550
PIP072560
PIP072570
PIP072580
PIP072590
PIP072600
PIP072610
PIP072620
PIP072630
PIP072640
PIP072650
PIP072660
PIP072670
PIP072680

```

```

C C C
SECOND EQUATION
DO 297 I = 1, MESH
  II = I + MESH
  A{II,MH0} = H0A2{I}
  B{II,MH0} = H0B2{I}
297 CONTINUE

A AND B MATRIX ELEMENTS FOR THE TWO SPECIAL BOUNDARY
CONDITION EQUATIONS INVOLVING GAMMA.

FIRST EQUATION COEFFICIENTS
TEMPR = 4.000 / RE
D2P01 = DCMPX(TEMPR, 0.000)
TEMPPI = 20.000 / RE
D2Q01 = DCMPX(0.000, TEMPI)
TEMPR = ALSO / RE
TEMPPI = -AL2
DOP01 = DCMPX(TEMPR, TEMPI)
TEMPR = 6.000 * ALPHA
TEMPPI = -ALSO5 / RE
DQ001 = DCMPX(TEMPR, TEMPI)
TEMPR = AL4 - AL3RD2
TEMPPI = AL4TH / RE
DOH01 = DCMPX(TEMPR, TEMPI)
EOP01 = ONE
EQO01 = DCMPX(0.000, 3.000)
TEMPPI = -ALSO
EOH01 = DCMPX(0.000, TEMPI)

SECOND EQUATION COEFFICIENTS
TEMPPI = -16.000 / RE
D2P02 = DCMPX(0.000, TEMPI)
D2Q02 = DCMPX(TEMPPI, 0.000)
TEMPR = -AL4
TEMPPI = ALSO4 / RE
DOP02 = DCMPX(TEMPR, TEMPI)
DQO02 = DCMPX(TEMPPI, AL4)
TEMPR = -AL4TH / RE
TEMPPI = -AL3RD2
DOH02 = DCMPX(TEMPR, TEMPI)
EOP02 = DCMPX(0.000, -2.300)
EQO02 = DCMPX(-2.000, 0.300)
EOH02 = DCMPX(ALSO, 0.000)

C C C

```

188

```

      MESH2 = (MESH * 2) + 2
      IJOB = 1
      CALL EIGZC (AA, 100, BB, 100, MESH2, IJOB, EIGA, EIGB,
      1 EIGVEC, 100, WK, INEER, 150)
      IF (INEER.EQ.0) WRITE(6,150)
150  FORMAT(1X, 'ALL EIGENVALUES CONVERGED WITHIN 30 ',
      1 'ITERATIONS')
155  IF (INEER.NE.0) WRITE(6,155) INEER
      IF (FORMAT(1X, 'FAILED TO CONVERGE ON THE', I4, 1X,
      1 'TH EIGENVALUE', //))
      DO 165 I = 1, MESH2
      EIGVAL(I) = EIGA(I)/EIGB(I)
      GAMR(I) = DREAL(EIGVAL(I))
165  CONTINUE
      NGAM = 1
      GAMMAX = GAMR(1)
      DO 170 I = 2, MESH2
      IF (GAMR(I) .LT. GAMMAX) GO TO 169
      GAMMAX = GAMR(I)
      NGAM = I
169  CONTINUE
170  CONTINUE
      WRITE(6,175) NGAM, GAMMAX, MESH, ALPHA, RE
175  IF (FORMAT(1X, 'LEAST STABLE EIGENVALUE NR', I3, 1X, '= ', D27.18, 4X,
      1 'MESH = ', I3, 4X, 'ALPHA = ', D10.3, 4X, 'REYNOLDS NR = ', D17.10, /))
      *****
      PART VI
      VERIFY THAT THE LEAST STABLE EIGENVALUE AND CORRESPONDING
      EIGENVECTOR SATISFY THE GOVERNING PARTIAL DIFFERENTIAL
      EQUATIONS. RESIDJAL ERROR IS OUTPUT AS EPSILON.

      DO 351 I = 1, MESH2
      SUMA = ZERO
      SUMB = ZERO
      DO 350 J = 1, MESH2
      SUMA = SUMA + (A(I,J) * EIGVEC(J,NGAM) )
      SUMB = SUMB + ( B(I,J) * EIGVEC(J,NGAM) )
350  CONTINUE
      ERROR(I) = SUMA - ( SUMB * EIGVAL(NGAM) )
351  CONTINUE
      WRITE(6,375) 15X, 'EPSILON = A * X - GAMMA * B * X', /
375  FORMAT(1X, //, 15X, 'ERROR(I), I = 1, MESH2)
      WRITE(6,380) (ERROR(I), I = 1, MESH2)

```

PIP08170
 PIP08180
 PIP08190
 PIP08200
 PIP08210
 PIP08220
 PIP08230
 PIP08240
 PIP08250
 PIP08260
 PIP08270
 PIP08280
 PIP08290
 PIP08300
 PIP08310
 PIP08320
 PIP08330
 PIP08340
 PIP08350
 PIP08360
 PIP08370
 PIP08380
 PIP08390
 PIP08400
 PIP08410
 PIP08420
 PIP08430
 PIP08440
 PIP08450
 PIP08460
 PIP08470
 PIP08480
 PIP08490
 PIP08500
 PIP08510
 PIP08520
 PIP08530
 PIP08540
 PIP08550
 PIP08560
 PIP08570
 PIP08580
 PIP08590
 PIP08600
 PIP08610
 PIP08620
 PIP08630
 PIP08640

380 FORMAT(1X,2D30.18)

CCCCCCCCCCCC

PART VII

COMPUTATION OF AXIAL PERTURBATION VELOCITY U(R).

OUTPUT THE EIGENVECTOR CORRESPONDING TO THE LEASE STABLE

EIGENVALUE, GAMMA*.

```

DO 400 I = 1, MESH
  II = I + MESH
  P(II) = EIGVEC(II,NGAM)
  Q(II) = EIGVEC(II,NGAM)
  400 CONTINUE
  H0 = EIGVEC(MH0,NGAM)
  Q0 = EIGVEC(H00,NGAM)
  WRITE(6,401) EIGVAL(NGAM)
  401 FORMAT(1X,///,5X,'EIGENVECTOR CORRESPONDING TO',2D27.18,/)
  DO 402 I = 1, MESH
    II = I + MESH
    WRITE(6,404) I, P(II), I, Q(II)
    404 FORMAT(2X,12,2D28.18,2X,12,2D23.18)
    402 CONTINUE
    H0 = H00
    403 WRITE(6,403) H0, Q0
    403 FORMAT(1X,/,2X,10,2D28.18,2X,10,2D28.18,/)
  
```

COMPUTATION OF DQ(R)

```

DO 411 J = 1, 3
  DQ(J) = ZERO
  QOD1QA = ZERO
  DO 410 K = 1, 6
    AAXQ1 = AAXISQ(1,J,K)
    IF(J.EQ.3) AAXQ1 = ZERO
    DO 409 J = DO(J) + Q(K) * AAXISQ(1,J,K)
    QOD1QA = QOD1QA + AAXQ1
  410 CONTINUE
  DQ(J) = DQ(J) - (QOD1QA + Q0)
  411 CONTINUE

DO 420 J = 4, M
  DQ(J) = ZERO
  DO 420 K = 1, 7
    L = J - 4 + K
  
```

C

PIP086550
PIP08660
PIP08660
PIP08670
PIP08680
PIP08690
PIP08700
PIP08710
PIP08720
PIP08730
PIP08740
PIP08750
PIP08760
PIP08770
PIP08780
PIP08790
PIP08800
PIP08810
PIP08820
PIP08830
PIP08840
PIP08850
PIP08860
PIP08870
PIP08880
PIP08890
PIP08900
PIP08910
PIP08920
PIP08930
PIP08940
PIP08950
PIP08960
PIP08970
PIP08980
PIP08990
PIP09000
PIP09010
PIP09020
PIP09030
PIP09040
PIP09050
PIP09060
PIP09070
PIP09080
PIP09090
PIP09100
PIP09110
PIP09120

```

C
420  DQ(J) = DQ(J) + (Q(L) * A1DER2(K))
      CONTINUE
C
DO 431 J = 1,3
  L = J + M
  DQ(L) = ZERO
  HOD1QA = ZERO
  DO 430 K = 1,6
    AWAQ1 = AWAQ1 + Q(1,J,K)
    IF (J.EQ.1) AWAQ1 = ZERO
    KK = 7 - K
    N = MM + K
    HTEMP = 1.0D0 - ((2.0D0 * DPLDAT(KK) - 1.0D0) / DMESH)
    BETA = DCMFLX(HTEMP,0.0D0)
    HOD1QA = HOD1QA + (AWAQ1 * BETA)
    DQ(L) = DQ(L) + (Q(N) * AWAQ1(1,J,K))
  CONTINUE
430  HOD1QA = HOD1QA + TWJ
      IF (J.EQ.1) HOD1QA = ZERO
      DQ(L) = DQ(L) + (HOD1QA * H0)
431  CONTINUE
C
DO 440 I = 1, MESH
  U(I) = RAD(I) * ((THREE*Q(I)) + (RAD(I)*D2(I)) - (ONEING*P(I)))
  CONTINUE
C
C
C      REARRANGE DATA FOR PLOT ROUTINE
M2 = MESH + 2
DO 450 I = 1, MESH
  II = M2 - I
  III = II - 1
  U(II) = U(III)
  RAD(II) = RAD(III)
450  CONTINUE
      RAD(1) = ZERO
      RAD(M2) = ONE
      U(1) = ZERO
      U(M2) = ZERO
      DO 460 I = 1, M2
        RADR(I) = DREAL(RAD(I))
460  CONTINUE
C
C
C      COMPUTE THE NORMALIZED PERTURBATION VELOCITY AND
      NORMALIZED AMPLITUDE AND OUTPUT THE RESULTS.
      DO 465 I = 1, M2

```

```

PIPO9130
PIPO9140
PIPO9150
PIPO9160
PIPO9170
PIPO9180
PIPO9190
PIPO9200
PIPO9210
PIPO9220
PIPO9230
PIPO9240
PIPO9250
PIPO9260
PIPO9270
PIPO9280
PIPO9290
PIPO9300
PIPO9310
PIPO9320
PIPO9330
PIPO9340
PIPO9350
PIPO9360
PIPO9370
PIPO9380
PIPO9390
PIPO9400
PIPO9410
PIPO9420
PIPO9430
PIPO9440
PIPO9450
PIPO9460
PIPO9470
PIPO9480
PIPO9490
PIPO9500
PIPO9510
PIPO9520
PIPO9530
PIPO9540
PIPO9550
PIPO9560
PIPO9570
PIPO9580
PIPO9590
PIPO9600

```


AD-A126 767

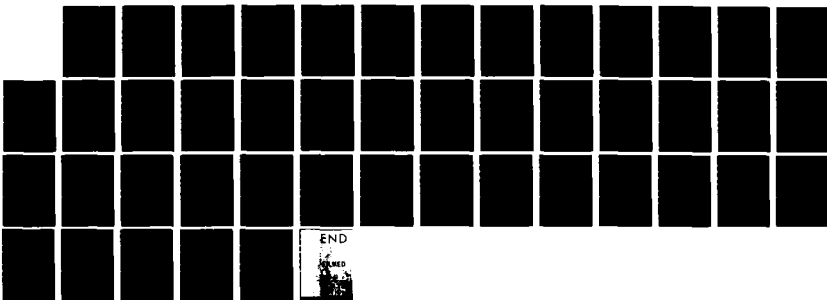
A NUMERICAL ANALYSIS OF PIPE FLOW STABILITY(U) NAVAL
POSTGRADUATE SCHOOL MONTEREY CA D B WALLACE DEC 82

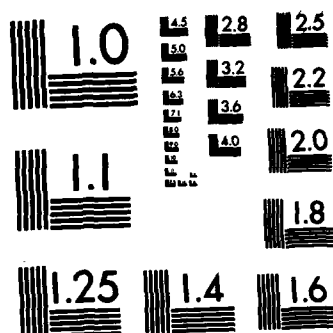
3/3

UNCLASSIFIED

F/G 20/4

NL





MICROCOPY RESOLUTION TEST CHART
NATIONAL BUREAU OF STANDARDS-1963-A

[illegible]

```

PIP1010100
PIP1010110
PIP1010120
PIP1010130
PIP1010140
PIP1010150
PIP1010160
PIP1010170
PIP1010180
PIP1010190
PIP1010200
PIP1010210
PIP1010220
PIP1010230
PIP1010240
PIP1010250
PIP1010260
PIP1010270
PIP1010280
PIP1010290
PIP1010300
PIP1010310
PIP1010320
PIP1010330
PIP1010340
PIP1010350
PIP1010360
PIP1010370
PIP1010380
PIP1010390
PIP1010400
PIP1010410
PIP1010420
PIP1010430
PIP1010440
PIP1010450
PIP1010460
PIP1010470
PIP1010480
PIP1010490
PIP1010500
PIP1010510
PIP1010520
PIP1010530
PIP1010540
PIP1010550
PIP1010560

```

```

180 GO TO 19
    CONTINUE
    CALL PLOT (0.0,0.0,999)
    STOP
    END

```

CCCCC

SUBROUTINE TITLE1

SUBROUTINE TO WRITE TITLE ON PLOTS

SUBROUTINE TITLE1(XO,YO,RMESH,ALPLOT,REPLCT,GAMPLT)

```

RN = 1.0
YHT = 0.14
CALL NEWPEN(2)
CALL SYMBOL(XO,YO,YHT)
1: NORMALIZED PERTURBATION VELOCITY VS RADIUS',0.0,42)
YHT = 0.08
DELY = 0.20
CALL NEWPEN(1)
YO = YO - 0.8
XO = XO + 2.5
XN = XO + .75
CALL SYMBOL(XO,YO,YHT,'N',0.0,-1)
CALL NUMBER(XN,YO,YHT,RN,0.0,-1)
YO = YO - DELY
CALL SYMBOL(XO,YO,YHT,'MESH',0.0,9)
CALL NUMBER(XN,YO,YHT,RMESH,0.0,-1)
YO = YO - DELY
CALL SYMBOL(XO,YO,YHT,'ALPHA',0.0,2)
CALL NUMBER(XN,YO,YHT,ALPLOT,0.0,2)
YO = YO - DELY
CALL SYMBOL(XO,YO,YHT,'REY NR',0.0,9)
CALL NUMBER(XN,YO,YHT,REPLCT,0.0,1)
YO = YO - DELY
CALL SYMBOL(XO,YO,YHT,'GAMMA',0.0,9)
CALL NUMBER(XN,YO,YHT,GAMPLT,0.0,4)
YO = YO - 3.4
CALL SYMBOL(XO,YO,YHT,'OCTAGON = U (REAL)',0.0,17)
YO = YO - DELY
CALL SYMBOL(XO,YO,YHT,'DIAMOND = U (IMAG)',0.0,17)
YO = YO - DELY
CALL SYMBOL(XO,YO,YHT,'TRIANGLE = U AMPL',0.0,17)

```

WRITE THE AXIS LABELS

XO = XO - 2.55

CCCC

```

YO = YO + 0.3
YHT = 0.12
CALL SYMBOL(XO,YO,YHT,'NORMALIZED PERTURBATION VELOCITY',90.,32)
XO = XO + 2.8
YO = YO - 1.3
CALL SYMBOL(XO,YO,YHT,'PIPE RADIUS',0.0,11)
RETURN
END

```

```

/*GO,SYN DD *
2 1 5
-0.754144464179988427D+00
0.372212354450365063D+00
0.619005328596801241D+00
-0.285375962107755191D+00
0.483027432405761783D-01

2 2 5
0.128374777975133259D+01
-0.257055456877836686D+01
-0.138809946714031485D+01
-0.104795737122556964D+00
0.35030590927518066D-02

1 1 4
-0.1026515151515138D+01
0.1367727272727271D+01
-0.4431818181818135D+00
0.719696969696969474D-01

1 2 4
-0.602272727272726405D+00
0.340909090909091733D-01
0.647727272727273373D+00
-0.79545454545454470D-01

9 0 0
0.137690108792184640D+01
-0.611956039076375066D+00
-0.330456261101242083D+00
-0.11240008809946189D+00
0.169987788632325644D-01
-0.442650976909413263D+01
0.780067100848626405D+01
-0.484236234458257542D+01
0.173889875666073834D+01
-0.270697651470296355D+00

2 1 5
-0.541666666666665808D+01
-0.244444444444444176D+01
-0.4999999999999994837D+00
0.952380952380948859D-01

```

```

PIP10570
PIP10580
PIP10590
PIP10600
PIP10610
PIP10620
PIP10630
PIP10640
PIP10650
PIP10660
PIP10670
PIP10680
PIP10690
PIP10700
PIP10710
PIP10720
PIP10730
PIP10740
PIP10750
PIP10760
PIP10770
PIP10780
PIP10790
PIP10800
PIP10810
PIP10820
PIP10830
PIP10840
PIP10850
PIP10860
PIP10870
PIP10880
PIP10890
PIP10900
PIP10910
PIP10920
PIP10930
PIP10940
PIP10950
PIP10960
PIP10970
PIP10980
PIP10990
PIP11000
PIP11010
PIP11020
PIP11030
PIP11040

```


4	3	6	0.10000000000000000852650+01
-0.	0.	6222222222222222804090+01	
-0.	0.	9200000000000000457590+01	
-0.	0.	6448979591836899050+01	
-0.	0.	1987654320987697790+01	
-0.	0.	1652892561983525520+00	
3	1	5	-0.17499999999999997510+02
-0.	0.	11111111111111076090+00	
0.	0.	1200000000000013720+01	
-0.	0.	3469387755102073950+00	
0.	0.	4320987654321039110-01	
3	2	5	0.13499999999999996800+02
-0.	0.	3888888888888882130+01	
-0.	0.	1421085471520200370-13	
-0.	0.	5510204081632665840+00	
-0.	0.	6790123456790178590-01	
3	3	5	-0.155000000000000011370+02
-0.	0.	9888888888888910600+01	
-0.	0.	600000000000000053290+01	
-0.	0.	1448979591836749850+01	
0.	0.	6790123456789909350-01	
2	1	4	-0.46666666666666665850+01
-0.	0.	21111111111111110270+01	
-0.	0.	31999999999999999930+00	
0.	0.	3401360544217685210-01	
2	2	4	0.9999999999999999786840+00
-0.	0.	24444444444444449300+01	
-0.	0.	13200000000000001170+01	
-0.	0.	8163265306122451100-01	
1	1	3	0.249999999999999998830+01
0.	0.	2222222222222222930+00	
-0.	0.	19999999999999999730-01	
1	2	3	-0.45000000000000003550+01
0.	0.	1333333333333333300+01	
0.	0.	18000000000000000000+00	
9	0	0	1150.0000
0.	0	00	1150.0000
0.	5	00	1150.0000
2.	3	00	1150.0000


```

4.300 0.000
8.000 0.000
16.000 0.000
32.000 0.000
0.500 0.000
1.300 0.000
2.400 0.000
4.800 0.000
8.000 0.000
16.000 0.000
32.000 0.000
/*
*/

```

C. MAIN INVESTIGATIVE PROGRAM FOR $n = 6$

PIP0000010
PIP0000020
PIP0000030
PIP0000040
PIP0000050
PIP0000060
PIP0000070
PIP0000080
PIP0000090
PIP0000100
PIP0000110
PIP0000120
PIP0000130
PIP0000140
PIP0000150
PIP0000160
PIP0000170
PIP0000180
PIP0000190
PIP0000200
PIP0000210
PIP0000220
PIP0000230
PIP0000240
PIP0000250
PIP0000260
PIP0000270
PIP0000280
PIP0000290
PIP0000300
PIP0000310
PIP0000320
PIP0000330
PIP0000340
PIP0000350
PIP0000360
PIP0000370
PIP0000380
PIP0000390
PIP0000400
PIP0000410
PIP0000420
PIP0000430
PIP0000440
PIP0000450
PIP0000460
PIP0000470
PIP0000480

//WALLACE JOB (2027,0084), 'THESES N = 6', CLASS=C
//*MAIN LINES={20}
// EXEC FRTXCLGP, INSL=DP, REGION.GO=2048K
//PORT.SYSIN DD

C*****

THIS PROGRAM WAS DEVELOPED TO PERFORM A NUMERICAL ANALYSIS
OF THREE DIMENSIONAL PIPE FLOW STABILITY FOR AXIAL WAVE
NUMBER $N = 6$. THE PROGRAM IS DIVIDED INTO EIGHT PARTS.
THE FIRST PART COMPUTES THE CENTRAL FINITE DIFFERENCE
COEFFICIENTS FOR THE DERIVATIVES OF $P(R)$ AND $Q(R)$ AT THE
INTERIOR MESH POINTS ALONG THE PIPE RADIUS. IN THE SECOND
PART, PRE-COMPUTED NON-CENTRAL FINITE DIFFERENCE
COEFFICIENTS FOR THE DERIVATIVES OF $P(R)$ AND $Q(R)$ AT POINTS
NEAR THE AXIS AND WALL ARE READ IN AS DATA. THE THIRD PART
COMPUTES THE VORTICITY TRANSPORT EQUATION COEFFICIENTS OF
 $P(R)$ AND $Q(R)$ AND THEIR RESPECTIVE DERIVATIVES AT ALL RADIAL
MESH POINTS (STATIONS). THE FOURTH PART COMPUTES THE A AND B
MATRIX ELEMENTS, WHICH MAKE-UP THE EIGENSYSTEM TO BE SOLVED
IN THE FORMAT, $A * X = GAMMA * B * X$. IN THE FIFTH PART
THE A AND B MATRICES COMPRISING THE EIGENSYSTEM ARE SOLVED
IN THE SUBROUTINE EIGZC. THE RESULTING EIGENVALUES AND
CORRESPONDING EIGENVECTOR REPRESENT GAMMA AND THE COLUMN
VECTOR X, RESPECTIVELY, AND ARE SOLUTIONS OF THE GOVERNING
PARTIAL DIFFERENTIAL EQUATIONS. THE SIXTH PART VERIFIES
THE SOLUTION OF THE PDE AND THE MAGNITUDE OF THE RESIDUAL
IS DETERMINED. THE SEVENTH PART COMPUTES THE NORMALIZED

```
DATA ZERO /0.0D0,0.0D0/,ONE/(1.0D0,0.0D0)/,FOUR/(4.0D0,0.0D0)/
DDATA SIXING/0.0B0,5.0B0/,
DDATA AXISO/72*(0.0D0,0.0D0)/,AVALLO/72*(0.0D0,0.0D0)/
DDATA A1DERO/7*(0.0D0,6.0D0)/,A2DERO/7*(0.3D0,0.0D0)/
DDATA A3DERO/7*(0.0D0,0.0D0)/,A4DERO/7*(0.0D0,0.0D0)/
DDATA AAXISP/20*(0.0D0,6.0D0)/,AHALP/20*(0.0B0,0.0B0)/
DDATA AAXISRP/5*(0.0D0,6.0D0)/,A2DRP/5*(0.0D0,0.0D0)/
DDATA YI(1)0.0/,YI(2)/1.0/,YI(1)/0.0/,YI(2)/6.0/
DDATA FRESH/50/
```

DATA 000000/000000

PART I

COMPUTE CENTRAL DIFFERENCE COEFFICIENTS FOR FOURTH ORDER

DERIVATIVE OF $Q(R)$ AT INTERIOR MESH POINTS.

DMESH = DFL0AT (MESH)

```

H4TH = DMESH ** 4
ATEMP = (-1.0D0/6.0D0) * H4TH
A4DERQ(1) = A4DERX(1)
A4DERQ(7) = A4DERX(1)
ATEMP = 2.000 * H4TH
A4DERQ(2) = DCMLX(ATEMP, 0.0D0)
A4DERQ(6) = A4DERX(2)
ATEMP = -6.5D0 * H4TH
A4DERQ(3) = DCMLX(ATEMP, 0.0D0)
A4DERQ(5) = A4DERX(3)
ATEMP = (56.0D0/6.0D0) * H4TH
A4DERQ(4) = DCMLX(ATEMP, 0.0D0)

```

COMPUTE CENTRAL DIFFERENCE COEFFICIENTS FOR THIRD ORDER

DERIVATIVE OF $Q(R)$ AT INTERIOR MESH POINTS.

```

H3RD = DRESH ** 3
ATEMP = 0.125D0 * H3RD
A3DERO{1} = DCMPLX(A1EMP, 0.0D0)
A3DERO{2} = -A3DERO{1}
A3DERO{3} = -A3DERO{2}
ATEMP = (13.0D0/8.0D0) * H3RD
A3DERO{4} = DCMPLX(A1EMP, 0.0D0)
A3DERO{5} = -A3DERO{4}

```

COMPUTE CENTRAL DIFFERENCE COEFFICIENTS FOR SECOND ORDER

UUU

```

PIP000490
PIP000500
PIP000510
PIP000520
PIP000530
PIP000540
PIP000550
PIP000560
PIP000570
PIP000580
PIP000590
PIP000600
PIP000610
PIP000620
PIP000630
PIP000640
PIP000650
PIP000660
PIP000670
PIP000680
PIP000690
PIP000700
PIP000710
PIP000720
PIP000730
PIP000740
PIP000750
PIP000760
PIP000770
PIP000780
PIP000790
PIP000800
PIP000810
PIP000820
PIP000830
PIP000840
PIP000850
PIP000860
PIP000870
PIP000880
PIP000890
PIP000900
PIP000910
PIP000920
PIP000930
PIP000940
PIP000950

```

```

AXIAL PERTURBATION VELOCITY U(R). THE EIGHTH AND LAST
PART PLOTS THE PERTURBATION VELOCITY VERSUS PIPE RADIUS.
REQUIRED SUBROUTINES ARE INCLUDED AT THE END OF THE PROGRAM
LISTING. THIS IS A GENERALIZED PROGRAM FOR VARIABLE SIZED
MESH UP TO A MAXIMUM MESH SIZE OF 50. BECAUSE OF THE
LARGE AMOUNT OF MEMORY REQUIRED TO RUN THIS PROGRAM, IT
CAN ONLY BE RUN IN THE BATCH MODE (MVS). AVERAGE CPU TIME
REQUIRED FOR ONE SET OF DATA, I.E. ONE AXIAL WAVE NUMBER
AND ONE REYNOLDS NUMBER, IS 61 SECONDS.

```

```

DEFINE PROGRAM VARIABLES AND ARRAYS.

```

```

COMPLEX*16 A(100,100), B(100,100), ANALLO(4,3,6), A1DERQ(7)
COMPLEX*16 ZERO, ONE, A3ISO(4,3,6), A3DERQ(7), A1DERQ(7)
COMPLEX*16 A2DERQ(7), A3DERQ(7), A1DERQ(7), A1DERQ(7)
COMPLEX*16 D3Q1(50), D3Q2(50), D3Q3(50), D3Q4(50), D3Q5(50)
COMPLEX*16 D4Q1(50), D4Q2(50), D4Q3(50), D4Q4(50), D4Q5(50)
COMPLEX*16 E1Q1(50), E1Q2(50), E1Q3(50), E1Q4(50), E1Q5(50)
COMPLEX*16 AA(100,100), AALLP(2,2,5), A1DERP(5), A2DERP(5)
COMPLEX*16 D2P1(50), D2P2(50), D2P3(50), D2P4(50), D2P5(50)
COMPLEX*16 DOP1(50), DOP2(50), DOP3(50), DOP4(50), DOP5(50)
COMPLEX*16 EIGA(100,100), EIGB(100,100), EIGVEC(100,100), EIGVAL(100)
COMPLEX*16 AA(100,100), BB(100,100), SIXING, FOUR
COMPLEX*16 Q(50,50), P(50,50), RAD(52), UNORN(52)
COMPLEX*16 ERROR(100), SUMA, SUMB
REAL*8 GAMR(100), GAMH(100), AX, DX, D1MESH
REAL*8 HATH(100), H2ND, H1ST, HTEMP, ATEMP, AATEMP, WATEMP, R, RE, ALPHA
REAL*8 TEMPR(100), TENPI, SI, GN, R2, R3, R4, R5
REAL*8 AL2, AL12, AL14, AL24, AL3, ALSQ2, ALSQ6, ALSQ9, ALSQ24, ALSQ36
REAL*8 ALSQ57, AL4TH, AL3RD2
REAL*8 UAMP(52), AMPHAX, ANTEMP, JANMOR(52), URDP(52), UIDP(52)
REAL*4 RADR(52), OR(52), UI(52), AMPNOR(52)
REAL*4 Y1(2), Y1(2), ALPLOT, REPLCT, GAMPLIT, RMESH
INTEGER MESH, N, NH, H2, INAX, NP, MIP, MESH2, NGAN

```

```

INITIALIZE THE COEFFICIENT ARRAYS AND SEVERAL CONSTANTS

```

CCCCCCCCCCCCCCCCCCCCCCCCCCCCCCCC

CCC

```

PIP01450
PIP01460
PIP01470
PIP01480
PIP01490
PIP01500
PIP01510
PIP01520
PIP01530
PIP01540
PIP01550
PIP01560
PIP01570
PIP01580
PIP01590
PIP01600
PIP01610
PIP01620
PIP01630
PIP01640
PIP01650
PIP01660
PIP01670
PIP01680
PIP01690
PIP01700
PIP01710
PIP01720
PIP01730
PIP01740
PIP01750
PIP01760
PIP01770
PIP01780
PIP01790
PIP01800
PIP01810
PIP01820
PIP01830
PIP01840
PIP01850
PIP01860
PIP01870
PIP01880
PIP01890
PIP01900
PIP01910
PIP01920

```

DERIVATIVES OF P(R) AND Q(R) AT INTERIOR MESH POINTS.

```

H2ND = DMESH ** 2
ATEMP = (-1.0D0/12.0D0) * H2ND
A2DERQ(2) = DCMPLEX(ATEMP, 0.0D0)
A2DERQ(6) = A2DERQ(2)
ATEMP = (16.0D0/12.0D0) * H2ND
A2DERQ(3) = DCMPLEX(ATEMP, 0.0D0)
A2DERQ(5) = A2DERQ(3)
ATEMP = -2.5D0 * H2ND
A2DERQ(4) = DCMPLEX(ATEMP, 0.0D0)
A2DERP(1) = A2DERQ(2)
A2DERP(2) = A2DERQ(3)
A2DERP(3) = A2DERQ(4)
A2DERP(4) = A2DERQ(5)
A2DERP(5) = A2DERQ(5)

```

COMPUTE CENTRAL DIFFERENCE COEFFICIENTS FOR FIRST ORDER

DERIVATIVES OF P(R) AND Q(R) AT INTERIOR MESH POINTS.

```

H1ST = DMESH
ATEMP = (1.0D0/12.0D0) * H1ST
A1DERQ(2) = DCMPLEX(ATEMP, 0.0D0)
A1DERQ(6) = -A1DERQ(2)
ATEMP = (-8.0D0/12.0D0) * H1ST
A1DERQ(3) = DCMPLEX(ATEMP, 0.0D0)
A1DERQ(5) = -A1DERQ(3)
A1DERP(1) = A1DERQ(2)
A1DERP(2) = A1DERQ(3)
A1DERP(3) = A1DERQ(4)
A1DERP(4) = A1DERQ(5)
A1DERP(5) = A1DERQ(5)

```

PART II

READ IN PRE-COMPUTED NON-CENTRAL DIFFERENCE COEFFICIENTS FOR

ALL DERIVATIVES OF P(R) AT POINTS NEAR THE AXIS.

BOUNDARY CONDITION AT THE AXIS IS: P(0) = 0.

```

41 READ(5,49) I,J,K
   IF(I.EQ.9) GO TO 44
   HTEMP = DMESH ** I
   DO 42 KKK = 1,K
   READ(5,*) AATEMP

```

```

AATMP = AATMP * HTEMP
AAISP(I,J,KKK) = DCHPLX(AATMP,0.0D0)
CONTINUE
GO TO 41
42 CONTINUE
44 CONTINUE

```

CCCCCCCC

```

READ IN PRE-COMPUTED NON-CENTRAL DIFFERENCE COEFFICIENTS FOR
ALL DERIVATIVES OF P(R) AT POINTS NEAR THE WALL.
BOUNDARY CONDITION AT THE WALL IS: P(1) = 0

```

```

45 READ(5,49) I,J,K
IF(I.EQ.9) GO TO 47
HTEMP = DMESH ** I
JJ = 3 - J
SIGN = 1.0D0
IF(I.EQ.1) SIGN = -SIGN
DO 46 KKK = 1,K
KK = 6 - KKK
READ(5,*) WATMP
WATMP = WATMP * HTEMP * SIGN
AWALLP(I,JJ,KK) = DCHPLX(WATMP,0.0D0)
CONTINUE
GO TO 45
46 CONTINUE
47 CONTINUE
49 FORMAT(I1,1X,I1,1X,I1)

```

CCCCCCCC

```

READ IN PRE-COMPUTED NON-CENTRAL DIFFERENCE COEFFICIENTS FOR
ALL DERIVATIVES OF Q(R) AT POINTS NEAR THE AXIS.
BOUNDARY CONDITIONS AT THE AXIS ARE: DQ(0) = 0 AND Q(0) = 0.

```

```

51 READ(5,49) I,J,K
IF(I.EQ.9) GO TO 54
HTEMP = DMESH ** I
DO 52 KKK = 1,K
READ(5,*) AATMP
AATMP = AATMP * HTEMP
AAISO(I,J,KKK) = DCHPLX(AATMP,0.0D0)
CONTINUE
GO TO 51
52 CONTINUE
54 CONTINUE

```

CCCC

```

READ IN PRE-COMPUTED NON-CENTRAL DIFFERENCE COEFFICIENTS FOR
ALL DERIVATIVES OF Q(R) AT POINTS NEAR THE WALL.

```

PIP01930
 PIP01940
 PIP01950
 PIP01960
 PIP01970
 PIP01980
 PIP01990
 PIP02000
 PIP02010
 PIP02020
 PIP02030
 PIP02040
 PIP02050
 PIP02060
 PIP02070
 PIP02080
 PIP02090
 PIP02100
 PIP02110
 PIP02120
 PIP02130
 PIP02140
 PIP02150
 PIP02160
 PIP02170
 PIP02180
 PIP02190
 PIP02200
 PIP02210
 PIP02220
 PIP02230
 PIP02240
 PIP02250
 PIP02260
 PIP02270
 PIP02280
 PIP02290
 PIP02300
 PIP02310
 PIP02320
 PIP02330
 PIP02340
 PIP02350
 PIP02360
 PIP02370
 PIP02380
 PIP02390
 PIP02400


```

PIP02892
PIP02900
PIP02910
PIP02920
PIP02930
PIP02940
PIP02950
PIP02960
PIP02970
PIP02980
PIP02990
PIP03000
PIP03010
PIP03020
PIP03030
PIP03040
PIP03050
PIP03060
PIP03070
PIP03080
PIP03090
PIP03100
PIP03110
PIP03120
PIP03130
PIP03140
PIP03150
PIP03160
PIP03170
PIP03180
PIP03190
PIP03200
PIP03210
PIP03220
PIP03230
PIP03240
PIP03250
PIP03260
PIP03270
PIP03280
PIP03290
PIP03300
PIP03310
PIP03320
PIP03330
PIP03340
PIP03350
PIP03360

```

```

AL12 = 12.000 * ALPHA
AL14 = 14.000 * ALPHA
AL24 = 24.000 * ALPHA
ALSO = ALPHA * ALPHA
ALSO2 = ALSO * ALSO
AL4TH = ALSO * ALSO
ALSO6 = 6.000 * ALSO
ALSO9 = 9.000 * ALSO
ALSO24 = 24.000 * ALSO
ALSO36 = 36.000 * ALSO
ALSO57 = 57.000 * ALSO
AL3RD2 = 2.000 * ALSO * ALPHA

      COMPUTE THE INCREMENTAL PIPE RADIUS AT INTERIOR MESH POINTS.

DO 60 I = 1,MESH
R = (DPLOAT(I) - 0.500) / DMESH
R2 = R * R
R3 = R * R * R
R4 = R * R * R * R
R5 = R * R * R * R * R
RAD(I) = DCMLPX(R,0.000)

      VORTICITY TRANSPORT EQN COEFFICIENTS FOR P(R), DP(R) & D2P(R)

      FIRST EQUATION FIRST QUADRANT
TEMPR = (R2 * (36.000 + ALSO * R2)) / RE
D2P1(I) = DCMLPX(TEMPR,0.000)
TEMPR = ((252.000 * R) + (ALSO3 * R2)) / RE
D1P1(I) = DCMLPX(TEMPR,0.000)
TEMPR = -(972.000 + (ALSO257 * R2) + (AL4TH * R4)) / RE
TEMP1 = -AL2 * R2 * (36.000 - (36.000 * R2) + (ALSO * R4))
DOP1(I) = DCMLPX(TEMPR,TEMP1)
TEMPR = (36.000 * R2) + (ALSO * R4)
EOP1(I) = DCMLPX(TEMPR,0.000)

      V T E COEFFICIENTS FOR Q(R), DQ(R), D2Q(R) AND D3Q(R)

      FIRST EQUATION SECOND QUADRANT
TEMP1 = (6.000 * R2) / RE
D3Q1(I) = DCMLPX(TEMP1,0.000)
TEMP1 = (66.000 * R) / RE
D2Q1(I) = DCMLPX(TEMP1,0.000)
TEMPR = AL12 * (R2 - R4)
TEMP1 = - (42.000 + (ALSO6 * R2)) / RE
D1Q1(I) = DCMLPX(TEMPR,TEMP1)

```

CC C

CC C C C

CC C C C C

PIP033370
 PIP033380
 PIP033390
 PIP033400
 PIP033410
 PIP033420
 PIP033430
 PIP033440
 PIP033450
 PIP033460
 PIP033470
 PIP033480
 PIP033490
 PIP033500
 PIP033510
 PIP033520
 PIP033530
 PIP033540
 PIP033550
 PIP033560
 PIP033570
 PIP033580
 PIP033590
 PIP033600
 PIP033610
 PIP033620
 PIP033630
 PIP033640
 PIP033650
 PIP033660
 PIP033670
 PIP033680
 PIP033690
 PIP033700
 PIP033710
 PIP033720
 PIP033730
 PIP033740
 PIP033750
 PIP033760
 PIP033770
 PIP033780
 PIP033790
 PIP033800
 PIP033810
 PIP033820
 PIP033830
 PIP033840

```

CCCCC
TEMPR = AL24 * ((2.000 * R) - R3) / RE
DQ01(I) = - ((768.000 / R) + (ALS236 * R)) / RE
TEMP1 = 6.000 * R2
E1Q1(I) = DCMPLX(0.000,TEMP1)
TEMP1 = 24.000 * R
EQ01(I) = DCMPLX(0.000,TEMP1)

      VORTICITY TRANSPORT EQN COEFFICIENTS FOR P(R), DP(R) & D2P(R)

      SECOND EQUATION THIRD QUADRANT

TEMP1 = - (24.000 * R2) / RE
D2P2(I) = - DCMPLX(0.000,TEMP1)
TEMP1 = - ((158.000 * R) / RE
D1P2(I) = - DCMPLX(0.000,TEMP1)
TEMP1 = - AL24 * (R2 - R4)
TEMP1 = (648.000 + (ALSQ24 * R2)) / RE
DOP2(I) = DCMPLX(TEMP1,TEMP1)
TEMP1 = - 12.000 * R2
EOP2(I) = DCMPLX(0.000,TEMP1)

      V T E COEFFICIENTS FOR Q(R), DQ(R), D2Q(R), D3Q(R) AND D4Q(R)

      SECOND EQUATION FOURTH QUADRANT

TEMPR = - R3 / RE
D4Q2(I) = - DCMPLX(TEMPR,0.000)
TEMPR = - ((14.000 * R2) / RE
D3Q2(I) = - DCMPLX(TEMPR,0.000)
TEMPR = (R * (21.000 + (ALSQ2 * R2))) / RE
TEMP1 = AL2 * (R3 - R5)
D2Q2(I) = DCMPLX(TEMPR,TEMP1)
TEMP1 = (315.000 + (ALSQ14 * R2)) / RE
TEMP1 = AL14 * (R2 - R4)
D1Q2(I) = DCMPLX(TEMPR,TEMP1)
TEMPR = - ((1152.000 / R) + (ALS256 * R) + (AL4TH * R3)) / RE
TEMP1 = - ((56.000 * ALPHA * (R - R3)) + (AL3RD2 * (R3 - R5)))
DQ02(I) = - DCMPLX(TEMPR,TEMP1)
TEMP1 = - R3
E2Q2(I) = DCMPLX(TEMPR,0.000)
TEMPR = - 7.000 * R2
E1Q2(I) = DCMPLX(TEMPR,0.000)
TEMPR = (28.000 * R) + (ALSO * R3)
EQ02(I) = DCMPLX(TEMPR,0.000)
      60 CONTINUE
C*****

```



```

PIP04330
PIP04340
PIP04350
PIP04360
PIP04370
PIP04380
PIP04390
PIP04400
PIP04410
PIP04420
PIP04430
PIP04440
PIP04450
PIP04460
PIP04470
PIP04480
PIP04490
PIP04500
PIP04510
PIP04520
PIP04530
PIP04540
PIP04550
PIP04560
PIP04570
PIP04580
PIP04590
PIP04600
PIP04610
PIP04620
PIP04630
PIP04640
PIP04650
PIP04660
PIP04670
PIP04680
PIP04690
PIP04700
PIP04710
PIP04720
PIP04730
PIP04740
PIP04750
PIP04760
PIP04770
PIP04780
PIP04790
PIP04800

```

```

C C FIRST EQUATION SECOND QUADRANT
DO 250 J = 1,3
DO 250 K = 1,6
KK = K + MESH
AORDER = ZERO
IF (K.EQ.J) AORDER = ONE
A(J,KK) = AAXISO(3,J,K)*D3Q1(J) + AAXISO(2,J,K)*D2Q1(J) +
1 A(J,KK) = AAXISO(1,J,K)*D1Q1(J) + AORDER*EQQ1(J)
250 B(J,KK) = AAXISO(1,J,K)*E1Q1(J) +
CONTINUE - 3
M = MESH
DO 260 J = 4,M
DO 260 K = 1,7
L = J - 4 + K
LL = L + MESH
AORDER = ZERO
IF (L.EQ.J) AORDER = ONE
A(J,LL) = A2DERQ(K)*D2Q1(J) + AORDER*EQQ1(J)
1 A(J,LL) = A1DERQ(K)*E1Q1(J) +
260 B(J,LL) = A1DERQ(K)*E1Q1(J)
CONTINUE 3
MM = M - 3
DO 265 J = 1,3
L = J + M
DO 265 K = 1,6
KK = 7 - K
NN = MM + MESH
AORDER = ZERO
IF (N.EQ.L) AORDER = ONE
A(L,NN) = AVALLO(3,J,K)*D3Q1(L) + AVALLO(2,J,K)*D2Q1(L) +
1 A(L,NN) = AVALLO(1,J,K)*D1Q1(L) + AORDER*EQQ1(L)
265 B(L,NN) = AVALLO(1,J,K)*E1Q1(L)
CONTINUE

C C A AND B MATRIX ELEMENTS IN TERMS OF P(R)
C C SECOND EQUATION THIRD QUADRANT
C C
DO 270 J = 1,2
JJ = J + MESH
DO 270 K = 1,5
AORDER = ZERO
IF (K.EQ.J) AORDER = ONE
A(JJ,K) = AAXISP(2,J,K)*D2P2(J) + AAXISP(1,J,K)*D1P2(J) +
1 B(JJ,K) = AORDER*EQP2(J)

```

```

270 CONTINUE
DO 275 J = 3, MP
  JJ = J + MESH
DO 275 K = 1, 5
  L = J - 3 + K
  AODER = ZERO
  IF (L.EQ.J) AODER = ONE
  A(JJ,L) = A2DERP(K)*D2P2(J) + A1DERP(K)*D1P2(J) + AODER*DOP2(J)
  B(JJ,L) = AODER*EOP2(J)
275 CONTINUE
DO 280 J = 1, 2
  L = J + MP
  LL = L + MESH
DO 280 K = 1, 5
  N = MMP + K
  AODER = ZERO
  IF (N.EQ.L) AODER = ONE
  A(LL,N) = AVALLP(2,J,K)*D2P2(L) + AVALLP(1,J,K)*D1P2(L) +
  1 AODER*DOP2(L)
  B(LL,N) = AODER*EOP2(L)
280 CONTINUE
CCCCC

      A AND B MATRIX ELEMENTS IN TERMS OF Q(R)
      SECOND EQUATION FOURTH QUADRANT

DO 285 J = 1, 3
  JJ = J + MESH
DO 285 K = 1, 6
  KK = K + MESH
  AODER = ZERO
  IF (K.EQ.J) AODER = ONE
  1 A(JJ,KK) = AAXISO(4,J,K)*D4Q2(J) + AAXISO(3,J,K)*D3Q2(J) +
  2 AAXISO(2,J,K)*D2Q2(J) + AAXISO(1,J,K)*D1Q2(J) +
  3 AODER*DQ2(J)
  B(JJ,KK) = AAXISO(2,J,K)*E2Q2(J) + AAXISO(1,J,K)*E1Q2(J) +
  1 AODER*EQ2(J)
285 CONTINUE
DO 290 J = 4, M
  JJ = J + MESH
DO 290 K = 1, 7
  L = J - 4 + K
  LL = L + MESH
  AODER = ZERO
  IF (L.EQ.J) AODER = ONE
  A(JJ,LL) = A4DERQ(K)*D4Q2(J) + A3DERQ(K)*D3Q2(J) +
  1 A2DERQ(K)*D2Q2(J) + A1DERQ(K)*D1Q2(J) +
  2 AODER*EQ2(J)
  B(JJ,LL) = A2DERQ(K)*E2Q2(J) + AODER*EQ2(J)

```

10
8820
8830
8840
8850
8860
8870
8880
8890
8900
8910
8920
8930
8940
8950
8960
8970
8980
8990
9000
9010
9020
9030
9040
9050
9060
9070
9080
9090
9100
9110
9120
9130
9140
9150
9160
9170
9180
9190
9200
9210
9220
9230
9240
9250
9260
9270
9280
9290
9300
9310
9320
9330
9340
9350
9360
9370
9380
9390
9400
9410
9420
9430
9440
9450
9460
9470
9480
9490
9500
9510
9520
9530
9540
9550
9560
9570
9580
9590
9600
9610
9620
9630
9640
9650
9660
9670
9680
9690
9700
9710
9720
9730
9740
9750
9760
9770
9780
9790
9800
9810
9820
9830
9840
9850
9860
9870
9880
9890
9900
9910
9920
9930
9940
9950
9960
9970
9980
9990
1000

210

211

```

C      OUTPUT THE EIGENVECTOR CORRESPONDING TO THE LEAST STABLE
C      EIGENVALUE, GAMMA*.
C
      DO 400 I = 1, MESH
      II = I + MESH
      P(I) = EIGVEC(I, NGAM)
      Q(I) = EIGVEC(II, NGAM)
      CONTINUE
      WRITE(6, 401) EIGVAL(NGAM)
      FORMAT(1X, //, 5X, 'EIGENVECTOR CORRESPONDING TO', 2D27.18, /)
      DO 402 I = 1, MESH
      II = I + MESH
      WRITE(6, 404) I, P(I), II, Q(I)
      FORMAT(2X, I2, 2D28.18, 2X, I2, 2D23.18)
      CONTINUE
C      COMPUTATION OF DQ(R)
C
      DO 410 J = 1, 3
      DQ(J) = ZERO
      DO 410 K = 1, 6
      DQ(J) = DQ(J) + (Q(K) * AAXIS2(1, J, K))
      CONTINUE
C
      DO 420 J = 4, M
      DQ(J) = ZERO
      DO 420 K = 1, 7
      L = J - 4 + K
      DQ(J) = DQ(J) + (Q(L) * A1DER2(K))
      CONTINUE
C
      DO 430 J = 1, 3
      L = J + M
      DQ(L) = ZERO
      DO 430 K = 1, 6
      KK = 7 - K
      N = MM + K
      DQ(L) = DQ(L) + (Q(N) * AVAL2(1, J, K))
      CONTINUE
C
      DO 440 I = 1, MESH
      B(I) = (RAD(I) ** 2) * ((FOUR * Q(I)) + (RAD(I) * DQ(I)) -
      1) * (SIXING * P(I) * RAD(I))
      CONTINUE
C      REARRANGE DATA FOR PLOT ROUTINE
C

```

PIP06730
 PIP06740
 PIP06750
 PIP06760
 PIP06770
 PIP06780
 PIP06790
 PIP06800
 PIP06810
 PIP06820
 PIP06830
 PIP06840
 PIP06850
 PIP06860
 PIP06870
 PIP06880
 PIP06890
 PIP06900
 PIP06910
 PIP06920
 PIP06930
 PIP06940
 PIP06950
 PIP06960
 PIP06970
 PIP06980
 PIP06990
 PIP07000
 PIP07010
 PIP07020
 PIP07030
 PIP07040
 PIP07050
 PIP07060
 PIP07070
 PIP07080
 PIP07090
 PIP07100
 PIP07110
 PIP07120
 PIP07130
 PIP07140
 PIP07150
 PIP07160
 PIP07170
 PIP07180
 PIP07190
 PIP07200

```

C
      M2 = MESH + 2
      DO 450 I = 1, MESH
        II = M2 - I
        III = II - 1
        U(II) = U(III)
        RAD(II) = RAD(III)
      CONTINUE
      RAD(1) = ZERO
      RAD(M2) = ONE
      U(1) = ZERO
      U(M2) = ZERO
      DO 460 I = 1, M2
        RADR(I) = DREAL(RAD(I))
      CONTINUE
      450
      460

      C      COMPUTE THE NORMALIZED PERTURBATION VELOCITY AND
      C      NORMALIZED AMPLITUDE AND OUTPUT THE RESULTS.
      C
      DO 465 I = 1, M2
        UAMP(I) = CDABS(U(I))
      CONTINUE
      AMPMAX = UAMP(1)
      IMAX = 1
      DO 470 J = 2, M2
        UAMP(J)
        IF (UAMP(J) .GT. AMPMAX) GO TO 471
        AMPMAX = UAMP(J)
      CONTINUE
      IMAX = J
      465
      470
      471
      472
      WRITE(6,472) // 23X 'NORMALIZED PERTURBATION VELOCITY',
      1 24X 'NORMALIZED AMPLITUDE', /
      DO 475 K = 1, M2
        UAMNOR(K) = UAMP(K) / AMPMAX
        AMPNOR(K) = UAMNOR(K)
        UNORM(K) = U(K) / U(IMAX)
        URDP(K) = DREAL(UNORM(K))
        UR(K) = URDP(K)
        UIDP(K) = DIMAG(UNORM(K))
        UI(K) = UIDP(K)
        KK = K - 1
      CONTINUE
      475
      WRITE(6,466) KK, URDP(K), UIDP(K), UAMNOR(K)
      466
      475
      C
  
```



```
*****  
C  
C  
C  
C  
C  
C  
PART VIII  
  
PLOT THE NORMALIZED PERTURBATION VELOCITY VS PIPE RADIUS.  
  
IPLOT = IPLOT + 1  
RMESH = FLOAT(MESH)  
ALPLOTT = ALPHA  
REPLOTT = RE  
GAMPLT = GAMMAX  
CALL PLOTC(RADR, UR, M2, 1, 1, 1, 1, 0, -1, 0, 0, 1, 0, -1, 0, 1, 0, 5, 0, 5, 0}  
CALL PLOTC(RADR, UI, M2, 2, 1, 5, 1, 1, 0, 0, 1, 0, -1, 0, 1, 0, 5, 0, 5, 0}  
CALL PLOTC(RADR, AMPNDR, H2, 3, 1, 2, 1, 1, 0, 0, 1, 0, -1, 0, 1, 0, 5, 0, 5, 0}  
CALL PLOTC(X1, Y1, 2, 3, 1, 0, 1, 1, 1, 6, 0, 1, 6, -1, 0, 1, 0, 5, 0, 5, 0},  
XO = 0.15  
YO = 5.6  
IF(IPLOT.EQ.4) IPLOT = 1  
IF( {IPLOT.EQ.2} } YO = 12.1  
IF( {IPLOT.EQ.3} } YO = 18.6  
CALL TITLE1(YO, YO, RMESH, ALPLOTT, REPLOTT, GAMPLT)  
GO TO 19  
CONTINUE  
CALL PLOT(0.0, 0.0, 999)  
STOP  
END  
  
180  
.....  
SUBROUTINE TITLE1  
  
SUBROUTINE TO WRITE TITLE ON PLOTS  
  
SUBROUTINE TITLE1(XO, YO, RMESH, ALPLOTT, REPLOTT, GAMPLT)  
RN = 6.0  
YHT = 0.14  
CALL NEWPEN(2)  
CALL SYMBOL{XO, YO, YHT,  
1,NORMALIZED PERTURBATION VELOCITY VS RADIUS*,0.0,42)  
YHT = 0.08  
DELY = 0.20  
CALL NEWPEN(1)  
YO YO - 0.8  
XO XO + 2.5  
XN XO + .75  
CALL SYMBOL(XO, YO, YHT,'N  
CALL NUMBER(XN, YO, YHT,RN,0.0,-1),  
YO XO - DELY
```

UUUU

PIP09610
 PIP09620
 PIP09630
 PIP09640
 PIP09650
 PIP09660
 PIP09670
 PIP09680
 PIP09690
 PIP09700
 PIP09710
 PIP09720
 PIP09730
 PIP09740
 PIP09750
 PIP09760
 PIP09770
 PIP09780
 PIP09790
 PIP09800

0
 0D0
 1150:0D0
 1150:0D0
 1150:0D0
 1150:0D0
 1150:0D0
 1150:0D0
 2300:0D0
 2300:0D0
 2300:0D0
 2300:0D0
 2300:0D0
 2300:0D0
 0.0D0

9 0 0
 0 0.5D0
 1 0.5D0
 2 0.5D0
 4 0.5D0
 8 0.5D0
 16 0.5D0
 32 0.5D0
 0 0.5D0
 1 0.5D0
 2 0.5D0
 4 0.5D0
 8 0.5D0
 16 0.5D0
 32 0.5D0
 -1.0D0
 /*

[illegible]

220

221


```

CCE00970
CCE00980
CCE00990
CCE01000
CCE01010
CCE01020
CCE01030
CCE01040
CCE01050
CCE01060
CCE01070
CCE01080
CCE01090
CCE01100
CCE01110
CCE01120
CCE01130
CCE01140
CCE01150
CCE01160
CCE01170
CCE01180
CCE01190
CCE01200
CCE01210
CCE01220
CCE01230
CCE01240
CCE01250
CCE01260
CCE01270
CCE01280
CCE01290
CCE01300
CCE01310
CCE01320
CCE01330
CCE01340
CCE01350
CCE01360
CCE01370
CCE01380
CCE01390
CCE01400
CCE01410
CCE01420
CCE01430
CCE01440

```

```

DO 171 I = 1,3
DO 171 J = 1,3
A3(I,J) = A6(I,J)
171 CONTINUE
CALL LINV2F(A3,3,3,A3INV,10,WKAREA,IER)
CC
    COMPUTE THE CC MATRICES FOR APPROPRIATE POINTS.
DO 310 K = 1,3
XK = DFLOAT(K)
H(K) = (2.0D0*XK - 1.0D0)/2.0D0
C(K,3,1) = 1.0D0
C(K,3,1) = 0.0D0
C(K,4,1) = 0.0D0
C(K,3,2) = 1.0D0
C(K,4,2) = 0.0D0
C(K,4,3) = 1.0D0
KK = 6
KK6 = 6
DO 330 I = 1,4
PACT = 1.0D0
DO 325 J = 1,K6
JK = J+KK
XJ = DFLOAT(J)
PACT = PACT*XJ
C(K,I,JK) = (H(K)*J)/PACT
325 CONTINUE
KK = KK+1
KK6 = KK6-1
330 CONTINUE
DO 331 K = 1,3
DO 331 I = 1,4
C(K,I,1) = 0.0D0
331 CONTINUE
CC
    CONVERT THE 3 DIMENSIONAL CC MATRICES TO APPROPRIATE 2
    DIMENSIONAL MATRICES.
DO 200 I = 1,4
DO 200 J = 1,6
C4X61(I,J) = C(1,I,J)
200 CONTINUE
DO 201 I = 1,4
DO 201 J = 1,6
C4X62(I,J) = C(2,I,J)

```

201	CONTINUE	=	1,4	
	DO 202 J	=	1,6	
	DO 202 J	=	1,6	C(3,I,J)
202	C4X63(I,J)			
	CONTINUE			
	DO 203 J	=	1,4	
	DO 203 J	=	1,5	
	DO 203 J	=	1,5	C4X61(I,J)
203	C4X51(I,J)			
	CONTINUE			
	DO 204 J	=	1,4	
	DO 204 J	=	1,4	
	DO 204 J	=	1,4	C4X61(I,J)
204	C4X41(I,J)			
	CONTINUE			
	DO 220 J	=	1,3	
	DO 220 J	=	1,3	
	DO 220 J	=	1,3	C4X61(I,J)
220	C3X31(I,J)			
	CONTINUE			
	DO 205 J	=	1,4	
	DO 205 J	=	1,5	
	DO 205 J	=	1,5	C4X62(I,J)
205	C4X52(I,J)			
	CONTINUE			
	DO 206 J	=	1,4	
	DO 206 J	=	1,4	
	DO 206 J	=	1,4	C4X62(I,J)
206	C4X42(I,J)			
	CONTINUE			
	DO 208 J	=	1,3	
	DO 208 J	=	1,3	
	DO 208 J	=	1,3	C4X62(I,J)
208	C3X32(I,J)			
	CONTINUE			
	DO 207 J	=	1,4	
	DO 207 J	=	1,5	
	DO 207 J	=	1,5	C4X63(I,J)
207	C4X53(I,J)			
	CONTINUE			

UUUUUU

CC MATRIX FOR POINTS NEAR THE BOUNDARIES AS REQUIRED.

CALL	VMUL	FF	(C4	XY61	A5	INV	4	6	6	4	C4	6A61	4	IER
CALL	VMUL	FF	C4	XY62	A5	INV	4	6	6	4	C4	6A62	4	IER
CALL	VMUL	FF	C4	XY63	A5	INV	4	6	6	4	C4	6A63	4	IER
CALL	VMUL	FF	C4	XY52	A5	INV	4	6	6	4	C4	5A52	4	IER
CALL	VMUL	FF	C4	XY53	A5	INV	4	6	6	4	C4	5A53	4	IER
CALL	VMUL	FF	C4	XY42	A4	INV	4	5	5	4	C4	5A42	4	IER
CALL	VMUL	FF	C4	XY41	A4	INV	4	5	5	4	C4	5A41	4	IER
CALL	VMUL	FF	C3	XY32	A3	INV	3	4	4	3	C3	3A32	3	IER
CALL	VMUL	FF	C3	XY31	A3	INV	3	4	4	3	C3	3A31	3	IER


```

WRITE(2,20) (C33A32(1,J),J=1,NPTS)
ND = 9
NP = 0
NPTS = 0
WRITE(2,22) ND,NP,NPTS
225 WRITE(2,225) COEFFICIENTS TO APPROXIMATE Q(0) FOR N = 0. TAKEN',
1. FROM THE TOP ROW OF THE ACINV MATRIX.
WRITE(2,20) (A6INV(1,J),J=1,6)
*****
A MODIFIED SUBPROGRAM TO COMPUTE AA MATRIX ELEMENTS FOR
THE BOUNDARY CONDITIONS NEAR THE AXIS AND THE WALL FOR
N = 0, 1 AND 6. THE APPLICABLE BOUNDARY CONDITIONS ARE:
Q(1) = 0 AND DQ(1) = 0 FOR N = 0 AT THE WALL.
Q(0) = VARIABLE AND DQ(0) = 0 FOR N = 1 AT THE AXIS.
Q(1) = -H(0) AND DQ(0) = 2H(0) FOR N = 1 AT THE WALL.
Q(0) = 0 AND DQ(0) = 0 FOR N = 6 AT THE AXIS.
Q(1) = 0 AND DQ(1) = 0 FOR N = 6 AT THE WALL.
*****
COMPUTE THE AA MATRICES AND THEIR INVERSES.
DO 400 I = 1,6
FACT = 1.0D0
XI = DFLOAT(I)
H(I) = {2.0D0+XI-1.0D0}/2.0D0
DO 400 J = 1,6
XJ = DFLOAT(J)
FACT = FACT*(XJ+1.0D0)
A6(I,J) = (H(I)**(J+1))/FACT
400 CONTINUE
CALL LINV2F(A6,6,6,A5INV,10,HKAREA,IER)
DO 401 I = 1,5
DO 401 J = 1,5
A5(I,J) = A6(I,J)
401 CONTINUE
CALL LINV2F(A5,5,5,A5INV,10,HKAREA,IER)
DO 402 I = 1,4

```

```

DO 402 J = 1,4
A4(I,J) = A6(I,J)
402 CONTINUE
CALL LINV2P(A4,4,4,A4INV,10,WKAREA,IER)
DO 403 I = 1,3
DO 403 J = 1,3
A3(I,J) = A6(I,J)
403 CONTINUE
CALL LINV2P(A3,3,3,A3INV,10,WKAREA,IER)

      COMPUTE THE CC COEFFICIENT MATRICES FOR APPROPRIATE POINTS.
DO 405 K = 1,3
XK = DFLOAT(K)
H(K) = (2.0D0*XK - 1.0D0)/2.0D0
C(K,2,1) = 0.0D0
C(K,3,1) = 0.0D0
C(K,4,1) = 0.0D0
C(K,3,2) = 1.0D0
C(K,4,2) = 0.0D0
C(K,4,3) = 1.0D0
KK = 0
K6 = 6
DO 406 I = 1,4
FACT = 1.0D0
DO 407 J = 1,K6
JK = J+KK
XJ = DFLOAT(J)
FACT = FACT*XJ
C(K,I,JK) = (H(K)**J)/FACT
407 CONTINUE
KK = KK+1
K6 = K6-1
406 CONTINUE
405 CONTINUE

      CONVERT THE 3 DIMENSIONAL CC MATRICES TO APPROPRIATE 2
      DIMENSIONAL MATRICES.
DO 408 I = 1,4
DO 408 J = 1,6
C4X61(I,J) = C(1,I,J)
408 CONTINUE
DO 409 I = 1,4
DO 409 J = 1,6
C4X62(I,J) = C(2,I,J)
409 CONTINUE

```

4 10	D0 410 I = 1,6 D0 410 J = C (3, I, J) C4X63(I, J) CONTINUE
4 11	D0 411 I = 1,3 D0 411 J = C4X61(I, J) C3X51(I, J) CONTINUE
4 12	D0 412 I = 1,2 D0 412 J = C4X61(I, J) C2X41(I, J) CONTINUE
4 13	D0 413 I = 1,3 D0 413 J = C4X61(I, J) C1X31(I, J) CONTINUE
4 14	D0 414 I = 1,5 D0 414 J = C4X62(I, J) C3X52(I, J) CONTINUE
4 15	D0 415 I = 1,2 D0 415 J = C4X62(I, J) C2X42(I, J) CONTINUE
4 16	D0 416 I = 1,3 D0 416 J = C4X62(I, J) C1X32(I, J) CONTINUE
4 17	D0 417 I = 1,3 D0 417 J = C4X63(I, J) C3X53(I, J) CONTINUE

PRE-MULTIPLY THE PROPER AA INVERSE MATRIX BY THE PROPER
CCC MATRIX FOR POINTS NEAR THE BOUNDARIES AS REQUIRED.

CCC MATRIX FOR POINTS NEAR THE BOUNDARIES AS REQUIRED.

419
WRITE
FORMAT
2,418

228

```

CCE04333
CCE04340
CCE04350
CCE04360
CCE04370
CCE04380
CCE04390
CCE04400
CCE04410
CCE04420
CCE04430
CCE04440
CCE04450
CCE04460
CCE04470
CCE04480
CCE04490
CCE04500
CCE04510
CCE04520
CCE04530
CCE04540
CCE04550
CCE04560
CCE04570
CCE04580
CCE04590
CCE04600
CCE04610
CCE04620
CCE04630
CCE04640
CCE04650
CCE04660
CCE04670
CCE04680
CCE04690
CCE04700
CCE04710
CCE04720
CCE04730
CCE04740
CCE04750
CCE04760
CCE04770
CCE04780
CCE04790
CCE04800

```

```

ND = 9
NP = 0
NPTS = 0
WRITE(2,221) ND,NP,NPTS
WRITE(2,420)
420 FORMAT(1X, 'COEFFICIENTS TO APPROXIMATE D22(0) FOR N = 1.',
1 'TAKEN FROM THE FIRST ROW OF THE A6INV MATRIX.')
WRITE(2,20) (A6INV(1,J),J=1,6)
*****
C A SUBPROGRAM USED TO COMPUTE THE NONCENTRAL FINITE
DIFFERENCE COEFFICIENTS FOR THE DERIVATIVES OF P(R) AT
POINTS NEAR THE BOUNDARIES. COMPUTE THE AA MATRIX ELEMENTS
FOR THE BOUNDARY CONDITIONS NEAR THE AXIS AND WALL.
THE APPLICABLE BOUNDARY CONDITIONS FOR N = 1 AND 6 ARE:
P(1) = I H(0), A VARIABLE, FOR N = 1 AT THE WALL.
P(0) = 0 FOR N = 6 AT THE AXIS.
P(1) = 0 FOR N = 6 AT THE WALL.
*****
C COMPUTE THE AA MATRICES AND THEIR INVERSES.
DO 500 I=1,5
PACT = 1.0D0
XI = DFL0AT(I)
H(I) = (2.0D0*XI-1.000)/2.0D0
DO 500 J=1,5
XJ = DFL0AT(J)
PACT = PACT+XJ
A5(I,J) = (H(I)**J)/PACT
500 CONTINUE
CALL LINV2F(A5,5,5,A5INV,10,NKAREA,IER)
DO 501 I=1,4
DO 501 J=1,4
A4(I,J) = A5(I,J)
501 CONTINUE
CALL LINV2F(A4,4,4,A4INV,10,NKAREA,IER)
C COMPUTE THE CC COEFFICIENT MATRICES FOR APPROPRIATE POINTS.

```



```
C
C2X51(1,1) = 1.0D0
C2X51(2,1) = 0.0D0
FACT = 1.0D0
DO 502 J = 2,5
  XJ = DPL0AT(J)
  FACT = FACT*(XJ-1.0D0)
  C2X51(1,J) = (H(1)*(J-1))/FACT
CONTINUE
DO 503 J = 2,5
  JJ = J-1
  C2X51(2,J) = C2X51(1,JJ)
CONTINUE
DO 504 J = 1,4
  C1X41(1,J) = C2X51(1,J)
CONTINUE
C2X52(1,1) = 1.0D0
C2X52(2,1) = 0.0D0
FACT = 1.0D0
DO 505 J = 2,5
  XJ = DPL0AT(J)
  FACT = FACT*(XJ-1.0D0)
  C2X52(1,J) = (H(2)*(J-1))/FACT
CONTINUE
DO 506 J = 2,5
  JJ = J-1
  C2X52(2,J) = C2X52(1,JJ)
CONTINUE
DO 507 J = 1,4
  C1X42(1,J) = C2X52(1,J)
CONTINUE

      PRE-MULTIPLY THE PROPER AA INVERSE MAIRIX BY THE PROPER
      CC MATRIX FOR POINTS NEAR THE BOUNDARIES AS REQUIRED.

CALL VHULFFF(C2X51,A5INV,2,5,5,2,5,C25A51,2,IER)
CALL VHULFFF(C2X52,A5INV,2,5,5,2,5,C25A52,2,IER)
CALL VHULFFF(C1X41,A4INV,1,4,4,1,4,C14A41,1,IER)
CALL VHULFFF(C1X42,A4INV,1,4,4,1,4,C14A42,1,IER)
WRITE(2,508)
FORMAT(1X,5F9.2)
WRITE(2,509)
FORMAT(1X,1NONCENTRAL FINITE DIFFERENCE COEFFICIENTS THAT ARE REQUIRED
1TIED NEAR THE BOUNDARIES FOR N= 1 AND 6.,//1X,
2THE COEFFICIENTS APPEAR IN THE
3.FORMAT REQUIRED BY THE MAIN PROGRAM, EXCLUDING COMMENTS.://1X,
4.THE APPLICABLE BOUNDARY CONDITIONS FOR N= 1 AND 6 ARE: ://1X,

```

```

50 P(1) = I H(0) A VARIABLE FOR N = 1 AT THE WALL. ' , // , 1X,
60 P(0) = 0 FOR N = 5 AT THE AXIS: ' , // , 1X,
70 P(1) = 0 FOR N = 6 AT THE WALL: ' , // , 1X,

```

```

      - 0      2 1 5
      F(1) = 1
      ND = 1
      NNPTS = 2, 22 1)
      WURRITE(2, 20)
      NNPTS = NP + 1
      ND = 1
      NNPTS = 2, 22 1)
      WURRITE(2, 20)
      ND = 1
      NNPTS = NPTS - 1
      NNPTS = 2, 22 1)
      WURRITE(2, 20)
      NNPTS = NP + 1
      ND = 1
      NNPTS = 2, 22 1)
      WURRITE(2, 20)
      NNPTS = 0
      ND = 0
      NNPTS = 2, 22 1)
      WURRITE(2, 20)

```

A SUBPROGRAM USED TO COMPUTE THE MATRIX ELEMENTS FOR THE BOUNDARY CONDITIONS NEAR THE AXIS FOR $N = 1$. THE APPLICABLE BOUNDARY CONDITION IS:

DP(0) = 0 FOR N = 1 AT THE AXIS.

```

600      DO 600 I = 1,5
        A5(I,1) = 1.6D0
        CONTINUE
601      DO 601 I = 1,4
        A4(I,1) = 1.6D0
        CONTINUE
        C2X51(1,1) = 0.0D0
        C2X52(1,1) = 0.0D0
        C1X42(1,1) = 0.0D0
        C1X42(1,1) = 0.0D0
        CALL LINV2F(A5,5,5
        CALL LINV2F(A4,4,4

```

```

CCCCC
      PRE-MULTIPLY THE PROPER AA INVERSE MATRIX BY THE PROPER
      CC MATRIX FOR POINTS NEAR THE BOUNDARIES AS REQUIRED.

      CALL VMULFF(C2X51, A5INV, 2, 5, 5, 2, 5, C25A51, 2, IER)
      CALL VMULFF(C2X52, A5INV, 2, 5, 5, 2, 5, C25A52, 2, IER)
      CALL VMULFF(C1X41, A4INV, 1, 4, 4, 1, 4, C14A41, 1, IER)
      CALL VMULFF(C1X42, A4INV, 1, 4, 4, 1, 4, C14A42, 1, IER)
      WRITE(2, 605)
      FORMAT(1X, //)
605  WRITE(2, 606)
      FORMAT(1X, //)
606  FORMAT(1X, //)
      1. THE COEFFICIENTS TO APPROXIMATE P(J) FOR N = 1.,
      2. THE COEFFICIENTS TO APPROXIMATE D2P(0) FOR N = 1.,
      3. THE COEFFICIENTS TO APPROXIMATE D2P(0) FOR N = 1.,
      4. THE APPLICABLE BOUNDARY CONDITION IS: ., ., ., 1X,
      5. DP(0) = 0 FOR N = 1 AT THE AXIS. ., ., ., //)
      ND = 1
      NP = 1
      NPTS = 5
      WRITE(2, 221) ND, NP, NPTS
      WRITE(2, 20) (C25A51(2, J), J=1, NPTS)
      NP = NP + 1
      WRITE(2, 221) ND, NP, NPTS
      WRITE(2, 20) (C25A52(2, J), J=1, NPTS)
      ND = 1
      NP = 1
      NPTS = NPTS - 1
      WRITE(2, 221) ND, NP, NPTS
      WRITE(2, 20) (C14A41(1, J), J=1, NPTS)
      NP = NP + 1
      WRITE(2, 221) ND, NP, NPTS
      WRITE(2, 20) (C14A42(1, J), J=1, NPTS)
      ND = 0
      NP = 0
      NPTS = 0
      WRITE(2, 221) ND, NP, NPTS
      WRITE(2, 615)
      615  FORMAT(1X, //)
      1. TAKEN FROM THE FIRST ROW OF THE A5INV MATRIX.
      WRITE(2, 20) (A5INV(1, J), J=1, 5)
      WRITE(2, 616)
      616  FORMAT(1X, //)
      1. TAKEN FROM THE SECOND ROW OF THE A5INV MATRIX.
      WRITE(2, 20) (A5INV(2, J), J=1, 5)
      STOP
      END

```

```

* * * * *
* FILENAME:  RUNDATA EXEC
* * * * *
* THIS EXEC ALLOWS THE USER TO RUN A FORTRAN H EXTENDED PROGRAM ON
* VM/CMS THAT REQUIRES INPUT DATA AND/OR PRODUCES OUTPUT DATA.
* * * * *
* THE INPUT DATA IS STORED ON THE USER'S DISK UNDER THE SAME FILENAME
* ASSIGNED TO THE MAIN PROGRAM WITH FILETYPE = <DATAIN>.  THE MAIN
* PROGRAM MUST USE, READ(3,NNN) , I.E. DEVICE CODE 3.  THE OUTPUT DATA
* FROM THE FORTRAN PROGRAM WILL BE SENT TO A FILE ON THE USER'S DISK
* HAVING THE SAME FILENAME WITH FILETYPE = <DATAOUT2>.  USE
* WRITE(2,NNN) , I.E. DEVICE CODE 2.  THE USER ALSO HAS THE CAPABILITY
* TO LOAD AND EXECUTE PRE-COMPILED, (FILETYPE = TEXT), SUBROUTINES
* THAT RESIDE ON THE USER'S DISK WHICH ARE CALLED BY THE MAIN PROGRAM.
* * * * *
* TYPE THE COMMAND:  RUNDATA <PN>
* * * * *
* THE OUTPUT IS SENT TO DISK, A FILE IS CREATED AS <PN> <DATAOUT2>.
* * * * *
* IF DEVICE CODE 6 IS ALSO USED IN THE MAIN PROGRAM, I.E. WRITE(6,NNN),
* THE OUTPUT WILL AUTOMATICALLY GO TO THE TERMINAL AS WELL.
* * * * *
* FORTHX 61
* FILEDEF 03 DISK 61 DATAIN (LRECL 80
* FILEDEF 02 DISK 61 DATAOUT2 (BLOCK 130
* FILEDEF 06 TERMINAL
* LOAD 61 (START
* ERASE 61 TEXT *
* ERASE 61 LISTING *
* ERASE LOAD MAP
* EXIT

```

LIST OF REFERENCES

1. Reynolds, O., "An Experimental Investigation of the Circumstances Which Determine Whether the Motion of Water Shall be Direct or Sinuous, and the Law of Resistance in Parallel Channels", Phil. Trans. Royal Society, 174, pp. 935-982, 1883.
2. Salwen, H., and Grosch, C. E., "The Stability of Poiseuille Flow in a Pipe of Circular Cross-section", Journal of Fluid Mechanics, v. 54, part 1, p. 93, 6 March 1972.
3. Garg, V. K., and Rouleau, W. T., "Linear Spatial Stability of Pipe Poiseuille Flow", Journal of Fluid Mechanics, v. 54, part 1, p. 113, 25 November 1973.
4. Gill, A. E., "The Least Damped Disturbances to Poiseuille Flow in a Circular Pipe", Journal of Fluid Mechanics, v. 61, part 1, p. 97, 27 March 1973.
5. Davey, A., and Drazin, P. G., "The Stability of Poiseuille Flow in a Pipe", Journal of Fluid Mechanics, v. 36, part 2, p. 209, 22 August 1968.
6. McIntire, L. V., and Lin, C. H., "Finite Amplitude Instabilities of Second Order Fluids in Plane Poiseuille Flow", Journal of Fluid Mechanics, v. 52, part 2, p. 273, 31 March 1971.
7. Huang, L. M., and Chen, T. S., "Stability of Developing Flow Subject to Non-axisymmetric Disturbances", Journal of Fluid Mechanics, v. 63, part 1, p. 183, 16 April 1973.
8. Leite, R. J., An Experimental Investigation of the Stability of Axially Symmetric Poiseuille Flow, Report No. OSR-TR-56-2, U.S. Air Force Contract AF 18(600)-350, November 1956.
9. Garg, V. K., "Stability of Developing Flow in a Pipe: Non-axisymmetric Disturbances", Journal of Fluid Mechanics, v. 110, p. 209, 15 April 1980.
10. Harrison, W. F., On the Stability of Poiseuille Flow, Ae.E. Thesis, Naval Postgraduate School, Monterey, California, December 1975.
11. Arnold, M. J., Investigation of Pipe Flow Instability and Results for Wave Number Zero, M. S. Thesis, Naval Postgraduate School, Monterey, California, December 1978.

12. Naval Postgraduate School Report NPS67-78-006, A Basic Reformulation of the Pipe Flow Stability Problem and Some Preliminary Numerical Results, by T. H. Gawain, 1 September 1977.
13. Naval Postgraduate School Report NPS67-79-003, A General Linearized Theory of the Stability of Fully Developed Pipe Flow with Particular Reference to the Boundary Conditions at the Axis, by T. H. Gawain, February 1979.
14. Ketter, R. L., and Prawel, S. P. Jr., Modern Methods of Engineering Computation, p. 227, McGraw-Hill, 1969.
15. Gawain, T. H., and Ball, R. E., "Improved Finite Difference Formulas for Boundary Value Problems", International Journal for Numerical Methods in Engineering, v. 12, p. 1151, June 1977.
16. Schlichting, H., Boundary Layer Theory, p. 516, McGraw-Hill, 1968.

INITIAL DISTRIBUTION LIST

	No.	Copies
1. Defense Technical Information Center Cameron Station Alexandria, Virginia 22314	2	
2. Library, Code 0142 Naval Postgraduate School Monterey, California 93940	2	
3. Department Chairman, Code 67 Department of Aeronautics Naval Postgraduate School Monterey, California 93940	1	
4. Professor T. H. Gawain, Code 67Gn Department of Aeronautics Naval Postgraduate School Monterey, California 93940	4	
5. LT David B. Wallace, USN VQ - 1 DET ATSUGI, JAPAN Box 43 FPO Seattle, Washington 98767	1	

END

FILMED

5-83

DTIC